www.biohealthcongress.com

Second International Congress on Biological and Health Sciences Proceedings Book

ONLINE 24-25-26-27 FEBRUARY 2022

ISBN: 978-605-71368-1-7

Veterinary And Public Health Association

SECOND INTERNATIONAL CONGRESS ON BIOLOGICAL AND HEALTH SCIENCES PROCEEDINGS BOOK

All authors are responsible for the contents of their abstracts.

https://www.biohealthcongress.com/(biohealthcongress@gmail.com)

Editor
Ulaş ACARÖZ
Published: 20/03/2022
ISBN: 978-605-71368-1-7

Editor's Note

The first 'International Congress on Biological and Health Sciences' was organized online and free of charge. We are very happy and proud that various health sciencerelated fields attended the congress. By this event, the distinguished and respected scientists came together to exchange ideas, develop and implement new researches and joint projects. There were 23 invited speakers from 11 different countries and also more than 400 submissions were accepted. More than 50 countries contributed to the congress. We would like to thank all participants and supporters. Hope to see you at our next congress.

Best wishes from Turkey

Assoc. Prof. Dr. Ulaş ACARÖZ

HONORARY BOARD

Prof. Dr. Mehmet Karakaş, President of Afyon Kocatepe University, Turkey. (Honorary President).

Prof. Dr. Alparslan Ceylan, Krgyz-Turkish Manas University, Kyrgyzstan.

Assoc. Prof. Dr. Dobri Yarkov, President of Trakia University, Bulgaria.

Prof. Dr. Erinda Lika, Vice-President of Agricultural University of Tirana, Albania.

Prof. Dr. Haurichenka Mikalai Ivanavich, President of Vitebsk Stata Academy of Veterinary Medicine, Belarus.

Prof. Dr. Hazım Tamer Dodurka, President of Istanbul Rumeli University, Turkey.

Prof. Dr. Jerzy Stojko, Vice-President of Medical University of Silesia, Poland.

Prof. Dr. Nihat Şındak, President of Siirt University, Turkey.

Prof. Dr. Mehmet Emin Erkan, President of Şırnak University, Turkey.

Prof. Dr. Sergey Pozyabin, President of Moscow State Academy of Veterinary Medicine and Biotechnology, Russia.

Prof. Dr. Talat Naseer Pasha, President of University of Education Lahore, Pakistan.

Prof. Dr. Turan Civelek, Dean of Afyon Kocatepe University, Faculty of Veterinary Medicine, Turkey.

ORGANIZING COMMITTEE

Dr. Richard Dietrich, Ludwig Maximilians University Munich, Germany, Honorary Member of Committe.

Assoc. Prof. Dr. Ulaş Acaröz, Afyon Kocatepe University, Turkey, President.

Prof. Dr. Kui Zhu, China Agricultural University, China, President.

Prof. Dr. Abdullah Eryavuz, Afyon Kocatepe University, Turkey, Congress General Secretary.

Prof. Dr. Halil Selçuk Biricik, Afyon Kocatepe University, Turkey, Member of Committee.

Assoc. Prof. Dr. Andrea Armani, Pisa University, Italy, Member of Committee.

Prof. Dr. İsmail Küçükkurt, Afyon Kocatepe University, Turkey, Member of Committee.

Prof. Dr. Sinan Ince, Afyon Kocatepe University, Turkey, Member of Committee.

Prof. Dr. Zeki Gürler, Afyon Kocatepe University, Turkey, Member of Committee.

Assoc. Prof. Dr. Halil Yalçın, Burdur Mehmet Akif Ersoy University, Turkey, Member of Committee.

Assoc. Prof. Dr. Damla Arslan Acaröz, Afyon Kocatepe University, Turkey, Member of Committee.

Assist. Prof. Dr. Merve Keskin, Bilecik Seyh Edebali University, Turkey, Member of Committee.

Assist. Prof. Dr. Tuncer Çakmak, Van Yuzuncu Yil University, Turkey, Member of Committee.

Dr. Alexander Atanasoff, Trakia University, Bulgaria, Member of Committee.

Dr. Mehmet Aydın Akalan, Afyon Kocatepe University, Turkey, Member of Committee.

Dr. Fahriye Kan, Afyon Kocatepe University, Turkey, Member of Committee.

CONGRESS SECRETARY

Ali Soylu, Member of Congress Secretary.

Barış Kaçmaz, Member of Congress Secretary.

Büşra Boduroğu, Member of Congress Secretary.

Duygu Uğurlu, Member of Congress Secretary.

Fatih Küçükbüğrü, Member of Congress Secretary.

Hacı İbrahim Koç, Member of Congress Secretary.

İpek Çam Çomak, Member of Congress Secretary.

Melike Akay, Member of Congress Secretary.

Nurtaç Küçükbüğrü, Member of Congress Secretary.

Ömer Gümüştaş, Member of Congress Secretary.

Sermet Genay, Member of Congress Secretary.

Sezen Evrenkaya, Member of Congress Secretary.

CONGRESS TECHNICAL SUPPORT

Osman Doğanay, Member of Congress Technical Support

Mehmet Yalvaç, Member of Congress Technical Support

Okan Dilki, Member of Congress Technical Support

İbrahim Halil Yıldız, Member of Congress Technical Support

SCIENTIFIC COMMITTEE

Prof. Dr. Abdelhanine Ayad, University of Bejaia.
Prof. Dr. Abdul Ahad, Chittagong Veterinary and Animal Sciences University.
Prof. Dr. Abdulridha Taha Sarhan, Hila University.
Prof. Dr. Abdullah Eryavuz, Afyon Kocatepe University.
Prof. Dr. Adilbay Esimbetov, Samarkand Institute of Veterinary Medicine.
Prof. Dr. Agnieszka Najda, University of Life Sciences in Lublin.
Prof. Dr. Ahmet Çakır, Ankara University.
Prof. Dr. Adriana Morar, Banat University of Agronomical Sciences and Veterinary Medicine.
Prof. Dr. Ahmet Güner, Selçuk University.
Prof. Dr. Alev Gürol Bayraktar, Ankara University.
Prof. Dr. Ali Aydın, İstanbul University Cerrahpaşa.
Prof. Dr. Ali Belge, Aydın Adnan Menderes University.
Prof. Dr. Anil Pushpakumara, University of Peradeniya.
Prof. Dr. Aneela Zameer Durrani, University of Veterinary &Animal Sciences, Lahore-Pakistan.
Prof. Dr. Armağan Çolak, Atatürk University.
Prof. Dr. Artay Yağcı, Muğla Sıtkı Koçman University.
Prof. Dr. Asım Kart, Burdur Mehmet Akif Ersoy University.
Prof. Dr. Aydın Vural, Dicle University.
Prof. Dr. Ayhan Baştan, Ankara University.
Prof. Dr. Ayhan Filazi, Ankara University.
Prof. Dr. Aysun Çevik Demirkan, Afyon Kocatepe University.
Prof. Dr. Bahri Patır, Bingöl University.
Prof. Dr. Beniamino Terzo Cenci Goga, Università degli Studi di Perugia.
Prof. Dr. Belgin Sarımehmetoğlu, Ankara University.
Prof. Dr. Birol Kılıç, Süleyman Demirel University.
Prof. Dr. Canan Hecer, Near East University.
Prof. Dr. Cumali Özkan, Van Yuzuncu Yil University.
Prof. Dr. El khasmi Mohammed, University Hassan II of Casablanca.
Prof. Dr. Ender Yarsan, Ankara University.
Prof. Dr. Ergün Ömer Göksoy, Aydın Adnan Menderes University.
Prof. Dr. Erinda Lika, Agricultural University of Tirana.
Prof. Dr. Ertan Emek Onuk, Ondokuz Mayıs University.
Prof. Dr. Erwin Märtlbauer, Ludwig Maximilian University of Munich.
Prof. Dr. Evgeny Eskov, Russian State Agrarian University.
Prof. Dr. Esma Kozan, Afyon Kocatepe University.
Prof. Dr. Esra Akkol, Gazi University.
Prof. Dr. Fatma Seda Bilir Ormancı, Ankara University.
Prof. Dr. Fatih Hatipoğlu, Selçuk University/Kyrgyz-Turkish Manas University.
Prof. Dr. Fatih Mehmet Birdane, Afyon Kocatepe University.
Prof. Dr. Fatih Mehmet Kandemir, Atatürk University.

Prof. Dr. Fatima Wariaghlii, Université Mohammed V Agdal.
Prof. Dr. Figen Çetinkaya, Uludağ University.
Prof. Dr. Gaspar Ros Berruezo, University of Murcia.
Prof. Dr. Gökhan Oto, Van Yuzuncu Yil University.
Prof. Dr. Gülden Zehra Omurtag, İstanbul Medipol University.
Prof. Dr. Gürhan Çiftçioğlu, T.C. İstanbul Kültür University.
Prof. Dr. Hakan Öner, Burdur Mehmet Akif Ersoy University.
Prof. Dr. Hakan Öztürk, Ankara University.
Prof. Dr. Hakan Yardımcı, Ankara University.
Prof. Dr. Halil Selçuk Biricik, Afyon Kocatepe University.
Prof. Dr. Handan Saliha Yıldız, Afyonkarahisar Health Sciences University.
Prof. Dr. Hasan Hüseyin Hadimli, Selçuk University.
Prof. Dr. Hatice Çiçek, Afyon Kocatepe University.
Prof. Dr. Haydar Özdemir, Ankara University.
Prof. Dr. Hom Bahadur Basnet, Agricultre and Forestry University.
Prof. Dr. Hülya Özdemir, Van Yuzuncu Yil University.
Prof. Dr. İbrahim Demirkan, Afyon Kocatepe University.
Prof. Dr. İbrahim Hakkı Ciğerci, Afyon Kocatepe University.
Prof. Dr. İlker Camkerten, Aksaray University.
Prof. Dr. İsa Özaydın, Kafkas University.
Prof. Dr. İsmail Alkan, Van Yuzuncu Yil University.
Prof. Dr. İsmail Şen, Kyrgyz-Turkish Manas University.
Prof. Dr. Iahtasham khan, University of Veterinary &Animal Sciences, Lahore-Pakistan.
Prof. Dr. İzzet Karahan, Balıkesir University.
Prof. Dr. Jani Mavromati, Agricultural University of Tirana.
Prof. Dr. Jezie A. Acorda, University of the Philippines Los Banos.
Prof. Dr. Kálmán Imre, Banat University of Agronomical Sciences and Veterinary Medicine.
Prof. Dr. Katerina Blagoevska, Ss. Cyril and Methodius University in Skopje.
Prof. Dr. Korhan Altunbaş, Afyon Kocatepe University.
Prof. Dr.Koula Doukani, University of Ibn Khaldoun – Tiaret.
Prof. Dr. Pavel Krasochko, Vitebsk Stata Academy of Veterinary Medicine.
Prof. Dr. Petr Krasochko, Vitebsk Stata Academy of Veterinary Medicine.
Prof. Dr. Kui Zhu, China Agricultural University.
Prof. Dr.Lamia Hamrouni Bel Hadj Brahim, University of Carthage.
Prof. Dr. Loğman Aslan, Van Yuzuncu Yil University.
Prof. Dr. Maria G. Campos, University of Coimbra.
Prof. Dr. Mario Giorgi, University of Pisa.
Prof. Dr. Masood Akhtar, Bahauddin Zakariya University.
Prof. Dr. Mehmmet Çalıcıoğlu, Fırat University.
Prof. Dr. Mehmet Elmalı, Hatay Mustafa Kemal University.
Prof. Dr. Mehmet Emin Erkan, Sırnak University.
Prof. Dr. Meryem Eren, Erciyes University.
Prof. Dr. Metin Bayraktar, Fırat University/Kyrgyz-Turkish Manas University.
Prof. Dr. Mitat Şahin, Kafkas University.
Prof. Dr. Miyase Çınar, Kırıkkale University.

Prof. Dr. Mohammad Amjad Kamal, Sichuan University, King Abdulaziz University, Daffodil International University, Novel Global Community Educational Foundation.
Prof. Dr. Muhammad Ovais Omer, University of Veterinary &Animal Sciences, Lahore-Pakistan.
Prof. Dr. Murat Çetin Rağbetli, Karamanoğlu Mehmetbey University.
Prof. Dr. Murat Kanbur, Erciyes University.
Prof. Dr. Murat Yıldırım, Kırıkkale University.
Prof. Dr. Mustafa Ardıç, Aksaray University.
Prof. Dr. Mustafa Karakaya, Selçuk University.
Prof. Dr. Mustafa Nizamlıoğlu, Gelişim University.
Prof. Dr. Mustafa Numan Bucak, Selçuk University.
Prof. Dr. Mustafa Yıldız, Afyon Kocatepe University.
Prof. Dr. Müjgan Özdemir Erdoğan, Afyonkarahisar Health Sciences University.
Prof. Dr. Naim Deniz Ayaz, Kırıkkale University.
Prof. Dr. Nalan Bayşu Sözbilir, Afyon Kocatepe University.
Prof. Dr. Nebahat Bilge Oral, Kafkas University.
Prof. Dr. Neşe Demirtürk, Afyonkarahisar Health Sciences University.
Prof. Dr. Nihad Fezjic, University of Sarajevo.
Prof. Dr. Niraldo Paulino, Universidade Bandeirante de São Paulo (UNIBAN).
Prof. Dr. Oğuz Sarımehmetoğlu, Ankara University.
Prof. Dr. Oscar Herrera Calderon, Universidad Nacional Mayor de San Marcos.
Prof. Dr. Osman Sağdıç, Yildiz Technical University.
Prof. Dr. Ömer Çetin, İstanbul University Cerrahpaşa.
Prof. Dr. Otilia Bobis, USAMV Cluj-Napoca.
Prof. Dr. Özal Özcan, Afyonkarahisar Health Sciences University.
Prof. Dr. Özer Ergün, İstanbul Sağlık ve Teknoloji University.
Prof. Dr. Özlem Küplülü, Ankara University.
Prof. Dr. Özgür Kaynar, Kastamonu Univesity.
Prof. Dr. Recep Keşli, Selçuk University.
Prof. Dr. Sefa Çelik, Afyonkarahisar Health Sciences University.
Prof. Dr. Selim Sekkin, Aydın Adnan Menderes University.
Prof. Dr. Semra Kayaardı, Celal Bayar University.
Prof. Dr. Sergey Pozyabin, President of Moscow State Academy of Veterinary Medicine and Biotechnology, Russia.
Prof. Dr. Seyfullah Haliloğlu, Selçuk University.
Prof. Dr. Sinan İnce, Afyon Kocatepe University.
Prof. Dr. Silvia Patruica, Banat University of Agronomical Sciences and Veterinary Medicine.
Prof. Dr. Sokol Duro, Agricultural University of Tirana.
Prof. Dr. Tamer Dodurka, İstanbul Rumeli University.
Prof. Dr. Tarık Haluk Çelik, Ankara University.
Prof. Dr. Tülay Büyükoğlu, Burdur Mehmet Akif Ersoy University.
Prof. Dr. Ufuk Tansel Şireli, Ankara University.
Prof. Dr. Uğur Günşen, Bandırma Onyedi Eylül University.
Prof. Dr. Ümit Gürbüz, Selçuk University.
Prof. Dr. Vassya Bankova, Bulgarian Academy of Sciences.
Prof. Dr. Vedat Sağmalıgil, Near East University.
Prof. Dr. Yahya Kuyucuoğlu, Selçuk University.

Prof. Dr. Yakup Can Sancak, Van Yuzuncu Yil University.
Prof. Dr. Yavuz Osman Birdane, Afyon Kocatepe University.
Prof. Dr. Zafer Gönülalan, Erciyes University / Yozgat Bozok University.
Prof. Dr. Zehra Hajrulai-Musliu, Ss. Cyril and Methodius University in Skopje.
Prof. Dr. Zeki Gürler, Afyon Kocatepe University.
Assoc. Prof. Dr. Andrea Armani, Pisa University.
Assoc. Prof. Dr. Ali Evren Haydardedeoğlu, Aksaray University.
Assoc. Prof. Dr. Ayşe Güneş Bayır, Bezmialem Vakıf University.
Assoc. Prof. Dr. Begüm Yurdakök Dikmen, Ankara University.
Assoc. Prof. Dr. Behnam Rostami, University of Zanjan.
Assoc. Prof. Dr. Bekir Oğuz, Van Yuzuncu Yil University.
Assoc. Prof. Dr. Beyza Ulusoy, Near East University.
Assoc. Prof. Dr. Bojan Blagojevic, University of Novi Sad.
Assoc. Prof. Dr. Camelia Tulcan, Banat University of Agromical Sciences and Veterinary Medicine.
Assoc. Prof. Dr. Damla Arslan Acaröz, Afyon Kocatepe University.
Assoc. Prof. Dr. Didem Pekmezci, Ondokuz Mayıs University.
Assoc. Prof. Dr. Dilek Dülger, Karabük University.
Assoc. Prof. Dr. Deyan Stratev, Trakia University.
Assoc. Prof. Dr. Dinko Dinkov, Trakia University.
Assoc. Prof. Dr. Doğukan Özen, Ankara University.
Assoc. Prof. Dr. Dzmitry Barysavets, Institute of Experimental Veterinary Medicine named of S.N. Vyshelessky.
Assoc. Prof. Dr. Elena Stepanova, Institute of Experimental Veterinary Medicine named of S.N. Vyshelessky.
Assoc. Prof. Dr. Ekin Emre Erkılıç, Kafkas University.
Assoc. Prof. Dr. Eray Alçığır, Kırıkkale University.
Assoc. Prof. Dr. Esra Özgül, Afyonkarahisar Health Sciences University.
Assoc. Prof. Dr. Gamze Çakmak, Van Yuzuncu Yil University.
Assoc. Prof. Dr. Güzin Camkerten, Aksaray University.
Assoc. Prof. Dr. Halil Yalçın, Burdur Mehmet Akif Ersoy University.
Assoc. Prof. Dr. Hüsamettin Ekici, Kırıkkale University.
Assoc. Prof. Dr. İbrahim Küçükaslan, Dicle University.
Assoc. Prof. Dr. İlhan Aydın, Republic of Turkey Ministry of Agriculture and Forestry General Directorate of Agricultural Research and Policies.
Assoc. Prof. Dr. İsmail Küçükkurt, Afyon Kocatepe University.
Assoc. Prof. Dr. Levent Altıntaş, Ankara University.
Assoc. Prof. Dr. Leyla Mis, Van Yuzuncu Yil University.
Assoc. Prof. Dr. Mehmet Cengiz, Atatürk University.
Assoc. Prof. Dr. Mehmet Nuri Konya, Afyonkarahisar Health Sciences University.
Assoc. Prof. Dr. Mehmet Özkan Timurkan, Atatürk University.
Assoc. Prof. Dr. Mehmet Sağlam, Aksaray University.
Assoc. Prof. Dr. Meysam Sharifdini, Guilan University of Medical Sciences.
Assoc. Prof. Dr. Mian Muhammed Awais, Bahauddin Zakariya University.
Assoc. Prof. Dr. Mokhtar Benhanifia, University Mustapha Stambouli.
Assoc. Prof. Dr. Mustafa Yipel, Hatay Mustafa Kemal University.
Assoc. Prof. Dr. Mahir Murat Cengiz, Atatürk Üniversity.
Assoc. Prof. Dr. Nizamettin Koçkara, Erzincan Binali Yıldırım University.

Assoc. Prof. Dr. Nuray Varol, Gazi University.
Assoc. Prof. Dr. Ömer Hazman, Afyon Kocatepe University.
Assoc. Prof. Dr. Özge Sızmaz, Ankara University.
Assoc. Prof. Dr. Özgül Küçükaslan, Dicle University.
Assoc. Prof. Dr. Özgür Albuz, Dr. Abdurrahman Yurtaslan Ankara Onkoloji Eğitim ve Araştırma Hastanesi
Assoc. Prof. Dr. Özgür Genç Şen, Van Yuzuncu Yil University.
Assoc. Prof. Dr. Pasupuleti Visweswara Rao, Universiti Malaysia Sabah.
Assoc. Prof. Recep Kara, Afyon Kocatepe University.
Assoc. Prof. Dr. Saad Mukhlif Mhadi, Anbar University.
Assoc. Prof. Dr. Saadet Belhan, Van Yuzuncu Yil University.
Assoc. Prof. Dr. Sefa Küçükler, Atatürk University.
Assoc. Prof. Dr. Segueni Narimane, University of Constantine.
Assoc. Prof. Dr. Seyda Cengiz, Atatürk University.
Assoc. Prof. Dr. Seyda Şahin, Sivas Cumhuriyet University.
Assoc. Prof. Dr. Tanveer Hussain, Virtual University of Pakistan.
Assoc. Prof. Dr. Turhan Turan, Sivas Cumhuriyet University.
Assoc. Prof. Dr. Ulaş Acaröz, Afyon Kocatepe University.
Assoc. Prof. Dr. Yasin Demiraslan, Burdur Mehmet Akif Ersoy University.
Assoc. Prof. Dr. Zafer Pekmezci, Ondokuz Mayıs University.
Assoc. Prof. Dr. Zeynep Karapınar, Balıkesir University.
Assist Prof. Dr. Aamir Iqbal, Gomal University.
Assist Prof. Dr. Ahmad Ali, University of Mumbai.
Assist Prof. Dr. Ali Ekber Ün, Ankara Yıldırım Beyazıt University.
Assist Prof. Dr. Ali Soleimanzadeh, Urmia University.
Assist Prof. Dr. Ali Emrah Bıyıklı, Alanya Alaaddin Keykubat University.
Assist. Prof. Dr. Arash Pourgholaminejad, Guilan University of Medical Sciences.
Assist. Prof. Dr. Ashwaq Jabbar, University of Thiqar.
Assist. Prof. Dr. Asim Faraz, Bahauddin Zakariya University.
Assist. Prof. Dr. Azim Şimşek, Isparta Uygulamalı Bilimler University.
Assist. Prof. Dr. Burcu Güçyetmez Topal, Afyonkarahisar Health Sciences University.
Assist. Prof. Dr. Olgun Topal, Afyonkarahisar Health Sciences University.
Assist. Prof. Dr. Abdur Rahman Sial, University of Veterinary &Animal Sciences, Lahore-Pakistan.
Assist. Prof. Dr. Ali Timuçin Atayoğlu, Istanbul Medipol University.
Assist. Prof. Dr. Bora Özarslan, Kırıkkale University.
Assist. Prof. Dr. Burcu İrem Omurtag Korkmaz, Marmara University.
Assist. Prof. Dr. Cafer Yıldırım, Eskişehir Osmangazi University.
Assist. Prof. Dr. Cihat Öztürk, Kırşehir Ahi Evran University.
Assist. Prof. Dr. Çiğdem Ürkü Atanasov, İstanbul Univetrsity.
Assist. Prof. Dr. Eren Kuter, Burdur Mehmet Akif Ersoy University.
Assist. Prof. Dr. Engin Berber, University of Tennessee.
Assist. Prof. Dr. Ejaz Ahmad, Bahauddin Zakariya University.
Assist. Prof. Dr. Ezgi Topbaş Bıyıklı, Alanya Alaaddin Keykubat University.
Assist. Prof. Dr. Fahriye Zemheri Navruz, Bartın University.
Assist. Prof. Dr. Firas Alalı, Kerbala University.
Assist. Prof. Dr. Fatih Ramazan İstanbullugil, Kyrgyz-Turkish Manas University.
Assist. Prof. Dr. Fulya Altınok-Yipel, Hatay Mustafa Kemal University

Assist. Prof. Dr. Gözde Ede, Burdur Mehmet Akif Ersoy University.
Assist. Prof. Dr. Gültekin Bilgin, Bezmialem Vakıf University.
Assist. Prof. Dr. Hamide Nur Çevik Özdemir, Afyonkarahisar Health Sciences University.
Assist. Prof. Dr. Hande Sultan Şahiner, Aydın Adnan Menderes University.
Assist. Prof. Dr. Hasan Hüseyin Demirel, Afyon Kocatepe University.
Assist. Prof. Dr. Hasan Ufuk Çelebioğlu, Bartın University.
Assist. Prof. Dr. Hayri Demirbaş, Afyonkarahisar Health Sciences University.
Assist. Prof. Dr. İbrahim Durmuş, Afyon Kocatepe University.
Assist. Prof. Dr. İbrahim Sözdutmaz, Erciyes University.
Assist. Prof. Dr. Kamala Badalova, Azerbaijan Medical University.
Assist. Prof. Dr. Mehmet Cemal Adıgüzel, Atatürk University.
Assist. Prof. Dr. Mentor Alishani, University of Prishtina.
Assist. Prof. Dr. Merve Keskin, Bilecik Şeyh Edebali University.
Assist. Prof. Dr. Muharrem Satılmış, Bakırçay University.
Assist. Prof. Dr. Muhammet Yasin Tekeli, Erciyet University.
Assist. Prof. Dr. Muhsin Öztürk, İstanbul Sağlık ve Teknoloji University..
Assist. Prof. Dr. Murat Yeşil, Afyonkarahisar Health Sciences University.
Assist. Prof. Dr. Mustafa Özbek, Van Yuzuncu Yil University.
Assist. Prof. Dr. Mustafa Eser, Anadolu University.
Assist. Prof. Dr. Ömer Çakmak, Istanbul Esenyurt University.
Assist. Prof. Dr. Pakize Özyürek, Afyonkarahisar Health Sciences University.
Assist. Prof. Dr. Rabia Mehtap Tuncay, Van Yuzuncu Yil University.
Assist. Prof. Dr. Risto Uzunov, Ss. Cyril and Methodius University in Skopje.
Assist. Prof. Dr. Rüştü Taştan, Kocaeli University.
Assist. Prof. Dr. Selahattin Konak, Afyon Kocatepe University.
Assist. Prof. Dr. Selma İnfal Kesim, Selçuk University.
Assist. Prof. Dr. Shah Nawaz Sial, Riphah College of Veterinary Sciences.
Assist. Prof. Dr. Şaban Keskin, Bilecik Şeyh Edebali University.
Assist. Prof. Dr. Sibel Doğan, Medipol University.
Assist. Prof. Dr. Şükrü Önalan, Van Yuzuncu Yil University.
Assist. Prof. Dr. Mahendra Singh Tomar, Sri Venkateswara Veterinary University.
Assist. Prof. Dr. Tuncer Çakmak, Van Yuzuncu Yil University.
Dr. Aleksandar Joksimović, University of Montenegro.
Dr. Ali Soyucok, Burdur Mehmet Akif Ersoy University.
Dr. Alice Giusti, Pisa University.
Dr. Anna Kurek-Gorecka, Medical University of Silesia in Katowice.
Dr. Aytaç Ünsal Adaca, Ankara University.
Dr. Cemil Şahiner, Aydın Adnan Menderes University.
Dr. Dilara Fayetörbay Kaynar, Kastamonu University.
Dr. Dmitry Morozov, Vitebsk Stata Academy of Veterinary Medicine/ FAO National Coordinator of Belarus
Dr. Erdem Danyer, Republic of Turkey Ministry of Agriculture and Forestry, Veterinary Control Central Research Institute.
Dr. Esin Keleş Arslan, Republic of Turkey Ministry of Agriculture and Forestry, International Center For Livestock Research and Traning.
Dr. Fahriye Kan, Afyon Kocatepe University, Turkey, Member of Committee.

Dr. Halil Ozancan Arslan, Republic of Turkey Ministry of Agriculture and Forestry, International Center For Livestock Research and Traning.
Dr. Krešimir Matanović, University of Zagreb.
Dr. Lara Tinacci, Pisa University.
Dr. Mehmet Akalan, Afyon Kocatepe University.
Dr. Ömer Barış İnce, Pamukkale University.
Dr. Pelin Koçak Kızanlık, Aydın Adnan Menderes University.
Dr. Sedat Sevin, Ankara University.
Dr. Seda Ekici, Republic of Turkey Ministry of Agriculture and Forestry, Veterinary Control Central Research Institute.
Dr. Serol Korkmaz, Republic of Turkey Ministry of Agriculture and Forestry, Pendik Veterinary Control Institute.
Dr. Stefan Stangaciu, Romanian Apitherapy Society.
Dr. Tohid Rezaei Topraggaleh, Tabriz University of Medical Sciences.
Dr. Wassan Nori, Mustansiriyah University.

CONTENTS

PROCEEDINGS BOOK

Second International Congress on Biological and Health Sciences
ONLINE 24-25-26-27 FEBRUARY 2022

Comparison of Different Virus Sampling Technics in a Bovine Coronavirus Model

Gizem Aytogu[1], Berfin Kadiroğlu[1] Kadir Yesilbag [1]

[1]Department of Virology, Bursa Uludag University, Faculty of Veterinary Medicine, 16059, Bursa, Turkey

Corresponding author: kyesilbag@uludag.edu.tr

Abstract:
The recent pandemic and the attention of researches on the effects of synthetic or natural products on protection or control of diseases, have increased investigations of the antiviral effects of various compounds. But pre-analytical conditions like choosing sampling area, material to be used, storage conditions or mediums can affect the performance of a laboratory analyses. The aim of this study was to compare 14 different sampling techniques to determine the sampling model suitable for antiviral efficacy trials in a Bovine Coronavirus (BCoV) model. We compared collection methods of; aspirating whole drop / small droplets of virus suspensions or wetted smeared dry virus contaminated area, swab sampling of smeared virus contaminated dry area or virus droplets by using pre-wetted or dry rayon swab material, recovering virus particles from cellulose filter paper. We also compared BCoV titers at 2nd and 12th hours after inicial of incubation at room temperature for each condition. The highest virus titers were obtained by aspiration of 0.2, 2 and 5ml virus suspensions with same virus concentrations. Recovered virus titers reached 75%, 71% and 71%, respectively compared to the control virus titer value at second hour. Lowest values determined in the swab sampling by pre-wetting (44-52%). After the virus containing speciemens was kept at room temperature for 12 hours, the highest titers (compared to the virus control titers) were obtained in the virus particles housed in 5 ml liquid (83%) and the lowest titers were obtained in swab sampling of the virus particles leaved in a dry environment (25%). According to the results obtained in this study, it is evaluated that the preference of the aspiration method will contribute to obtaining the maximum virus titer in the studies to be conducted.

Keywords: aspiration, bovine coronavirus, cellulose filter paper sampling methods, swab, virus titration.

1. Introduction

In the light of today's epidemics/pandemics there is need for an effective disinfectant or antiviral as a control/protection method. In the last decade, researches on the effects of synthetic or natural products in this direction have gained attention. Some have been accelerated, and some have been commercialized, due to the search created by the novel coronavirus disease virus (SARS-CoV-2) pandemic. However, literature researchs show that most of the studies have been performed on animal models. Looking at the rest, it is seen that there is no standard accepted method. The chosen materials at detection procedure affects the analyse results. The use of nucleic acid stabilization mix instead of virus transport medium when swab sampling has been shown to improve the sensitivity of COVID-19 tests 1. As shown in mentioned study that products that can be used during sampling can affect the correct positivity, it is inevitable that the sampling method or the experimental protocol will affect the results to be obtained. Therefore, in this study it was aimed to determinate the most appropriate sampling model that can be selected in antiviral efficacy trials, which will give the highest recovery of virus particules.

2. Material and methods

2.1. Viruses and Cell lines

BCoV, strain Mebus which is a reference strain for BCoV classified in the genus of Betacoronavirus including SARS-CoV-2 was used as the virus in this study. The viral stock is used from the stock of Bursa Uludag University Faculty of Veterinary Medicine, Virology Department, which has been stored at −80 ◦C. The titer (50% Tissue Culture Infectivity Dose, TCID50) of the virus was log10 10 6.25 / 0.1 ml for main stock.

MDBK cell line were used for the titration assays as well as for propagation of the virus. Cells were maintained in Dulbecco's Modified Eagles Medium (DMEM) supplemented with heat treated 10 % fetal calf serum (FCS), 100 UI/mL Penicillin/Streptomycin and 250 µL/mL Amphotericin B solution. All cell cultures were grown at 37 °C, in 5% CO2 athmosphere.

2.2. Sampling methods

In this study, 14 different experimental conditions other than control well was performed for comparison of the re-collection of the virus suspensions, which has same amount of virus titer. In order to evaluate the recovery of BCoV at different times (2nd hour and 12th hour) each experimental conditions were prepared as doubled. The experiment prepared for each condition was repeated 3 times. The studied conditions are indicated in the Table-1.

Before starting to the experiments, 1:5 diluation of 100 TCID50 (106.25) virus suspension prepared in DMEM (without FDS or any supplement/protector). Samples taken from this diluent at 0, 2nd and 12th hour was applied to virus titration assay as internal control (IC) for each analyses.

Experiment A: 0.2 ml virus suspension released in to the perti dishes as a whole drop. After incubation at room temperature for 2 and 12 hours seperately, 1.8ml DMEM was added on the suspension and collected from the petri dish. Samples taken at this point used in virus titration assays.

Experiment B: 0.2 ml virus suspension released in to the perti dishes and spreaded as smear on the surface of petri dish. This inoculation incubated at room temperature for 2 and 12 hours seperately, 1.8 ml DMEM was added on the suspension and collected from the petri dish. Samples taken at this point used in virus titration assays.

Experiment C: 0.2 ml virus suspension droped on to the 3x3cm cut cellulose filter paper and incubated at room temperature for 2 and 12 hours seperately. At the end of the incubation period papers placed into 1.8 ml DMEM and vortexed 5 times for 10 seconds. Samples taken at this point used in virus titration assays.

Experiment D: Total of 0.2 ml virus suspension released in to the perti dishes as 10 small amount droplets into petri dish. This inoculation incubated at room temperature for 2 and 12 hours seperately, 1.8 ml DMEM was added on the suspension and collected from the petri dish. Samples taken at this point used in virus titration assays.

Experiment E: 2 ml virus suspension released in to the perti dishes as a whole drop. After incubation at room temperature for 2 and 12 hours seperately samples taken at this point used in virus titration assays.

Experiment F: 5 ml virus suspension released in to the perti dishes as a whole drop. After incubation at room temperature for 2 and 12 hours seperately samples taken at this point used in virus titration assays.

Experiment G: : 0.2 ml virus suspension released in to the perti dishes and spreaded as smear on the surface of petri dish. After incubation at room temperature for 2 and 12 hours seperately, swab samples were taken by dry swab material, placed into 1.8 ml DMEM and incubated for 30 min. Samples taken after vortexing the swab was used in virus titration assays.

Experiment H: 0.2 ml virus suspension released in to the perti dishes and spreaded as smear on the surface of petri dish. After incubation at room temperature for 2 and 12 hours seperately, swab samples were taken by dry swab material, placed into 1.8 ml DMEM. Collected samples vortexed 5 times for 10 sec. and virus titration assays was applied.

Experiment I: 0.2 ml virus suspension released in to the perti dishes and spreaded as smear on the surface of petri dish. After incubation at room temperature for 2 and 12 hours seperately, swab samples were taken by wettened swab material, placed into 1.8 ml DMEM and incubated for 30 min. Samples taken after vortexing the swab used in virus titration assays.

Experiment J: 0.2 ml virus suspension released in to the perti dishes and spreaded as smear on the surface of petri dish. After incubation at room temperature for 2 and 12 hours seperately, swab samples were taken by wettened swab material, placed into 1.8 ml DMEM. Collected samples vortexed 5 times for 10 sec. and virus titration assays was applied.

Experiment K: Total of 0.2 ml virus suspension released in to the perti dishes as 20 small amount droplets into petri dish. This inoculation incubated at room temperature for 2 and 12 hours, collected by a dry swab and left in 1.8 ml DMEM for 30 min. at +4 °C. Swab material vortexed 5 times for 10 sec. and virus titration assays was applied.

Experiment L: Total of 0.2 ml virus suspension released in to the perti dishes as 20 small amount droplets into petri dish. This inoculation incubated at room temperature for 2 and 12 hours, collected by a dry swab and left in 1.8 ml DMEM and vortexed five times for 10 sec. and subjected to virus titration assays.

Experiment M: Total of 0.2 ml virus suspension released in to the perti dishes as 20 small amount droplets into petri dish. This inoculation incubated at room temperature for 2 and 12 hours, collected by a pre-wetted swab and left in 1.8 ml DMEM for 30 min. at +4 °C. Swab material vortexed 5 times for 10 sec. and virus titration assays was applied.

Experiment N: Total of 0.2 ml virus suspension released in to the perti dishes as 20 small amount droplets into petri dish. This inoculation incubated at room temperature for 2 and 12 hours, collected by a prewetted swab

and left in 1.8 ml DMEM and vortexed five times for 10 sec. Collected samples vortexed 5 times for 10 sec. and virus titration assays was applied.

2.3. Virus titration assay

In all the experimental conditions after the determined incubation periods, virus titration tests were immediately applied by infectivity assay in cell culture. Ten-fold serial dilutions of the samples were made in DMEM. One hundred µl of virus dilution placed into 4 replicate wells of 96-well tissue culture plates. Virus diluent mixed with an equal amount of cell suspension (2×10^5 cells/mL) and incubated at 37 °C, 5% CO_2 atmosphere. Cells were observed daily for 7 days and the virus titers ($TCID_{50}$) were determined according to the Spearman-Kârber method.

3. Results

BCoV Mebus strains were titrated for two different hours to obtain $TCID_{50}$ in simple format. Titration assay applied for 14 different sampling conditions with three repetitions. Each repetitive sample of one condition were titrated seperately and simultaneously withought freezing or maintaining at any other conditions. Results are summarized in Table 1. For the all experiment conditions, the titer values of all repeated samples were similar to each other, with a difference of only one well detectable cytopathogenic effect (CPE) of virus growth on a 96-well plate. Though, for the evaluation of the results, it was preferred to take the average of the titer values of the three samples repeated for each condition. The virus in control well analyzed in both experiments had highest titers, around 4,75 and 4 log 10 TCID50/ml. The titers calculated for both time periods and each condition were differed. According to the three replicative assays virus titer results values ranged between 0,75 -3,75 log 10 separately, apart from the control results.

For second hour evaluations, when values were compared, titer values obtained from the experimental assays were 75-44% similar to the titer values of their control. But those values were decreased for 12th hour titrations. According to titer values comparison, experiment values mostly similar with 70% and 25% lowest similarity was seen in 12th hour. The method in which virus particles collected maximum in the second hour was the condition that 0.2 mL virus suspension was incubated as a whole drop. The following highest concentration of virus particles collection method was the experimental setup in which the virus suspensions at higher volumes (2 and 5 mL) were kept as a single drop. It was observed that the lowest titer obtained in the condition where the small drops collected with wet swab and kept in the medium for 30 min. When the averages of all the titer values obtained in the dry and wet swab studies were compared, it was seen that there was a difference of 0.1 log 10 between them. It was observed that keeping the swab stick in the medium for half an hour increased the detectable virus titer values obtained in all swab uses, except collection of smeared virus particles at 12th hour.

Similarly, in the 12th hour comparisons, it was observed that the least titer losses were obtained in conditions where the virus particles were kept in a liquid as a whole droplet, especially 5 mL droplet (17%). It was seen that the highest loss (75%) was obtained in the collection with dry swab of virus particles left on the surface

by the smear method and waited in medium. In all experimental conditions the least titer loss when the 2nd hour and 12th hour titer values compared was detected when the virus particles kept in the 5ml single drop.

Table Ledgends and Footnotes

Table 1. Average of titration values obtained from different experimental design.

	Experiment Design¡													
Titration	**IC**	**A**	**B**	**C**	**D**	**E**	**F**	**G**	**H**	**I**	**J**	**K**	**L**	**M**	**N**
2nd h*	**4.8**	**3.6**	**2.9**	**2.5**	**3.4**	**3.4**	**3.4**	**2.8**	**2.4**	**2.3**	**2.2**	**2.5**	**3.0**	**2.1**	**2.5**
12th h*	**4**	**2.8**	**2.5**	**1.8**	**2.4**	**2.3**	**3.3**	**1**	**1.5**	**1.1**	**1.8**	**1.5**	**2.4**	**1.3**	**2**

IC: Internal control, A:Whole drop (200 µl), B: Smear (200 µl), C: Porrous paper /fabric (200 µl), D: Droplets (20 µl x10), E: Whole drop (2 ml), F: Whole drop (5 ml), G: Smear (200 µl)+dry swab + incubation 30 min. in media, H: Smear (200 µl) +dry swab, I: Smear (200 µl)+wet swab+ incubation 30 min. in media, J: Smear (200 µl)+wet swab, K: Droplets (20 µl x10)+dry swab+ incubation 30 min. in media, L: Droplets (20 µl x10)+dry swab, M: Droplets (20 µl x10)+wet swab+ incubation 30 min. in media, N: Droplets (20 µl x10)+ wet swab

*: Average of 2nd and 12th hour $TCID_{50}$ 10^{x} titer values ¡: All samples (except E and F samples) were collected in 2 ml dmem and then vortexed. E and F samples directly collected.

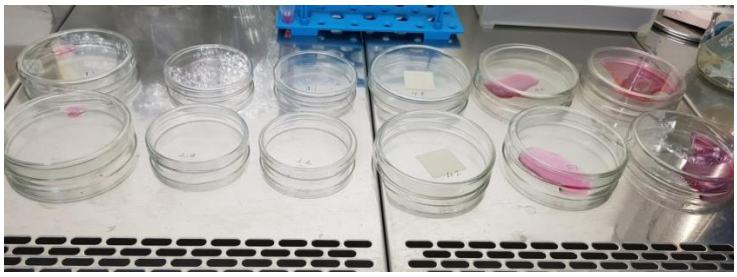

Figure 1. The experimental setup of petri dishes incubated at room temperature

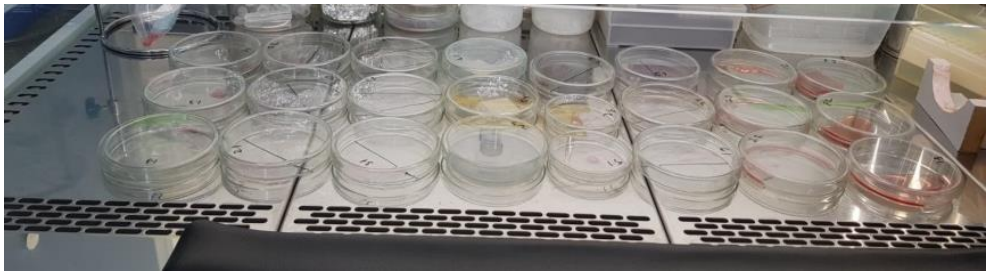

Figure 2. The experiment was repeated 3 times under the same conditions

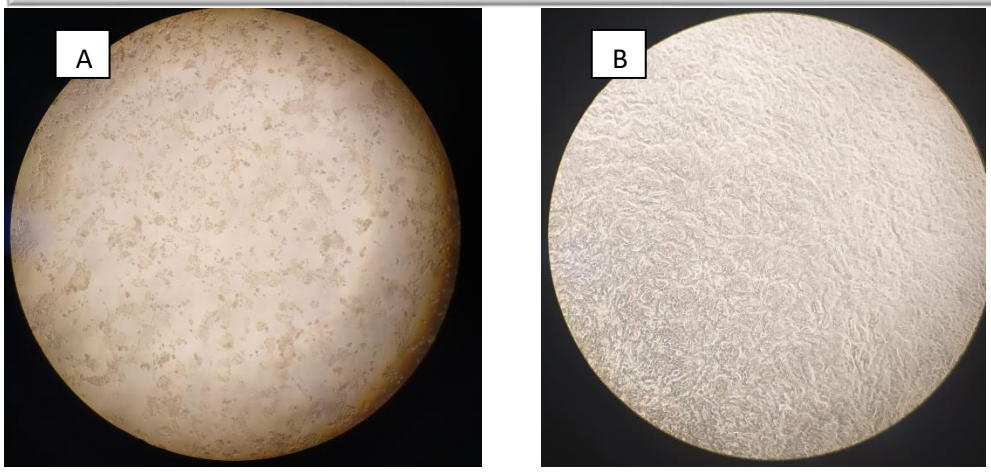

Figure 3. Cell image on day 3 under an invert microscope in 96-well plates, A: Coronavirus infected MDBK cell, B: MDBK cell control

4. Discussion

We reviewed the literatures and lack of measurements on this topic led us to the need to design to determine the best sampling methods for an antiviral efficinecy investigation whether it inqluides a liquid based material or dry surfaced equipment. Though direct liquid sampling, virus contaminated solid material or swab sampling methods were investigated. Swab sampling assays are usually most preferred and recommended procedure for most viral disease as SARS-CoV-2 (H et al., 2020; Kahamba et al., 2020). For this reason, 8 of the 14 different methods used in this study implemented for swab sampling. In a study examining the effect of three different types of nylon swab on SARS-CoV-2 sampling, swab composition and structure has been shown to have a significant impact on the amount of fluid sample adsorbed, volume of fluid sample released into buffer(Kahamba et al., 2020). Though differences had been related to viral capture capacity, extraction capacity and recovery efficiency of collected samples. On the other hand, in a study which utilizes the effects of 6 different (cotton, polyester, synthetic flocked or fiber) swabs and transport mediums (DMEM, PBS, 100 % ethanol, 0.9 % normal saline and VTM) for the molecular detection of SARS-CoV-2, it was found that there was no meaningful difference for the collection and detection of SARS-CoV-2(Garnett et al., 2020). A study showed that RNA recovery of norovirus with the use of pre-wetted cotton swab ranged from 7 -52% (Scherer et al., 2009). In another study which compares virus recovery from fomites by different sampling methods it was concluded that the most effective method was recovery from nonporous fomites using prewetted polyester-tripped swabs (Julian et al., 2011). In our study, recovery was more successful in the use of dry swab (Experiment G-H-K-L). And the recovering range of virus titers with wet and dry swab were found to be 50-63% and 44-52%, respectively, compared to the control virus titer using DMEM as transport medium at second hour. Although only rayon swab material has been tested, the results show that the dry swab material at the time of sampling gives higher virus titer. This situation can be taken into consideration in the selection of the swab materials that is presented as a ready kit in the transport medium or contained separately from the medium. When collecting swab samples, the sample may be provided from a moist (liquid applied surface, cell culture supernatant ex.) or dry (fabric, mask, gas/ light treated surfaces) surface. Due to the high virus titers obtained with dry swab material in this study, when the titers of the sample taken from a dry surface and the wet droplet surface were compared, re obtained titre vallues were ranged between 50-58% and 52-63%, respectively. Since those values are at about similar rates, it can be said that the swab-related sampling area/surface may not cause differences.

In a study which investigates pre-analytic steps effects on molecular assay, it was shown that there was no significant difference between woven or flocked swab sampling(Ferguson et al., 2017). In our study not a woven swab was used but a cellulose filter paper preferred. And virus titers reached up to 52% values, similar as swab sampling. In a more comprehensive methodology study, Spyridaki et. al. showed that virus detection rate changed by 88% (wash), 79% (aspirate), 77% (swab) and 74% (brush) (IS et al., 2009). Those values were compatible with our findings. According to all sampling conditions we found that the most recovery rates was reached by aspirating the whole fluid samples (ExperimentsA, D, E, F). For 0.2, 2 and 5ml virus suspensions with same virus concentrations virus titers reached 75%, 71% and 71%, respectively. Therefore, choosing sampling with aspiration method may increase the chance of viral detection rates. In cases where the viral load is low, preference of high sensitivite techniques may increase the chance of success with swab sampling.

Survival rates of viruses in enviromental conditions like laboratories or hospital is another area of interest for researchers. Lai et. al. reported the highest survival time of Severe Acute Respiratory Syndrome Coronavirus in stool samples with virus transport medium and showed that virus can remain alive in respiratory specimens like nasopharyngeal aspirate, throat and nasal swab, and viral transport medium for more than 7 days at room temperature(MY et al., 2005). In our study highest titers were reached at aspiration of whole drop virus suspensions both at 2 and 12 hours of inoculation at room temperature. It has been observed that the opposite of this situation is in the conditions where the virus particles leaved in a dry environment, asthe lowest virus titer was obtained in the condition sampled through swab sampling after being spread on the petri dish and kept at room temperature for 12 hours (25-45%). But it was also realised that incubation of the swab material in medium does not encreased the recovery change of swab samplig of dry surfaces. According to the data obtained from this study, it was seen that in the samples to be taken from the dry surface at 12th hour, aspiration of the virus material from the exposed surface provides a higher virus titer (63%).

5. Conclusion

There are some studies examining the recovery rate of viruses or their interactions on different surfaces or compounds. However, there are few methodology studies to obtain more sensitive results while performing those studies. Choosing the methods to obtain the maximum virus titer in experimental or antiviral efficiency studies will prevent false negative results obtained from samples where low virus titers are examined. In this study, the differences between collecting viruses from a small surface glass area are discussed. And it was determined that aspiration method gave higher results in virus recovery compared to other sampling methods. Preferring this method may provide more sensitive results in areas with low virus concentrations or in experiments to be conducted for efficacy analysis.

6. References

Ferguson J, Krevolin M, Lewinski RA, Marlowe EM. Comparison of Two Swabs (Woven and Flocked) used for the Collection of Endocervical Specimens for Chlamydia trachomatis and Neisseria gonorrhoeae testing on the cobas® 4800 System 2017; In:, ECCMID 2017, (ESCMID 2017)

Garnett L, Bello A, Tran KN, Audet J, Leung A, Schiffman Z, Griffin BD, Tailor N, Kobasa D, Strong JE. Comparison analysis of different swabs and transport mediums suitable for SARS-CoV-2 testing following shortages. Journal of Virological Methods. 2020; 285, 113947

Péré H, Podglajen I, Wack M, Flamarion E, Mirault T, Goudot G, Hauw-Berlemont C, Le L, Caudron E, Carrabin S, Rodary J, Ribeyre T, Bélec L, Veyer D, Fewer S. Nasal Swab Sampling for SARS-CoV-2: a Convenient Alternative in Times of Nasopharyngeal Swab Shortage. Journal of clinical microbiology. 2020; 58 (J Clin

Microbiol).

Spyridaki IS, Christodoulou I, de Beer L, Hovland V, Kurowski M, Olszewska-Ziaber A, Carlsen K-H, Lødrup-Carlsen K, van Drunen CM, Kowalski ML, Molenkamp R, Papadopoulos NG. Comparison of four nasal sampling methods for the detection of viral pathogens by RT-PCR-A GA(2)LEN project. Journal of virological methods. 2009; 156, 102–106 (J Virol Methods).

Julian TR, Tamayo FJ, Leckie JO, Boehm AB. Comparison of surface sampling methods for virus recovery from fomites. Applied and Environmental Microbiology. 2011; 77, 6918–6925.

Kahamba TR, Noble L, Stevens W, Scott L. Comparison of three nasopharyngeal swab types and the impact of physiochemical properties for optimal SARS-CoV-2 detection. medRxiv. 2020; 2020.10.21.20206078 (Cold Spring Harbor Laboratory Press).

MY L, PK C, WW L. Survival of severe acute respiratory syndrome coronavirus. Clinical Infectious Diseases. 2005; 41 (Clin Infect Dis).

Scherer K, Mäde D, Ellerbroek L, Schulenburg J, Johne R, Klein G. Application of a Swab Sampling Method for the Detection of Norovirus and Rotavirus on Artificially Contaminated Food and Environmental Surfaces. Food and Environmental Virology 2009; 1:1, 1, 42–49 (Springer).

Second International Congress on Biological and Health Sciences
ONLINE 24-25-26-27 FEBRUARY 2022

Investigation of the Mechanism of α-Tocopherol in Reducing Lipid Accumulation in 3T3-L1 Adipocyte via CTRP3 gene Expression

Meliha KOLDEMİR GÜNDÜZ[1], Güllü KAYMAK[2], Ertan KANBUR[3]

[1]Kutahya Health Sciences University, Faculty of Engineering and Natural Sciences, Department of Basic Sciences of Engineering, Kutahya, TURKEY

[2]Kutahya Health Sciences University, Training and Research Center, Kutahya, TURKEY

[3]Bursa Uludağ University, Faculty of Medicine, Department of Immunology, Bursa, TURKEY

Corresponding author: meliha.koldemirgunduz@ksbu.edu.tr

Abstract:
Obesity is a complicated medical condition characterized by excessive fat deposition in the body as a result of excessive food consumption and insufficient physical exercise. Obesity, which develops as a result of excessive fat accumulation, is a worldwide pandemic social problem. Adipose tissue is known as an endocrine organ and a regulator of energy homeostasis. Recently, it has been accepted that changes in the biological function of adipose tissue rather than changes in adipose tissue mass play an important role in physiological and pathological processes. The aim of this study is to investigate the role of α-tocopherol in reducing fat accumulation in 3T3-L1 adipocytes via gene expression of a new adipocytokine, CTRP3. *In vitro*, 3T3-L1 fibroblast cells (ATCC® CL - 173) were differentiated into adipocyte cells. Fat accumulation in 3T3-L1 adipocyte cells was detected by oil red-o staining method. As a result of the application of different doses of α-tocopherol to 3T3-L1 adipocytes, the cytotoxic activity on adipocytes was determined by MTT method. CTPR3 and PPAR-γ gene expressions were determined with qPCR. The IC_{50} value was found to be 104 µg/ml after 48 hours of α-tocopherol administration to 3T3-L1 adipocytes. As a result of the application of 50, 104 and 200 µg/ml α-tocopherol to 3T3-L1 adipocytes, the fat accumulation in the cells decreased in a dose-dependent manner, according to the fat accumulation analysis performed with the Oil red o staining method. As a result of administration of α-tocopherol to adipocyte cells, CTRP3 expression levels were found to be higher compared to control cells. When control and adipocyte cells treated with 104 µg/ml α-tocopherol were compared, PPAR-γ gene expression levels were found to be lower. In obese individuals, the use of α-tocopherol with dietary habits or supplements may be beneficial in reducing dose-related side effects in the use of hybrid drugs in the treatment of obesity by reducing lipid accumulation in adipocytes.

Keywords: 3T3-L1 adipocyte, Obesity, Alpha-tocopherol, CTRP3, PPAR-γ

1. Introduction

Obesity is a major health problem worldwide. The health and social complications it creates increases day by day. According to the World Health Organization data, approximately 1.9 billion of the adult world population is overweight and more than 650 million of them are obese (Emami et al. 2021). Obesity is a chronic disease

that occurs when the energy taken into the body through diet is higher than the energy used by the body (Koldemir-Gündüz et al. 2019). Complications that are known to be associated with obesity which many studies have been conducted on their mechanisms are hypertension, diabetes mellitus, coronary heart disease, and dyslipidemia.

Considering the high prevalence and severity of obesity, the number of weight control drugs is much less compared to other chronic diseases. Despite ample evidence of significant weight loss effects and the safety of pharmacotherapy of these drugs for patients unable to lose weight with lifestyle changes, these drugs are still not used sufficiently. The main reason for this issue is the side effects of these drugs. These side effects develop depending on the drug dosage (Koldemir-Gündüz M 2021). Many chemicals, herbal and nutritional supplements are used for the treatment of obesity, in addition to pharmacotherapy, low-calorie diets, and increased conventional physical activity, of which their effectiveness varies according to the condition, amount, and the duration of use of the patient. One such nutritional supplement is vitamin E, whose effects on body weight and mass have been extensively studied (Emami et al. 2021).

Vitamin E, which has an antioxidant effect, plays an important role in energy metabolism associated with the expression of various genes (Azzi et al. 2004). Vitamin E consists of four tocopherols and four tocotrienol isomers, of which α-tocopherol and γ-tocopherol are the most commonly found ones in diet (Traber MG 2007). α-tocopherol contributes to the regulation of genes involved in various cell functions (Gray et al. 2011). α- It has been shown that α-tocopherol increases adiponectin expression through the activation of PPARγ, which is the master regulator of adiponectin expression (Gray et al. 2011). Vitamin E can control energy balance and weight by increasing adiponectin expression. In addition, vitamin E shows cholesterol-lowering effects (Zhao et al. 2016). Vitamin E prevents the accumulation of cholesterol that leads to obesity through amplification of inflammatory responses (Tall AR and Yvan-Charvet L 205) and increased insulin resistance (Taverne et al. 2013).

Cytokines, known as adipocytokines or adipokines, play important roles in fat and carbohydrate metabolism, inflammation, hunger, and satiety signal pathways. Adipogenesis is a process of cell differentiation and plays an important role in adipose development and systemic energy homeostasis (Abdik et al. 2021). Adipogenesis is regulated by various transcription factors such as CCAAT-enhancing binding proteins (C/EBPa) and peroxisome proliferator-activated receptor-gamma (PPARγ). PPARγ is also required to maintain the differentiation and fat deposition mechanism (Shao et al. 2016). C1q/TNF-related protein-3 (CTRP3) is a new adipocytokine that has recently emerged as an important regulatory adipokine of obesity and related

metabolic diseases (Chen et al. 2019). CTRP3 has effects on glucose, lipid metabolism, and inflammation (Bei et al. 2020). Studies have shown that CTRP3 can be a potential target in the treatment of obesity (Guo et al. 2020).

In this study, the cytotoxic effects of α-tocopherol on 3T3-L1 adipocytes were evaluated. Moreover, the role of α-tocopherol in reducing fat deposition in 3T3-L1 adipocytes was investigated through gene expression analyses of a new adipocytokine, CTRP3.

2. Materials and Methods

2.1. Cell Culture

The 3T3L-1 fibroblast (CL-173™) cell line used in this study was obtained from the American Type Culture Collection (ATCC) (Manassas, USA). Cells were cultured in Dulbecco's modified Eagle's medium (DMEM) containing, 10% Fetal Bovine Serum (FBS; ATCC, USA) and penicillin/streptomycin (100 µg/ml; Gibco, US). Cells were maintained at 37ºC with 5% CO_2 in a humidified chamber.

2.2. Adipocyte Differentiation from 3T3-L1 Fibroblasts

Differentiation of 3T3-L1 fibroblast cells was performed according to the Miard et al. protocol (Miard et al. 2009). Briefly, a medium supplemented with 10µg/ml insulin + 1µM dexamethasone + 0.5 mM 3-isobutyl-1-methylxanthine was added to 3T3-L1 fibroblast cells in DMEM-FBS and incubated for 3 days. Then, the cells medium was changed every two days for three times with DMEM-FBS medium containing 10 µ/ml insulin. Subsequently, the lipid content formed by the differentiation of 3T3-L1 fibroblast cells into adipocyte cells was determined by the oil red O staining method (Lillie and Ashburn 1943).

2.3. Cytotoxicity Assay

An MTT-based cytotoxicity assay was performed according to the Yerlikaya et al. method (2010) to evaluate the effects of α-tocopherol on 3T3-L1 adipocytes. Briefly, equal numbers of cells were seeded into 96-well plates and grown to an exponential phase. Subsequently, cells were treated with various doses of α-tocopherol (1 µg/ml, 2.5 µg/ml, 5 µg/ml, 10 µg/ml, 25 µg/ml and 50 µg/ml) for 48 hours. Cell survival was determined by reading the absorbances at 570 nm with a Bio-Rad Smartspec Plus spectrophotometer. The results were analyzed with GraphPad Prism 5 program and the IC_{50} value of α-tocopherol was obtained by using nonlinear regression to fit the data to the log(inhibitor) vs. response. Viability rates of cells after α-tocopherol administration was calculated compared to untreated control cells. The viability of untreated cells

was considered to be 100% and the viability percentages of cells were calculated as follows. % viability: (Treated cell / untreated cell) X100

2.4. RNA Isolation and Real-Time PCR Analysis

The expression of CTRP3 and PPAR γ gene was determined by quantitative real-time PCR using ABI StepOnePlus (Applied Biosystems, Germany) instrument. Total RNA was extracted from cells using the RNeasy Protect Mini Kit (Qiagen, Germany) according to the manufacturer's protocol. Total RNA samples were diluted in DNase–RNase-free sterile water and stored at -80°C until use. The Transcriptor HiFi cDNA Synthesis Kit (Roche) was used for cDNA synthesis. Data were analyzed using $2^{-\triangle\triangle}$Ct and GAPDH was used as a reference gene. Primer sequences were: CTRP3 (forward) 5'-GCT GTT TCC CAG AGG ACT GAC T-3', (reverse) 5'- AGG GCA AGA TGG CTG TAA GGT-3'; PPAR γ (forward) 5'-CCC ACC TTC GGA ATC AG-3' and (reverse) 5'-AAT GCT GAA ATC AAC TGT GGT A-3'; GAPDH (forward) 5'-AGG GCA AGA TGG CTG TAA GGT-3' and (reverse) 5'-GGG ACC AAC TTC GGA ATC AG-3'.

2.5. Statistical analysis

The data are shown as the means with their standard errors. All the statistical analyses were performed in GraphPad Prism 5 software. The significance of the differences between all the groups was analyzed by a one-way ANOVA followed by Bonferroni's multiple comparison post-test. A p-value <0.05 was considered significant.

3. Results

3.1. Cytotoxic Effects of α-tocopherol on 3T3-L1 Adipocytes

Initially, we examined the antiproliferative and cytotoxic effects of α-tocopherol in 3T3-L1 Adipocytes. Adipocytes were treated with increasing doses of the α-tocopherol (1 µg/ml, 2.5 µg/ml, 5 µg/ml, 10 µg/ml, 25 µg/ml and 50 µg/ml.) in a logarithmic growth phase for a period of 48 h, then viability was determined by an MTT-based cytotoxicity assay. An IC_{50} of 104.5 µg were calculated upon α-tocopherol treatment, indicating that 3T3-L1 adipocytes were sensitive to the α-tocopherol.

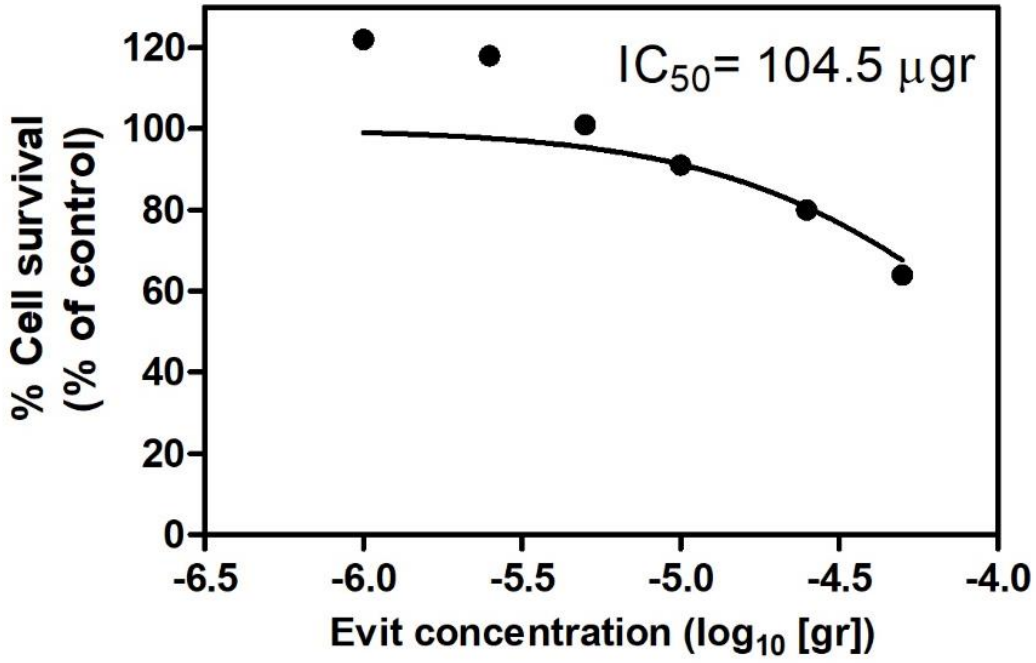

Figure 1. MTT graph after 48 hours α-tocopherol application to adipocyte cells

The % survival rates of 3T3-L1 adipocyte cells were also calculated after MTT-based cytotoxicity (Figure 2) to reflect variable effects of α-tocopherol dosage on cell proliferation. Cell viability of 50 µg/ml, 25 µg/ml, 10 µg/ml, 5 µg/ml, 2.5 µg/ml and 1 µg/ml α-tocopherol treated cells were 64%, 80%, 91%, %101, 118% and 122% respectively when normalized to control cells. It was determined that 50 µg/ml and 25 µg/ml α-tocopherol exposure had an anti-proliferative effect on adipocytes while other administered α-tocopherol doses did not produce any antiproliferative effect on 3T3-L1 adipocytes (Figure 2).

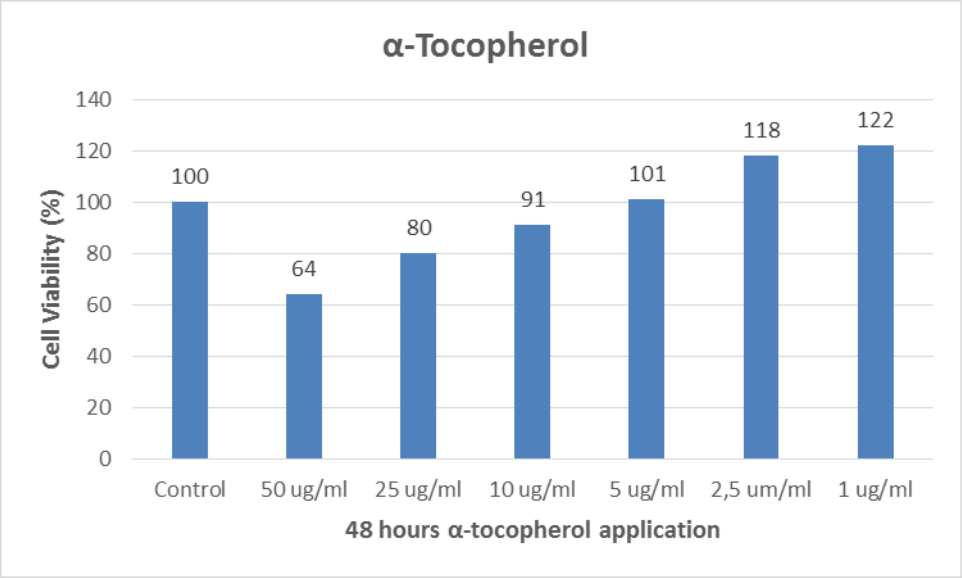

Figure 2. Different concentrations of α-tocopherol have cytotoxic effects in adipocytes. The MTT test was performed after 3T3-L1 adipocytes were treated 50 µg/ml, 25 µg/ml, 10 µg/ml, 5 µg/ml, 2.5 µg/ml and 1 µg/ml α-tocopherol for 48 hours.

3.2. Effect of α-tocopherol Application on Lipid Accumulation

Oil Red-O staining was performed to visualize oil droplets after mature adipocyte formation. Different amounts of α-tocopherol (50 µg/ml, 104 µg/ml and 200 µg/ml) were administered to mature adipocytes. A high amount of oil droplets was observed in control cells. Depending on the α-tocopherol doses, lipid accumulation in adipocytes was significantly reduced (Figure 3). These results indicate that α-tocopherol reduces the fat content in adipocytes. This shows that α-tocopherol may be effective in the treatment of obesity.

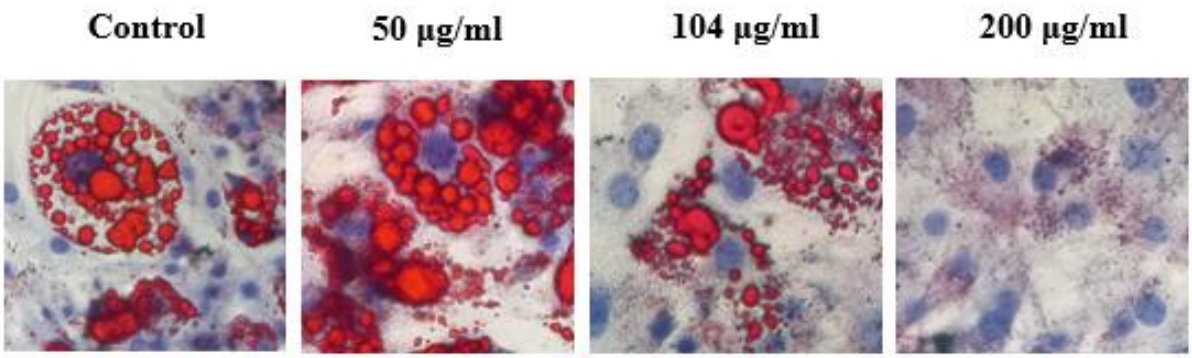

Figure 3. Effects of α-tocopherol on 3T3-L1 adipocytes. Oil Red O staining of adipocytes treated with 50 µg/ml, 104 µg/ml and 200 µg/ml α-tocopherol.

3.3. Differences in CTRP3 and PPARγ mRNA Expression Levels

CTRP3 and PPARγ gene expression levels were analyzed after 50 µg/ml, 104 µg/ml and 200 µg/ml α-tocopherol administration to adipocyte cells. When 3T3-L1 adipocytes treated with 50 µg/ml α-tocopherol for 48 hours were compared with control adipocyte cells, CTRP3 and PPARγ gene expression levels were increased by about 1.8 and 5.58-fold, respectively ($p<0.001$) (Figure 4). When 3T3-L1 adipocytes treated with 104 µg/ml α-tocopherol for 48 hours were compared with control adipocyte cells, CTRP3 gene expression levels were found to be increased by 2.14-fold ($p<0.001$) and PPARγ gene expression levels were found to decreased by 0.05-fold ($p<0.001$) (Figure 4). When 3T3-L1 adipocytes were treated with 200 µg/ml α-tocopherol for 48 hours and control adipocyte cells were compared, CTRP3 and PPARγ gene expression levels were found to increase 3.51 ($p<0.001$) and 1.2-fold ($p<0.01$) respectively (Figure 4).

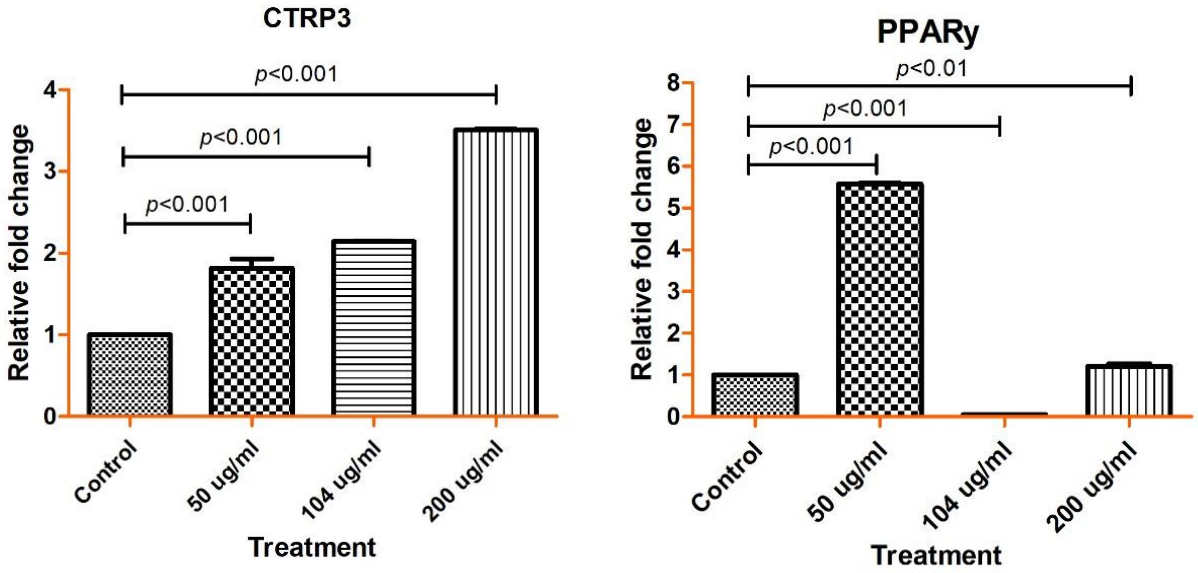

Figure 4. Relative mRNA expression levels of CTRP3 and PPARγ genes on α-tocopherol treated groups and control cells. Gene expression levels were determined in fully differentiated cells by real-time PCR and were normalized to GAPDH mRNA levels.

4. Discussion

Obesity is a major public health problem driven largely by associated diseases such as insulin resistance, type 2 diabetes, dyslipidemia, and cancer. The aetiology of obesity is complex with environmental and genetic influences. The main mechanism of its development is the imbalance between the energy received and spent by the body. Excess energy is stored as adipose tissue (Hammes et al. 2012). However, we know little about the participation of transcription factors in this modulation.

Majima et al. have investigated the relationship between lipid accumulation and α-tocopheryl succinate in 3T3-L1 adipocytes and showed that vitamin E ester α-tocopheryl succinate can suppress lipid accumulation in adipocytes by regulating lipid metabolic cell signals (Mahima et al. 2021). In our study, we determined that α-tocopherol decreased lipid accumulation in a dose-dependent manner by the Oil Red O staining method.

The expression of adipogenesis-related CTRP3 and PPARγ genes was investigated in 3T3-L1 adipocytes to evaluate the therapeutic effect of α-tocopherol. In a study investigating the relationship between the serum level of a new adipokine, CTRP3, and obesity, the serum CTRP3 level was found to be lower in obese patients (Deng et al. 2015). Chen et al. have investigated the serum CTRP3 levels in obese children on obesity, insulin sensitivity and pancreatic beta-cell function and found that CTRP3 serum levels were significantly reduced in obese children compared to controls, and insulin-resistant obese subjects had lower CTRP3 levels in contrast

to non-insulin-resistant obese subjects. (Chen et al. 2019). Li et al. (2018) investigated the relationship between CTRP3 gene expression level and adipose tissue inflammation in obese mice and found that CTRP3 gene expression level was lower in obese mice than in healthy control mice. Li et al. reported that obesity impairs glucose metabolism and insulin sensitivity by decreasing CTRP3 (Li et al. 2018). In this study, CTRP3 gene expression levels have been found to significantly increase when adipocyte cells treated with different doses of α-tocopherol were compared with control adipocytes. An increased level of CTRP3 mRNA may indicate inhibition of lipogenesis.

In anti-adipogenic studies, PPARγ gene expression levels are lower than in control adipocyte cells. In this study, the mRNA level of PPARγ was found to be 0.05-fold lower when adipocyte cells treated with the IC_{50} dose (104 µM) of α-tocopherol were compared with control adipocyte cells.

5. Conclusion

In obese individuals, the use of α-tocopherol may be beneficial within dietary habits or supplements for reducing dose-related side effects of drug combinations in the treatment of obesity by reducing lipid accumulation in adipocytes.

6. References

Abdik H, Cumbul A, Hayal TB, Abdik EA, Taşlı PN, Kırbaş OK, Baban D, Şahin F. Sodium Pentaborate Pentahydrate ameliorates lipid accumulation and pathological damage caused by high fat diet induced obesity in BALB/c mice, J Trace Elem Med Biol. 2021; 66: 126736.

Azzi A, Gysin R, Kempna P, Munteanu A, Villacorta L, Visarius T, et al. Regulation of gene expression by a-tocopherol. Biol Chem. 2004; 385: 585e91.

Bei G, Tongtian Z, Feng X, Xiao L, Fuxingzi L, Su-Kang S, Feng W, Jia-Yu Z, Yi W, Ming-Hui Z, Qiu-Shuang X, Ullah MHE, Ling-Qing Y. New Insights Into Implications of CTRP3 in Obesity, Metabolic Dysfunction, and Cardiovascular Diseases: Potential of Therapeutic. Interventions, Front Physiol. 2020; 3: 570270.

Chen T, Wang F, Chu Z, Shi X, Sun L, Lv H, Zhou W, Shen J, Chen L, Hou M. Serum CTRP3 Levels In Obese Children: A Potential Protective Adipokine Of Obesity, Insulin Sensitivity And Pancreatic β Cell Function. Diabetes Metab Syndr Obes. 2019; 20(12): 1923-1930.

Deng W, Li C, Zhang Y, Zhao J, Yang M, Tian M, Li L, Zheng Y, Chen B, Yang G. Serum C1q/TNF-related protein-3 (CTRP3) levels are decreased in obesity and hypertension and are negatively correlated with parameters of insulin resistance.' Diabetology & Metabolic Syndrome. 2015; 7: 33.

Emami MR, Jamshidi S, Zarezadeh M, Khorshidi M, Olang B, Hezaveh ZS, Sohouli M, Aryaeian N. Can vitamin E supplementation affect obesity indices? A systematic review and meta-analysis of twenty-four randomized controlled trials. Clin Nutr. 2021; 40 (5): 3201-3209.

Gray B, Swick J, Ronnenberg AG. Vitamin E and adiponectin: proposed mechanism for vitamin E-induced improvement in insulin sensitivity. Nutr Rev. 2011; 69: 155e61.

Hammes TO, dos Santos Costa C, Rohden F, et al. Parallel down-regulation of FOXO1, PPARγ and adiponectin mRNA expression in visceral adipose tissue of class III obese individuals. Obes Facts. 2012; 5: 452-459.

Guo B, Zhuang T, Xu F, Lin X, Li F, Shan S-K, Wu F, Zhong J-Y, Wang Y, Zheng M-H, Xu Q-S, Ehsan UMH, Yuan L-Q. New Insights Into Implications of CTRP3 in Obesity, Metabolic Dysfunction, and Cardiovascular Diseases: Potential of Therapeutic Interventions. Front. Physiol. 2020; 11: 570270.

Koldemir Gündüz M. Obezite Tedavisinde Yeni Nesil Yaklaşımlar. Obeziteye Multidisipliner Bakış. Özyiğit F. (Eds). Akademisyen Kitabevi A.Ş., 2021; pp.399-408.

Koldemir-Gündüz M, Çevik M, Çağatay P, Süsleyici B. The effects of oral antidiabetics on adipogenesis related gene expressions in 3T3-L1, AML12 cell lines and their co-cultures. Eurasian J. Bio. Chem. Sci. 2019; 2: 29-37.

Li X, Jiang L, Yang M, Wu YW, Sun JZ. Impact of weight cycling on CTRP3 expression, adipose tissue inflammation and insulin sensitivity in C57BL/6J mice, Experimental and Therapeutic Medicine. 2018; 16: 2052-2059.

Lillie RD, Ashburn LL. Supersaturated solutions of fat stains in dilute isopropanol for demonstration of acute fatty degeneration not shown by Herxheimer's technique. Archs.Path.,1943; 36: 432.

Majima D, Mitsuhashi R, Yamasaki M, Kajimoto K, Fukuta T, Kogure K. Suppression of Lipid Accumulation in 3T3-L1 Adipocytes by α-Tocopheryl Succinate. Biol. Pharm. Bull. 2021; 44: 46–50.

Miard S, Dombrowski L, Carter S, Boivin L, Picard F. Aging alters PPARgamma in rodent and human adipose tissue by modulating the balance in steroid receptor coactivator-1, Aging Cell. 2009; 8: 449-459.

Shao X, Wang M, Wei X, Deng S, Fu N, Peng Q, Jiang Y, Ye L, Xie J, Lin Y. Peroxisome proliferator-activated receptor-γ: master regulator of adipogenesis and obesity. Current Stem Cell Research & Therapy. 2016; 11: 282–289.

Tall AR, Yvan-Charvet L. Cholesterol, inflammation and innate immunity. Nat Rev Immunol. 2015; 15: 104e16.

Taverne F, Richard C, Couture P, Lamarche B. Abdominal obesity, insülin resistance, metabolic syndrome and cholesterol homeostasis. PharmaNutrition 2013; 1: 130e6.

Traber MG. Vitamin E regulatory mechanisms. Annu Rev Nutr 2007; 27: 347e62.

Yerlikaya A, Okur E, Şeker S, Erin N. Combined effects of the proteasome inhibitor bortezomib and Hsp70 inhibitors on the B16F10 melanoma cell line. Mol Med Rep. 2010; 3: 333–339.

Zhao L, Fang X, Marshall M, Chung S. Regulation of obesity and metabolic complications by gamma and delta tocotrienols. Molecules. 2016; 21: 344.

Second International Congress on Biological and Health Sciences
ONLINE 24-25-26-27 FEBRUARY 2022

Production and optimization of lipase by Anoxybacillus flavitermus MOB61 using cooking oil as substrate

Mustafa Ozkan Baltaci[1]

[1]Department of Molecular Biology and Genetics, Science Faculty, Ataturk University, Erzurum, Turkey

Corresponding author: ozkanbaltaci@atauni.edu.tr

Abstract:
The main source of industrial enzymes is microorganisms. The use of microorganisms in the production of enzymes has some important advantages. Compared to enzymes derived from herbal and animal sources, microbial enzymes can demonstrate higher stability under extreme conditions and can be produced in higher quantities. In addition, the production of microbial enzymes can be carried out at low cost using organic wastes.Thermophilic microorganisms are considered as a crucial source of lipase, especially of industrial importance. Lipases produced by thermophilic microorganisms exhibit a very stable structure and high activity at high temperatures in organic solvents. Moreover, these lipases show high resistance to chemical denaturation and can have high activity at alkaline pH values. Due to their high activity and stability at alkaline pH values and elevated temperatures, thermophilic lipases are mainly utilised in the detergent industry. Therefore, isolation, identification and characterization of thermophilic bacteria play an important role for the production of thermophilic lipase. In this study, lipase production and optimization was carried out with *Anoxybacillus flavitermus* MOB isolated from hot springs using cooking oil as a substrate. As a result of analysis, the optimal conditions were determined as; 3 g/L fish peptone, pH:7, 72 hours incubation time and temperature 50 ºC. Under optimized conditions lipase enzyme activity was increased approximately 3-fold (316 U/mL).

Keywords: optimization, production, lipase, *Anoxybacillus flavithermus*

1. Introduction

Lipids constitute an important part of the world's biomass. Lipolytic enzymes play an important role in the conversion of water-insoluble compounds. Lipolytic enzymes, lipases and esterases are characterized by their ability to hydrolyze short and long chain carboxylic acid esters (Chandra et al., 2020). Lipases are a group of enzymes abundant in nature which are hydrolytic enzymes that catalyze the hydrolysis of triacylglycerol to glycerol and free fatty acids. Naturally, lipase enzymes are found in every living organism but the main source

of industrial enzymes is microorganisms (Oliart-Ros et al., 2021). The use of microorganisms in the production of enzymes has some important advantages. Compared to enzymes derived from herbal and animal sources, microbial enzymes can demonstrate higher stability under extreme conditions and can be produced in higher quantities (Patel et al., 2020). In addition, the production of microbial enzymes can be carried out at low cost using organic wastes. Microorganisms having ability to produce enzymes can be screened easily and quickly and the genetic modifications required to increase enzyme production can be performed more easily on microbial cells.

Thermophilic microorganisms are considered as a crucial source of lipase, especially of industrial importance. Lipases produced by thermophilic microorganisms exhibit a very stable structure and high activity at high temperatures in organic solvents. Moreover, these lipases show high resistance to chemical denaturation and can have high activity at alkaline pH values. Due to their high activity and stability at alkaline pH values and elevated temperatures, thermophilic lipases are mainly utilised in the detergent industry (Abu et al., 2021).

In literature, it has been reported that species of bacteria such as *Bacillus*, *Geobacillus* and *Thermomonas* can be used as promising sources of thermophilic lipases (Balaji et al., 2020; Druteika et al., 2020). Moreover, studies on the discovery of new microorganisms which are able to produce these enzymes are constantly increasing due to the industrial and biotechnological importance of thermophilic enzymes. Enzymes are supposed to be produced in large quantities in order to respond to increasing demands. However, the average cost is regarded as a major issue. To solve this problem, agricultural wastes or by-products are used as inexpensive substrates for microorganisms. For instance, waste materials such as coconut, lemon peel, coffee peel and soybean residues are used as cost-effective substrates for the production of microbial lipases. Similarly, researchers reported that waste frying oil (cooking oil) would be a suitable substrate for the production of microbial lipase (Nunes et al., 2021).

Therefore, the present study was carried out to produce lipase from thermophilic bacteria using the waste cooking oil as substrate and to increase the enzyme production efficiency by optimizing some culture conditions.

2. Materials and Methods

2.1. Screening of lipase-producing microorganisms

Six bacteria were screened for their lipase-producing ability. Screening experiments were performed in medium containing 10 ml/L frying oil and 3 g/L Bushnell Haas salt medium (pH: 7.0). To do this, the screening medium was inoculated with 1 mL (OD600nm= 1.0) of seed culture under aseptic conditions. After inoculation, the vials were incubated at 55 °C for 48 hours (Baltaci et al., 2020). Further lipase activities were analyzed and the best lipase producer strain was selected for further experiments.

2.2. Idetification of the best strain

The strain which has the highest lipase activities was subjected to molecular identification by analyzing 16S rDNA sequence. For this purpose Genomic DNA isolation of the test strains was performed according to the Promega WizardR Genomic DNA Purification Kit (A2360) protocol. 16S rRNA region, was amplified using 27F (5'-AGAGTTTGATCCTGGCTCAG-3') and 1492R (5'-GGTTACCTTGTTACGACTT-3') primers, and 30 µL volume of PCR mixture containing, 13.1 µL ddH_2O, 3 µL 10X PCR buffer, 1.8 µL $MgCl_2$, 1.2 µL DMSO, 0.6 µL dNTP, 3 µL (5µM) reverse primer (1492R), 3 µL (5 µM) forward primer (27F), 0.3 µL Taq DNA polymerase and 4 µL template DNA. PCR amplification was performed according to the following protocol: Initial denaturation for 5 min at 94°C, followed by 35 cycles of denaturation at 94°C for 1 min, annealing at 55°C for 30 s, extension at 72°C for 30 s, and final extension at 72°C for 5 min. The PCR products were visualized on a 1% agarose gel. The amplified fragments were cloned into *Escherichia coli* JM101 strain with the pGEM-T Easy Cloning Vector (Promega, Southampton, UK) according to the instructions of the manufacturer. After the cloning, plasmid isolation was carried out by selecting colonies that gave the positive result, and the sequence analysis was made by the Macrogen Company (Netherlands). The 16S rRNA obtained was compared with the other bacterial series in GenBank and EzTaxon (http://blast.ncbi.nlm.nih and http://www.eztaxon.org). A

phylogenetic tree was constructed with Mega4 software based on the 16S rDNA sequences of the strains closer to isolates (Baltaci et al., 2017).

2.3. Optimization for Maximum Lipase Production

Test strain were inoculated in lipase production medium (described above) and some culture parameters were optimized. Firstly, the incubation time parameter has been optimized (with 12 h intervals up to 96 h). Then, nitrogen sources (yeast extract, fish peptone, and ammonium sulfate) and concentration (0-4 g/L), temperature (35-60^{o}C with 5 ^{o}C intervals), and initial pH (6-10 with 1 interval) parameters were studied, respectively(Baltaci et al., 2020).

2.4. Statistical Analysis

All the measurements were taken in three biological and two technical replicates. The variance analysis was carried out according to the One-Way ANOVA Test using the Prism software 7.0 (GraphPad Software, San Diego, CA).

3. Results

3.1. Screening of lipase-producing microorganisms

Lipase producing potentials of six thermophilic bacteria isolated from hot springs were determined. As a result of the analysis, MOB61 strain showed the highest lipase activity and growth in screening medium. Detailed results are given in table 1.

Table 1. Screening of lipase activity

Isolates	Bacterial growth (OD_{600})	Lipase enzyme activity (U/ml)
MOB11	1.24	46.8
MOB25	1.16	49.5
MOB36	0.78	26.8
MOB42	0.9	32.2
MOB53	1.35	51.6
MOB61	1.58	74.2

After the best strain was determined, this bacterium was identified by molecular methods and a phylogenetic tree was constructed via Mega4 program (Figure 1). According to sequence analysis, the isolate coded MOB61 was found to belong to *Anoxybacillus flavitermus* at a rate of 99%.

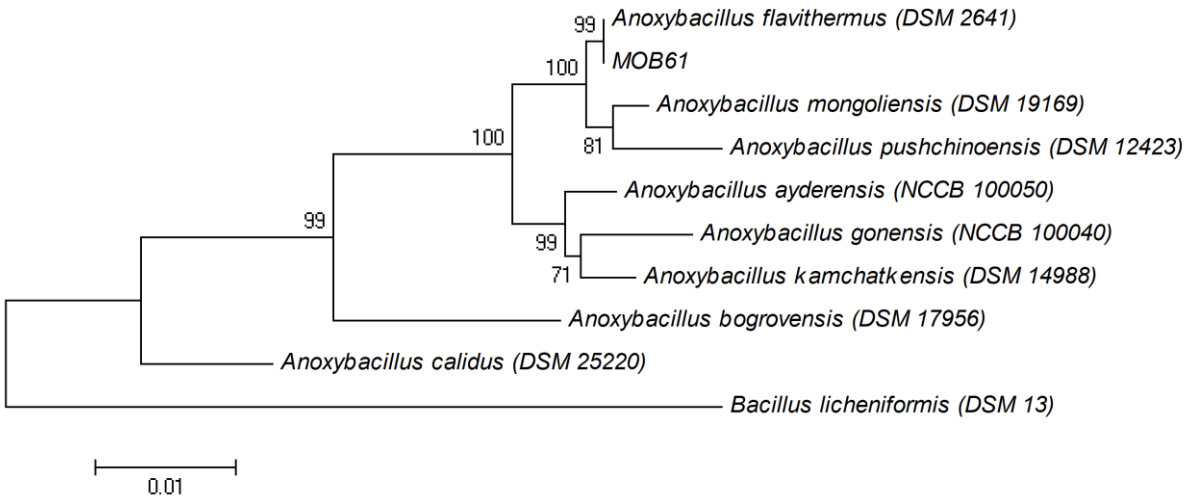

Figure 1. Neighbor-joining showing the phylogenetic position of strain MOB61 based on 16S rDNA gene sequence comparison

3.2. Optimization of Culture Conditions

Effect of Incubation time

To determine the effect of the incubation period on the lipase enzyme activity, MOB61was incubated at 40°C for 96 h. The enzyme activity was assayed with 12 h intervals. The results showed that there was continuous increase in the lipase activity from 12th to 72 th h. Maximum enzyme activity was detected at 72th h.

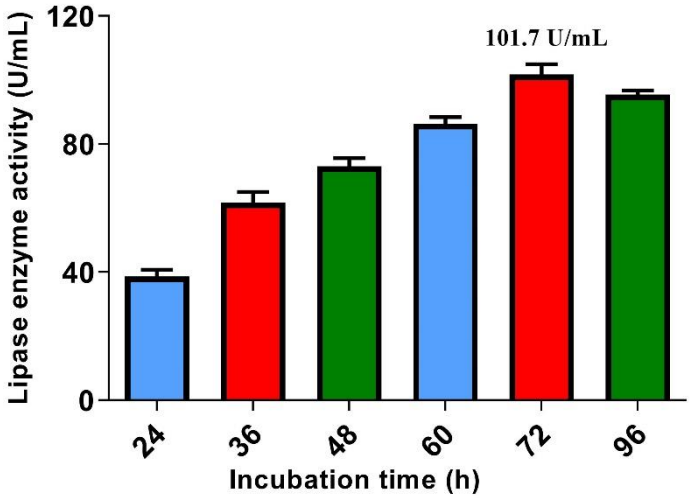

Figure 2. The effect of incubation time. Culture conditions: Temperature; 40 °C, initial pH 6.0, nitrogen source 0 g/L

Effect of Nitrogen Sources

To increase the enzyme activity nitrogen sources such as yeast extract, Fish peptone, and ammonium sulfate, were added to the medium at different concentrations (0-4 g/L). As shown in Figure 3 among the three nitrogen sources, the highest lipase activity was achieved with 3 g/L fish peptone.

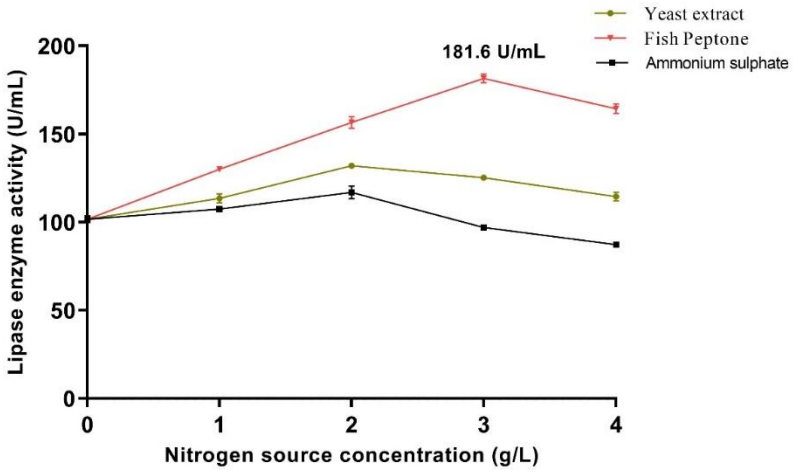

Figure 3. The effect of nitrogen source. Culture conditions: Temperature; 40 °C, initial pH 6.0, incubation time 72 h.

Effect of temperature

MOB61 were incubated for 72 h in the presence of 3 g/L fish peptone at different temperatures (35-60 °C).

After the incubation, it was determined that the maximum activity was achieved at 50 °C.

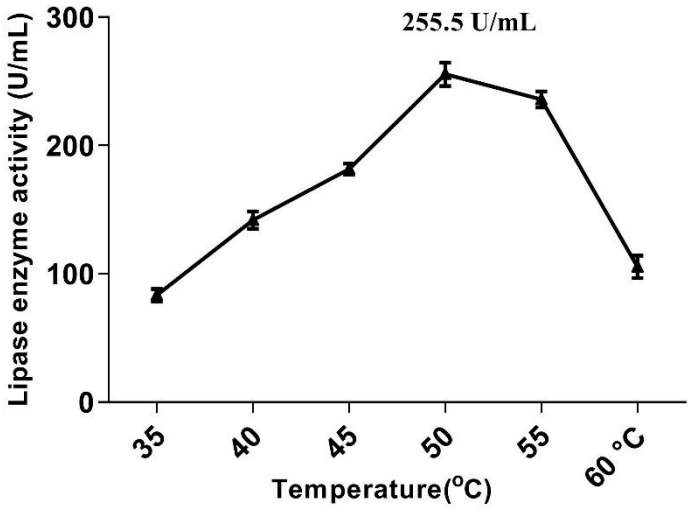

Figure 4. The effect of temperature. Culture conditions: initial pH 6.0, incubation time 72 h, nitrogen sources 3 g/L Fish peptone

Effect of pH

In the last stage of the optimization study, the effect of pH parameter on the enzyme activity was investigated. The optimum enzyme activity was achived at pH 7.

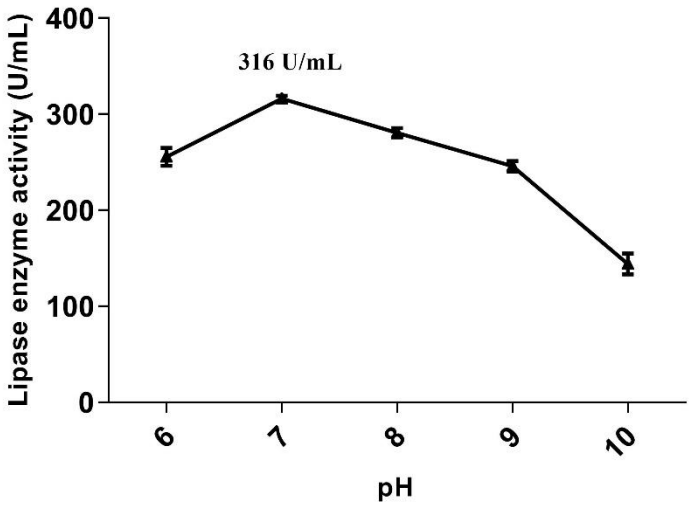

Figure 5. The effect of temperature. Culture conditions: temperature 50, incubation time 72 h, nitrogen sources 3 g/L Fish peptone

4. Discussion

Lipases are among the most important enzyme with industrial and biotechnological interest. Although these enzymes are present in many organisms, their industrial scale production is mainly carried out using microorganisms (Abusham et al., 2009). Studies demonstrated that some nutritional factors (nitrogen and carbon sources) as well as physical and chemical factors affect the production of microbial lipases (Fickers et al., 2004). It is well known that production of microbial enzymes including lipases are significantly affected by culture parameters such as substrate concentration, temperature, pH, surfactants, incubation time, oxygen concentration, shaking speed and incubation time. Therefore, in the present study, some (temperature, oil

concentration, pH and incubation time) of these culture parameters were optimized to enhance lipase production.

The first stage of the study was focused on determining the effect of incubation time on lipase

production. The results showed that there was continuous increase in the lipase activity from 12th to 72 th h. Maximum enzyme activity was detected at 72th h. On the other hand lipase activity showed decrease after 72th h. This decrease was probably due to the lost of the enzyme stability.

It has been reported in the literature that concentrations of nitrogen sources, temperature, and pH significantly affect the amount of enzyme produced. Therefore, these parameters were optimized. As a result of analysis, the optimal conditions were determined as; 3 g/L fish peptone, pH:7, and temperature 50 ^{o}C.

5. Conclusion

As a result of analysis, the optimal conditions were determined as; 3 g/L fish peptone, pH:7, 72 hours incubation time and temperature 50 ^{o}C. Under optimized conditions lipase enzyme activity was increased approximately 4-fold (316 U/mL).In addition, the production of lipase enzyme from a waste material such as cooking oil has been carried out successfully.

6. References

Abu ML, Mohammad R, Oslan SN, Salleh A. 2021. The use of response surface methodology for enhanced production of a thermostable bacterial lipase in a novel yeast system. Prep Biochem Biotech 51:350-360.

Abusham RA, Rahman RNZRA, Salleh AB, Basri M. 2009. Optimization of physical factors affecting the production of thermo-stable organic solvent-tolerant protease from a newly isolated halo tolerant Bacillus subtilis strain Rand. Microb Cell Fact 8.

Balaji L, Chittoor JT, Jayaraman G. 2020. Optimization of extracellular lipase production by halotolerant Bacillus sp. VITL8 using factorial design and applicability of enzyme in pretreatment of food industry effluents. Prep Biochem Biotech 50:708-716.

Baltaci MO, Genc B, Arslan S, Adiguzel G, Adiguzel A. 2017. Isolation and Characterization of Thermophilic Bacteria from Geothermal Areas in Turkey and Preliminary Research on Biotechnologically Important Enzyme Production. Geomicrobiol J 34:53-62.

Baltaci MO, Orak T, Taskin M, Adiguzel A, Ozkan H. 2020. Enhancement of Amylase and Lipase Production from Bacillus licheniformis 016 Using Waste Chicken Feathers as Peptone Source. Waste Biomass Valori 11:1809-1819.

Chandra P, Enespa, Singh R, Arora PK. 2020. Microbial lipases and their industrial applications: a comprehensive review. Microb Cell Fact 19.

Druteika G, Sadauskas M, Malunavicius V, Lastauskiene E, Statkeviciute R, Savickaite A, Gudiukaite R. 2020. New engineered Geobacillus lipase GD-95RM for industry focusing on the cleaner production of fatty esters and household washing product formulations. World J Microb Biot 36.

Fickers P, Nicaud JM, Gaillardin C, Destain J, Thonart P. 2004. Carbon and nitrogen sources modulate lipase production in the yeast Yarrowia lipolytica. J Appl Microbiol 96:742-749.

Nunes PMB, Fraga JL, Ratier RB, Rocha-Leao MHM, Brigida AIS, Fickers P, Amaral PFF. 2021. Waste soybean frying oil for the production, extraction, and characterization of cell-wall-associated lipases from Yarrowia lipolytica. Bioproc Biosyst Eng 44:809-818.

Oliart-Ros RM, Badillo-Zeferino GL, Quintana-Castro R, Ruiz-Lopez II, Alexander-Aguilera A, Dominguez-Chavez JG, Khan AA, Nguyen DD, Nadda AK, Sanchez-Otero MG. 2021. Production and Characterization of Cross-Linked Aggregates of Geobacillus thermoleovorans CCR11 Thermoalkaliphilic Recombinant Lipase. Molecules 26.

Patel R, Prajapati V, Trivedi U, Patel K. 2020. Optimization of organic solvent-tolerant lipase production by Acinetobacter sp. UBT1 using deoiled castor seed cake. 3 Biotech 10.

Second International Congress on Biological and Health Sciences
ONLINE 24-25-26-27 FEBRUARY 2022

An In Vitro Investigation of the Interaction of Genomic DNA with Copper Chloride

Elisha Apatewen Akanbong[1], Alparslan Kadir Devrim[2]

[1]Kirikkale University, Institute of Health Sciences, Department of Biochemistry, Kirikkale, Turkey

[2]Izmir Bakırçay University, Menemen Vocational School, Izmir, Turkey

Corresponding author: akanbongelisha605@gmail.com

Abstract:
Some metal ions are essential in the maintenance of DNA stability and structure, but some are also known to be mutagenic and carcinogenic. Relevant facts about the mutagenicity and carcinogenicity of metal ions were obtained from several research studies conducted on the interactions between d-block elements and DNA. Copper (Cu) complexes have the aptitude for interacting with DNA due to their three-dimensional structure, cationic ability, the tendency of hydrolyzing DNA, and their redox ability. In order to produce more effective and safer therapeutic agents, there is the need to exploit the interaction of DNA with metal complexes. Despite that, DNA-metal complexes interaction has not been fully elucidated. Thus, studies investigating the interaction of DNA with $CuCl_2$ is extremely limited. Hence, this study aimed to provide data on that. UV-absorbance spectrophotometry was adopted in investigating the interaction of the ct-DNA with $CuCl_2$. Combinations of ct-DNA with prepared concentrations of $CuCl_2$ (1000 µM, 500 µM, 250 µM, 125 µM, and 62.5 µM) were made in sterile water. Following that, their absorbance intensities were measured. Also, the absorbance intensity of only DNA (positive control) and only $CuCl_2$ (negative control) was measured. All measurements were done using MultiskanGO UV-absorbance spectrophotometer and prior to the measurements, it was calibrated with nuclease-free water. The data obtained from this study indicate that $CuCl_2$ incited an increment in ct-DNA absorption intensity (hyperchromism), hence, bind to the DNA via groove binding.

In conclusion, $CuCl_2$ has the aptitude for interacting with DNA and can bind to DNA via groove binding. Thus, it could be used in the development of therapeutic agents such as anticancer agents, as the increment in the absorption intensity of the ct-DNA could be due to a degradation of the ct-DNA incited by the $CuCl_2$. However, further studies on the interaction of DNA with copper compounds ($CuCl_2$) and the possible DNA cleavage activity of copper compounds would provide further data.

Keywords: ct-DNA, $CuCl_2$, DNA-Interaction, Metal Complexes, UV-vis Spectrophotometry

[#]The present paper is produced from a portion of the masters' thesis of the first author under the supervision of the second author.

1. Introduction

DNA is a nucleic acid, a genetic material that mediates crucial processes like; transcription, recombination, cell survival and proliferation (Williams and Da Silva 2005). Some metal ions are essential in the maintenance of

DNA stability and structure, but some are also known to be mutagenic and carcinogenic. Relevant facts about the mutagenicity and carcinogenicity of metal ions were obtained from several research studies conducted on the interactions between d-block elements and DNA (Lippert 2008). Modifying or inhibiting the activity of a cell's DNA is an essential medical research that enhances the development of new therapeutic agents, mainly anticancer agents (Hurley 2002). A wide range of fields including material and biological sciences develop and apply metal-containing compounds (Boerner and Zaleski 2005, Zhang and Lippard 2003).

Copper (Cu) complexes have the aptitude for interacting with DNA due to their three-dimensional structure, cationic ability, the tendency of hydrolyzing DNA and their redox ability (Boerner and Zaleski 2005). In order to produce more effective and safer therapeutic agents, there is the need to exploit the interaction of DNA with metal complexes (Bhattacharjee et al. 2021, Pages et al. 2015). Nonetheless, the interaction of DNA with metal complexes has not been fully elucidated (Hannon and Reedijk 2015). Thus, studies investigating the interaction of DNA with $CuCl_2$ are extremely limited. Hence, this study aimed to provide data on that.

2. Materials and Methods

The DNA used in this study was isolated from calf thymus (ct-DNA) using Wizard Genomic Purification Kit (Promega, USA) and its concentration at Å 260/280 was 1.84, hence was appropriate for the conduction of UV-absorbance spectrophotometry. Also, procured $CuCl_2$ (AM0686890527, Merck, Germany) was prepared into 5 different concentrations; 1000 µM, 500 µM, 250 µM, 125 µM, and 62.5 µM. Following that, a combination of the ct-DNA was made with the various concentrations of the $CuCl_2$ at a 1:1 ratio in 0.2 ml sterile Eppendorf tubes and incubated at 37 ℃ for 1 hour. Prior to the measurement of all absorbance, the spectrophotometer (MultiskanGO UV-absorbance spectrophotometer) was calibrated with nuclease-free water. After the calibration, the absorbance of only DNA (positive control), only $CuCl_2$ (negative control), and ct-DNA + $CuCl_2$ was measured.

3. Results

The UV-absorbance spectrophotometric results obtained from the measurement of only ct-DNA (positive control), only $CuCl_2$ (negative control), and ct-DNA+$CuCl_2$ are presented in figure 1, 2, and 3, respectively. As expected, while the ct-DNA gave an absorbance peak at 260 nm, the various concentrations of the $CuCl_2$ did not manifest any absorbance at the aforementioned wavelength. The ct-DNA+$CuCl_2$ gave absorbance peaks at the wavelength 260 nm. However, the absorbance intensities of the ct-DNA+$CuCl_2$ were not as high as that of the positive control (only ct-DNA). Again, the absorption intensities obtained from the ct-DNA+$CuCl_2$ exhibited a concentration-dependent increment.

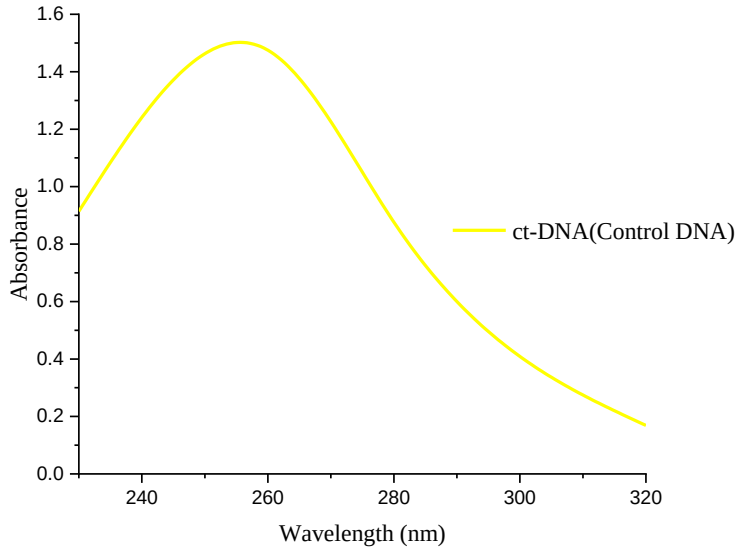

Figure 1. ct-DNA (Control DNA) UV-absorbance spectrophotometry graph.

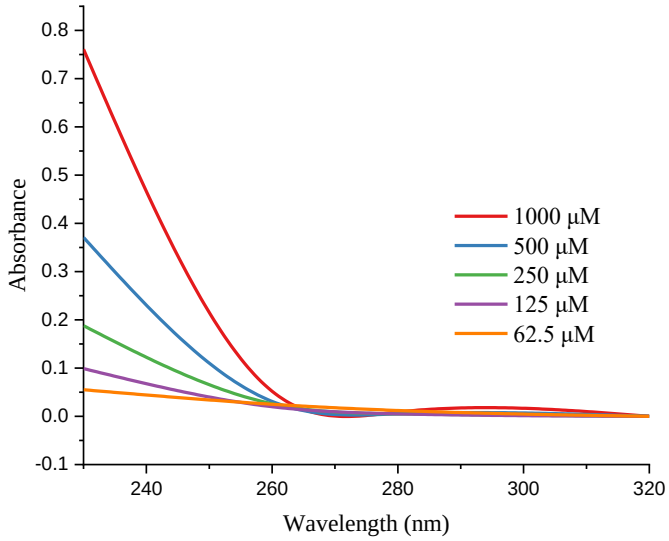

Figure 2. Only $CuCl_2$- UV-absorbance spectrophotometry graph.

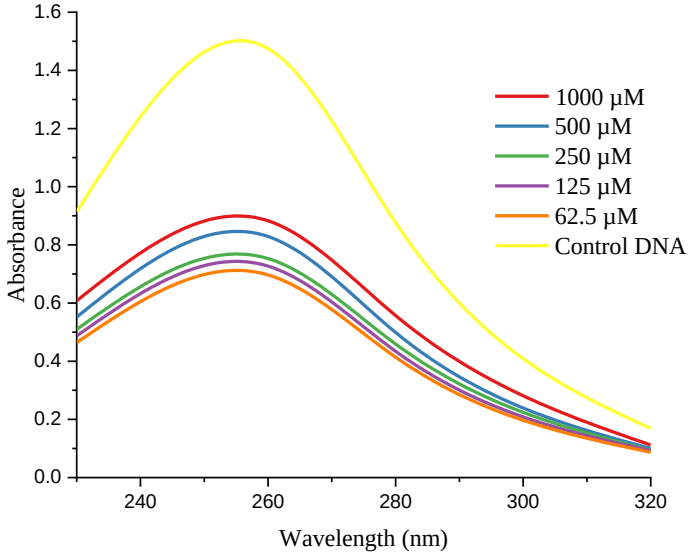

Figure 3. UV-absorbance spectrophotometry graph of ct-DNA + $CuCl_2$ (different concentrations)

4. Discussion

UV-vis absorbance spectrophotometry is one of the many methods used to study the interaction of DNA with metals. In view of that, in this study, the DNA binding potential and mode of binding of $CuCl_2$ to ct-DNA was investigated adopting this method. Hypochromism is often characterised by decrement in DNA absorption wave peak at 260 nm wavelength as the concentration of the binding molecule increases. When a binding molecule instigates hypochromism, then the molecule is said to had bind to DNA via intercalation (Chaveerach et al. 2010; Chen et al. 2011). From the data obtained from the UV-absorbance spectrophotometry, it was observed that in addition to the control, the combinations of ct-DNA with the various concentrations of $CuCl_2$ gave wave peaks at 260 nm. However, $CuCl_2$ incited an increment in the absorption intensity of the ct-DNA in a concentration-dependent manner (Fig.3), even though, it did not give any wave peak at 260 nm when measured alone (Fig.2). Thus, $CuCl_2$ instigated hyperchromism. The instigation of hyperchromism by the $CuCl_2$ indicates that $CuCl_2$ probably bind to the ct-DNA via groove binding and not by intercalation (Dey et al. 2010, Vijayalakshmi et al. 2000).

5. Conclusion

$CuCl_2$ has the aptitude for interacting with DNA and can bind to DNA via groove binding. Thus, it could be used in the development of therapeutic agents such as anticancer agents, as the increment in the absorption intensity of the ct-DNA could be due to a degradation of the ct-DNA incited by the $CuCl_2$. However, further studies on the interaction of DNA with copper compounds ($CuCl_2$) and the possible DNA cleavage activity of copper compounds would provide further data.

6. References

Bhattacharjee A, Das S, Das B, & Roy P. Intercalative DNA binding, protein binding, antibacterial activities and cytotoxicity studies of a mononuclear copper (II) complex. Inorganica Chimica Acta. 2021; 514 (August 2020): 119961.

Boerner LJK, & Zaleski JM. Metal complex-DNA interactions: From transcription inhibition to photoactivated cleavage. Current Opinion in Chemical Biology. 2005; 9 (2): 135–144.

Chaveerach U, Meenongwa A, Trongpanich Y, Soikum C, & Chaveerach P. DNA binding and cleavage behaviors of copper (II) complexes with amidino-O-methylurea and N-methylphenyl-amidino-O-methylurea, and their antibacterial activities. Polyhedron. 2010; 29 (2): 731–738.

Chen D, Milacic V, Frezza M, & Dou QP. Metal complexes, their cellular targets and potential for cancer therapy. Current Pharmaceutical Design. 2009; 15 (7): 777–791.

Dey S, Sarkar S, Paul H, Zangrando E, & Chattopadhyay P. Copper (II) complex with tridentate N donor ligand: Synthesis, crystal structure, reactivity and DNA binding study. Polyhedron. 2010; 29 (6): 1583–1587.

Hannon MJ, & Reedijk J. Metal interactions with nucleic acids. Dalton Transactions. 2015;

44 (8): 3503–3504.

Hurley LH. DNA and its associated processes as targets for cancer therapy. Nature Reviews Cancer. 2002; 2 (3): 188–200.

Lippert B. Coordinative bond formation between metal ions and nucleic acid bases. Nucleic Acid-Metal Ion Interactions (Ed. Hud, NV). 2008; 39–74.

Pages BJ, Ang DL, Wright EP, & Aldrich-Wright JR. Metal complex interactions with DNA. Dalton Transactions. 2015; 44 (8): 3505–3526.

Vijayalakshmi R, Kanthimathi M, Subramanian V, & Nair BU. Interaction of DNA with [Cr (Schiff base) (H2O) 2] ClO4. Biochimica et Biophysica Acta (BBA)-General Subjects . 2000; 1475 (2): 157–162.

Williams RJP, & Da Silva JJRF. The chemistry of evolution: the development of our ecosystem. Elsevier. 2005.

Zhang CX, & Lippard SJ. New metal complexes as potential therapeutics. Current Opinion in Chemical Biology. 2003; 7 (4): 481–489.

Evaluation of Acrosome Integrity of Frozen-Thawed Simmental Bull Semen with Different Staining Methods

Emre KARA, Mesut ÇEVİK

Department of Reproduction and Artificial Insemination, Faculty of Veterinary Medicine, Ondokuz Mayıs University, TR-55200, Samsun, Turkey

Corresponding author: cevikm@omu.edu.tr

Abstract:

The indicators in predicting spermatozoa fertilizing ability include individual motility and movement scores, but the indicators have not been able to accurately predict the spermatozoa fertilizing ability, Acrosome integrity of spermatozoa cells is an important indicator of the success of the fertilization. Semen cryopreservation results in sublethal damage to sperm due to membrane deterioration and an increased number of spermatozoa that undergo acrosome reaction, these damages lead to fertility reduction. The objective of this study was to compare three methods of staining in order to evaluate bull sperm viability and acrosome integrity after cryopreservation. In the study, 55 semen straws obtained from Simmental bulls with known breeding quality and frozen at different times were used as the main material. A 30-second slow thawing protocol at 37°C was used to thaw frozen semen straws. Motility, spermatozoa concentration, plasma membrane integrity and acrosome integrity parameters of all thawed semen were analyzed. In the evaluation of acrosome integrity, three different complicated staining protocols were applied and the results obtained were compared and an efficient and appropriate staining protocol was tried to be determined. The Computer-Aided Sperm Analyzer (CASA), (SCA®, Microptic, Barcelona, Spain) was used to assess frozen-thawed sperm motility, concentration and movement characteristics. Plasma membrane integrity is vital for spermatozoa because the plasma membrane integrity plays an important role in regulating all of the processes in cells. The percentage of plasma membrane integrity in frozen Simental bull semen used in this study ranged from 42-78% and can be considered good. According to our study results, spermatozoa acrosome integrity can be easily tested using the Coomassie Blue, Trypan Blue-Giemsa and Spermac staining procedures. TBG staining was not very effective in evaluating frozen semen because diluent components were also stained, causing

difficulty in analyzing the staining results. In addition, analysis of TBG and Spermac staining results takes more time than Coomassie blue staining results.

Keywords: Acrosome integrity, frozen-thawed semen, HOST, Simmental bull

*: *This work was supported by the Project Management Office of Ondokuz Mayıs University with the project numbered PYO.VET.1904.21.010.*

1. Introduction

The predicting ability of semen fertility of the laboratory tests is still limited, especially because of the complexity of sperm and fertilization process. Therefore, it is necessary to increase the accuracy of the prediction of bull fertility using other tests that the accuracy of the reproductive potential estimate of the bull is in turn improved. Another equally important indicator that can be specifically used to determine the fertilizability of spermatozoa is acrosomal integrity of spermatozoa (Sitepu and Marisa, 2020). Motility and kinematic parameters serve as indicators in predicting the fertilizing ability of spermatozoa, but the indicators are still unable to precisely indicate the fertilizing ability of the spermatozoa. The motility and the individual motion of the spermatozoa only indicate that live spermatozoa are able to move normally and pass through female reproductive tract. It is necessary for spermatozoa to be acrosome-intact to achieve successful fertilization by activating the function of acrosome reaction at the right time, releasing enzymes and facilitating spermatozoa to penetrate zona pellucida. Semen freezing process will result in the exposure of spermatozoa to low temperature in liquid nitrogen (-196 ^{o}C). The cryopreservation process will cause cold shock, osmotic stress and formation of ice crystals (Yaniz et al., 2021). It is known that spermatozoa have three types of membranes, which are plasma membrane, mitochondrial membrane, and acrosomal membrane. The membranes contain polyunsaturated fatty acids (PFA) and hence are very susceptible to oxidative stress, especially during cryopreservation procedures (Silva and Gadella, 2006). Oxidative stress is one of the factors that increase cell damage due to increase reactive oxygen species (ROS). Excessive ROS production in sperms is dangerous due to its negative effects on functional sperm count. The membrane of spermatozoa is susceptible to oxidation due to the presence of ROS as it is rich in unsaturated fatty acids. Such lipid peroxidation chain reactions occur continuously because each reaction generates a ROS, which leads to a new lipid peroxidation reaction and ultimately damages the entire plasma membrane of the spermatozoa. Lipid peroxidation can alter membrane functions and thus reduce the metabolism, morphology, motility and

fertility of spermatozoa. Acrosome integrity is one of the determining factors for fertilization. Only with the acrosome, intact spermatozoa can penetrate the zona pellucida and fuse with the oocyte plasma membrane (Prihantoko et al., 2020; Umamageswari et al., 2012).

The acrosome integrity of spermatozoa can be observed using various staining methods such as Trypan Blue-Giemsa (TBG), Giemsa, Sperm Blue, Spermac and Coomassie Blue (CB). TBG staining has been used in examining the acrosome of the spermatozoa of various species such as bull and pig (Larson and Miller, 1999; Saad et al., 2011; Umamageswari et al., 2012), while CB staining has been reported on the spermatozoa of rabbits and human (Cross and Stanley, 1989; Kovacs and Foote, 1992). The mentioned staining methods have high affinity for protein and are expected to be capable of staining the acrosome of spermatozoa. TBG is staining capable of binding to cell protein. Giemsa is known to have low molecular weight and able to pass through cell membrane that protects the acrosome of spermatozoa. A previous study showed that Trypan Blue-Giemsa staining is considered to be simpler and easier than Coomassie Blue staining. In addition to the two abovementioned staining methods, another study (Almadaly et al., 2014) has been conducted to assess the acrosomal integrity of spermatozoa using Giemsa staining, which was a simpler and easier method, by combining methanol fixation and Giemsa staining. Given that acrosomal integrity is very crucial in fertilization processes, the study aimed at evaluating the quality and acrosomal integrity of frozen spermatozoa of Simmental bulls and determining the most effective staining method in assessing the acrosomal integrity of frozen spermatozoa.

2. Materials and Methods

Sperm samples and experimental design

In the study, a total of 55 frozen sperm straws from the semen of the Simmental bull were used. A 30-second thawing protocol at 37°C was used, which is used as the gold standard for thawing frozen sperm pipettes. All thawed sperm were tested for motility, viability, concentration, plasma membrane integrity and acrosome integrity parameters.

Sperm motility

The Computer-Aided Sperm Analyzer (CASA), (SCA®, Microptic, Barcelona, Spain) was used to assess frozen-thawed sperm motility and movement characteristics. Total motility (0-100%), progressive motility (0-100%), VAP (mean path velocity, m/ s–1), VSL (straight-line velocity, m/ s–1), VCL (curvilinear velocity, m/ s–1) and ALH (lateral head change, m), BCF (Crossover frequency rhythm Hertz (Hz) values were measured and recorded in at least 5 microscope fields in the software system.

Hypoosmotic Swelling Test

The HOS test was used to evaluate the functional membrane integrity of sperm. 1 ml of the HOST solution (7.35 g sodium citrate and 13.51 g fructose per 1 l of distilled water) was collected and placed in an eppendorf tube at 37°C. It was incubated at 37°C for 30 minutes after adding 10 µl of the semen sample to the HOST solution. After incubating the mixture, one drop was placed on the slide and a smear was obtained. After drying the slide at a 45-degrees angle, this slide was examined at 40x magnification under the microscope, and 200 sperm per slide were counted. Membrane-intact spermatozoa were characterized by swollen tail, while sperms with damaged membrane were characterized by straight tails. The percentage of HOS-positive sperm was calculated with those with a coiling tail.

Staining Procedures

a- Trypan Blue-Giemsa Staining

First, a 0.25% Trypan blue (Sigma Cell Culture, T-6146) (w/v) staining solution was prepared in 0.81% NaCl, isotonic and pH neutral (6.9-7.2). Dyes 86 ml of 1N HCl and 14 ml of formaldehyde solution 37% w/v for fixation; and 0.2g of neutral red were prepared. Acrosome staining was prepared from 2.5-7.5% Giemsa stock solution with distilled water (pH 6.9). Then, it was started to paint. In this staining, Trypan blue and semen were mixed with an automatic pipette on one side of the slide and smeared with a coverslip. The preparations were then left to dry. Dried preparations were fixed in a formaldehyde-neutral rejection solution in a steep gelatin for 2-5 minutes. It was then quickly rinsed with distilled water. It was dyed at 40 ºC with 7.5% Giemsa for 2-4 hours, and it was quickly passed through distilled water. In this second distilled water run, the preparations were left in distilled water for 2 minutes. Two hundred cells were evaluated under a microscope at 400x magnification. Acrosome-intact spermatozoa were characterized by purple head, while those with damaged acrosome were characterized by pale lavender.

Coomassie Blue G-250

Sperm were fixed with 4% paraformaldehyde solution (110 mM Na2HPO4, 2.5 mM NaH2PO4, 4% paraformaldehyde pH 7.4) for 10 min at 24°C. Sperm were centrifuged and washed twice using 1.5 ml of 100mM ammonium acetate (pH: 9.0). The final sperm pellet was resuspended in 1 ml of 100 mM ammonium acetate, 50 µl of the sperm suspension was smeared on glass microscope slides using another glass slide and air dried. Sperm on the slides were incubated in freshly made Coomassie stain (0.22% Coomassie Blue G-250

(Fisher Scientific, Fair Lawn, NJ), 50% methanol, 10% glacial acetic acid, 40% water) for 2 min. Slides were washed thoroughly using distilled water to remove excess stain. Slides were air-dried and coverslips were placed on slides and sealed using Permount mounting medium (Fisher Scientific). Stained two hundred sperm cells were examined under a microscope at 400x magnification.

Spermac Staining

To determine acrosome integrity, the commercial kit Spermac® were used. For Spermac® staining, a smear was made with semen and allowed to air dry at 37°C for 10 min. The slide was plunged seven times in the fixative solution before immersion for 10 min and washed in clean tap water seven times. Excess water was dried with tissue paper without touching the smear. The slide was plunged seven times in solution A and immersed for 90 sec and washed as described before. Then it was plunged in solution B seven times and immersed for one minute, washed and plunged in solution C seven times and immersed for 80 sec and then washed one last time. Then it was allowed to air dry at 37°C. All the slides were read using a light microscope (Nikon Corporation, Tokyo, Japan) and a 1000X objective lens, under oil immersion. The acrosomes and the equatorial zone are stained light green, while the rest of the head appears in red, and both the tail and the intermediate piece will be dark green. Qualitative and quantitative estimates of acrosomal integrity may thus be rapidly and simply obtained. Stained two hundred sperm cells were examined under a microscope.

Statistical analyses

Statistics Data were analyzed using the statistical software SAS System for Windows (SAS Institute Inc, Cary, NC, USA, 2000). Fifty-five semen straws (n=55) were used for each group. The correlations between the staining methods used in the determination of acrosomal integrity and other parameters were evaluated by "Pearson Correlation Coefficients Analysis". Again, Covariance Analysis was used to determine the relationship and interaction degrees between important spermatological parameters and acrosomal integrity.

3. Results

Spermatozoa motility will decrease due to the freezing process because the thawing process of frozen spermatozoa will result in some spermatozoa with low viability and less progressive motility than those of fresh semen. In *Table 1* summarized the effects of some important sperm parameters on acrosome integrity and staining procedures. It has been determined that there is a significant and remarkable relationship between the sperm thawing parameters, progressive motility and especially total motility, and the detection

of acrosome integrity of staining procedures (P<0.001). When the effects of spermatozoa kinematic parameters (VCL, VAP, VSL, STR, LIN, WOB, ALH, BCF) on the effectiveness of staining procedures used for the determination of acrosomal integrity are evaluated, especially VCL and ALH kinematic parameters, as well as BCF with acrosomal integrity, direct and it was determined that they had a significant positive interaction (P < 0.001). Other parameters VAP, VSL; STR, LIN and WOB values are VCL; It was determined that they were not as effective in detecting acrosomal integrity as ALH and BCF (P > 0.05). No statistically significant interaction was found between sperm concentration and staining procedures, especially acrosomal integrity, as well as other spermatological parameters (P > 0.05).

Plasma membrane integrity is an absolute necessity for spermatozoa. Plasma membrane serves as first defense of cells against external environment that can damage the cells. The examination results showed mean spermatozoa membrane integrity of 59.10±1.00, and the maximum and minimum values ranged from 42.00% to 78.00% (Table 1). Very strong and significant positive interactions were determined between HOST, which is used to determine the plasma membrane integrity of spermatozoa, and acrosomal integrity of spermatozoa (P < 0.001). In other words, according to this correlation, it is possible to say that the acrosomal integrity is highly preserved in sperm with high plasma membrane integrity, and the interaction between these two parameters is extremely effective in determining the fertility of the sperm.

The success of fertilization is determined by the presence/the status of acrosome, which is able to activate the function of the acrosome reaction and the fusion of oocyte. Table 1 also summarized the percentages of the intact acrosome of the Simmental bulls identified using CB, TBG or Spermac with the values between 94,85±0,30, 85,98±0,42 and 88,78±0,42%, respectively. When the staining methods used in the detection of acrosomal integrity are compared among themselves in terms of detection success, it is possible to say that the CB method is more successful than the others. After that, the sperm staining procedure and finally the TBG method were found to be effective. The difference between them was found to be statistically significant (P < 0.05). However, all three staining procedures are methods that can be used easily in detecting the acrosomal status of spermatozoa.

According to the results of the “Pearson Correlation Coefficients Analysis”, there is a very strong 86% positive correlation between spermatozoa motility and progressive motility (P<0.001, **). The relationship between these two basic parameters is already known and accepted relations. It was determined that there was a 40% negative correlation between sperm kinematic parameters, BCF, and spermatozoa concentration. A positive correlation was also determined between the Coomassie blue staining method, which was used for the determination of acrosomal integrity and was determined as the most successful procedure, and VCL, one of

the kinematic parameters (P < 0.05). In addition, it was determined that there was a positive correlation between motility and progressive motility and Coomassie blue and Trypan blue-Giemsa staining (P < 0.05).

Table 1. Effects of some important sperm parameters on acrosome integrity and staining procedures

Parameters		n	Mean±SEM	P Value	Minimum	Maximum
Motility		55	72,93±1,56	0,011	48,34	91,91
Progressive motility		55	53,07±1,51	0,462	28,48	79,91
VCL		55	96,90±2,16	0,028	65,15	130,26
VAP		55	50,33±1,19	0,886	34,15	70,93
VSL		55	34,49±1,07	0,806	23,00	53,46
STR		55	61,75±0,73	0,177	52,44	72,24
LIN		55	35,37±0,77	0,139	26,02	48,17
WOB		55	53,28±0,59	0,395	46,54	64,09
ALH		55	4,39±0,09	0,023	3,05	5,88
BCF		55	6,54±0,15	0,095	4,90	10,90
Sperm concentration		55	102,30±3,53	0,809	45,14	180,24
Plasma membrane integrity (%)		55	59,10±1,00	0,003	42,00	78,00
Acrosome Integrity (%)	Coomassie Blue Stain	55	94,85±0,30[a]	0,000	87,00	98,00
	Trypan Blue-Giemsa Stai	55	85,98±0,42[b]	-8,872	76,00	93,00
	Spermac stain	55	88,78±0,42[c]	-6,072	82,00	95,00

4. Discussion

The acrosomal membrane must remain intact until zonal attachment occurs, prior to and during the passage of spermatozoa into the isthmus. Early acrosome reactions render the spermatozoa infertile and therefore it is important to evaluate acrosome integrity before assisted reproductive techniques. After freezing and thawing, spermatozoa moves more slowly than fresh semen. Additionally, freezing process also damages spermatozoa and it makes their movement slower. The decrease in the motility of the spermatozoa after freezing and thawing may be in the range of 24-64% [Ata et al., 2014]. The reason why the motility decreases is that the spermatozoa experience cold shocks and excessive osmotic stress. The decrease in the motility relates to mitochondrial activity [Hincapie et al., 2021]. Plasma membrane integrity is vital for spermatozoa because the plasma membrane integrity plays an important role in regulating all of the processes in cells [Kang et al., 2020]. Phospholipids found in skim milk egg yolks play a role in protecting the plasma membrane

from the effects of cold shock [Prihantoko et al., 2020]. Therefore, it can be used as semen extender to protect spermatozoa from the effects of cold shock.

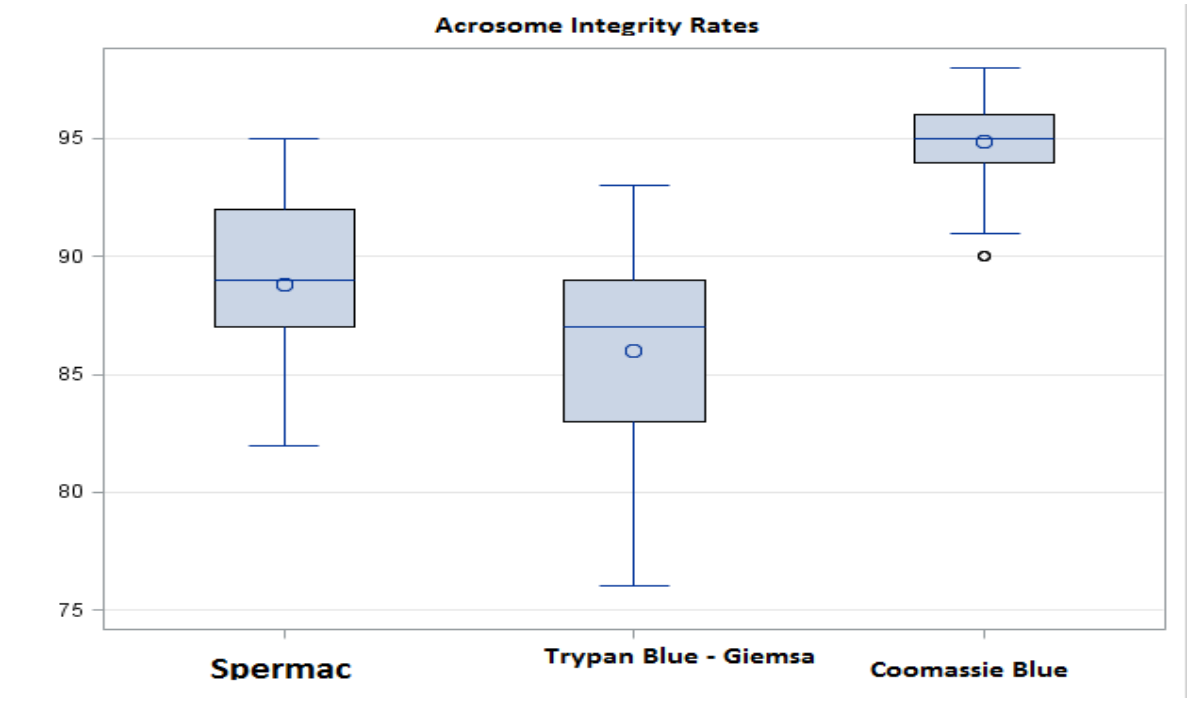

Figure 1. Success status of staining methods used to determine acrosomal integrity

In all mammals, the capacitation and the subsequent acrosome reaction of spermatozoa represent essential steps for successful fertilization and formation of a zygote. The determination of the ability of spermatozoa to activate the acrosome reaction is supposed to be a useful parameter in evaluating infertility [Jancovicova et al., 2008]. One of the key processes in mammalian fertilization is the acrosome reaction (AR) usually triggered in spermatozoa upon their biding to the zona pellucida of the egg. The AR involves fusion between the plasma membrane and the underlying outer acrosomal membrane, which results in the release of the acrosomal contents [Yaniz et al., 2021]. Acrosomes play a crucial role in the process of fertilization. Spermatozoa binding to the zona pellucida will stimulate acrosome reaction and cause the release and the activation of acrosome enzymes, allowing spermatozoa to penetrate the zona pellucida [Van der Horst and Maree, 2009; Way et al., 1995]. It can be assumed that the Giemsa can stain the membrane proteins. The damaged acrosome can be observed on the basis of the results of spermatozoa staining, whether they absorb color or not.

The TBG staining was not quite effective in assessing frozen semen because the extender components were also stained, which caused the difficulty in analyzing the results of the staining. Additionally, the analysis of the Spermac and TBG staining results was more time consuming that that of CB staining results. The analysis of the acrosomal status using the CB staining is more efficient than that using the Spermac and TBG staining.

Recent reports indicate that the sperm membrane integrity is influenced by centrifugation (Weiss, et al., 2004), therefore another possible explanation for the different staining patterns obtained on bull sperm is that the juxtaposition of the plasma membrane with the nuclear membrane over the equatorial region was disrupted by the centrifugation process and allowed the diffusion of the dyes in that portion of the head (Maxwell & Johnson, 1997). Several staining techniques have been used to assess both acrosomal integrity and viability of ejaculated bovine spermatozoa (Nur et al., 2011; Silva and Gadella, 2006; Almadaly et al., 2014). These methods typically are used on thawed cryopreserved spermatozoa, or on spermatozoa incubated in semen extenders that were used to cryopreserve the spermatozoa. The results of the study showed that Coomassie Blue staining is a simple, inexpensive and reliable staining method in frozen-thawed Simmental bull semen. With this method, both morphological and acrosomal integrity examination were performed in a single smear, allowing rapid evaluation of spermatozoa. It can be said that this method is a very advantageous method, considering that this staining method is very easy, can be applied easily in field conditions and can be obtained very quickly in terms of morphological characteristics of spermatozoa.

As a result, it has been revealed that this method is a fast working method in frozen-thawed semen of Simmental bulls and does not require complex laboratory conditions in the calculation of dead live and acrosomal / morphological disorders. Male fertility assessment based on test inseminations is expensive and time consuming, and it would be useful to have simple in vitro test for predicting potential bull fertility. Spermatozoa from bulls with superior field fertility displayed increased acrosomal integrity and head width. In all likelihood, the repeated analysis of more ejaculates would increase the chance of finding associations between in vitro sperm quality and bull fertility. In agreement with our study, Yaniz et al. [2021] have described that acrosome integrity, together with viability, were the only sperm attributes that were significantly different between high and low fertility bulls. In fact, Yaniz et al. [2021] observed that both viability and acrosome integrity could serve as bull fertility biomarkers in the field, while Felipe-Perez et al. [2008] described an association between sperm motility and velocity with bull fertility. Given the difficulty in clearly discerning the sperm acrosome in most animal species, its evaluation is usually limited to research or to occasional studies of sperm quality.

5. Conclusion

In our study, we showed that frozen-thawed sperm obtained from Simmental bulls can be stained with Trypan blue-Giemsa, Spermac and Coomassie blue staining processes and their acrosomal status can be clearly determined. These dyeing procedures are simple, inexpensive and reliable. It does not require fluorescent or

DIC optics and 400x magnification is sufficient to view sperm and determine acrosomal status. The staining techniques described here can be easily applied in studies to determine fertilization and infertility status.

6. References

Almadaly E, Foad F, Mostafa S, Tetsuma M. Plasma membrane integrity and morphology of frozen-thawed bull spermatozoa supplemented with desalted and lyophilized seminal plasma. Global Veterinaria. 2014; 13(5): 753-766.

Ata A, İnanç ME, Kankavi O, Gülay ÖY, Gülay MŞ. Epididimal ve dondurulmuş çözülmüş Holstain boğa spermasında farklı boyama yöntemlerinin karşılaştırılması. MAKÜ Sag. Bil. Enst. Derg. 2014; 2(1): 1-12.

Cross NL, Stanley M. Methods for Evaluating the Acrosomal Status of Mammalian Sperm. Biology of Reproduction. 1989; 41: 635-641.

Felipe-Perez YE, Juarez-Mosqueda ML, Hernandez-Gonzalez EO, Valencia JJ. Viability of fresh and frozen bull sperm compared by two staining techniques. *Acta Veterinaria Brasilica*. 2008; 2(4): 123-130.

Hincapie JJ, Monroy CL, Matamoros IA. Effect of refreezing on the plasma membrane integrity, acrosome, viability, morphology and individual motility in bovine sperm. Clinical Research in Animal Science. 1(3). CRAS. 000513. 2021.

Jancovicova J, Michal S, Jana A, Lubica H. Acrosomal and viability status of bovine spermatozoa evaluated by two staining methods. Acta Veterinaria Hungarica. 2008; 56(1): 133-137.

Kang S-S, Kim U-H, Lee M-S, Lee S-D, Cho S-R. Spermatozoa motility, viability, acrosome integrity, mitochondrial membrane potential and plasma membrane integrity in 0.25 mL and 0.5 mL straw after frozen-thawing in Hanwoo bull. J Anim Reprod Biotechnol. 2020; 35:307-314.

Kovacs A, Foote RH. Viability and acrosome staining of bull, boar and rabbit spermatozoa. Biotechnology Histochemical. 1992; 67(3): 120-124.

Larson JL, Miller DJ. Simple histochemical stain for acrosomes on sperm from several species. Molecular Reproduction and Development. 1999; 52:445–449.

Nur Z, Zık B, Üstüner B, Tütüncü Ş, Sağırkaya H, Özgüden C, Günay Ü, Doğan İ. Effect of freezing rate on acrosome and chromatin integrity in ram semen. Ankara Üniv Vet Fak Derg. 2011; 58: 267-272.

Prihantoko KD, Yuliastuti F, Haniarti H, Kusumawati A, Widayati DT, Budiyanto A. The acrosome integrity examination of post-thawed spermatozoa of several ongole grade bull in Indonesia using Giemsa staining method. The 4th Animal Production International Seminar, IOP Conf. Series: Earth and Environmental Science 478. 2020; 012042, doi:10.1088/1755-1315/478/1/012042.

Saad A-E, Alhamidi AR, Alkahtani S, Sandouka MAE. Determination of the Arabian Sand Gazelle sperm and acrosomes defects by using Spermac staining technique. Asian Journal of Biological Sciences. 2011; 4(2): 138-147.

Silva PFN, Gadella BM. Detection of damage in mammalian sperm cells. Theriogenology. 2006; 65: 958-978.

Sitepu SA, Marisa J. Acrosome integrity spermatozoa test with addition of gentamicin and sweet orange essential oil in Simmental bull liquid semen. Asian Journal of Advanced Research and Reports. 2020; 9(3): 1-5.

Umamageswari J, Joseph C, Kulasekar K, Kalathara J, sridev P. Assesment of acrosomal integrity of dog spermatozoa Spermac staining technique. Indian Journal of Animal Reproduction. 2012; 33 (2): 51-53.

Van der Horst G, Maree L. SpermBlue: A new universal stain for human and animal sperm which is also amenable to automated sperm morphology analysis. Biotechnic and Histochemistry. 2009; 1-10, iFirst article.

Way AL, Henault MA, Killian GJ. Comparison of four staining methods for evaluating acrosome status and viability of ejaculated and cauda epididymal bull spermatozoa. Theriogenology. 1995; 43: 1301-l 316.

Yaniz JL, Palacin I, Silvestre MA, Hidalgo CO, Tamargo C, Santolaria P. Ability of the ISAS3Fun method to detect sperm acrosome integrity and its potential to discriminate between high and low field fertility bulls. Biology. 2021; 10: 1135.

Second International Congress on Biological and Health Sciences
ONLINE 24-25-26-27 FEBRUARY 2022

Thalamus, Hypothalamus, Amygdala, Mamillary Body Volume Ratios Obtained by MRICloud Method in Alzheimer's Patients

Meryem Esma DÜZ[1], Nurullah YÜCEL[2]

[1]Necmettin Erbakan University, Meram Medicine Faculty, Department of Anatomy

[2] Health Sciences University Hamidiye Medicine Faculty, Department of Anatomy

Corresponding author: duzmeryemesma@gmail.com

Abstract:

Alzheimer's disease (AD) affects more than 35 million people around the worldwide and its incidence is predicted to triple by 2050. According to The World Health Organization, Turkey will be one of the four countries with the highest AD in the world in 2050. In the literature, pathological involvement has been observed in subcortical structures that play a role in cognitive process in AD.Therefore we aimed to determine the changes in volume ratios in Alzheimer's disease. The study included 24 AD,16 CG, a total of 40 people.Telencephalon (Telen), Brain Spinal Fluid (CSF), Thalamus (Thal), Hypothalamus (HypoTh), Amygdala (Amyg), Mamillary body (Mama) data was obtained from the Type2 L5 statistics table in the web based MRICloud program. The SPSS 27.0 program was used in the analysis of the data. TelenL / AmygL, TelenL / MamaL, TelenR / AmygR and TelenR / MamaR ratios were found to be higher in the AH group (p <05). Although the rates of TelenL / ThalL, TelenL / HypoThL and TelenR / ThalR were higher in the AD group, no significant difference was observed (p> 05). CSF / TotAmyg, CSF / ThalamT, CSF / TotHypoth and CSF / TotMam ratios were found to be higher in AH group (p <05). The higher ratio of the thalamus, hypothalamus, corpus amygdalaodieum and mamillary body volumes to the CSF which are subcortical structures of the limbic system makes think that these rates may be more specific for diagnosis in AD group. Multicenter studies with more AH are needed to support the decrease of volumes of the thalamus, hypothalamus, corpus amygdalaodieum and mamillary body are shrinking in patients with AH.

Keywords: Alzheimer's Disease, MRICloud, Thalamus, Hypothalamus, Amygdala, Mamillary Body

Introduction

Alzheimer's disease (AD) is the most common type of dementia and forms for 60-70% of dementia cases. Initially, AD manifests as progressive memory loss and is accompanied by other cognitive dysfunctions such as visual-spatial abnormalities, orientation difficulties, walking problems, and language impairment. These cognitive disorders affect daily living activities more. In addition, dementia and most of its behavioral psychological symptoms usually occur during the course of the disease (1).

Thalamus constitutes the largest part of the diencephalon. The two thalamus are separated from each other by the third ventricular cavity and are interconnected by interthalamic adhesion. It creates a great station for all senses except smell and evaluates sensations such as pain and touch. Thalamic neurons send projections to the sensory area of the cerebral cortex. The thalamus also integrates motor functions that transmit impulses from the cerebellum and corpus striatum to the motor area of the cerebral cortex. Connections of the thalamus with the limbic system affect mood, behavior and memory (2)

Hypothalamus is part of the diencephalon and forms the walls and base of the lower part of the third ventricle. The hypothalamus is separated from the thalamus by a shallow groove in the wall of the third ventricle called the hypothalamic sulcus. Hypothalamus can be seen on the ventral surface of the brain, just behind the chiasma opticum (tuber cinereum and mamillary body), but its portions are located on the dorsal of the chiasma opticum. Tuber cinereum, meaning "gray bulge", is a protrusion located between the optic chiasma opticum and mamillary body. are paired structures that form the posterior part of the hypothalamus (3).

Amygdala is located in the temporal lobe of the cerebral hemisphere. It extends deep into the uncus and connects with the anterior end of the cornu inferius ventriculi lateralis. Superiorly, It is connected with the anterior part of nucleus lentiformis. Inferiorly, it is connected with the gyrus semilunaris, gyrus ambiens and gyrus uncinatus, namely the anterior part of the gyrus parahippocampalis. The anterior end of the nucleus caudatus is connected with the lower end of the stria terminalis. There is a region of substriatal gray matter with cholinergic neurons in the region between the amygdala and the nucleus lentiformis These neurons make up the nucleus basalis (4).

Mamillar region includes nucleus mamillaris and nucleus hypothalamicus posterior. Three to four nucleus mamillaris combine to form the mamillary body. Mamillary body is located on the ventral surface of the

hypothalamus. Unlike other hypothalamic nuclei associated with the functions of the endocrine and / or autonomic nervous systems, the mammillary nuclei are an important target projection area that transmits emotional inputs of the hippocampal formation through the fornix. In addition, the informations are transmitted to the nuclei mamillaris via the nucleus tegmentalis anterior and posterior. The nucleus hypothalamicus posterior contains cells sensitive to the drop in blood temperature. This core acts as a "thermostat" and regulates body temperature by maintaining heat and promoting heat production. While heat is protected by vasoconstriction of the cutaneous vessels, it is produced by the increase in thyroid activity and vibration (5).

AD affects more than 35 million people around the world, and its incidence is estimated to triple by 2050. Countries with a significant number of people currently affected are China, the Western Pacific, Western Europe and the USA. 350-400 thousand in Turkey is estimated to be suffering from Alzheimer's. In 2050, according to World Health Organization data, Turkey would be the most Alzheimer's patients is one of four countries in the world. There are about 400 thousand Alzheimer's patients in Turkey. It is predicted that Alzheimer's disease will become more common with aging in the coming years. When we evaluate these patients with their families, it is seen that AD is an important public health problem affecting large masses. AD disease not only affects the person but also brings serious psychosocial and economic burden to caregivers, families and society. ADs need the support and observation of the caregiver. For this reason, caregiving family members also experience severe strain and burnout (6).

In recent years, the most commonly used imaging method in radiolocigal studies is computed tomography (CT), which measures tissue density. However, compared to CT, magnetic resonance (MR) images can provide a large number of sequences. It reflects not only the structure of the organization, but also functional metabolism and dynamic changes. MR imaging provides enhanced tissue contrast.It has a multidimensional volume and does not require radiation dose. Various MRI methods have been used to examine AD, including resting state functional MRI, voxel-based morphometry, diffusion tensor imaging, as well as arterial spin labeling. MRI is a non-invasive imaging technique that creates cross-section images of internal structures using non-ionizing electromagnetic radiation. Recently, the use of automated methods to calculate structures such as volume, cortical thickness, and subcortical segmentation of the hippocampus has increased (9). One of these methods is the morphometry analysis method and provides this service free, online, fully automated, widely used MRICloud site for large-scale multimodal processing (7).

MRICloud offers web-based volume calculation through automatic analysis of brain data. Technically, Brain Imaging Information Technology Initiative and MRI unit in hdr format are used. In addition, it creates a text report that includes the infrastructures of the brain such as cerebrospinal fluid (CSF), substantia grisea, substantia alba and brain hemispheres, cerebellum and brainstem, intracranial spaces and the volumes of tissues. Its reliability and accuracy in whole brain segmentation has been extensively tested and validated (10-11). Therefore, in our study, we used MRICloud, a widely applied neuroimaging method for free, online, fully automated, large-scale multimodal processing (8,9).

The neuropathology underlying AD has a predominantly cortical distribution, but there is some evidence of subcortical involvement in AD. It has been suggested that the role of the hippocampus and the basal ganglia in balance control is important. Neuroimaging studies have enabled researchers to clarify the brain areas responsible for the clinical symptoms of AD. Several structural factors have been associated with postural imbalances, such as ventricular size, white matter hyperintensities, whole brain atrophy, hippocampal volume, and focal atrophy of the fronto-parietal or sensorimotor regions. However, despite the evidence for the role of subcortical structures in postural control, subcortical structures have not been the focus of previous studies. Finally, we aimed to determine the role of subcortical structures in AD. In the literature, there are studies assuming that specific subcortical structures will show significant volume loss in AD patients compared to postural imbalance (10)

In our study, we wanted to examine how Thalamus, Hypothalamus, Amygdala, mamillary body, which connects both hemisphere structures, are affected in patients with Alzheimer's disease. We used mrıcloud assisted morphometry analysis as the method of investigation. We think that volumetric changes occurring in these pathways may be helpful in diagnosing and staging Alzheimer's disease (7)

Materials and Methods

Approval was obtained for this study from the Non-Invasive Research Ethics Committee of Istanbul Medipol University, with decision number 170, dated February 19, 2020. According to DSM-V (Diagnostic and Statistical Manual of Mental disorders, 5 th edition) diagnostic criteria, 24 Alzheimer's patients (AH) (Mini The demographic characteristics and cranial MRI data of a total of 40 individuals, who were diagnosed with a mental test score of 24 and below and those aged 55 and cold, and 16 control group (CG) were scanned using retrospective methods. Left Telencephalon (TelenL), Right Telencephalon (TelenR), Cerebrospinal Fluid (CSF), Left Thalamus (ThalL), Right Thalamus (ThalR), Left Hypothalamus (HypoThL), Right Hypothalamus (HypoThR),

Leftgdala (AmygL), Rightgdala (AmygL) (AmygR), Left Mammillary Body (MamaL), Right Mammillary Body (MamaR), Total Amygdala (TotAmyg), Total Thalamus (TotThalam), Total Hypothalamus (TotHypoth), Total Mamillary Body (TotMam), Total Telencephalon (TotTelen), TelenL / AmygL, TelenL / ThalL, TelenL / HypoThL, TelenL / MamaL, TelenR / AmygR, TelenR / ThalR, TelenR / HypoThR, TelenR / MamaR, CSF / TotAmyg, CSF / ThalamT, CSF / TotHypoth, CSF / TotMam in total 28 data web derived from the Type 2 L5 Statistics table using the MRICloude based program. The data were evaluated in IBM SPSS Statisrtics Version 22.0 package program. Descriptive statistics and Independent Samples T Test statistical analysis methods were used in the evaluation. From the patient files; Date of birth, Gender, Diseases, drugs used, Mini mental test score and MR images were obtained.

Results

It was determined that the mean age of the AD group was 72.3 ± 7.7 years, and the mean age of KG was 68.9 ± 7.5 years. While 58% of the people in the Alzheimer's group were women, 56% of the people with CG were women (Table 1).

Table1. AH and CG average ages (years) and distribution by gender

		Alzheimer Grubu			Kontrol Grubu			p
		Ort±ss/n-%		Medyan	Ort±ss/n-%		Medyan	
Yaş		72,3 ± 7,7		72,5	68,9 ± 7,5		67,0	0,173 [t]
Cinsiyet	Kadın	14	58%		9	56%		0,896 [X²]
	Erkek	10	42%		7	44%		

[t] Bağımsız örneklem t test / [X²] Ki-kare test

MRICloud report gives the maximum, minimum and average values of TelenL, TelenR, CSF, AmygL, AmgR, ThalL, ThalR, HypoThL, HypoThR, MamL, MamR separately. We obtained TotAmyg, TotThalm, TotHypoth, TotMam, TotTelen data by collecting the right and left volume values (Table 2).

Table 2. Data of Anatomical Structures Obtained from MRICloud Report

	Min-Mak	Medyan	Ort±ss
TelenL (x10³)	347,4 - 516,7	448,6	444,5 ± 45,9
TelenR (x10³)	360,4 - 530,5	440,9	446,6 ± 43,6
CSF (x10³)	71,0 - 198,8	130,4	141,4 ± 36,5
AmygL	817,0 - 1767,0	1199,0	1204,3 ± 264,5
AmygR	821,0 - 2081,0	1300,0	1373,5 ± 293,5
ThalL	2849,0 - 5965,0	4645,0	4673,7 ± 576,0
ThalR	3618,0 - 5663,0	4690,5	4719,7 ± 505,9
HypoThL	385,0 - 584,0	510,0	508,1 ± 45,9
HypoThR	519,0 - 692,0	579,0	595,0 ± 48,7
MamL	42,0 - 105,0	75,5	74,8 ± 15,8
MamR	40,0 - 115,0	80,5	80,1 ± 18,9
TotAmyg	1665,0 - 3848,0	2481,5	2577,7 ± 541,7
TotThalam	6467,0 - 11619,0	9315,5	9393,4 ± 1046,8
TotHypoth	909,0 - 1276,0	1088,0	1103,2 ± 82,3
TotMam	91,0 - 220,0	154,0	154,9 ± 31,6

TelenL and TelenR values did not differ significantly (p> 0.05) between Alzheimer and control groups. In the Alzheimer group, DiencL, ResistanceR values were significantly lower (p <0.05) than the control group. Mesenc, Metenc, Myelen values did not differ significantly (p> 0.05) between Alzheimer and control groups. The CSF value in the Alzheimer group was significantly higher (p <0.05) than the control group. AmygL and AmgR values were significantly lower in the Alzheimer group than the control group (p <0.05). ThalL and ThalR values were significantly lower in the Alzheimer group than the control group (p <0.05). HypoThL value was significantly lower in the Alzheimer group than the control group (p <0.05). HypoThR value did not differ significantly (p> 0.05) between Alzheimer and control groups. MamL and MamR values were significantly lower in the Alzheimer group than in the control group (p <0.05). (Table 3)

Table 3. Calculation of the volume of right and left anatomical data in AH and CG

	Alzheimer Grubu		Kontrol Grubu		p	
	Ort±ss	Medyan	Ort±ss	Medyan		
TelenL (x10³)	438,1 ± 47,6	444,8	454,1 ± 43,0	466,0	0,298	t
TelenR (x10³)	440,9 ± 43,3	436,8	455,1 ± 44,1	460,8	0,298	t
CSF (x10³)	157,1 ± 32,3	156,8	117,8 ± 29,7	120,6	***0,001***	t
AmygL	1076,0 ± 200,9	1018,0	1396,8 ± 232,6	1400,5	***0,000***	m
AmygR	1259,1 ± 249,1	1194,5	1544,9 ± 276,7	1528,5	***0,002***	t
ThalL	4518,4 ± 598,5	4535,5	4906,7 ± 465,7	4920,0	***0,035***	t
ThalR	4560,3 ± 502,2	4482,0	4958,7 ± 420,7	4932,0	***0,013***	t
HypoThL	494,6 ± 47,3	487,0	528,4 ± 36,4	529,0	***0,020***	t
HypoThR	587,6 ± 37,6	579,0	606,2 ± 61,5	587,5	0,456	m
MamL	67,9 ± 13,9	65,0	85,2 ± 12,5	86,0	***0,000***	t
MamR	72,8 ± 18,0	72,0	91,0 ± 15,0	87,0	***0,002***	t

[t] Bağımsız örneklem t test / [m] Mann-whitney u test

In the Alzheimer group, TotAmyg, TotThalm, TotHypoth, TotMam, TotTelen values were significantly lower than the control group (p <0.05). The TotTelen value did not differ significantly (p> 0.05) between Alzheimer's and control groups (Table 4).

Table 4. Calculation of Total Volumes of Anatomical Data in AH and KG

	Alzheimer Grubu		Kontrol Grubu		p	
	Ort±ss	Medyan	Ort±ss	Medyan		
TotAmyg	2335,1 ± 433,4	2211,5	2941,7 ± 489,4	2866,5	***0,000***	t
TotThalam	9078,7 ± 1054,5	9152,0	9865,4 ± 864,7	9717,0	***0,018***	t
TotHypoth	1082,2 ± 75,4	1067,0	1134,6 ± 84,4	1131,0	***0,047***	m
TotMam	140,7 ± 28,2	135,0	176,2 ± 24,0	176,5	***0,000***	m
TotTelen (x10³)	879,1 ± 89,6	883,8	909,2 ± 86,9	926,8	0,298	t

[t] Bağımsız örneklem t test / [m] Mann-whitney u test

TenL / ThalL, TelenL / HypoThL, TelenR / TahlR, TelenR / HypoThR values did not differ significantly (p> 0.05) between Alzheimer's and control groups. In the Alzheimer group, TelenL / AmygL TelenL / MamaL, TelenR / AmygR, TelenR / MamaR values were significantly higher than the control group (p <0.05) (Table 5).

Tablo 5. Ratio of right and left Telencephalon volumes to anatomical formation volumes measured in AH and KG

	Alzheimer Grubu		Kontrol Grubu		p	
	Ort±ss	Medyan	Ort±ss	Medyan		
TelenL/AmygL	417,3 ± 71,9	414,5	332,4 ± 59,2	316,3	***0,000***	m
TelenL/ThalL	99,3 ± 22,4	96,0	92,8 ± 7,0	91,5	0,481	m
TelenL/HypoThL	890,3 ± 102,6	898,7	861,5 ± 86,2	845,8	0,360	t
TelenL/MamaL	6773,5 ± 1897,0	6320,4	5415,4 ± 788,4	5341,6	***0,009***	m
TelenR/AmygR	361,0 ± 68,0	359,4	302,7 ± 60,1	281,5	***0,008***	t
TelenR/ThalR	98,0 ± 15,9	95,4	91,9 ± 6,4	90,0	0,219	m
TelenR/HypoThR	751,4 ± 70,1	750,8	756,2 ± 94,0	744,2	0,659	m
TelenR/MamaR	6425,8 ± 1813,1	5824,1	5112,0 ± 866,4	5046,7	***0,004***	m

[t] Bağımsız örneklem t test / [m] Mann-whitney u test

In the Alzheimer group, CSF / TotAmyg, CSF / TotThalm, CSF / TotHypo, CSF / TotMama values were significantly higher than the control group ($p < 0.05$) (Table 6).

Table 6. Ratio of Cerebrospinal Fluid Volumes to Total Anatomical Formation Volumes Measured in AH

	Alzheimer Grubu		Kontrol Grubu		p	
	Ort±ss	Medyan	Ort±ss	Medyan		
CSF/TotAmyg	69,2 ± 18,2	69,0	41,5 ± 15,1	38,2	***0,000***	t
CSF/ThalamT	17,7 ± 4,8	18,3	12,1 ± 3,4	12,0	***0,000***	t
CSF/TotHypoth	145,3 ± 29,2	146,7	103,4 ± 22,3	102,3	***0,000***	t
CSF/TotMam	1168,2 ± 388,4	1064,6	675,4 ± 164,4	686,4	***0,000***	m

[t] Bağımsız örneklem t test / [m] Mann-whitney u test

Discussion

Cognitive impairment leading to neuropathological findings in Alzheimer's disease contributed to the concentration on the medial temporal lobe. Pathologies in other areas are likely to play a key role in impairing memory starting at the earliest stages of the disease. One of these areas is limbic thalamus.

The main nuclei of the limbic thalamus are nucleus thalamicus anterior, nucleus thalamicus laterais and nucleus dorsalis medialis. If anterior thalamic dysfunctions are present from the early stages of cognitive impairment, a larger system analysis is required. Among the various groups of thalamic nuclei, the limbic

thalamus is important for cognition. Nucleus thalamicus anterior from the thalamic nucleus shows the clearest structural changes with normal aging. Anterior thalamic dysfunctions are characterized by episodic memory loss. Structural MRI provides information on the condition of the thalamus during the progression of Alzheimer's disease and best reflects the late stages of neural dysfunction in the progression of the disease (11).

The realization that Alzheimer's disease has a long course of treatment over decades makes it desirable to examine the state of thalamus in healthy people at high genetic risk of Alzheimer's disease. At first, this logic is questionable. Because of it is 'presymptomatic', thalamic abnormalities are examined when there is no impairment in memory. In fact, memory loss in the "presymptomatic" stages is often hidden by "cognitive reserve." Presymptomatic patients may have smaller memory defects that do not reach the threshold, although they do not have a fully developed memory problem in standard neuropsychological tests. Therefore, damage to the anterior regions of the thalamus may be a critical threshold when the symptoms of Alzheimer's disease first appear (11).

Animal studies provide strong evidence that the central nervous system (CNS) directly regulates bone remodeling from the hypothalamus via the neural and neurohumoral arms. The neural arm provides hypothalamic control of bone remodeling through leptin-mediated increased sympathetic nervous system activity. The neurohumoral arm provides hypothalamic control of anterior pituitary hormones such as growth hormone (GH) and insulin-like growth factor-1 (IGF-1). There are studies showing that low bone density is associated with low hypothalamus volumes in early stage AD. The hypothalamic structural change associated with AD, bone remodeling is thought to alter the neural and neurohumoral regulatory systems and cause bone loss. A moderate relationship has been observed between hypothalamic atrophy and bone loss. Atrophy in the hypothalamus has been associated with increased leptin in the AD group (12).

Preclinical models of Alzheimer's disease (AD) show that volumetric reductions in medial temporal lobe structures occur before clinical onset. It has been observed that the risk in AD is associated with reduced volume (hippocampus / amygdala). Neuroimaging studies have observed atrophic changes in the amygdala in the early stages of AD. Both the hippocampus and amygdala are thought to be key subcortical nodes affected by AD-related neurodegeneration (13).

Alzheimer's disease (AD) is characterized by the extracellular accumulation of amyloid peptides (Aβ) and intracellular aggregation of hyperphosphorylated Tau proteins (hp-Tau). Aβ peptides have distinct

extracellular accumulation, whereas hp-Tau neurofbrillers lead to entanglement. In order to analyze the progression, timing and relationships of Tau and Aβ pathologies, the subiculo-fornico-mammillary system in the human brain was examined, and Aβ deposits, complex nodes, neurofibrillary tangles and ghost nodes were observed in the mamillary body (14).

Result

The limbic system subcortical structures cause cognitive dysfunction in neurodegenerative diseases. In the literature, pathological involvements have been observed in cognitive dysfunction in AD and in subcortical structures that play a role in the cognitive process. In addition, it has been observed that most of the hippocampal fibers in the fornix cause atrophy in the mamillary body and amyloid plaque (Aβ) accumulation in the axons extending from the fornix to the mamillary body (14).

In our study, we wanted to take attention to the fact that there may be volume changes in the subcortical structures of the limbic system in patients with Alzheimer's. The fact that the ratio of thalamus, hypothalamus, amygdala and mamillary body volumes, which are subcortical structures of the limbic system, to cerebrospinal fluid is higher in AD group than CG suggests that this ratio may be more specific in diagnosis and staging of AD. This study was conducted with a single center and a limited number of patients and control groups. Multi-center studies and more studies with AD are needed to support the reduction of thalamus, hypothalamus, amygdala and mamillary body volumes.

References

1. Huang LK, Chao SP, Hu CJ. Clinical trials of new drugs for Alzheimer disease. Journal of Biomedical
2. Singh V. Textbook of clinical neuroanatomy. Elsevier, Inc.2010,2nd Edition, Ghaziabad, NCR, Delhi, p:89.
3. Blumenfeld H. Neuroanatomy through Clinical Cases, Sinauer Associates, Inc.2010, 2th Edition, Sunderland, U.S.A.p:792-793
4. Bhuiyan PS, Rajgopal L, Shyamkishore K. Limbic system. In: Inderbir Singh's Textbook of Human Neuroanatomy. Eds: Bhuiyan PS, Rajgopal L,Shyamkishore K. Jaypee Brothers Medical Publishers. Inc.2014,9th Edition, Mumbai, Maharashtra, India, p:215
5. Patestas MA, Gartner LP. Blackwell Science Ltd a Blackwell Publishing Company. İn:A Textbook of Neuroanatomy.Inc. 2006, First Edition, MA, USA, P:370
6. Sengoku R. Aging and Alzheimer's disease pathology. Neuropathology. 2019; doi:10.1111/neup.12626
7. Rezende TJR, Campos BM, Hsu J, Li Y, Ceritoglu C, Kutten K, Faria AV.Test–retest reproducibility of a multi-atlas automated segmentation tool on multimodality brain MRI. Brain and Behavior. 2019; 9(10): e01363
8. Feng Q, Chen Y, Liao Z,Jian H, Mao D,Wang M, Yu E , Ding Z. Corpus Callosum Radiomics-Based Classification Model in Alzheimer's Disease: A Case-Control Study. Front. Neurology.2018;

9. McGinley LM, Kashlan ON, Chen KS, Bruno ES, Hayes JM, Backus C, Feldman EL. Human neural stem cell transplantation into the corpus callosum of Alzheimer's mice. Annals of Clinical and Translational Neurology.2017); 4(10), 749–755
10. Lee YW, Lee H, Chung IS & Yi HA. Relationship between postural instability and subcortical volume loss in Alzheimer's disease. Medicine.2017; 96(25), e7286.
11. Aggleton JP, Pralus A, Nelson AJD, & Hornberger M. Thalamic pathology and memory loss in early Alzheimer's disease: moving the focus from the medial temporal lobe to Papez circuit. Brain.2016;139(7), 1877–1890. doi:10.1093/brain/aww083
12. Loskutova, N., Watts, A. S., & Burns, J. M. The cause-effect relationship between bone loss and Alzheimer's disease using statistical modeling. Medical Hypotheses. 2019;122, 92–97
13. Murray AN, Chandler HL, & Lancaster TM. Multimodal hippocampal and amygdala subfield volumetry in polygenic risk for Alzheimer's disease. Neurobiology of Aging.2021;98, 33–41.
14. Thierry M, Boluda S, Delatour B, Marty S, Seilhean D, Duyckaerts C. Human subiculo-fornico-mamillary system in Alzheimer's disease: Tau seeding by the pillar of the fornix. Acta Neuropathologica.2019; doi:10.1007/s00401-019-02108-7

Second International Congress on Biological and Health Sciences
ONLINE 24-25-26-27 FEBRUARY 2022

Preoperative Pulmonary Rehabilitation in Lung Transplant Candidates: Scoping Review

Esra PEHLİVAN

University of Health Sciences, Faculty of Hamidiye Health Sciences, Department of Physiotherapy and Rehabilitation, Istanbul, Turkey

Corresponding author: esra.pehlivan@sbu.edu.tr, fztesrakambur@yahoo.com

Abstract:
Implementation of pulmonary rehabilitation (PR) during the waiting period for lung transplantation (LTx) is one of the routine applications of transplantation centers. There are few studies related to PR practices in this period. The content and effects of PR vary in these cases in the terminal stage. The aim of this study is to examine the effectiveness of PR in lung transplant candidates. Before February 2022, two main databases were searched: PubMed and Web of Science. The search was limited to in the last 5 years. Articles on pulmonary rehabilitation in lung transplant candidates were included. Key words were "lung transplantation", "preoperative" and "pulmonary rehabilitation". A total of 20 articles were found without time constraints. When the time interval was chosen as the last 5 years, a total of 5 articles were identified. After reading the full texts, 2 studies were found that fulfil the inclusion criteria. One of these articles was a review and one was a randomized controlled trial. In the review study, researchers were reporting positive effects of PR on quality of life and exercise capacity. The second study was a randomized controlled trial and it was reported that PR improved exercise capacity, muscle strength and decreased the perception of dyspnea. Preoperative PR has positive effects on the clinical status of the waiting list LTx candidates. Preoperative PR improves the exercise capacity and muscle strength of the patients and positively affects the quality of life. More randomized controlled studies and meta-analyses are needed on this subject.

Keywords: lung transplantation, pulmonary rehabilitation, exercise, quality of life.

1. Introduction

Lung transplantation is the last treatment option in terminal respiratory patients. Preparation for lung transplantation is extremely important to increase the success of surgery. In this period, it is aimed to bring the patient to the optimal health status (Spruit, Singh et al. 2013).

Pulmonary rehabilitation (PR) are multidisciplinary programs that help to safely improve the physical condition of chronic respiratory patients (Nici, Donner et al. 2006, Maltais, Decramer et al. 2014, Holland, Cox et al. 2021). Although it has been shown to be effective in many chronic respiratory diseases such as chronic obstructive pulmonary disease, interstitial lung disease and cystic fibrosis, information on the results of rehabilitation practices in lung transplantation is limited (Yeung and Keshavjee 2014, Weill, Benden et al. 2015).

The aim of the study is to examine the content and effectiveness of pulmonary rehabilitation (PR) practices during the waiting period for lung transplantation.

2. Materials and Methods

This study was a scoping review. Before February 2022, two main databases were searched: PubMed and Web of. The search was limited to in the last 5 years. Articles on pulmonary rehabilitation in lung transplant candidates were included. Key words were "lung transplantation", "preoperative" and "pulmonary rehabilitation". The full texts of the articles were examined. Studies that did not meet the inclusion criteria were excluded. The methodologies of the articles were reviewed and summarized.

3. Results

A total of 20 articles were found without time constraints. When the time interval was chosen as the last 5 years, a total of 5 articles were identified. After reading the full texts, 2 studies were found that fulfil the inclusion criteria.

One of these was a review study (Hoffman, Chaves et al. 2017). Two review authors independently selected the studies, assessed study quality and extracted data. Studies in any language were included. Researchers searched the Cochrane Library, MEDLINE, EMBASE, CINAHL and PEDro databases. 2 RCTs, and two quasi-experimental and two retrospectives studies, involving 1305 participants were included in the review. 5 studies included an enhancement reported in quality of life using the Short Form 36 questionnaire. All studies included exercise capacity evaluated through 6 min walk test and in five of them, there were improvements in this outcome after PR. The researchers were reporting positive effects of PR on quality of life and exercise capacity.

The second study was a randomized controlled trial (Pehlivan, Balci et al. 2018). Thirty-nine cases with a mean age of 36 years were included in the study. The content of the program included aerobic training, peripheral muscle strengthening and breathing exercises. All patients underwent preoperative pulmonary rehabilitation for at least 3 weeks. In pulmonary rehabilitation outcome evaluations, a decrease in dyspnea, an increase in exercise capacity and peripheral muscle strength, an improvement in quality of life and a decrease in depression were detected. As a result, researchers report that PR increases exercise capacity, muscle strength and decreases the perception of dyspnea.

Table 1. Summary of the articles.

	Study Type	Number of the cases	Pulmonary rehabilitation program content	Results
Hoffman at al.	Systematic Review	1305	Aerobic exercise training and/or resistance exercise training.	QOL↑ Exercise capacity↑
Pehlivan at al.	RCT	39	Aerobic training, peripheral muscle strengthening and breathing exercises.	QOL↑ Exercise capacity ↑ Dyspnea↓ Peripheral muscle strength↑

RCT: randomized controlled trial, QOL: quality of life

4. Discussion

Lung transplantation is a surgical intervention performed to prolong survival in individuals with advanced lung diseases such as chronic obstructive pulmonary disease (COPD), cystic fibrosis, idiopathic pulmonary fibrosis, and pulmonary hypertension (Kugler, Gottlieb et al. 2013). Patients who are considered to have an indication for transplantation by a chest diseases specialist are referred to the transplantation center. Here, a detailed examination is carried out and the transplant is placed on the waiting list. Surgery is performed when a suitable donor is found.

Pulmonary rehabilitation is a comprehensive intervention designed to improve not only exercise, education and behavioral changes, but also the physical and psychological state of individuals, based on detailed patient evaluation and subsequent patient-specific therapies in individuals with chronic respiratory disease (Spruit, Singh et al. 2013). PR is also routinely applied in lung transplant candidates.

In the British Thoracic Society (BTC) 2013 guideline, PR should be used to reduce dyspnea (evidence level A), supervised (evidence level A) and supervised at least twice a week (evidence level D), include strength and endurance training in the program. It is emphasized that it is necessary (evidence level B) and that it can be applied intermittently and continuously (evidence level A) (Bolton, Bevan-Smith et al. 2013).

There are no guidelines on how to exercise and patient education in patients who will undergo LTx. Programs similar to general PRs in chronic diseases are implemented (Downs 1996, Spruit, Singh et al. 2013). It is noteworthy that aerobic and peripheral muscle strengthening programs were chosen similarly in the studies reviewed in this review.

Exercise capacity is severely restricted in lung transplant candidates. This is primarily due to the inability of the ventilatory and circulatory system to meet the increased demand with exercise. In these patients, minute

ventilation is increased, pulmonary mechanisms are insufficient, and early oxygen desaturation is observed (Oelberg, Systrom et al. 1998, Systrom, Pappagianopoulos et al. 1998). The common result of the two studies mentioned is that the exercise capacity of the patients increased.

The quality of life is greatly reduced in terminal lung patients. There is also a decrease in the quality of life in transplant candidates and in the post-transplant period. In the pre-transplant period, the quality of life of patients whose mobility, daily living activities are reduced and their occupational, social and emotional relationships are affected in relation to the disease symptoms also decreases (Feltrim, Rozanski et al. 2008). It was reported that the quality of life of the cases increased in the randomized controlled studies and compilation studies included in the review.

5. Conclusion

Implementation of pulmonary rehabilitation during the waiting period for lung transplantation improves the exercise capacity and peripheral muscle strength of the patients and reduces the perception of dyspnea. These positive improvements in patient clinics have positive effects on quality of life. More randomized controlled studies and meta-analyses are needed on the subject.

6. References

1. Spruit MA, Singh SJ, Garvey C, et al. An official American Thoracic Society/European Respiratory Society statement: key concepts and advances in pulmonary rehabilitation. American journal of respiratory and critical care medicine. Oct 15 2013;188(8):e13-64.

2. Holland AE, Cox NS, Houchen-Wolloff L, et al. Defining Modern Pulmonary Rehabilitation. An Official American Thoracic Society Workshop Report. Annals of the American Thoracic Society. May 2021;18(5):e12-e29.

3. Maltais F, Decramer M, Casaburi R, et al. An official American Thoracic Society/European Respiratory Society statement: update on limb muscle dysfunction in chronic obstructive pulmonary disease. American journal of respiratory and critical care medicine. May 1 2014;189(9):e15-62.

4. Nici L, Donner C, Wouters E, et al. American Thoracic Society/European Respiratory Society statement on pulmonary rehabilitation. American journal of respiratory and critical care medicine. Jun 15 2006;173(12):1390-1413.

5. Weill D, Benden C, Corris PA, et al. A consensus document for the selection of lung transplant candidates: 2014--an update from the Pulmonary Transplantation Council of the International Society for Heart and Lung Transplantation. The Journal of heart and lung transplantation : the official publication of the International Society for Heart Transplantation. Jan 2015;34(1):1-15.

6. Yeung JC, Keshavjee S. Overview of clinical lung transplantation. Cold Spring Harbor perspectives in medicine. Jan 1 2014;4(1):a015628.

7. Hoffman M, Chaves G, Ribeiro-Samora GA, Britto RR, Parreira VF. Effects of pulmonary rehabilitation in lung transplant candidates: a systematic review. Feb 3 2017;7(2):e013445.

8. Pehlivan E, Balci A, Kilic L, Kadakal F. Preoperative Pulmonary Rehabilitation for Lung Transplant: Effects on Pulmonary Function, Exercise Capacity, and Quality of Life; First Results in Turkey. Experimental and clinical

transplantation : official journal of the Middle East Society for Organ Transplantation. Aug 2018;16(4):455-460.

9. Kugler C, Gottlieb J, Warnecke G, et al. Health-related quality of life after solid organ transplantation: a prospective, multiorgan cohort study. Transplantation. Aug 15 2013;96(3):316-323.

10. Bolton CE, Bevan-Smith EF, Blakey JD, et al. British Thoracic Society guideline on pulmonary rehabilitation in adults. Thorax. Sep 2013;68 Suppl 2:ii1-30.

11. Downs AM. Physical therapy in lung transplantation. Physical therapy. Jun 1996;76(6):626-642.

12. Systrom DM, Pappagianopoulos P, Fishman RS, Wain JC, Ginns LC. Determinants of abnormal maximum oxygen uptake after lung transplantation for chronic obstructive pulmonary disease. The Journal of heart and lung transplantation : the official publication of the International Society for Heart Transplantation. Dec 1998;17(12):1220-1230.

13. Oelberg DA, Systrom DM, Markowitz DH, et al. Exercise performance in cystic fibrosis before and after bilateral lung transplantation. The Journal of heart and lung transplantation : the official publication of the International Society for Heart Transplantation. Nov 1998;17(11):1104-1112.

14. Feltrim MI, Rozanski A, Borges AC, Cardoso CA, Caramori ML, Pego-Fernandes P. The quality of life of patients on the lung transplantation waiting list. Transplantation proceedings. Apr 2008;40(3):819-821.

Second International Congress on Biological and Health Sciences
ONLINE 24-25-26-27 FEBRUARY 2022

An indigenous animal genetic resource: Oriental pigeon

Evren ERDEM[1], Fatma Tülin ÖZBAŞER BULUT[2], Eser Kemal GÜRCAN[3], Mehmet İhsan SOYSAL[3]

[1]University, Faculty of Veterinary Medicine, Department of Animal Husbandry, Kırıkkale, Turkey; [2]Tekirdağ Namık Kemal University, Faculty of Veterinary Medicine, Department of Animal Husbandry, Tekirdağ, Turkey; [3]Tekirdağ Namık Kemal University, Faculty of Agriculture, Department of Animal Husbandry, Tekirdağ, Turkey.

Corresponding author: evrenerdem@kku.edu.tr

Abstract:

This study aimed to determine the morphological characteristics of the Oriental pigeon, which is one of our indigenous animal genetic resources. The research was carried out on the oriental pigeon genotype in the hands of the breeder in Tekirdağ, Balıkesir provinces, and Lüleburgaz district, with the ethics committee decision of Tekirdağ Namık Kemal University (2017/09). The study consisted of 100 pigeons (52 male and 48 female) from seven different breeders. Each pigeon was morphologically examined in detail and body measurements were determined. Three eye colors (white- 75 %, white with yellow speckles - 15 %, white with red speckles 10 %) and six basic plumage colors (red- 29 %, black- 25 %, white- 23 %, yellow- 11 %, ashy or smoky- 5 %, tiger or speckled- 7 %) were identified in this pigeon genotype. Head length, beak length, beak depth, thoracic perimeter, tarsus diameter were significantly affected by sex and age group ($P < 0.01$; $P < 0.001$). Except for body length, male pigeons showed higher values than female pigeons. As a result of the present study, it is possible to say that the plumage color of Oriental pigeons is higher in percentages of red, black and white, and the body structure is larger than most other indigenous pigeon genotypes/breeds (Bursa oynarı, Cakal, Mulakat, Thrace roller, Alabadem and Muradiye Dönek pigeons). We suggest that the Oriental pigeon genotype should be preserved as an indigenous breed. Also, the relationship of the Oriental pigeon genotype with other pigeon genotypes bred in the Marmara region, and then with other breeds in Turkey should be revealed by genetic studies.

Keywords: Indigenous genetic resource, pigeon, Turkey

1. Introduction

The geography of Turkey the cradle of many civilizations, has a historical and geographical structure that includes many indigenous domestic genetic resources. One of these genetic resources is the pigeon, which has been traditionally bred in these lands for centuries. The traditional structure of pigeon breeding in Turkey has been transferred to the lower generations by the competent for centuries. People who have dealt with pigeon breeding for many years and transfer their experiences to each other are called fanciers (‘meraklı’ in Turkish). With the intensive and regular selection studies carried out by pigeon fanciers according to the desired traits (body traits, ornamental or flight display), many genotypes and breeds have emerged today. Oriental pigeons belong to the ‘roller pigeon’ group. These pigeons are famous for their aerial display characteristics. Ornamental features are of secondary importance. There have not been enough scientific studies on pigeons, which are considered an indigenous animal genetic resource. In recent years, some researchers have started to do research on domestic pigeon breeds in Turkey (Balcı et al. 2018, Erdem et al. 2018, Erdem et al. 2021, Özbaşer et al. 2016, Özbaşer et al. 2021, Soysal et al. 2011, Yıldırım et al. 2018). The study aimed to determine the morphological and morphometric characteristics of oriental pigeons, one of our indigenous animal genetic resources.

2. Materials and Methods

The research was carried out on the oriental pigeon genotype in the hands of the breeder in Tekirdağ, Balıkesir provinces, and Lüleburgaz district, with the ethics committee decision of Tekirdağ Namık Kemal University (2017/09). The study consisted of 100 pigeons (52 male and 48 female) from seven different breeders (14, 17, 27, 10, 8, 11, and 13 pigeons per breeder, respectively). The ages of pigeons were classified into four groups: 10 - 23 months of age (age group I), 24 - 35 months of age (age group II), 36-47 months of age (age group III), and 48 months and over (age group IV). Each pigeon was morphologically examined in detail concerning its plumage color, head type, eye color, head crest, presence or absence of head marks and body marks, wing and tail marks, and the presence or absence of muffs. Plumage color names of the pigeons were described as a result of consultation with local breeders. Body characteristics (Body weight, body length, trunk length, head length, head width, beak length, beak depth, chest depth, chest width, thoracic perimeter, wing length, wing span, tail length, and tarsus diameter) were determined individually for each pigeon (Erdem et al. 2021, Özbaşer et al, 2020). Effects of sex and age group on body weight and morphometric measurements were analyzed by using the *General Linear Model (GLM).* If GLM showed an acceptable level of significance ($P < 0.05$), Tukey's test was applied for post hoc comparison. Statistical analyses were performed using SPSS for Windows. A value of $P < 0.05$ was considered statistically significant (Dawson and Trapp 2011).

3. Results

The body structure of the Oriental pigeon genotype is long rectangular, and it has a specific body posture. The tail is withholding almost perpendicular to the horizontal line of the body in a normal posture, and the wings are kept below the horizontal line of the body, not touching the ground. Oriental pigeons did not have a 'crest'. The Oriental pigeons had leg feathers referred to as spats ('tozluk' in Turkish). Three eye colors (white - 75 %, white with yellow speckles - 15 %, white with red speckles 10 %) and six basic plumage colors (red, black, white, yellow, ashy or smoky, tiger or speckled were identified in this pigeon genotype. Red (plumage color was red) (29 %) (Figure 1. c), black (plumage color was black) (25 %) (Figure 1. a), white (plumage color was white) (23 %) (Figure 1. b), yellow (plumage color was yellow) (11 %) (Figure 1. f), ashy or smoky (body plumage grayish-blue with two transverse rows of dark stripes on the wings) (5 %) (Figure 1. d), tiger or speckled (plumage color was white, and the presence of irregular-shaped black, red or gray spots on the plumage color) (7 %) (Figure 1. g,h,ı) were classified as plumage colors (Table 1). Head length, beak length, beak depth, chest circumference, and tarsus diameter were significantly affected by sex and age group. Except for body length, male pigeons showed higher values than female pigeons ($P < 0.01$; $P < 0.001$) While age group II was higher than other age groups in terms of head width ($P < 0.001$), beak depth ($P < 0.01$), chest width ($P < 0.001$), wingspan ($P < 0.01$), age group III was higher than other age groups in head length ($P < 0.001$), chest circumference ($P < 0.001$), and tarsus diameter ($P < 0.001$) (Table 2).

Table 1. Morphological characteristics of Oriental pigeons (%).

Morphological characteristics	Ratio (%)
Eye color	
White	**75**
White with yellow speckles	**15**
White with red speckles	**10**
Plumage Color	
Red	**29**
Black	**25**
White	**23**
Yellow	**11**
Speckled (Tiger)	**7**
Ashy (Smoky)	**5**
Number of wing feathers	
11-1-11	**87**
10-1-11	**13**
Number of tail feathers	
14	**27**
15	**30**
16	**23**
17	**11**
18	**9**

Table 2. Morphometric characteristics of Oriental pigeons (X ± $S_{\bar{x}}$).

Variation factors	n	Body weight (g)	Head length (mm)	Head width (mm)	Beak length (mm)	Beak depth (mm)	Trunk length (cm)	Tail length (cm)
Sex		***	***	-	***	***	***	-
Male	52	457,70±1,76	52,33±0,21	21,16±0,12	18,84±0,07	5,58±0,05	10,26±0,07	14,07±0,10
Female	48	438,56±2,33	50,86±0,29	21,18±0,12	18,31±0,14	5,11±0,06	9,75±0,05	14,36±0,19
Age group		-	***	***	***	**	-	-
I	37	445,74±2,65	50,68±0,28^{a}	20,98±0,16^{a}	18,08±0,16^{a}	5,24±0,09^{ab}	10,08±0,08	14,36±0,22
II	41	451,63±3,12	52,16±0,32^{bc}	21,61±0,09^{b}	18,82±0,09^{b}	5,54±0,05^{b}	10,07±0,08	14,30±0,12
III	12	451,00±2,48	52,93±0,29^{c}	20,81±0,18^{a}	18,84±0,04^{b}	5,29±0,06^{ab}	9,85±0,06	14,02±0,21
IV	10	443,00±5,28	51,34±0,38^{ab}	20,48±0,18^{a}	19,16±0,19^{b}	5,05±0,11^{a}	9,75±0,18	13,54±0,27
Grand mean	100	448,51±1,73	51,62±0,19	21,17±0,08	18,59±0,08	5,35±0,04	10,02±0,05	14,21±0,10
Variation factors	n	Chest depth (mm)	Chest circumference (cm)	Chest width (mm)	Wing length (cm)	Wing span (cm)	Body length (cm)	Tarsus diameter (mm)
Sex		***	**	-	-	-	***	***
Male	52	61,23±0,45	23,90±0,14	58,46±0,36	26,67±0,29	61,73±0,52	35,30±0,22	4,70±0,03
Female	48	58,81±0,52	23,12±0,20	57,74±0,23	26,32±0,32	62,36±0,38	40,57±0,47	4,47±0,03
Age group		-	***	***	*	**	-	***
I	37	60,34±0,83	22,47±0,16^{a}	58,62±0,37^{c}	26,01±0,39^{ab}	62,29±0,46^{b}	37,31±0,58	4,46±0,04^{a}
II	41	59,65±0,39	23,98±0,15^{b}	58,64±0,27^{c}	27,00±0,30^{bc}	62,84±0,48^{b}	38,68±0,60	4,69±0,03^{b}
III	12	61,29±0,65	24,76±0,33^{c}	55,62±0,53^{a}	25,41±0,49^{a}	59,25±1,03^{a}	37,88±0,96	4,72±0,07^{b}
IV	10	59,33±0,87	24,16±0,32^{bc}	57,07±0,63^{b}	27,60±0,61^{c}	61,10±1,24^{ab}	36,25±0,91	4,52±0,07^{a}
Grand mean	100	60,07±0,36	23,53±0,13	58,11±0,22	26,50±0,21	62,03±0,33	37,83±0,36	4,59±0,03

- : P > 0.05; *: P < 0.05; **: P < 0.01; ***: P < 0.001, a–c: means within a column with different letters are significantly different (P < 0.05)

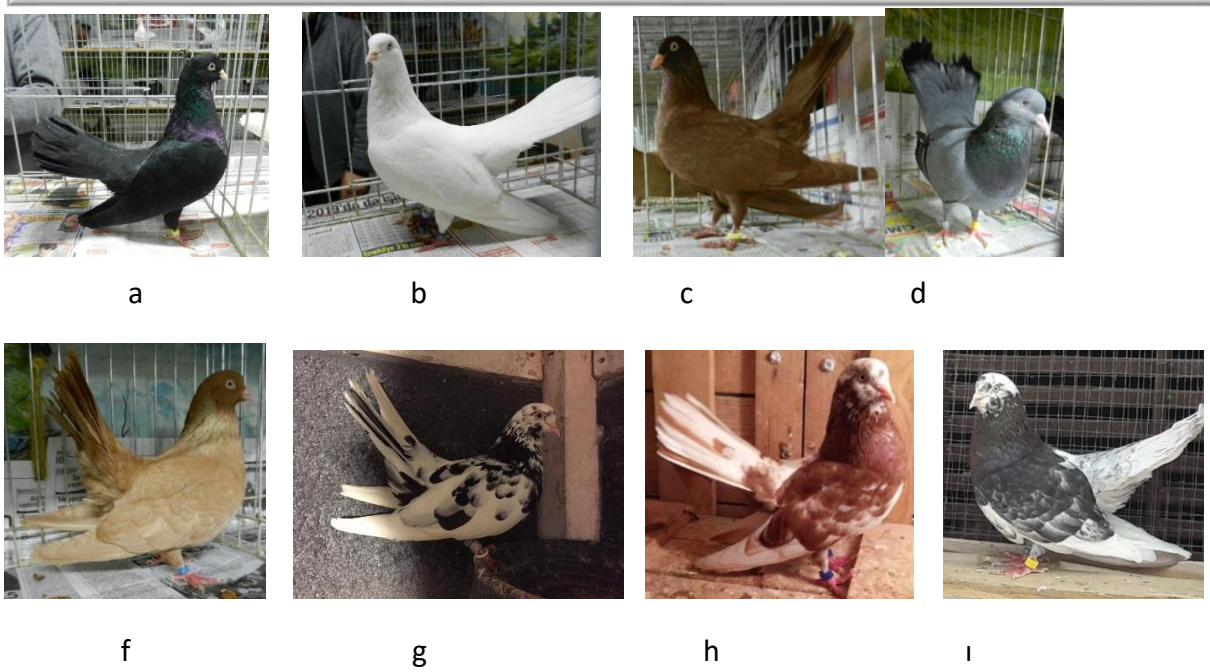

a b c d

f g h ı

Figure 1. Plumage colors of Oriental pigeons (a. Black, b. White, c. Red, d. Ashy/smoky f. Yellow, g. Black speckled, h. Red speckled, ı. Grey speckled)

4. Discussion

The ashy/smoky body plumage in Oriental pigeons (5 %) is identical to the blue plumage color found in Mulakat pigeons (79 %). In addition, it is possible that the red plumage color in Oriental pigeons (29 %) and the red plumage color, which covers most of the body in Cakal pigeons (100 %) are mutual traits. Many pigeon breeds/genotypes in Turkey have a body color called ‘speckled’, which can be considered a common trait. This body color is defined as tiger (kaplan in Turkish) in Oriental pigeons (7 %), ‘şeş’ in Edremit Kelebek roller pigeons (7 %), and kesper (keşbir in Turkish) in Squadron flyer pigeons (43.88 %). In the present study, the values obtained for the body weight (448,51 g), head width (21.17 mm), chest circumference (23,53cm), chest width (58.11 mm), body length (37,83 cm), and tarsus diameter (4,59 mm) in Oriental pigeons were higher than the Alabadem (321.17g, 18.67 mm, 19.78 cm, 51.70 mm, 31.56 cm, and 3.50 mm, respectively), Cakal (374.02 g, 18.94mm, 20.58 cm, 49.03 mm, 33.60 cm, and 4.25 mm, respectively), Mulakat (328.96 g, 19.03 mm, 20.87 cm, 51.02 mm, 34.23 cm, and 4.61 mm) and Muradiye Dönek pigeons (319.74 g, 18.56 mm, 19.34 cm, 49.94 mm, 35.10 cm, and 3.51 mm) (Erdem et al. 2018; Erdem et al., 2021; Özbaşer et al., 2016; Özbaşer et al., 2020; Özbaşer et al., 2021). As a result of the intense selection made by the fanciers with the desired characteristics (body structure, ornamental traits, and flight display) there is a high variation in terms of morphological characteristics among Turkey's indigenous pigeon genotypes. It may be possible to predict common traits by comparing studies. However, the relationship among genotypes should be determined by genetic studies.

5. Conclusion

As a result of the present study, it is possible to say that the plumage color of Oriental pigeons is higher in percentages of red, black and white, and the body structure is larger than most other indigenous pigeon genotypes/breeds (Alabadem, Bursa oynarı, Cakal, Mulakat, Thrace roller, and Muradiye Dönek pigeons). We suggest that the Oriental pigeon genotype should be preserved as an indigenous breed. Also, the relationship of the Oriental pigeon genotype with other pigeon genotypes bred in the Marmara region, and then with other breeds in Turkey should be revealed by genetic studies.

6. References

Balcı F, Ardıçlı S, Alpay F, Dinçel D, Soyudal B, Er M. The determination of some morphological characteristics of Bursa Oynarı pigeon breed. Ankara Üniversitesi Veteriner Fakültesi Dergisi. 2018; 65: 349-355.

Erdem H, Konyalı, C, Savaş T. Morphological characterization of Edremit Kelebek Roller Pigeons. Çanakkale Onsekiz Mart Üniversitesi Dergisi. 2018; 6 (2): 93-100.

Erdem, E., Özbaşer, F.T., Gürcan, E.K., Soysal, M.İ. The morphological and morphometric characteristics of Alabadem pigeons. Turkish Journal of Veterinary and Animal Sciences. 2021; 45: 372-379.

Özbaşer FT, Atasoy F, Erdem E, Güngör İ. Some morphological characteristics of squadron flyer pigeons (*Columba livia domestica*). Ankara Üniversitesi Veteriner Fakültesi Dergisi. 2016; 63: 171-177.

Özbaşer, F.T., Erdem, E., Gürcan, E.K., Soysal, M.İ. Morphological Characteristics of the Cakal, Mulakat and Oriental Pigeon Breeds Raised in the Marmara Region of Turkey. Agricultural Science Digest. 2020; 40 (3): 303-310.

Özbaşer, F.T., Erdem, E., Gürcan, E.K., Soysal, M.İ. The morphological characteristics of the Muradiye Dönek pigeon, a native Turkish genetic resource. Ankara Üniversitesi Veteriner Fakültesi Dergisi. 2021; 68: 107-112.

Soysal Mİ, Gürcan EK, Akar T, Alter K, Genç S. The determination of several morphological features of Thrace Roller Breeds in raised Thrace Region. Tekirdağ Ziraat Fakültesi Dergisi. 2011; 8(3): 61-68.

Yıldırım H, Dogan U, Cımrın T. Determination of the morphological characteristics of Scandaroon Pigeon grown in the central of Hatay Province *(Columba livia domestica).* The Eurasia Proceedings of Science, Engineering & Mathematics (EPSTEM). 2018; 2: 368-375.

Second International Congress on Biological and Health Sciences
ONLINE 24-25-26-27 FEBRUARY 2022

Methods Used in Detection of Carbapenemase Production

Hamide Kaya[1]

[1]Mersin University Faculty of Medicine Medical Microbiology

Corresponding author: hamidekirac@gmail.com

Abstract:
In recent years, the increase in hospitalization rates and the prevalence of hospital infections have made it difficult to control infections with resistant bacteria. Carbapenem-resistant Enterobactericeae family members are frequently isolated, especially in intensive care unit patients. Rapid interpretation of culture results and rapid and accurate reporting of resistance will facilitate the control of these infections. The most common mechanism of resistance to carbapenems is the production of carbapenemases. In this review, it is aimed to examine the methods used in the detection of resistance in carbapenemase producing isolates. Carbapenemases include class A, class B, and class D beta-lactamases in the Ambler classification. Class D beta-lactamases are more common in Turkey in epidemiological studies. In particular, OXA-48 is the most common carbapenemase. The phenotypic and genotype of carbapenemases can be determined by many methods. It is phenotypically defined by combined disk diffusion test, biochemical tests, immunochromatographic methods, modified Hodge test, chromogenic media and MALDI-TOF MS. Resistance gene regions can be detected by polymerase chain reaction or sequence analysis, which is one of the genotypic methods. Combined disk diffusion test is the most preferred method because it is easy to apply, low cost, and standardized. Other phenotypic tests are superior to the combined disk diffusion method in that it gives faster results. However, many tests are insufficient to detect resistance in some strains. Genotypic tests are not frequently preferred because they require high cost and technical infrastructure. Rapid and accurate detection of resistance mechanisms is required for the control of infection with resistant microorganisms. There is a need to develop new techniques with higher sensitivity and specificity compared to the standard method.

Keywords: Carbapenemase, Enterobactericeae, Nosocomial infections

1. Introduction

Today, carbapenems are the members of antibiotics with the widest spectrum of activity and rapid bactericidal action. Increasing multi-resistant bacterial infections increase the need for carbapenems (Basaran 2010). Like all beta-lactams, carbapenems contain a beta-lactam ring and are separated from the others by a hydroxyethyl side chain at position 6. Because of this feature, carbapenems are extremely resistant to beta-lactamase enzymes other than metallo beta-lactamases. Carbapenems differ from penicillins in that they have a carbon atom instead of sulfur at position 1 and a double bond between C2 and C3 in the five-membered thiazolidine ring. The trans configuration of the hydroxyethyl side chain of the sixth carbon confers both its broad spectrum and resistance to beta-lactamases of carbapenem (Topcu 2017). It is known that

carbapenems are not affected by AmpC and ESBL in bacteria. Carbapenems bind to PBP. Due to their general structure, their transition to bacterial cells is very good. Carbapenems are widely used in the treatment of infections caused by many microorganisms (Budak 2012). Carbapenems bind to PBP1 and PBP2 of gram-positive and gram-negative bacteria, causing cell lysis (Topcu 2017).

2. Carbapenemases Detection by phenotypic methods

Combined Disc Method

The first developed phenotypic method. Discs or tablets contain an inhibitory substance as well as carbapenem . Class A carbapenemases It is inhibited by boranic acid, while class B carbapenemases are inhibited by ethylenediaminetetraacetic acid (EDTA) or dipicolinic acid . Avibactam inhibits the OXA-48 enzyme. However, avibactam phenotypic it is not yet included in the tests (Porres-Osante 2014, Huang). Since OXA-48 enzyme and carbapenem resistant enterobacteria are seen in our country, the newly developed avibactam containing ceftazidime avibactam combination may be a solution to resistance (Kilic 2016).

Modified Hodge Test

The Modified Hodge test, which shows the presence of carbapenemase, is a phenotypic method that is easy to study. The E.coli ATCC 25922 strain used as an indicator is adjusted at 0.5 McFarland turbidity and diluted 1:10 and spread on Müller Hinton Agar medium. 10 µg into the center of the plate ertapenem or 10 µg Strains to be tested are planted in a straight line from all four sides of the 20-25 mm long disc towards the periphery by placing the meropenem disc. Inhibition by the tested isolate after 16-24 hours incubation in an oven at 37°C The increase in reproduction at the intersection point of the zone is checked. An increase in reproduction or clover appearance is considered positive for carbapenemase production and is also known as the cloverleaf test (Eraksoy 2018). Dilution methods cannot be routinely studied and it can detect all of the KPC, OXA and MBL enzymes, but it is not a useful method in terms of not being able to distinguish enzymes. The disadvantages of the test are that it is an open to interpretation and time-dependent test, its sensitivity is not the same in every carbapenemase species, and the sensitivity and specificity of the test differ according to the type of carbapenemase produced by the bacteria. While the sensitivity of the test was found to be successful in studies performed on KPC-producing strains , it was determined that the sensitivity was lower in OXA-48 and MBL-producing strains , and the results showed differences according to the disc and medium used. ESBL or AmpC producing strains, porin loss and alterations may cause false positive results. In order to increase the sensitivity in MBL detection , zinc addition to MHA medium is also added to the medium for resistance mechanisms such as AmpC production and porin loss. Modifications of the test were developed by adding cloxacillin (Topcu 2017, Kilic 2016).

Chromogenic media

Commercially produced chromogenic media can also show the presence of carbapenemase. Chrom ID carb medium and OXA-48 chromogenic When the strains to be tested on the media are cultivated, the presence of carbapenemase is evaluated according to their color and reproduction after incubation. Compared with the disc diffusion test, which is accepted as a standard method, it was found to be highly compatible (75%) in the literature (Demircan 2021).

Carbapenem Inactivation Method

A newly developed phenotypic requiring standardization carbapenemase detection method. It is a test that is inexpensive, easy to apply, and gives fast results. A suspension is prepared from the isolate to be tested and the meropenem disc is thrown into it. Two hours later, the disc was removed and *E. coli* ATCC 25922 strain known to be susceptible to meropenem was planted in Mueller Hinton agar, disc is placed in the middle of the medium. If an area of inhibition is not visible around the disc after six hours of incubation, the tested isolate should be it is thought to produce carbapenemase and inhibit the disc (Kilic 2016).

Biochemical or colorimetric tests

The CarbaNP test is a rapid test that can demonstrate carbapenem hydrolysis in less than two hours. It is based on the demonstration of pH change using the phenol red indicator. There are many studies in the literature stating that the test has high sensitivity and specificity. The Blue-Carba test is a derivative of the Carba NP test. It gives fast results. Bromothymol blue is used βas an indicator. The -CARBA test™ is another biochemical test that gives results in less than two hours (Kilic 2016, Giske 2013).

MALDI-TOF MS

Mass spectrometry is one of the proteomic methods recommended for rapid diagnosis recently. It is widely used in microbiology laboratories due to the highly accurate identification of bacteria. It can identify carbapenemase resistance by detecting carbapenems and degradation products of bacterial suspensions. Sensitivity and specificity are 87%. Each test costs about 1-2 dollars. MALDITOF-MS-based tests cannot identify the type of carbapenemase present (Lee 2022).

Immunochromatographic tests

Carbapenemases by antigen-antibody reactions on the chromatographic card It is an immunological test to detect epitopes. Five major carbapenemases (KPC, NDM, VIM, IMP and OXA-48-like carbapenemases) can be

detected within 15 minutes with the NG-Test® CARBA 5 (NG Biotech) test. The test is 100% sensitivity, 95.3 % specificity. RESIST 4 OKNV K (Coris BioConcept) test became available in 2018. It can detect clinically important carbapenemases (KPC, NDM, VIM and OXA-48) with 99.2% sensitivity and 100% specificity (Lee 2022).

Thin-layer chromatography (TLC)

Kanlıdrere et al. et all. describe a thin layer chromatography-based method for rapid detection of β-lactamases including carbapenemases. The method relies on the examination of changes in the migration rate of βlactams in chromatography, due to degradation by β-lactamase enzymes (Kanlidere 2019).

3. Genotypic Methods

Phenotypic methods have the advantage of being easy to implement, requiring simple equipment, and being easily accessible, molecular methods are used to confirm the results. Sensitivity and specificity are high.

Polymerase chain reaction

Common carbapenemase types such as VIM, KPC, IMP, NDM, OXA-48 can be detected in a short time using single or multiple RT PCR. However, it is not possible for every laboratory to routinely study special resistance groups with these methods, due to their high cost, special hardware materials and need for experienced personnel. Another disadvantage is the inability to detect new resistance genes or variant genes that have not yet been identified. For this reason, a molecular test with a negative result; tested strains cannot conclusively demonstrate the absence of carbapenem resistance (Kilic 2016).

Oligonucleotide Hybridization

DNA hybridization method is a carbapenemase detection method with high sensitivity and specificity, which can study important subtypes quickly and accurately from an isolate. Application of the method;

1) DNA extraction

2) dUTP labeled with biotin PCR using nucleotides

3) Primer in the microchip with the oligonucleotides of the amplified gene your probes hybridization

4) reading the fluorescence of the labeled nucleotides under UV.

Validated commercial products are available for the detection of carbapenemases. It gives results in 4-7 hours. Carbapenemases such as KPC, OXA, NDM, VIM, IMP and their variants can be tested on microchips

consisting of microplates. Thus, subgroups can also be identified. The disadvantages of the test are that it requires high cost and can be applied in competent laboratories.

Molecular analysis of clonal association

Molecular methods are also used to determine epidemiological data in addition to the detection and typing of carbapenemase genes. Identification of high-risk isolates, detection of potential epidemics and spreads, investigation of clonal relationships, sporadic disease with the strain causing the epidemic. It is used to find necessary data for surveillance, such as comparing strains. “Pulsed field gel electrophoresis” (PFGE) can be used for this purpose. in PFGE specific The genome extracted with restriction enzymes is cut from certain parts. By interpreting the pattern formed by DNA fragments, clonal relationships and closeness of strains are examined. Multilocus sequence typing (MLST), which is one of the sequence analysis methods, is one of the methods that has become widespread in molecular epidemiology. It is a method based on identifying the alleles of the internal parts of bacterial structural genes in the DNA sequence. For each isolate, the alleles at the locus determine the sequence type and allelic profile. With this method, the prevalence of specific resistance genes, allelic profiles in different geographies, regional or global spread of strains can be monitored by sequence typing (Kilic 2016).

4. Conclusion

Rapid and accurate detection of resistance mechanisms is required for the control of infection with resistant microorganisms. There is a need to develop new techniques with higher sensitivity and specificity compared to the standard method.

5. References

Başaran, S., Korten, V. (2010). Doripenem: Klinik Uygulamada Yeni Bir Karbapenem. *Klimik Dergisi.* 23(1): 2-5.

Budak, S., Aktas, Z., Erdem, H. (2012). Enterik Gram-Negatif Bakterilerde Laboratuvardan Kliniğe Karbapenemazlar. *J Infect Microb Antimicrob*.

Demırcan, Şerife Altun, et al. Karbapenemaz üreten Enterobacteriaceae üyelerinin belirlenmesinde kromojenik besiyerleri ve Rapidec Carba NP testin performanslarının değerlendirilmesi.

Eraksoy, Haluk. Karbapeneme Dirençli Enterobacteriaceae İnfeksiyonlarının Tedavisi: Başka Bir Şey Var mı?. *Klimik Dergisi*, 2018, 31.1: 1.

Giske, Christian G., et al. EUCAST Klinik ve/veya epidemiyolojik önemi olan direnç mekanizmaları ve direnç özelliklerini saptama kılavuzu V 1.0 (Temmuz 2013).

Huang, T.D., et al., Evaluation of avibactam-supplemented combination disk tests for the detection of OXA-48 carbapenemase-producing Enterobacteriaceae. Diagn Microbiol Infect Dis, 2014. 79(2): p. 252-4.

Kanlıdere, Zeynep; KARATUNA, Onur; KOCAGÖZ, Tanil. Rapid detection of beta-lactamase production including carbapenemase by thin layer chromatography. *Journal of Microbiological Methods*, 2019, 156: 15-19.

Kılıç, Ü., Demiray, T., & Altındiş, M. (2016). Karbapenemaz üreten enterobacterıaceae izolatlarının saptanmasında fenotipik ve genotipik metotlar. *Ankem Derg*, *30*(2), 62-75.

Lee, Y. L., Chen, H. M., Hii, M., & Hsueh, P. R. (2022). Carbapenemase-producing Enterobacterales infections: Recent advances in diagnosis and treatment. *International Journal of Antimicrobial Agents*, 106528.

Mulazımoğlu, L. (2010). 1986'dan gunumuze karbapenemler. *ANKEM Derg*. 24:33-5.

Murray, PR., Rosenthal, KS., Pfaller, MA. (2016). Tıbbi Mikrobiyoloji. İç: Aydın, D. Antibakteriyel İlaçlar, Başusatoğlu, A., Us AD. (Çeviri Ed.), 7. Baskı. Elsevier. Ankara: Pelikan Yayıncılık.17:165-173.

Porres-Osante, N., et al., Use of avibactam to detect Ambler class A carbapenemases and OXA-48 beta-lactamases in Enterobacteriaceae. Diagn Microbiol Infect Dis, 2014. 79(3): p. 399-400. 110.

Topcu, AW., Söyletir, G., Doğanay, M. (2017). Enfeksiyon Hastalıkları ve Mikrobiyolojisi, Etkenlere Göre Enfeksiyonlar. 4 Baskı, Nobel Tıp Kitabevleri, İstanbul.

Unat, E. K. (1988). Antibiyotiklerin Tarihçesi. *Tip tarihi arastirmalari= History of medicine studies*, *2*, 102-114..

Second International Congress on Biological and Health Sciences
ONLINE 24-25-26-27 FEBRUARY 2022

Are 5G Technologies Dangerous For The Kidneys Of Diabetic Patients?

Hava Bektas[1]

[1]Department of Biophysics, Medical School of Van Yuzuncu Yil University, Van, Turkey

Corresponding author: havva0009@hotmail.com, havabektas@yyu.edu.tr

Abstract:

The aim of this study was to explore the effects of fifth-generation (5G) Radiofrequency Radiation (RFR) emitted from mobile phone on histopathological changes in the kidney of diabetic and healthy rats. The study was carried out on 28 Wistar Albino adult male rats by dividing them into four groups: Healthy Sham (n=7), healthy 5G exposure (n=7), diabetic sham (n =7), diabetic 5G exposure (n =7). In the diabetic groups, diabetes mellitus was induced with 45 mg/kg streptozotocin (STZ). Rats in the exposure group were exposed to 3500 MHz RFR for 2h per day (5 days a week) for one month. The same procedure was applied to the rats in the sham groups except the generator was turned off. All the rats were sacrificed at the end of the experiment. Kidney tissues were collected for histopathological study. The SAR (Specific Absorption Rate) value was calculated as 1,02 W/kg. It was observed that kidney tissues of rats in healthy sham and healthy 5G exposure groups had normal histological structure. Tubular dilatation, enlargement of filtration range, atrophy of tubular microvilli were observed in Diabetic sham and Diabetic 5G exposure groups compared to the control group. However, these changes were found to be higher in the Diabetic exposure group according to Diabetic sham group. It has been determined that 5G RFR can increase diabetes-induced nephropathy, but it does not cause any effect in the kidney tissue of healthy rats. Based on this study, it is important to increase public consciousness of potential adverse effects of 5G RFR exposure.

Keywords: 5.Generation Technologies, radiofrequency radiation, diabetes mellitus, kidney,

[#] This work was supported by the Van Yuzuncu Yil University (grant number TYD-2021-9598).

1. Introduction

Electromagnetic (EM) pollution has become an important environmental problem worldwide, especially over the last decade. Cell phones, wireless internet providers and other wireless communication sources are important factors that rapidly increase EM pollution in today's world. Research results on the health effects of radio frequency radiation (RFR) emitted by wireless communication sources are of increasing concern to the public every day. With the increase in the number of 5G-based base stations and the Internet of Things (IoT), there will be RFR exposure above the frequencies that have been used extensively to date. Therefore,

determining whether 5G-sourced RFR has effects on living things will be a very important scientific contribution toward the elimination of the concerns that have been raised about this issue. Studies conducted on RFR exposure have reported that causes adverse effects, such as disturbed metabolic processes (Volkow et al., 2011), cancers (Hardell and Carlberg, 2020), cardiovascular diseases (Bandara and Weller, 2017), DNA damage (Bektas et al. 2020, Zothansiama et al. 2017), increase in free radical level and oxidative stress (Dasdag and Akdag 2016, Yakymenko et al. 2016), obesity and diabetes (Milham, 2014), etc. The impact of electromagnetic field (EMF) in rats causes decreased hemoglobin oxygen-binding capacity; i.e., hypoxia does not exclude kidney damage contributions (Singh et al. 2004). The kidneys could absorb EMF from originated cell phones (Oktem et al. 2005). Because the mobile phone is usually kept in a pocket that is very close to the kidney. Current concerns on mobile phone exposure are mainly focused on the kidney. The harmful effects of RFR exposure are poorly elucidated in vital organs such as the kidney. In the present study, therefore, we evaluated potentially harmful effects of RFR emitted from wireless technologies on the kidneys of healthy and diabetic rat models. In our country and in the world, the 3.5 GHz frequency band, which is the most suitable band to meet both coverage and high speed capacity needs, is accepted. For this reason, 3.5 GHz RF signals were be used in our study. In this study, it was investigated whether 5G technology caused toxic effects in kidneys of healthy and diabetic rats with histopathological analysis.

2. Materials and Methods

2.1.Subjects and animal care

Fourteen Wistar Albino adult male rats with initial average weight of 200-250 g were acquired from the Medical Science Application and Research Center of Yuzuncu Yil University. The rats were fed with standard pelleted food (Tavas Inc., Adana, Turkey) in a standard Plexiglas cage. They were separated equally into 4 groups such as healthy sham (n=7), healthy exposed to RFR (n=7), diabetic sham (n=7) and diabetic exposed to RFR (n=7), and kept on a 14/10 h light/dark schedule. During the study, the ambient temperature (22°C) and the relative humidity (45%) were maintained in the normal range for these animals. All animal procedures were in agreement with the Principles of Laboratory Animal Care and the rules of Scientific and Ethics Committee of Yuzuncu Yil University Health Research Center.

2.2.Induction of experimental diabetes

To induce experimental diabetes, the rats were fasted overnight (diabetic groups) and then 45 mg/kg of STZ was administered i.p. at a single dose. Blood samples were taken from rats 72 hr after STZ application for diabetes control. Blood glucose levels were measured by a glucometre (IME-DC). Blood glucose levels above 250 mg/dl were considered as diabetic (Öntürk & Özbek, 2007).

2.3.Exposure and field measurements

A GSM signal generator (3500 PM10 type Everest Comp., Adapazari, Turkey), which produces 3500 MHz band RF waveform identical to the one in mobile phones was used in the study to expose the rats. Emitted power (omnidirectional on the plane perpendicular to the antenna axis) of the generator was fixed during the exposure. The antenna of the generator was equivalent to that of a typical mobile phone. The rats were confined in a Plexiglas carousel and exposed to 3500 MHz RF exposure emitted from the generator. The carousel was surrounded with electromagnetic absorber material backed by metal to isolate outdoor electromagnetic fields from the test set-up during the study duration of one month. experimental set-up is illustrated in Figure 1.

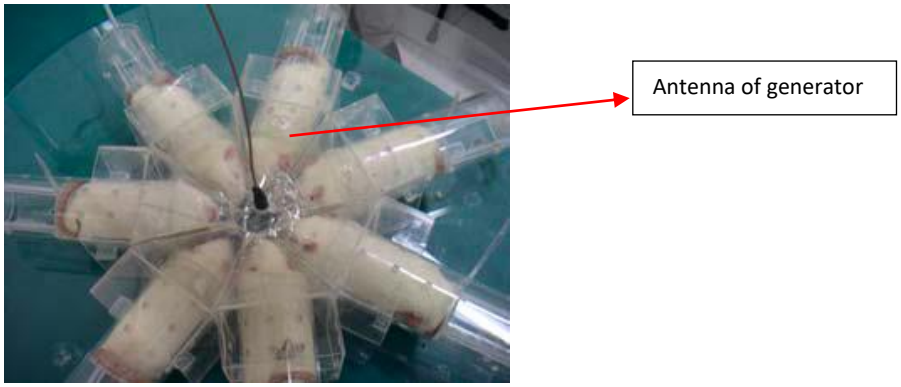

Figure 1. Exposure system.

The rats in the exposure groups were exposed to RFR 2 h per day (5 days a week) for one month. For the sham groups, the rats were placed in the carousel and the same procedure was applied to the rats except that the generator was turned off , i.e., no RF signal was present. The antenna of the generator was placed at the center of the Plexiglas Carousel to provide ideal exposure conditions. The distance of the antenna from the head of the rats was 1 cm. All rats were kept under identical conditions for one month with free access to food and water. At the end of first month, the rats were intraperitoneally administered a combination of 6 mg/kg of 2% xylazine hydrochloride (Rompun) and 75 mg/kg ketamine hydrochloride (Ketalar) for anesthesia. Afterward, the kidney of each rat was removed. All measurements, analysis and evaluations were performed by persons who were unaware of the groups so that the subsequent analysis could be performed blind.

2.4.Measurement of Power Density and Specific Absorption Rate (SAR)

Power density and electrical field measurements were performed by TES 593 (Shenzhen, Guangdong, P.R.C). Average power density around the brain was measured 3,1 W/m^2. However, electric field was measured between 39,1 V/m. The specific absorption rate was approximately calculated according to formula: SAR = $\frac{\sigma}{\rho} E^2$ (mW/g), where E is the root mean square value of the electrical field, s is the mean electrical conductivity of

tissue, and is the mass intensity. The values used to measure SAR based on article of Peyman et al. (2001)(Peyman et al., 2001). SAR value was found 1,2 W/kg, adopting $\sigma = 0.7$ S/m and $\rho = 1040$ kg/m^3.

2.5.Histopathological Evaluation

For histopathological evaluation, the kidney was fixed in 10% formalin solution. After going through routine histological tissue follow-up stages, it was embedded in paraffin. Sections of 5 µm thickness were taken on the microtome. Sections taken were stained with Hematoxylin-Eosin (HE) and examined with a light microscope (Olympus BX53, Japan). For histopathological evaluation, random sampling was made for each animal in the groups, and evaluation was made in an average of 10-12 fields. The findings were evaluated semi-quantitatively according to the degree of damage observed in the examined regions. Accordingly, It was rated as; - (normal tissue), minor damage: + (damage<25%), minor damage: ++ (25-50%), medium damage: +++ (50-75%), severe damage: ++++ (damage>75%).

3. Results

It was observed that kidney tissues of rats in healthy sham and healthy 5G groups had normal histological structure. Tubular dilatation, enlargement of filtration range, atrophy of tubular microvilli were observed in diabetic sham and diabetic exposure groups compared to the control group. However, these changes were found to be higher in the Diabetic exposure group according to diabetic sham group (Figure 2).

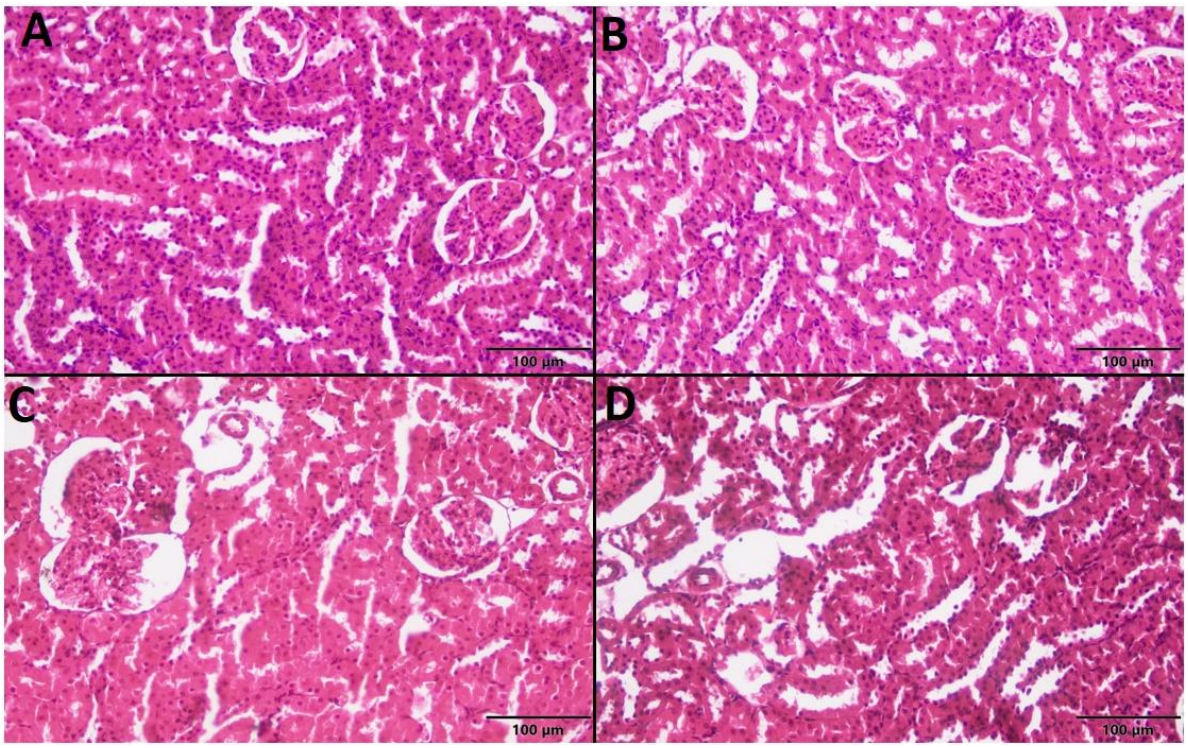

Figure 2. Light microscope images of the kidney tissues of the groups. A: Healthy Sham, B: healthy exposure, C: Diabetic sham, D: Diabetic exposure. H-E. x40.

4. Discussion

In this study, it was observed that kidney tissues of rats in healthy sham and healthy 5G groups had normal histological structure. Tubular dilatation, enlargement of filtration range, atrophy of tubular microvilli were observed in diabetic sham and diabetic exposure groups compared to the control group. However, these changes were found to be higher in the Diabetic exposure group according to Diabetic sham group.

In fact, diabetes causes histopathological changes in the kidneys through oxidative stress. Similar to our study, previous studies have reported pathological and functional changes in the kidneys in STZ-induced diabetes (Malik et al., 2017; Musabayane, 2012; Yamamoto, Nakamura, Noble, Ruoslahti, & Border, 1993). In addition, it has been stated that oxidative stress caused by hyperglycemia causes kidney damage (Kayama et al., 2015; Lee, Yu, Yang, Jiang, & Ha, 2003).

On the other hand, in this study, we found that histopathological changes caused by diabetes were more prominent in rats exposed to 5G RFR. Similarly to our results, it was reported that renal tissue was damaged due to exposure to RFR emitted from mobile phones (Al-Glaib et al. 2008). Moreover, it was stated that kidneys could mainly absorb the RFR from mobile phones because they are often carried in the belt (Oktem et al. 2005), which may influence serum creatinine level. Some studies carried on animals have shown that RFR raises serum creatinine, a marker of impaired renal tissue (Hasan et al. 2021, Morelli et al. 2005). This may be due to renal failure correlated with histopathologic changes.

In relation to histopathological alterations, Hasan et al., reported that exposure to RFR caused mononuclear cellular aggregates and intense venous congestion compared to the control mice (Hasan et al. 2021). Moreover, it was demonstrated that RFR exposure induces many atrophied glomeruli, infiltration of leucocytes between the tubules of the kidney, and vacuolation of some tubules (Bayazit 2009, Jaya et al. 2015). Chauhan et al. (2017) stated that RFR exposure causes shrunken glomeruli and irregular kidney tubules (Chauhan, Verma, Sisodia, & Kesari, 2017). It is a well-known fact that RFR lead to oxidative stress by increasing level of free radicals (Bektas et al. 2020, Dasdag and Akdag 2016). Free radicals damage the lipids of the cell and modify their composition and break protein boundary cause cell death. Oxidative stress is an important phenomenon in radiation induced tissue damage (Al-Glaib et al. 2008, Markov 2013). The histopathological changes observed in this study may be due to oxidative stress caused by both RFR and diabetes.

5. Conclusion

This study which is a preliminary investigation indicated that exposure to 5G RFR could lead to degenerative changes on kidney histopathology of diabetic rats. Comprehensive long-term studies at the molecular level are definitely required in order to draw precise conclusions.

6. References

Al-Glaib B, Al-Dardfi M, Al-Tuhami A, Elgenaidi A, Dkhil M. A technical report on the effect of electromagnetic radiation from a mobile phone on mice organs. Libyan Journal of Medicine. 2008; 3: 8-9.

Bandara P, Weller S. Cardiovascular disease: Time to identify emerging environmental risk factors. SAGE Publications Sage UK: London, England. 2017.

Bayazit V. 2009. Evaluation of potential carcinogenic effects of electromagnetic fields (EMF) on tissue and organs. Australian Journal of Basic and Applied Sciences 3:1043-1059.

Bektas H, Dasdag S, Bektas MS. Comparison of effects of 2.4 GHz Wi-Fi and mobile phone exposure on human placenta and cord blood. Biotechnology & Biotechnological Equipment. 2020; 34: 154-162.

Chauhan, P., Verma, H., Sisodia, R., & Kesari, K. K. (2017). Microwave radiation (2.45 GHz)-induced oxidative stress: Whole-body exposure effect on histopathology of Wistar rats. *Electromagnetic Biology and Medicine, 36*(1), 20-30.

Cheng J, Li F, Cui J, Guo W, Li C, Li W, Wang G, Xing X, Gao Y, Ge Y. Optimal conditions of LDR to protect the kidney from diabetes: exposure to 12.5 mGy X-rays for 8 weeks efficiently protects the kidney from diabetes. Life sciences. 2014; 103: 49-58.

Dasdag S, Akdag MZ. The link between radiofrequencies emitted from wireless technologies and oxidative stress. J Chem Neuroanat. 2016; 75: 85-93.

Hardell L, Carlberg M. Health risks from radiofrequency radiation, including 5G, should be assessed by experts with no conflicts of interest. Oncol Lett 20. 2020.

Hasan I, Amin T, Alam MR, Islam MR. Hematobiochemical and histopathological alterations of kidney and testis due to exposure of 4G cell phone radiation in mice. Saudi Journal of Biological Sciences. 2021; 28: 2933-2942.

Jaya P, Kataria S, Raichandani L, Raichandani S. A study of histological effects of chronic exposure to a 2G Cellphone Radiations (900–1900 MHz) on kidneys of albino rats. Sch. J. Appl. Med. Sci. 2015. 3: 257-260.

Kayama Y, Raaz U, Jagger A, Adam M, Schellinger IN, Sakamoto M, Suzuki H, Toyama K, Spin JM, Tsao PS. Diabetic cardiovascular disease induced by oxidative stress. International journal of molecular sciences. 2015. 16: 25234-25263.

Lee HB, Yu M-R, Yang Y, Jiang Z, Ha H. Reactive oxygen species-regulated signaling pathways in diabetic nephropathy. Journal of the American Society of Nephrology. 2003. 14: 241-245.

Malik S, Suchal K, Khan SI, Bhatia J, Kishore K, Dinda AK, Arya DS. Apigenin ameliorates streptozotocin-induced diabetic nephropathy in rats via MAPK-NF-κB-TNF-α and TGF-β1-MAPK-fibronectin pathways. American Journal of Physiology-Renal Physiology. 2017; 313: 414-422.

Markov MS. Effects of electromagnetic fields on biological systems. Taylor & Francis. p 121-122.

Milham S. 2014. Evidence that dirty electricity is causing the worldwide epidemics of obesity and diabetes. Electromagnetic biology and medicine. 2013; 33: 75-78.

Morelli A, Ravera S, Panfoli I, Pepe I. Effects of extremely low frequency electromagnetic fields on membrane-associated enzymes. Archives of biochemistry and biophysics. 2005; 441:191-198.

Musabayane C. The effects of medicinal plants on renal function and blood pressure in diabetes mellitus. South African Journal of Diabetes and Vascular Disease. 2012; 9: 114-119.

Oktem F, Ozguner F, Mollaoglu H, Koyu A, Uz E. Oxidative damage in the kidney induced by 900-MHz-emitted mobile phone: protection by melatonin. Archives of Medical Research. 2005; 36:350-355.

Öntürk, H., & Özbek, H. (2007). Deneysel diyabet oluşturulması ve kan şeker seviyesinin ölçülmesi. *Genel Tıp Derg, 17*(4), 231-236.

Peyman A, Rezazadeh A, Gabriel C. Changes in the dielectric properties of rat tissue as a function of age at microwave frequencies. Physics in Medicine & Biology. 2001; 46: 1617.

Singh M, Singh U, Singh K, Mishra A. Effect of 50-Hz powerline exposed magnetized water on rat kidney. Electromagnetic Biology and Medicine. 2004; 23: 241-249.

Volkow ND, Tomasi D, Wang G-J, Vaska P, Fowler JS, Telang F, Alexoff D, Logan J, Wong C. Effects of cell phone radiofrequency signal exposure on brain glucose metabolism. Jama. 2011; 305: 808-813.

Yakymenko I, Tsybulin O, Sidorik E, Henshel D, Kyrylenko O, Kyrylenko S. Oxidative mechanisms of biological activity of low-intensity radiofrequency radiation. Electromagnetic biology and medicine. 2016; 35: 186-202.

Yamamoto T, Nakamura T, Noble NA, Ruoslahti E, Border WA. Expression of transforming growth factor beta is elevated in human and experimental diabetic nephropathy. Proceedings of the National Academy of Sciences. 1993; 90: 1814-1818.

Zothansiama, Zosangzuali M, Lalramdinpuii M, Jagetia GC. Impact of radiofrequency radiation on DNA damage and antioxidants in peripheral blood lymphocytes of humans residing in the vicinity of mobile phone base stations. Electromagnetic biology and medicine. 2017; 36: 295-305.

Second International Congress on Biological and Health Sciences
ONLINE 24-25-26-27 FEBRUARY 2022

Effects of Medical Ozone Therapy on Xanthine Oxidase Activities in Paracetamol Treated Rats

Hakan Bağ[1], Seval Yılmaz[1], Emre Kaya[1], Feyza Aksu[2], Ahmet Kavaklı[2]

[1] Firat University, Faculty of Veterinary Medicine, Department of Biochemistry, Elazig, Turkey

[2] Firat University, Faculty of Medicine, Department of Anatomy, Elazig, Turkey

Corresponding author: hbag@firat.edu.tr

Abstract:

Paracetamol is one of the most widely used analgesics and antipyretic drugs. Paracetamol overdose has life-threatening effects on liver, kidney and heart so treatment of paracetamol-induced toxicity has life-saving importance. The aim of this study was to evaluate the efficacy of medical ozone therapy and the role of xanthine oxidase in the experimental model of paracetamol toxication. Twenty-eight healthy three-month-old male Wistar-Albino rats were used in this study. The animals were randomly divided into four experimental groups including 7 rats in each. These groups were arranged as follows: Control group, ozone group (150 µg/kg/day, i.p. for 3 weeks), paracetamol group (2 g/kg/ orally single dose) group, ozone (150 µg/kg/day, i.p. for 3 weeks)+paracetamol (2 g/kg/ orally single dose) group. Paracetamol was administered on the 21st day of ozone application. The animals were sacrificed at the end of the applications. Xanthine oxidase activity (the isoform that produces superoxide radical) was determined spectrophotometrically according to Hashimoto's method in tissues. There was a significant increase in xanthine oxidase, an important source of reactive oxygen species, activities in the blood ($p<0.001$), liver ($p<0.05$), kidney ($p<0.001$) and heart ($p<0.001$) tissues of rats treated paracetamol compared to the control group. It was determined that tissues taken from rats treated with ozone+paracetamol had lower xanthine oxidase in the blood ($p<0.001$), liver ($p<0.05$), kidney ($p<0.001$) and heart ($p<0.001$) tissues compared to the paracetamol group. This increased xanthine oxidase activity may be responsible for paracetamol-induced tissue damage. There was ozone showed protection against paracetamol-induced hepatotoxicity, nephrotoxicity and cardiotoxicity. However, before its clinical use, further studies should be planned to determine the possible side effects and long-term effects of ozone therapy.

Keywords: paracetamol, ozone therapy, xanthine oxidase, toxicity

1. Introduction

Paracetamol (N-acetyl-p-aminophenol, acetaminophen) is one of the most widely used members of the aniline family analgesic and antipyretic drug. Paracetamol is a ubiquitous and highly utilized over-the-counter

medication for the relief of pain and fever. Paracetamol is very safe when used in limited doses but the margin of safety is relatively narrow, leading to dose-dependent liver, kidney, heart injury in all mammalian species. Ninety percent of paracetamol is metabolized by glucuronidation and sulfation to non-toxic metabolites, 2% is excreted into the urine unchanged. Less than 10% of paracetamol is metabolized to reactive N-acetyl-p-benzoquinone imine (NAPQI) via the cytochrome p450 (CYP450) system. Normally, NAPQI is detoxified into harmless metabolites by conjugation of the sulfhydryl groups of glutathione (GSH) by glutathione-S-transferase into mercapturic acid, which is eliminated in the urine (Bertolini et al., 2006; Lancaster et al., 2015; Tezcan et al., 2018; Cavusoglu, 2021).

Studies have reported an additional mechanism by which NAPQI selectively inhibits electron transport system in mitochondria and leads to the cessation of ATP synthesis. All of these mechanisms result in ATP depletion and cell death. GSH can become depleted after large doses of paracetamol, allowing NAPQI to accumulate. When this happens, NAPQI interacts covalently with liver cell components, resulting in cellular toxicity and acute oxidative stress by forming reactive oxygen radicals within mitochondria. NAPQI binding to the cell membrane and sulfhydryl proteins causes liver, kidney and heart damage (Bertolini et al., 2006; Aminoshariae and Khan, 2015; Tezcan et al., 2018).

In the overdose of paracetamol, it causes severe hepatotoxicity as it is primarily metabolized in the liver. The kidneys are affected in the late stages of liver damage or rarely alone without liver damage. NAPQI is responsible for paracetamol-induced kidney damage caused by CYP450 enzyme systems. During the detoxification of this electrophilic intermediate, different conjugates are formed with sulfhydryl and glutathione moieties in cellular proteins. It has been reported that these conjugates increase oxidative damage and may be one of the mechanisms of toxicity. In parallel with the increase in oxidative stress, the consumption of antioxidant defense systems is also important for paracetamol-induced kidney damage (Hu et al., 1993).

One of the most important enzymatic sources producing reactive oxygen species in the organism is xanthine oxidase (XO). It is involved in the catabolism of purine nucleotides and catalyzes the reaction of hypoxanthine to xanthine and the oxidation of xanthine to uric acid. XO uses oxygen as the electron acceptor. Thus, hypoxanthine is converted to xanthine and xanthine into uric acid, while superoxide radical ($O_2^{\cdot-}$) and hydrogen peroxide (H_2O_2) is formed (Rootwelt et al., 1995).

Ozone is defined as three-atom molecules of oxygen (O_3). Ozone therapy is applied as a mixture of ozone and oxygen (O_3/O_2). Medical ozone has controversial and unclear effects on human cells, but recent studies have shown some beneficial effects. Medical ozone has been used for several decades in skin ulcerative lesions or

trauma, diabetic foot, arthritis, arterial obstruction, ulcerative colitis and spinal disk herniation, etc. It has been used in an empirical fashion in recent years for therapy of viral hepatitis (Li et al., 2007; León et al., 2008; Tezcan et al., 2018). The most important effect of ozone therapy is stimulation of antioxidative responses and preservation of mitochondrial integrity. In theory, the molecular effects of medical ozone therapy may protect patients from liver failure and decrease associated mortality when ozone is used at low doses (León et al., 2008; Tezcan et al., 2018)

In light of these data, we aimed to investigate the effects of ozone therapy as an antioxidant on the toxicity of paracetamol exposure by evaluating XO in the tissues of the rat.

2. Materials and Methods

In this investigation, 28 healthy adult male Wistar-Albino rats (8 weeks old, weighing 190–250 g) were used. The animals were obtained from the Firat University, Experimental Research Centre, Elazig, Turkey. The animals were kept under standard laboratory conditions (12-h light: 12-h dark and 24 ± 3°C). The protocol of this study was approved by the Local Ethics Committee. All experimental procedures were conducted in accordance with the Guide to the Care and Use of Laboratory Animals.

The rats were divided into four groups; each group containing 7 rats. Group 1 (control group) didn't receive any treatment, Group 2 (ozone group) received intraperitoneally 150 µg/kg/day ozone for 3 weeks (Siniscalco et al., 2018), Group 3 (paracetamol group) received orally 2 g/kg/single dose paracetamol (Ojo et al., 2006; Cavusoglu, 2021), Group 4 (ozone+paracetamol group) received a single dose of paracetamol before 20 days of ozone post-treatment. The ozone which was used in this study was obtained from the ozone generator. Ozone was applied to all rats once a day for 3 weeks according to their body weight. Paracetamol was administered on the 21st day of ozone application.

At the end of the administrations, rats were sacrificed and blood, liver, kidney and heart tissue samples were removed. Blood samples were taken into tubes containing anticoagulant (ethylenediaminetetraacetic acid-EDTA). After the blood samples with EDTA from which their plasma was separated were washed 3 times with saline (0.9% NaCl). After washing the erythrocytes, 0.2 ml was taken from the erythrocyte package formed and 1.8 ml of distilled water was added to it, and hemolysate was formed to study the enzyme activity. The collected liver, kidney and heart tissues were washed with physiological saline solution, diluted at a ratio of 1:10 with distilled water, and homogenised in a Potter-Elvehjem homogenizer (CAT R50D, Germany). The homogenate was centrifuged at 4°C at 3.000 rpm for 15 min to quantify XO activities. XO activity (the isoform that produces superoxide radical) was determined spectrophotometrically according to Hashimoto's method (1974) in tissues. In the experiment, after adding 2.8 ml of phosphate buffer (50 mM, pH 7.5) and 50 µl of xanthine (4 mM) to the blank and sample tubes, they were incubated at 37°C for 30 minutes. After incubation,

50 µl of sample was added to the blank tube and then 100 µl of trichloroacetic acid (TCA) was added to all tubes and the reaction was stopped. After the TCA addition, the tubes were mixed thoroughly and centrifuged at 3.800 rpm for 30 minutes. The absorbance at 293 nm was determined by taking the supernatant (Hashimoto, 1974).

In all statistical analyses, statistical significance between different groups was determined by using SPSS 22 software package. Shapiro-Wilk normality test was applied to determine whether the raw values of all the measured parameters showed normal distribution and as a result of the test, it was determined that the values in all parameters showed normal distribution. Based on the result of this test, one-way analysis of variance (ANOVA) was used to determine differences between groups, and post hoc Tukey test for paired comparisons. All values were calculated as mean ± standard error of the mean (mean ± SEM). The data obtained as a result of the study are expressed as mean and standard error. Statistically, $P<0.05$ values were accepted as significant.

3. Results

XO activities were given in Figures 1–4. XO activities in paracetamol treated groups were significantly higher than the control group in blood, liver, kidney and heart tissues. Paracetamol treated groups (group 3) showed an increase in XO activities by 23.04% ($p<0.001$), 6.82% ($p<0.05$), 13.56% ($p<0.001$), 16.97% ($p<0.001$) compared with the control group in blood, liver, kidney and heart tissues, respectively. Ozone with paracetamol treated groups provided showed a decrease in XO activity compared to the paracetamol treated groups of all tissues. Ozone improved the increased activity of XO caused by paracetamol. XO activities were significantly not different in ozone treated group (group 2) compared with the control group in all tissues.

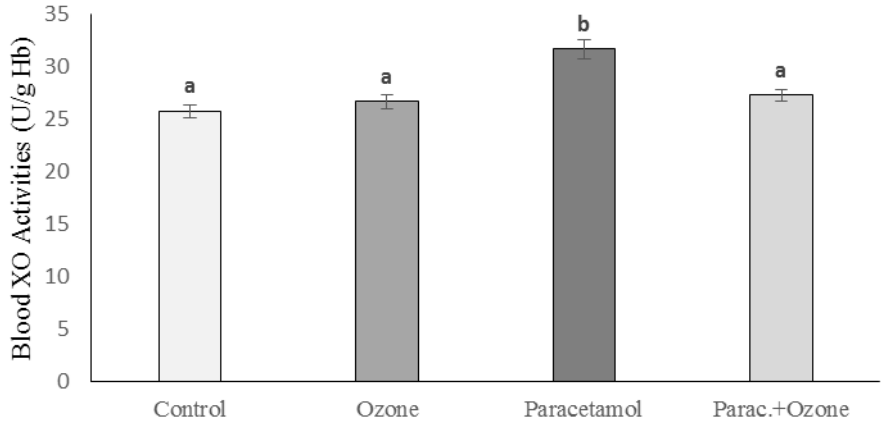

Figure 1: Effects of ozone on XO activities in blood tissue of paracetamol treated rats.

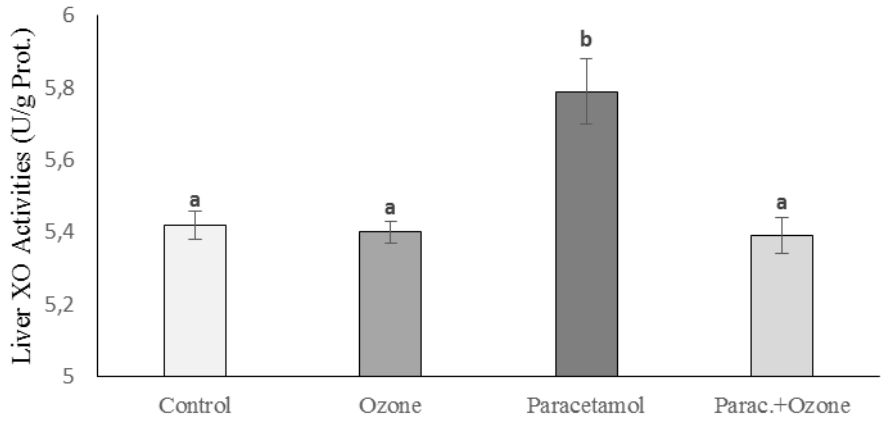

Figure 2: Effects of ozone on XO activities in liver tissue of paracetamol treated rats.

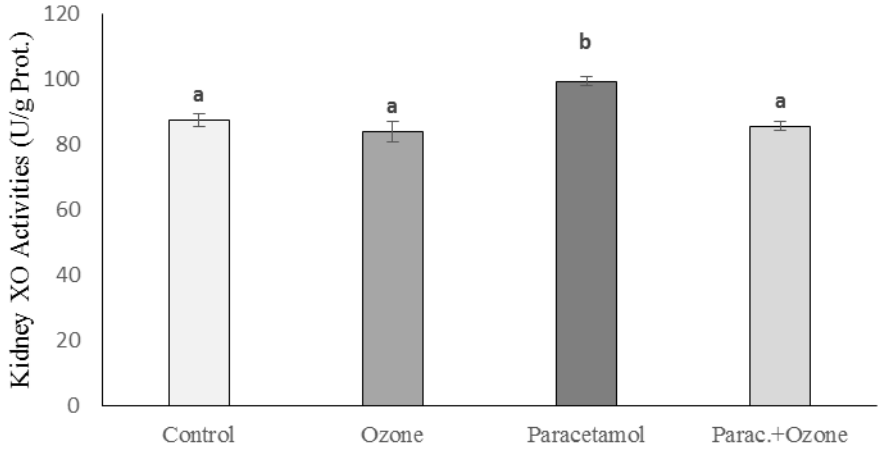

Figure 3: Effects of ozone on XO activities in kidney tissue of paracetamol treated rats.

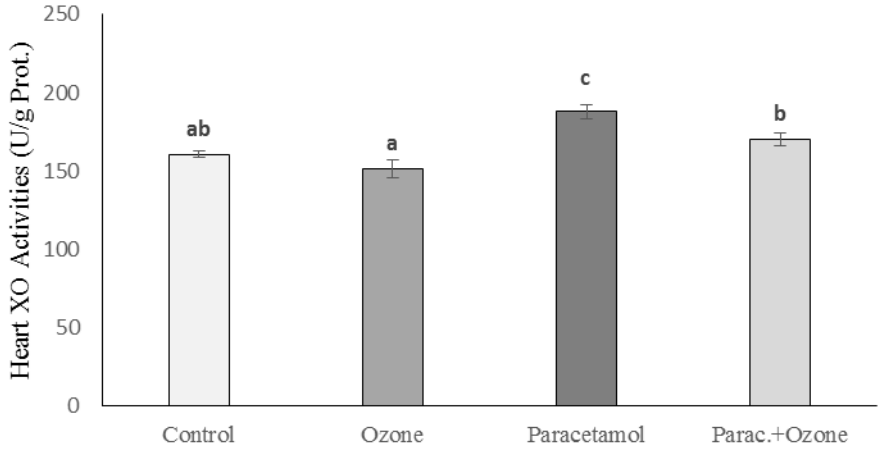

Figure 4: Effects of ozone on XO activities in heart tissue of paracetamol treated rats.

4. Discussion

Hepatic tissue injuries can be caused by generation of toxic metabolites in Phase 1 of drug metabolism, which induces the production and accumulation of reactive oxygen species (ROS). Living organisms respond to ROS by producing antioxidant enzymes, but once the free radicals and ROS exceed the regulatory ability of the body, a state of oxidative stress ensues (Atessahin et al., 2005; Yilmaz and Yilmaz, 2006; Yilmaz et al., 2018). Oxidative stress plays an essential role in liver diseases. Paracetamol it turned out to be hepatotoxic due to its very reactive intermediate (NAPQI), which is produced in the liver and kidney cells via the CYP450 metabolizing enzymes. In normal circumstances, this metabolite is detoxified by conjugating with GSH in phase 2 reactions, and only a small portion is oxidized via CYP450. In an overdose, mainly CYP450 transforms paracetamol to a highly reactive intermediary metabolite NAPQI, which overcomes the detoxification process and leads to liver, kidney cell damage. Semiquinone radicals obtained by one electron reduction of NAPQI covalently bind to molecules of the cellular membrane and increase the LPO. In this research, the effect of ozone on paracetamol-induced toxicity in rats was examined by determining its free radical scavenging activity, XO (Rašković et al., 2018; Ko et al., 2017; Tiwary et al. 2017).

The toxic effects of acetaminophen on other organ systems including the heart have also been reported. According to a report by Lip and Vale (1996), there is no decisive evidence suggesting acetaminophen overdose as having a direct cardiotoxic effect. Clinically significant disturbances of cardiac function after paracetamol poisoning have been recognized in two circumstances: First, in patients with hepatic damage who do not develop hepatic encephalopathy; secondly in association with paracetamol induced hepatic encephalopathy. There are many sparse reports of paracetamol induced cardiac effects in these two circumstances. Various cardiac effects could occur following paracetamol induced hepatic failure (Smilkstein, 1996; KhabazianZadeh et al., 2019). Price et al. (1991) describe a case of fatal paracetamol overdose which occurred in a 16-year-old female. Her serum paracetamol concentration 11.5 h post ingestion was 154 mg/L. Autopsy findings included centrilobular zonal liver necrosis, acute proximal renal tubular necrosis, and diffuse alveolar pulmonary damage. Das et al. (2010) studied the effect of taurine on paracetamol induced nephrotoxicity in mice. They observed that urea and creatinine levels were based on evaluating the effects of oxidative damage on renal function and these values increased.

XO catalyzes the conversion of xanthine to uric acid. Uric acid, an excretory product of purine catabolism, can act as a scavenger of ROS (such as hydroxyl radical ($OH^{\cdot}$) and $O_2^{\cdot-}$). Uric acid provides an antioxidant defense against oxidants and free radical-induced aging and cancer. In this study, XO activity was significantly elevated

in paracetamol-treated group compared with the control, whereas pretreatment with ozone in a dose of 150 µg/kg suppressed elevation induced by paracetamol administration. Ozone therapy showed protection against paracetamol induced hepatotoxicity, nephrotoxicity and cardiotoxicity (Pandey et al., 2003).

Ozone is administered as an O_2/O_3 mixture in medical procedures. Molecular studies demonstrated that ozone has dose-dependent effects. While high dose ozone stimulates harmful oxidative stress, low dose ozone (up to 20 mcg) stimulates antioxidant enzymes including superoxide dismutases, glutathione peroxidase, glutathione-S-transferases and catalase (Sagai and Bocci, 2011). Secondary to these findings, low dose ozone was chosen for the present study. Likewise, Costanzo et al. (2015) investigated intracellular effects of low dose ozone in an in vitro HeLa cell model. Their results showed that low concentrations of ozone had positive cellular responses in mitochondrial activation. The authors hypothesized that ozone promotes oxidative preconditioning and cells become resistant to free radicals (León et al., 1998). In another study, ozone therapy was used to investigate livers that were exposed to ionized radiation. The authors demonstrated that ozone therapy reduced lipid peroxidation and generation of free radicals which led to reduction of tissue damage associated with oxidative stress of radiation (Gultekin et al., 2013). Obstructive jaundice is another hepatocellular damage model. The effects of ozone on obstructive jaundice were found to be beneficial in this model in which ozone diminished the harmful results of hepatic fibrosis and periportal inflammation as shown by immunohistochemical examinations of the liver (Kocaman et al., 2016). Peralta et al. (1999) investigated ozone therapy which was administered via rectal insufflation in an ischemia/reperfusion model. The authors observed that ozone preserved GSH levels, increased superoxide dismutase levels as support for antioxidant defense system and maintained H_2O_2 levels. These improvements led to better liver enzyme results and lower lactate levels compared to control groups. In another study using a hepatic I/R model, it was shown that ozone protected liver by modulating endogenous nitric oxide concentrations and maintaining cellular redox balance Ajamieh et al. (2004). Ajamieh et al. (2002) compared ischemic preconditioning and ozone preconditioning on liver in terms of protecting against I/R injury. The authors found that both groups had comparable oxidative stress levels which were lower than control group. Both ischemic and ozone preconditioning groups exhibited similar protective effects including increased XO activities and attenuated malondialdehyde production which was considered to be associated with the same molecular mechanisms.

Gul et al. (2012) reported better hepatic enzyme results in the paracetamol+ozone group. Additionally, they reported on several oxidative stress markers such as malondialdehyde, superoxide dismutase and glutathione peroxidase. Based on these markers, they reported that paracetamol+ozone treatment group showed decreased oxidative stress and enhanced antioxidant defense system compared to paracetamol-alone group.

Signs of hepatic regeneration, diminished hepatic necrosis, and a significant reduction in periportal inflammation observed in group paracetamol+ozone support the biochemical analyses in terms of the healing effects of ozone.

5. Conclusion

It was concluded that ozone therapy has beneficial effects on paracetamol-induced toxicity as shown in the rat. The protective effect of ozone is shown at the tissue injury by upregulation of antioxidant defense system and beneficial effects on blood circulation and in oxygen metabolism. However, before its clinical use, further studies should be planned to determine the possible side effects and long-term effects of ozone therapy.

6. References

Ajamieh H, Merino N, Candelario-Jalil E, Menéndez S, Martinez-Sanchez G, Re L et al. Similar protective effect of ischaemic and ozone oxidative preconditionings in liver ischaemia/reperfusion injury. Pharmacol Res. 2002; 45 (4): 333-339.

Ajamieh HH, Menéndez S, Martínez- Sánchez G, Candelario- Jalil E, Re L, Giuliani A et al. Effects of ozone oxidative preconditioning on nitric oxide generation and cellular redox balance in a rat model of hepatic ischaemia–reperfusion. Liver Int. 2004; 24 (1): 55-62.

Aminoshariae A, Khan A. Acetaminophen: old drug, new issues. J Endod. 2015; 41 (5): 588-593.

Atessahin A, Yilmaz S, Karahan I, Ceribasi AO, Karaoglu A. Effects of lycopene against cisplatin-induced nephrotoxicity and oxidative stress in rats. Toxicology. 2005; 212 (2-3): 116-123.

Bertolini A, Ferrari A, Ottani A, Guerzoni S, Tacchi R, Leone, S. Paracetamol: new vistas of an old drug. CNS Drug Reviews, 2006; 12.(3-4): 250-275.

Cavusoglu B. Investigation of the effect of propolis on oxidative stress in a model of acetaminophen-induced hepatotoxicity in rats. Master thesis, Firat University Health Science Institute, Elazig, 2021.

Costanzo M, Cisterna B, Vella A, Cestari T, Covi V, Tabaracci G, et al. Low ozone concentrations stimulate cytoskeletal organization, mitochondrial activity and nuclear transcription. Eur J Histochem. 2015; 59 (2). 2515.

Das J, Ghosh J, Manna P, Sil PC. Taurine protects acetaminophen-induced oxidative damage in mice kidney through APAP urinary excretion and CYP2E1 inactivation. Toxicology. 2010; 269 (1): 24-34.

Gul H, Uysal B, Cakir E, Yaman H, Macit E, Yildirim AO et al. The protective effects of ozone therapy in a rat model of acetaminophen-induced liver injury. Environ Toxicol Pharmacol. 2012; 34 (1): 818-6.

Gultekin FA, Bakkal BH, Guven B et al. Effects of ozone oxidative preconditioning on radiation-induced organ damage in rats. J Radiat Res. (Tokyo). 2013; 54 (1): 36-44.

Hashimato S. A new spectrophotometric assay method of xanthine oxidase in crude tissue homogenate. Anal Biochem. 1974; 48: 137-145.

Hu JJ, Lee MJ, Vapiwala M, Reuhl K, Thomas P, & Yang CS. Sex-related differences in mouse renal metabolism and toxicity of acetaminophen. Toxicology and Applied Pharmacology. 1993; 122 (1): 16-26.

KhabazianZadeh F, Kazemi T, Nakhaee S, Patrick C, Mehrpour O. Acetaminophen poisoning-induced heart injury: a case-based review. Daru. 2019; 27 (2): 839-851.

Ko JW, Park SH, Shin, NR, Shin JY, Kim JW, Shin IS, Moon C, Heo JD,Kim JC, Lee IC. Protective effect and mechanism of action of diallyl disulfideagainst acetaminophen-induced acute hepatotoxicity. Food and Chemical Toxicology. 2017; 109: 28-37.

Kocaman H, Erginel B, Onder SY, Soysal FG, Keskin E, Celik A et al. The Role of Ozone Therapy in Hepatic Fibrosis due to Biliary Tract Obstruction. Eur J Pediatr Surg 2016; 26(01), 133-7.

Lancaster EM, Hiatt JR, Zarrinpar A. Acetaminophen hepatotoxicity: an updated review. Arch Toxicol. 2015; 89: 193.

León Fernández OS, Ajamieh HH, Berlanga J, Menéndez S, Viebahn-Hánsler R, Re L, & Carmona AM. Ozone oxidative preconditioning is mediated by A1 adenosine receptors in a rat model of liver ischemia/reperfusion. Transplant International. 2008; 21 (1): 39-48.

León OS, Menéndez S, Merino N, Castillo R, Sam S, Pérez L, et al. Ozone oxidative preconditioning: a protection against cellular damage by free radicals. Mediators Inflamm 1998; 7 (4): 289-294.

Li LJ, Yang YG, Zhang ZL et al. Protective effects of medical ozone combined with traditional Chinese medicine against chemically-induced hepatic injury in dogs. World J Gastroenterol. 2007; 13 (45): 5989-5994.

Lip GY, Vale JA. Does acetaminophen damage the heart? Clin Toxicol. 1996; 34 (2):145-147.

Ojo OO, Nadro MS., & Tella IO. Protection of rats by extracts of some common Nigerian trees against acetaminophen-induced hepatotoxicity. African Journal of Biotechnology. 2006; 5 (9): 755-760.

Pandey S, Parvez S, Sayeed I, Haque R, Bin-Hafeez B, Raisuddin S. Biomarkers of oxidative stress: a comparative study of river Yamuna fish Wallago attu (Bl. & Schn.). Sci Total Environ. 2003; 309 (1-3): 105-115.

Peralta C, Leon OS, Xaus C, Prats N, Jalil EC, Planell ES et al. Protective effect of ozone treatment on the injury associated with hepatic ischemia-reperfusion: antioxidantprooxidant balance. Free Radic Res. 1999; 31 (3): 191-196.

Price LM, Poklis A, Johnson DE. Fatal acetaminophen poisoning with evidence of subendocardial necrosis of the heart. J Forensic Sci. 1991; 36 (3): 930-935.

Rašković A, Bukumirović N, Paut Kusturica M, et al. Hepatoprotective and antioxidant potential of Pycnogenol® in acetaminophen-induced hepatotoxicity in rats. Phytother Res. 2018; 33 (3): 631-639.

Rootwelt T, Almaas R, Oyasaeter S, Moen A, Saugstad OD. Release of xanthine oxidase to the systemic circulation during resuscitation from severe hypoxemia in newborn pigs. Acta Paediatr. 1995; 84 (5): 507-511.

Sagai M, Bocci V. Mechanisms of Action Involved in Ozone Therapy: Is healing induced via a mild oxidative stress?. Med Gas Res. 2011; 1(1): 1.

Siniscalco D, Trotta MC, Brigida AL, Maisto R, Luongo,M, Ferraraccio F.,D'Amico M, Di Filippo C. Intraperitoneal administration of oxygen/ozone to rats reduces the pancreatic damage induced by streptozotocin. Biology. 2018; 11 (1): 10.

Smilkstein MJ. APAP-induced heart injury? Maybe yes, maybe no. next question? Clin Toxicol. 1996; 34 (2):155-156.

Tezcan AH, Ozturk O, Ustebay S, Adali Y, Yagmurdur H. The beneficial effects of ozone therapy in acetaminophen-induced hepatotoxicity in mice. Pharmacol Rep. 2018; 70 (2): 340-345.

Tiwary BK., Dutta S, Dey P, Hossain M, Kumar A, Bihani S, Nanda AK, ChaudhuriTK, Chakraborty R. Radical scavenging activities of lagerstroemia speciosa (L.) Pers. petal extracts and its hepato-protection in CCl4-intoxicated mice. BMC Complementary and Alternative Medicine. 2017; 17 (1), 55.

Yilmaz S, Kaya E, Karaca A, Karatas O. Aflatoxin B1 induced renal and cardiac damage in rats: Protective effect of lycopene. Res Vet Sci. 2018; 119: 268-275.

Yilmaz S, Yilmaz E. Effects of melatonin and vitamin E on oxidative-antioxidative status in rats exposed to irradiation. Toxicology. 2006; 22 2(1-2): 1-7.

Second International Congress on Biological and Health Sciences
ONLINE 24-25-26-27 FEBRUARY 2022

Live Weight Changes of Angora Goat Kids on Different Pasture

Hasan Hüseyin Şenyüz

Necmettin Erbakan University, Faculty of Veterinary Science, Ereğli, Konya, Türkiye

Correspond: hasansenyuzvet@yahoo.com

Abstract:

Angora goat (AG) is an important genetic source of Türkiye. It is the best adapted to Ankara region. The main yield of AG is mohair. In this study, the performance of AG kids was investigated which fed on pastures at different altitude after the weaning period. The project was carried out in the animals followed within the scope of the Ankara Goat Conservation Project on the Breeder Conditions conducted by General Directorate of Agricultural Research Policies (GDARP). For this purpose, birth, 90th and 180th days live weights (LW) of 67 kids were investigated between August and October fed in the pastures of Yalım Village in Kalecik District of Ankara. Kids remained with their mothers until 4 months of age and were fed with breast milk. They were weaned at the age of 4 months and divided into two groups; river (R, n: 30) and plateau (P, n: 37). The Irmak group were fed in the pasture at an altitude of 700 m at the coordinates 39.980794, 33.415731 and drank from the Kızılırmak river water. The plateau group, on the other hand, fed on the pasture at an altitude of 1300 m at the coordinates 40.025005, 33.374347 and drank spring water. While LW at birth and 90th days was higher in the river group than in the plateau group ($p<0.05$), LW at 180th days was higher in the plateau group ($p<0.05$). The LW of R group at birth, 90th and 180th days were respectively; 2.12±0.02, 15.59±.050 and 18.77±.43 kg. The LW of P group at the birth, 90th and 180th days were respectively; 2,03±0,02, 13,95±0,41 and 21,51±0,56 kg. As a result of the study, it was determined that the growth of grass in the high pasture is better and more efficient in the development of kids. It has been determined that the development of kids fed on high altitude pasture is better than low altitude.

Keywords: Angora goat, kid, pasture

Introduction:

Angora Goat is one of the important domestic animal resources of Turkiye. It came to Anatolia with the Turks in the 13th century. It has spread to the Ankara Region and has shown good adaptability. Therefore, its homeland is considered to be Turkey. Angora goat has been an important source of income in the Ottoman period and the Republican period of Türkiye. For this reason, it was forbidden to go abroad and taken abroad

from time to time with special permissions. The number of goat increased to 6 million and the mohair production to 10,000 tons during the time whwn it was grown (Kaynar, 2016). Although the number of goat has decreased due to different reasons such as mechanization, tendency to synthetic products, mass production demand and commercial competition especially after the European industrial revolution, the number of goat has started to increase and there are 287,020 Angora Goats now (TUİK, 2020). The number of Angora Goats and mohair production at the Ottoman and Republican periods are given in Figure 1.

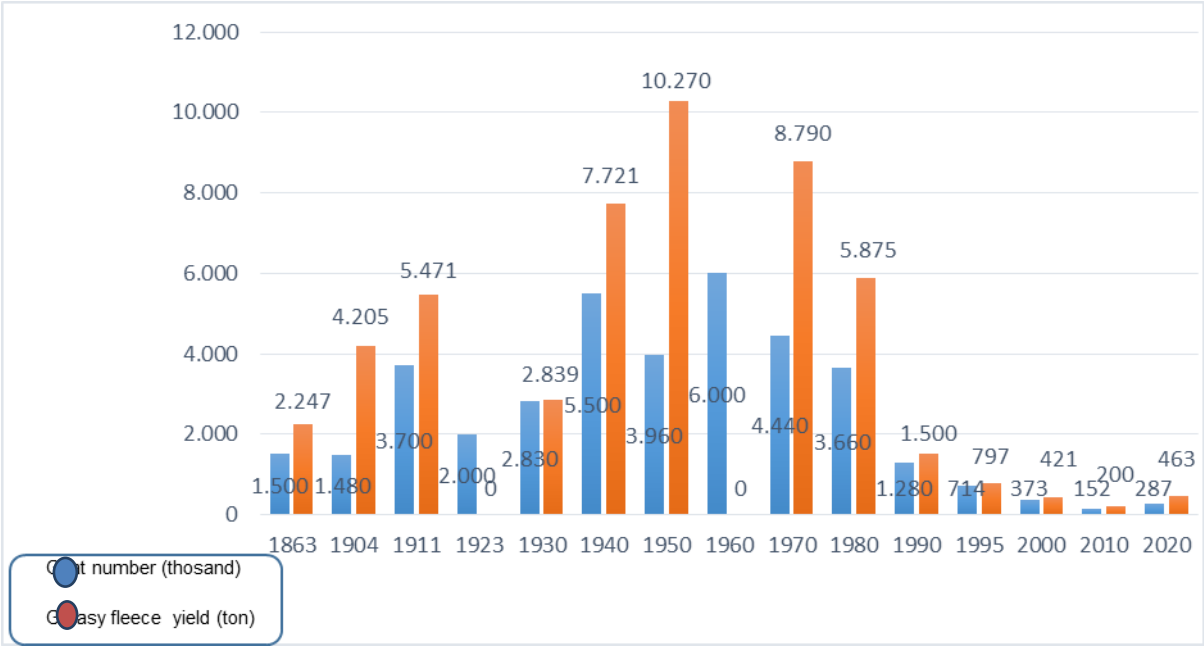

Figure 1: The number of goat and mohair yield for years (Kaynar, 2016; TUİK, 2020).

Angora Goats are small size, white color, rarely seen in yellow and black, covered with mohair up to the inferior extremities, and completely horned in males and females. Since the live weight is low (36 kg), the need of nutrients is lower than sheep and other goat breeds. It has the ability to evaluate poor pastures and turn them into yields (Erol et al. 2012). In the literature, the birth weight of Angora Goat kids were determined as 2.38 – 3.20 kg, the greasy fleece yield in goats was 1.46 – 2.54 kg, and the mohair diameter was in the range of 32.59 – 37.15 µ (Snyman, 2012; Erol et al. 2014,2017; Snyman, 2020; Şenyüz, 2021). The twinning rate is low and the birth rate is around 90%.

As the number of Angora Goats started to decrease in Turkey, the Ministry of Agriculture and Forestry started a conversation project as a precaution. For this purpose, Institute Conservation Project was initiated at the International Center for Livestock Research and Training (Lalahan) in 1997 and Conservation Project at the Breeder Conditions in 2005.

This study was carried out on animals followed within the scope of Breeder Conditions Protection Project implemented by the General Directorate of Agricultural Research and Policies of the Ministry of Agriculture and Forestry. For his purpose kids at the birth, 90th and 180th day live weight were investigated.

Material and Method:

This study was carried out within the scope of the Conservation Project of Ankara Goat in the Breeder Conditions which is carried out by the General Directorate of Agricultural Research and Policies. For this purpose, it was carried out in a private farm in Yahşihan District of Kırıkkale Province. The animals grazed in the pastures of Irmak Village (Yahşihan, Kırıkkale) and Yalım Village (Kalecik, Ankara) as pasture. Totally 110 goats and their kids were examined in this farm. Mating was done in a natural way with a free method. The mating period was in October-November. Also the birth season was March-April. The kids were weighed with an electronic scale with a precision of 10 g within the first 24 hours after the birth, and the live weight for 90th days and 180th days was weighed with a 100 g precision electronic scale. Weighing for 90th days was carried out on 10 August and 180th days weighed on 22 October. Kids were breastfed from birth to 4 months of age and were weaned at 4 months of age. The kids were divided into two groups at the age of 4 months. Irmak group (n=30) kids were grazed at 700 m altitude at the coordinates 39.980794, 33.415731 and drank Kızılırmak river water. The plateau group was drank natural spring water at the 1300 m altitude at the coordinates 40.025005, 33.374347. The animals were fed completely with pasture grass and no additional feeding was made during this period.

The kids birth, 90th and 180th days live weight were averaged with descriptive statistics, the difference between the groups was tested with ANOVA. In case of difference between groups, Tukey test was used and statistics were made using MINITAB software program.

Results:

The kids Birth weight, 90th days and 180th days live weight are given in Table 1. In terms of birth weight of kids, males were higher than females ($p<0.05$), and the river group was higher than the plateau group ($p<0.05$). Also in terms of 90th day live weight, males were higher than females, and the river group was higher than the plateau group ($p<0.05$). After the weaning, live weight of kids for 180th days was higher in the plateau group than in the river group ($p<0.05$).

Table 1: The birth, 90th and 180th live weight of kids.

	Birth Live Weight			90 th day Live Weight			180 th day Live Weight		
	n	Mean	P	n	Mean	P	n	Mean	p
Male	35	2.12±0.02[a]	0.01	35	15.62±0.45[a]	0.01	35	19.58±0.54	0.07
Female	32	2.01±0.02[b]		32	13.66±0.42[b]		32	21.05±0.57	
River	30	2.12±0.02[a]	0.01	30	15.59±0.50[a]	0.01	30	18.77±0.43[b]	0.01
Plateau	37	2.03±0.02[b]		37	13.95±0.41[b]		37	21.51±0.56[a]	
Overall	67	2.07±0.02		67	14.69±0.33		67	20.28±0.40	

Discussion and Conclusion:

Since Angora Goats are small animals, the birth weight of kids are also low. As in general, males have a higher birth weight than females. In this study, birth weight was higher in males than females ($p<0.05$). The birth weight of kids were lower than the literatüre (Snyman, 2012; Erol et al. 2014, 2017; Snyman 2020, Şenyüz, 2021). The reason of the low birth weight is thought to be related to the winter care and feeding conditions applied to the goats in the enterprise.

As expected, males kids 90th day body live weights were higher than in females. The kids 90th live weight is similar with Snyman (2012), Erol et al. (2014, 2017) and Şenyüz (2021), but lower than the values of Snyman (2020). Since the 90th day weighing period of the kids coincides with the spring months which a good quality pasture. Therefore, since the goats are fed at a good level, the development of the kid is at the same level in parallel.

The female kids 180th day live weight were were higher than males ($p<0.05$). The female kids were fed in plateau group in this period. Although the birth and 90th day live weight of the kids were higher in the river group, the 180th day live weight of the kids were higher in the plateau group ($p<0.05$). It is thought that this is due to the better quality of the plateau pasture and the feeding of the females in the plateau. The values stated in the literature (Erol et al. 2014; 2017) are similar with this study.

As a result of the study, it was observed that the quality of pasture is important in the feeding of Angora Goat kids, and the quality of pastures at high altitudes is better. It has been concluded that the development of kids grazing on high altitude pasture is better.

Acknowledge: The project consists of the data received within the scope of the Ankara Goat Conservation Project on the Breeder Conditions carried out by GDARP, and the author thanks GDARP

References:

1 - Erol H, Akçadağ Hİ, Ünal N, Akçapınar H. Milk yield and its effect on kids growth in Angora goats. Ankara Üniv Vet Fak Derg. 2012; 59: 129-134.

2 - Erol H, Ünal N, Ünal M, Akçadağ Hİ. Important production traits of Angora goats reared under conservation as a gene resource. Ankara Üniv Vet Fak Derg. 2014; 61 (3): 211-216.

3 - Erol H, Özdemir P, Odabaş E, Şenyüz HH, Ünal N, Behrem S. Investigation of various production traits of Angora goat herds kept as gene source both ex situ and ın situ conditions. Lalahan Hayvancılık Araştırma Enstitüsü Dergisi. 2017; 57 (1): 1-12.

4 - Kaynar İS. From Engürü to Ankara: Ankara's Economıc Change Between 1892 and 1962. Doctorate Thesis, Marmara University. 2016; Turkey. pp. 160-186.

5 - Minitab, LLC. (2006). Minitab. Inc., versão, 15.

6 - Snyman MA. Genetic analysis of body weight in South African Angora kids and young goats. South African Journal of Animal Science. 2012; 42 (2): 146-155. DOI: 10.4314/sajas.v42i2.7

7 - Snyman MA. Genetic analysis of reproduction, body weight and mohair production in South African Angora goats. Small Rumin.Res. 2020; https://doi.org/10.1016/j.smallrumres.2020.106183

8 - Şenyüz HH. Fertility, Live Weight, Survival Rate, Greasy Fleece Weight, and Quality Traits of Angora Goats in Turkey. *Small Ruminant Research*. 2021; *197*, 106332.

Second International Congress on Biological and Health Sciences
ONLINE 24-25-26-27 FEBRUARY 2022

First Report of an Unusual Monteggia Variant Fracture and Its Surgical Outcome in a Cat

Mehmet Zeki Yılmaz Deveci[1]

[1]Hatay Mustafa Kemal University, Faculty of Veterinary Medicine, Department of Surgery, Hatay, Turkey

Corresponding author: zekideveci@mail.com

Abstract:

Orthopedic surgical treatments on the elbow are challenging due to the complex anatomical structure. Among them, Monteggia fractures are special fractures that are rare. Although there are defined types for Monteggia fractures, there may be unusual Monteggia variant or equivalent fractures which are rarer. In this study, the aim was to report an unusual Monteggia variant fracture for the first time, that has not been described previously in a cat, and its surgical outcome. A male Bombay cat (5-year-old, 4.5 kg, intact, cryptorchid) was brought to Hatay Mustafa Kemal University Veterinary Health Research and Practice Hospital with a history of high fall and fractures of both forearms one day ago. As a result of clinical examination and radiographs, ulnar fracture accompanying cranio-lateral elbow dislocation was determined bilaterally. This atypical fracture dislocation was determined to be an unusual type of Monteggia variant fracture. After stabilization of the patient was achieved, open reduction was performed on both legs with a surgical approach. In surgical open reduction, ulnar fractures were fixed with Kirschner wire, locked mini titanium plate and screws; then elbow dislocations were fixed with two screws and orthopedic wire by lateral stabilization method. Due to the infection in the postoperative period, lateral stabilization of the right elbow was a failure on the seventh day and revised by reoperation. Despite the delayed union due to infection in the ongoing process, adequate fracture healing was achieved in 6 months with medical treatment and continuous check-ups. By examining previous studies, it was determined that this fracture was not classified as known Monteggia types due to ulnar fracture accompanying cranio-lateral elbow dislocation. Though there are reports of elbow dislocation along with diaphyseal forearm bones fractures, to aouthors knowledge, this is the first in which the complete elbow dislocation accompanies an ulnar fracture. In conclusion, with this study, a unique Monteggia variant fracture of a cat and its surgical outcome was presented.

Keywords: cat, dog, surgery, orthopaedics, veterinary.

1. Introduction

Elbow fracture dislocations result in pain, disfunction, instability, or stiffness, and surgical treatment is necessary in most cases. They are considered complex injuries that can provide a challenge even for experienced surgeons (Altug et al. 2015, Watts et al. 2019, Deveci et al. 2021). The elbow joint has got three synovial joints: humeroradial, humeroulnar, and proximal radioulnar. The humeroradial joint carries most of the forces of the forelimb, the humeroulnar joint restricts movement to the sagittal plane, and the radioulnar joint allows rotational (pronation/supination) movements. The joint capsule covers all the three articular

parts. The elbow stability is provided by periarticular structures and ligaments (Wiley and Galey 1985, Hung et al. 2003, Hassini et al. 2018, Watts et al. 2019). The collateral ligaments provides the primary stabilization (Fleming et al. 2004). Since the muscles do not cover the joint effectively, extreme direct loads or forces may result in fracture more than a dislocation (Wiley and Galey 1985, Modi et al. 2012).

Elbow fracture dislocations are more complex cases and mostly caused by motor vehicle accidents, falls, and other severe traumas (Modi et al. 2012, Madhar et al. 2013, Altug et al. 2015, Sing et al. 2016). Traumatic dislocations are mostly associated with soft tissue and ligament disruption (Frazier et al. 1991, Goni et al. 2015). The ligament ruptures are reported to be in up to 50% of dislocations (Frazier et al. 1991, Modi et al. 2012, Madhar et al. 2013, Hassini et al. 2018). Therefore, complex fracture dislocations such as Monteggia fractures are often accompanied by suffering significant damage of the soft tissues within the elbow joint and surroundings (Frazier et al. 1991, Goni et al. 2015, Hassini et al. 2018).

With this study, we report a very rare, unusual Monteggia variant fracture lesion consisting of bilateral cranio-lateral elbow dislocations with proximal ulna fractures in a 4.5-year-old cat. In this study, the aim is to report an unique Monteggia variant fracture for the first time, that has not been described previously in a cat, and its surgical outcome, in order to remind this rare type of fracture dislocation and also to provide a comprehensive review related to this uncommon lesion.

2. Materials and Methods

A male Bombay cat (5-year-old, 4.5 kg, intact, cryptorchid) was brought to Hatay Mustafa Kemal University Veterinary Health Research and Practice Hospital with a history of high fall and fractures of both forearms one day ago. Clinical examination revealed severe decrease in the both elbow's range of motion, crepitus, pain, and considerable swelling. As a result of radiographs, ulnar fracture accompanying cranio-lateral elbow dislocations was determined bilaterally (Figure 1). This atypical fracture dislocation was determined to be an unusual type of Monteggia variant fracture.

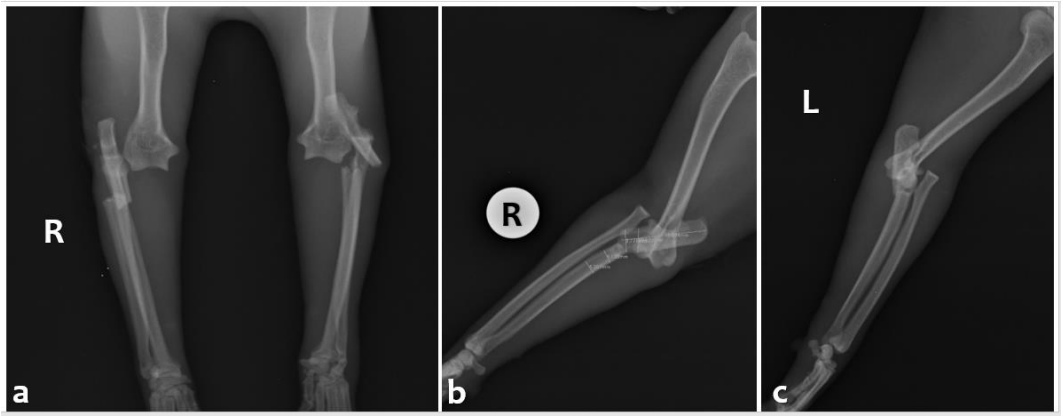

Figure 1. Preoperative cranio-caudal (a) and medio-lateral (b, c) radiographs

After stabilization of the patient was achieved, surgery was performed aiming to reduce and stabilize the ulnar fractures and elbow luxations of both forelimbs. After premedication with xylazine HCl (2 mg/kg IM, Alfazyne % 2, Egevet, Türkiye), general anaesthesia was induced with ketamine HCl (10 mg/kg IM, Alfamine %10, Egevet, Türkiye), followed by isoflurane (2-3 %, Isoflurane - USP, Adeka, Samsun, Türkiye) and 100% O_2. Isotonic NaCl solution (0.9%, Polifleks, Polifarma, Ankara, Türkiye; 5mL/kg/h IV) was administered intraoperatively. Antibiotic prophylaxis was ensured by cephazolin sodium (25 mg/kg, IM, Sefazol, Mustafa Nevzat, Istanbul, Türkiye). The cat was placed in lateral recumbency and caudolateral surgical approaches were performed to both elbows. In surgical open reduction, ulnar fractures were fixed with Kirschner wire, locked mini titanium plate and screws; then elbow dislocations were fixed with two screws and orthopedic wire by lateral stabilization method. Due to the infection in the postoperative period, lateral stabilization of the right elbow was a failure on the seventh day and revised by reoperation. Also antibiotics continued for a month because of the percistence of infection.

Postoperative radiographs revealed appropriate alignment and positioning of the implants used in the fixation of ulnar fractures and elbow dislocations except of a minimal non-compliance of the radial head in the left elbow, and confirmed anatomic reduction (Figure 2). Postoperative analgesia was provided with tolfenamic acid (3 mg/kg q24h per os / PO, Tolfedine, Novakim, Kocaeli, Türkiye and cephazolin sodium (25 mg/kg, IM, Sefazol, Mustafa Nevzat, İstanbul, Türkiye) administration was continued for seven days. The cat's activity was advised to be restricted for 8 weeks.

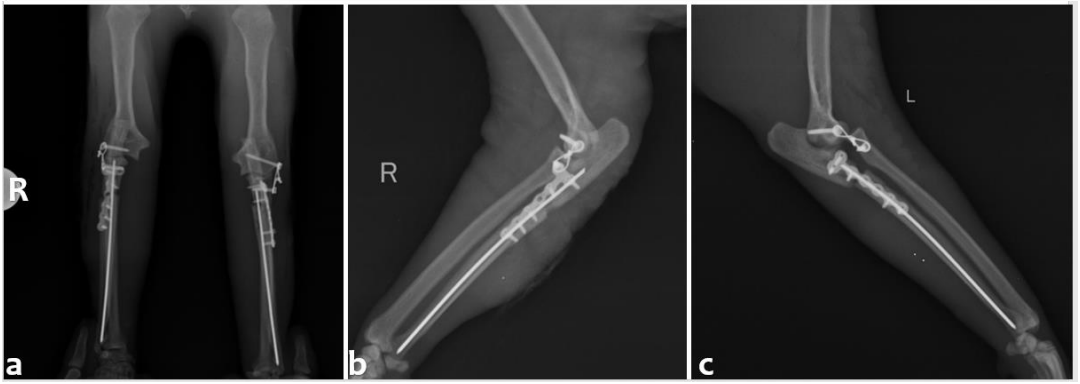

Figure 2. Postoperative cranio-caudal (a) and medio-lateral (b, c) radiographs

3. Results

Orthopaedic examinations after surgery (weekly) revealed a mild, weight-bearing lameness of the both forelimbs. Surgical site infection was affected the right forelimb and the complete blood count revealed an increased WBC. Radiographs revealed displacement of the orthopedic wire used for lateral stabilization of the right elbow at the seventh day and reoperated (Figure 3-4). Third week follow-up revealed a mild lameness and moderate muscle atrophy. Palpation of the elbow joint exhibited normal extension and mildly reduced flexion. There was not adequate callus formation (Figure 5). Second month follow-up revealed the screw migration of one in lateral stabilization and one in the mini titanium plate of the right elbow. The elbow was stable with improved range of motion, but a mild lameness and pain remained. Therefore, the migrated screws and orthopedic wire in the right forelimb removed at second month follow-up. Despite the delayed union due to infection in the ongoing process, at the third month it was still inadequate in terms of fracture healing (Figure 6). Physiotherapy exercises were recommended to increase muscle growth and the elbows range of motion.

Adequate fracture healing was achieved in 6 months with medical treatment with continuous follow-ups (Figure 7). Clinically the cat was with a good gait starting from three months and it was excellent at the sixth month follow-ups. One year follow-up radiographs revealed better fracture healing and remodeling (Figure 8). Clinical examinations revealed excellent muscle healing and good range of motion of both elbows. The cat's gait was excellent and there only remained a little

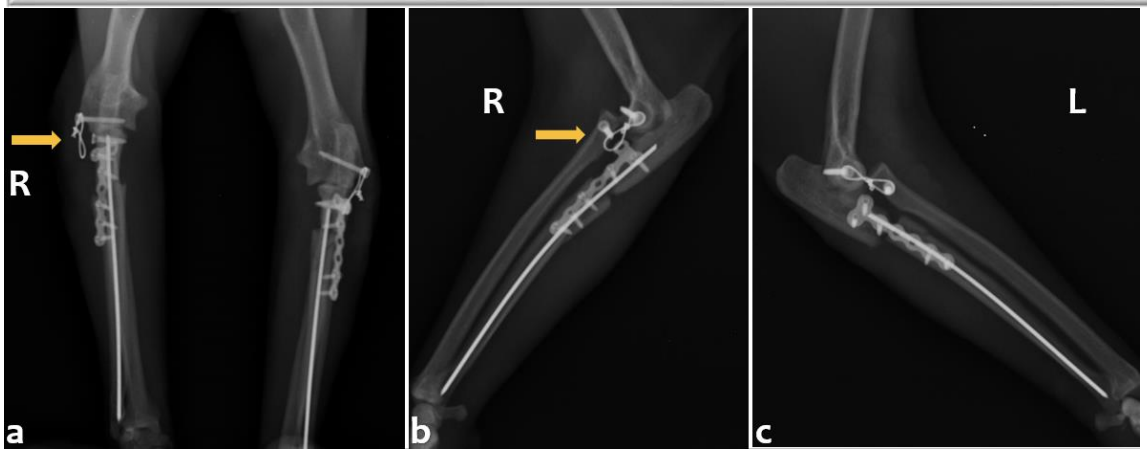

Figure 3. Postoperative seventh day cranio-caudal (a) and medio-lateral (b, c) radiographs

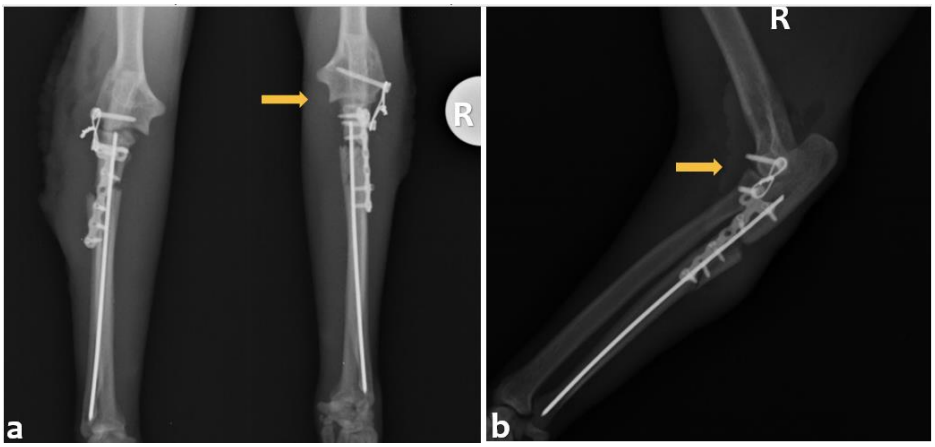

Figure 4. Postoperative cranio-caudal (a) and medio-lateral (b) radiographs of second surgery

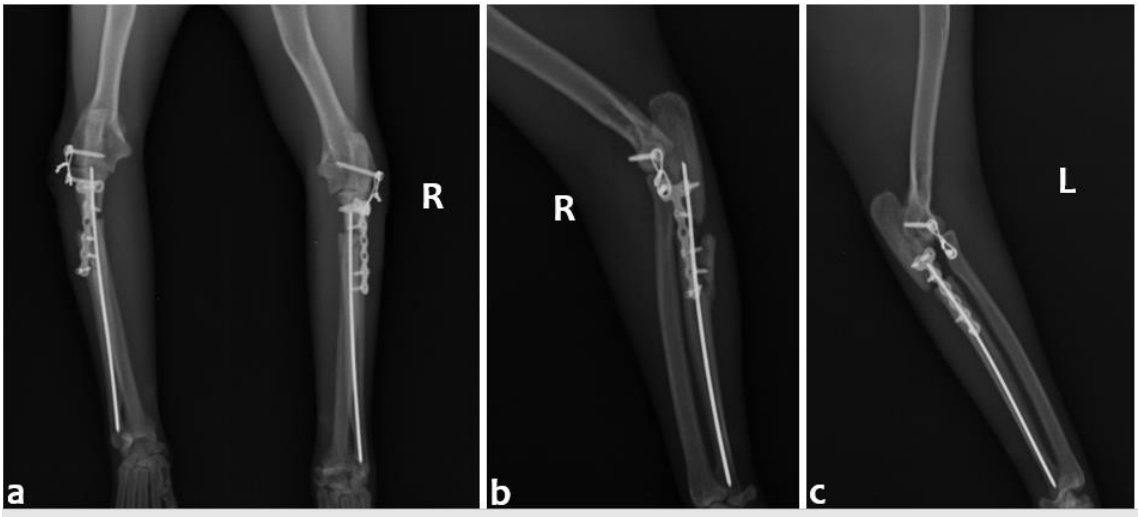

Figure 5. Postoperative third week cranio-caudal (a) and medio-lateral (b, c) radiographs

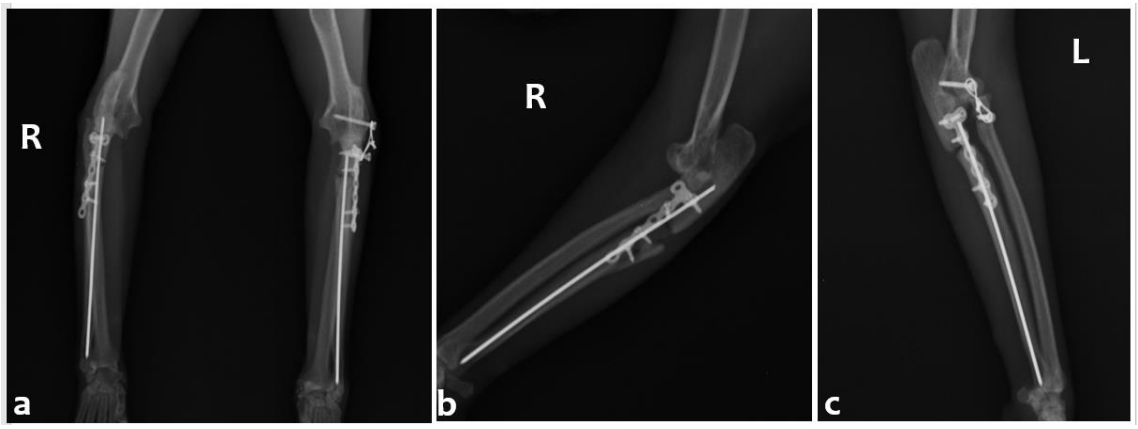

Figure 6. Postoperative third month cranio-caudal (a) and medio-lateral (b, c) radiographs

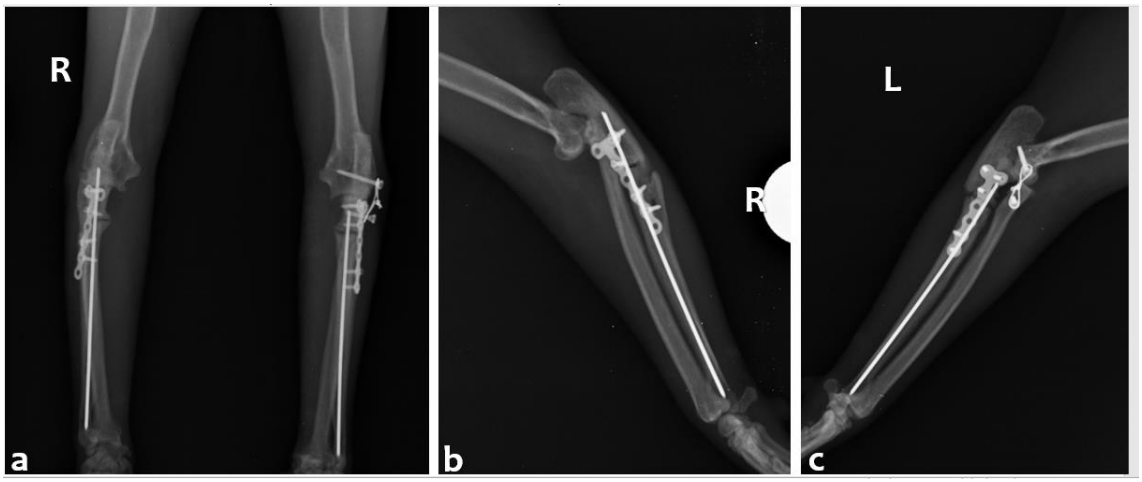

Figure 7. Postoperative sixth month cranio-caudal (a) and medio-lateral (b, c) radiographs

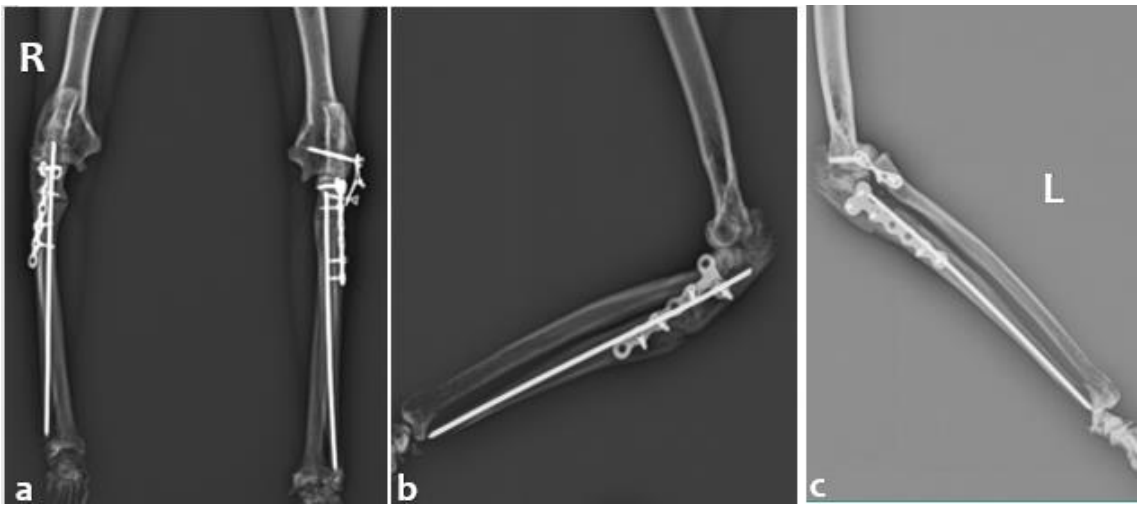

Figure 8. Postoperative one year cranio-caudal (a) and medio-lateral (b, c) radiographs

4. Discussion

The Monteggia fracture was described as an ulnar fracture with a dislocation of the radial head (Bush and Owen 2009). Monteggia fractures are special and rare among elbow fracture dislocations (Altug et al. 2015). The classification of Monteggia fractures as 4 types according to the direction of dislocation of the radial head was reported by Bado (1967). Also, Monteggia variant or equivalent lesions were described as special forms (Bush and Owen 2009, Hassini et al. 2018). Although there are defined types for Monteggia fractures, there may be even rarer unusual Monteggia variant fractures (Bush and Owen 2009). In fact, the information and experience about their physiopathological characteristics and therapeutic methodizing are lacking.
This study reports the successful repair of bilateral unusual Monteggia variant fractures of a cat caused by a high fall. The treatment was achieved by intraoperative manual reduction and stabilization using mini titanium plates, screws, and orthopedic wires. The cat returned to normal function with a good range of motion 6 months postoperatively.

The classical term of Monteggia fracture is defined as dislocation of the radial head accompanying an ipsilateral ulnar fracture at any level (Bush and Owen 2009). Pursuant to this definition, the orthopedic injury in our case may be classified as a Monteggia variant fracture since not only the radial head dislocated but complete elbow luxation. To the author's knowledge, there are no studies in cats or other animal species reported this type of fracture. Similar cases have been reported among complex elbow fracture dislocations in humans or other Monteggia variant fractures in animals (Bush and Owen 2009, Hassini et al. 2018). Contending accurate identification is important because a number of factors unique to this injury pattern can influence both treatment and prognosis (Ring et al. 1997).

The radiohumeral luxation may lead to the disruption of the joint capsule and the collateral ligaments. The ulnar fractures necessarily disrupt the annular ligament and at least the proximal portion of the interosseous membrane and ligaments if at the level of distal to the coronoid process. However, the interosseus ligament and interosseus membrane may remain preserved in other Monteggia fractures (Schwarz and Schrader 1984, Vallone and Schulz 2011, Garcia et al. 2021). In this case, the interosseus membrane and ligaments was remaining preserved because the complete elbow dislocation didn’t separate connections of the radius and ulna. Therefore, it was not necessary to apply a radioulnar positional screw in the surgical treatment and the prognosis was more favorable.

Osteoarthritis with consequent elbow range of motion reduction has been reported to be the most common complication after Monteggia fracture repair (Bado 1967, Schwarz and Schrader 1984, Garcia et al. 2021). In

the present case, septic osteoarthritis was caused by surgical site infection and lead to loosening of the implants in the right elbow. Although a strict aseptic technique and sterile inert implant materials were used, surgical site infection developed. Reoperation of the right elbow to renew lateral stabilization on the seventh day, and removal of three screws and orthopedic wire of the right elbow with the use of antibiotics enabled infection resolution. Even though this case was successfully treated, different implants and surgical methods may be considered to provide a better result for such cases.

5. Conclusion

By examining previous studies, it was determined that this fracture was not classified as known classic Monteggia types due to cranio-lateral elbow dislocation accompanying ulnar fracture. Though there are reports of elbow dislocation along with diaphyseal forearm bones fractures, to authors knowledge, this is the first in which a complete elbow dislocation is cranio-lateral accompanied an ulnar fracture. In conclusion, with this study, a unique Monteggia variant fracture of a cat that has not been reported previously and its surgical treatment was presented.

6. References

Altug ME, Deveci MZY, İşler CT, Yurtal Z, Gönenci R. Mustafa Kemal Üniversitesi Veteriner Fakültesi Cerrahi Kliniği'ne getirilen ortopedi olgularının genel değerlendirilmesi: 564 olgu (2009-2014). Harran Üniversitesi Veteriner Fakültesi Dergisi. 2017; 6(2): 158-62.

Bado JL. The Monteggia lesion. Clin Orthop Relat Res. 1967; 50: 71-86.

Bush MA, Owen MR. Type-IV variant Monteggia fracture with concurrent proximal radial physeal fracture in a domestic shorthaired cat. Veterinary and Comparative Orthopaedics and Traumatology. 2009; 22(03): 225-8.

Deveci MZY, Seyrek-İntaş D, Demirkan İ, Kaya U, Şirin ÖŞ, Altuğ ME. Perception of Teaching and Assessing Surgical Proficiency of Veterinary Surgery Postgraduate Programs in Turkey: Suggestions on Prospective Veterinary Surgery Specialist Training. International Journal of Veterinary and Animal Research (IJVAR). 2021; 4(3): 101-10.

Fleming FJ, Flavin R, Poynton AR, Glynn T. Elbow dislocation with ipsilateral open radial and ulnar diaphyseal fractures: a rare combination. Injury. 2004; 35: 90-92.

Frazier JL, Buschmann WR, Insler HP. Monteggia type I equivalent lesion: diaphyseal ulna and proximal radius fracture with a posterior elbow dislocation in a child. J Orthop Trauma. 1991; 5: 373-375.

Garcia M, Bismuth C, Deroy-Bordenave C. Repair of a Divergent Elbow Dislocation with Distal Ulnar Fracture in a Dog Using TightRope and External Skeletal Fixation. VCOT Open. 2021; 4(01): 58-64.

Goni V, Behera P, Meena UK, Gopinathan NR, Akkina N, Arjun RHH. Elbow dislocation with ipsilateral diaphyseal forearm bone fracture: a rare injury report with literature review. Chin J Traumatol. 2015; 18: 113-115.

Hassini L, Saidi A, Touati B, Fradj AB, Aloui I, Abid A. An unusual Monteggia equivalent type 1 lesion: diaphyseal ulna and radius fractures with a posterior elbow dislocation in a child. Chinese Journal of Traumatology. 2018; 21(02): 122-4.

Hung SC, Huang CK, Chiang CC, Chen TH, Chen WM, Lo WH. Monteggia type 1 equivalent lesion: diaphyseal ulna and radius fractures with a posterior elbow dislocation in an adult. Arch Orthop Trauma Surg. 2003; 123: 311-313.

Madhar M, Saidi H, Fikry T, Cermak K, Moungondo F, Schuind F. Dislocation of the elbow with ipsilateral forearm fracture. Six particular cases. Chir Main. 2013; 32: 299-304.

Modi P, Dhammi IK, Rustagi A, Jain AK. Elbow dislocation with ipsilateral diaphyseal fractures of radius and ulna in an adult is it type 1 or type 2 Monteggia equivalent lesion? Chin J Traumatol. 2012; 15: 303-305.

Ring D, Jupiter JB, Sanders RW, Mast J, Simpson NS. Transolecranon fracture-dislocation of the elbow. Journal of orthopaedic trauma. 1997;11 (8): 545-50.

Schwarz PD, Schrader SC. Ulnar fracture and dislocation of the proximal radial epiphysis (Monteggia lesion) in the dog and cat: a review of 28 cases. J Am Vet Med Assoc 1984; 185 (02): 190–194

Singh D, Awasthi B, Padha V, Thakur S. A very rare presentation of type 1 Monteggia equivalent fracture with ipsilateral fracture of distal forearm-approach with outcome: case report. J Orthop Case Rep. 2016; 6: 57-61.

Vallone L, Schulz K. Repair of Monteggia fractures using an Arthrex Tightrope systemand ulnar plating. Vet Surg 2011; 40 (06): 734–737

Watts AC, Singh J, Elvey M, Hamoodi Z. Current concepts in elbow fracture dislocation. Shoulder & Elbow. 2021; 13(4): 451-8.

Wiley JJ, Galey JP. Monteggia injuries in children. J Bone Joint Surg Br. 1985; 67: 728-731.

Second International Congress on Biological and Health Sciences
ONLINE 24-25-26-27 FEBRUARY 2022

Design of Orally Disintegrating Antihistaminic Tablet and Investigation of Kinetic Properties

Kutlu Sömek[1], Emek Möröydor Derun[1]

[1]Yıldız Technical University, Faculty of Chemical and Metallurgical Engineering, Chemical Engineering Department, İstanbul, Davutpaşa 34220, Turkey

Corresponding author: kutlusmk@gmail.com

Abstract:
Allergic rhinitis, which manifests itself with complaints such as runny nose, sneezing, nasal congestion, itching in the eyes, is a term used to describe the clinical symptoms associated with type 1 allergic diseases, defined as allergic rhinoconjunctivitis. The incidence of this disease, which is seen in all countries, in all ethnic groups and in people of all ages, is in the range of 10-40% on average. Allergic rhinitis has negative effects on the patient's quality of life and daily activities. Various therapeutic agents are used in the treatment of allergic rhinitis for eliminate and alleviate these effects. Among all these therapeutic agents, Bilastine stands out with its various properties. These are mainly features such as having low side effects, showing peripheral effects, not being metabolized and at the same time having a fast action compared to other antihistamines. However, Bilastine does not cause sedative or cardio-toxic effects. However, when used in tablet form, the bioavailability rate remains at 61%. So as to increase this rate and to minimize unwanted interactions in the gastrointestinal environment, the design in the form of "Orally Dispersible Tablets" will be the most appropriate method. In the study carried out for this purpose, direct compression method, which is the most widely used among the methods used to produce orally dispersible tablet form, such as Direct compression, fast melting technology, Sublimation, and lyophilisation was used. As a result of this study, the tablets obtained disintegrate in 40 seconds at a pH value of 6.8, which is the pH value of the mouth saliva, and the solubility value of this tablet was found to be 93%.

Keywords: Bilastine, orally disintegrating tablet, antihistaminic, rhino conjunctivitis.

1. Introduction

Respiration is a system that is directly affected by the atmosphere until the last breath of living things. The air in the breathing environment is filtered, humidified, heated, oxygen supplied to the body and carbon dioxide removed from the blood is carried out by the respiratory system. Since the respiratory system directly affects vital functions, it has gained some features that can tolerate some negative environmental effects over time. However, with the rapid industrialization in recent years, increasing indoor allergens and the effects of global warming, this system is becoming increasingly vulnerable. Currently, respiratory disorders that occur in the face of these negative effects are allergic rhinitis and asthma (Sanjay et. al. ,2011). Various therapeutic agents are used in order to increase the quality of life of people exposed to these diseases and to suppress the negative effects. Among these, agents in the group of H1 receptor antagonists are the most common used. Bilastine, which is in this group, has been widely used in recent years due to its low side effects, non-metabolization, low half-life and peripheral effects (Sadrani et al., 2021).

Among the drug groups in which the bilastine molecule is used, the most widely used are core tablet, solution and orally dispersible tablet forms. However, when these product forms are examined, the bioavailability rate

is approximately 60%, for this reason we need new tablet forms. In order to increase this rate and to minimize undesirable interactions in the gastrointestinal environment, the design in the form of an orally dispersible tablet would be the most appropriate method. Within the scope of the study carried out for this purpose, "Direct compression", which is the most widely used method among the methods used for the production of orally dispersible tablet form, such as "Direct compression, Fast melting technology, Sublimation, Lyophilisation" will be used (Sinko et al., 2006). This work based on 'Design of Orally Disintegrating Antihistaminic Tablet and Investigation of Kinetic Properties'.

2. Materials and Methods

2.1. Materials

Bilastine active pharmaceutical ingredient purchased from Lee Pharma, Micro Cyristalline Cellulose excipian material purchased from Ranq Pharmaceuticals and Excipients Co.; Other excipians Sodium Starch Glycolate and Primogel purchased from DFE Pharma; Crosscarmellose Sodium and Mannitol purchased from Raquette Frères Pharma; Polyplaston and Acdisol purchased from Ashland Inc., Menthol purchased from BASF Chemical; Aerosil 200 purchased from Evonik Industries, Talc purchased from Imerys SA., Acetonitrile and Methanol purchased from Scharlau.

2.2. Methods

2.2.1. Analytical Methods

For this study, instrumental device of High-Performance Liquid Chromatography was used. Firstly, suitable method for Bilastine raw material was made and then confirm and validation developed this method. Validation step is very critical process for analytical device. Because of this reason we use ICH Guideline Q2 (R1) validation of analytical procedure section (Anonymous).

Within the scope of the study, Distek Dissolution device was used to determine the dissolution rate and Erweka Disintegration device was used to disintegration time. The samples were taken into Waters HPLC vial for analysis after dissolution test, and then the analyzes were performed with a suitable HPLC method developed for Bilastine.

2.2.2. Synthesis of Bilastine Sublingual Tablet

For production of orally dispersible sublingual Bilastine tablet, "Direct Compression" method was used. All excipients were passed through a 60 mesh sieve. After all the materials were weighed, they were thoroughly mixed to obtain a homogeneous mixture. The resulting mixture was made into tablets at 40-60 N pressure, adjusted to 125 mg weight using a flat-shaped punch.

Figure 1. Produced Sublingual Tablet

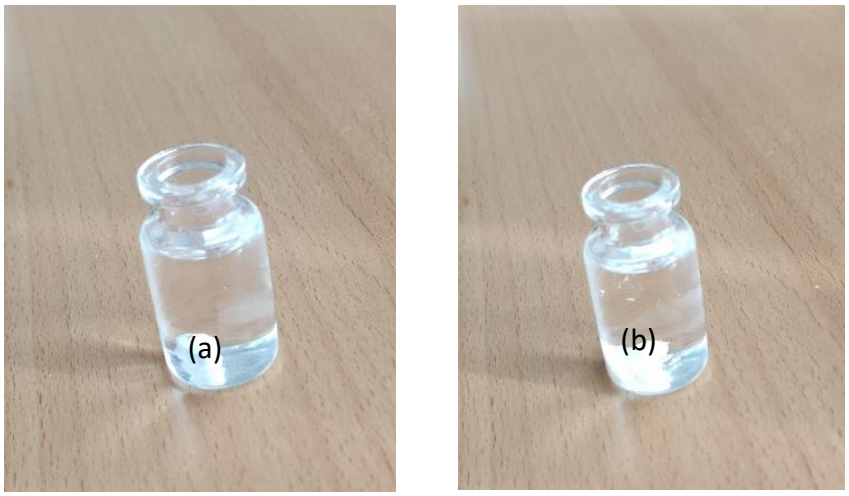

Figure 2. Disintagration of bilastine tablets in pH 6.8 solution (a) initially and,(b) after a while

3. Results

3.1. Results for Validation of Analytical Method

Mainly there is some validation parameter for use of validation. For instance, accuracy, precision, specificity, detection limit, quantitation limit and linearity range. During this study, Linearity step was used. In figure 3 include of linearity data for bilastine is given. It can be seen that the R^2 value which must be ≥ 0.98 in suitable method was found to be 0.999892.

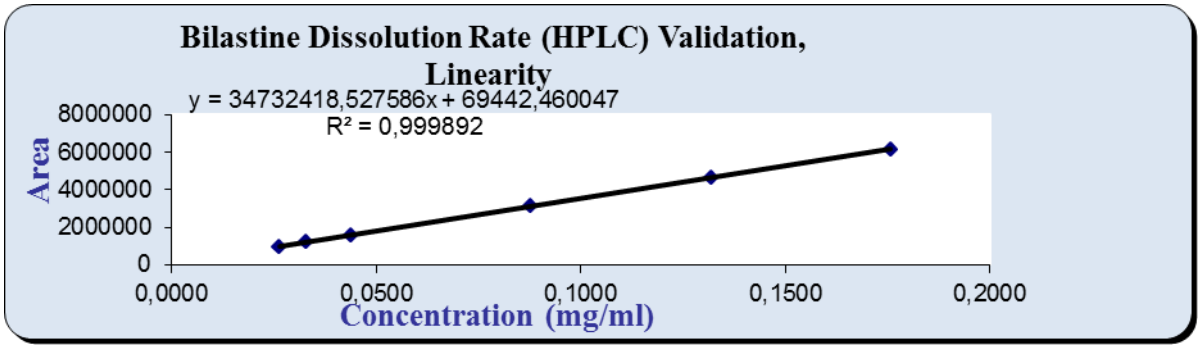

Figure 3. Linearity data of bilastine.

3.2. Results for Dissolution and Disintegration

Using HPLC device and some calculation, as it seen in the figure 4, dissolution rate was found to be 93%. The tablets obtained disintegrate in 40 seconds at a pH value of 6.8, which is the pH value of the mouth saliva.

Table 1. Dissolution Rate of Bilastine Tablets

Sample/Time (min)	5	10	15	20	30	45	60	Infinity	Tablet Weight (mg)
1	94.4	92.6	95.2	95.7	96.4	95.7	95.5	95.2	123.6
2	96.7	92.7	92.8	92.7	93.3	93.3	94.0	93.0	123.2
3	88.0	94.2	95.2	97.2	97.3	97.8	97.7	98.3	123.9
Mean	93.0	93.2	94.4	95.2	95.7	95.6	95.7	95.5	123.6
Std. Dev.	4.5	0.9	1.4	2.3	2.1	2.3	1.9	2.6	0.4
% RSD	4.8	1.0	1.5	2.4	2.2	2.4	1.9	2.8	0.3
MAX	96.7	94.2	95.2	97.2	97.3	97.8	97.7	98.3	123.9
MIN	88.0	92.6	92.8	92.7	93.3	93.3	94.0	93.0	123.2

4. Discussion

During this study, some formulation for good soluble drug tablet is tried and examined. As a result, produced tablets have 40 seconds disintagration time at pH value of 6.8, which is the pH value of the mouth saliva, and the solubility value of 93%.

5. Conclusion

So as to increase bio availability rate and to minimize unwanted interactions in the gastrointestinal environment, the design in the form of "Orally Dispersible Tablets" is to be the most appropriate method. For this purpose, direct compression method, which is the most widely used among the methods to produce orally dispersible tablet form is carried out in this study.

6. References

Sanjay N. Mandhane, Jigar H. Shah, Allergic rhinitis: An update on disease, present treatments and future prospects Rajamannar Thennati, International Immunopharmacology 11 (2011) 1646–1662

Sadrani Dolly A., Ajay N. Talele, Anuradha P. Prajapati, Sachin B. Narkhede, formulation development and evaluation of sublingual drug delivery system of bilastıne for allergic rhinoconjunctivitis, Indo American Journal of Pharmaceutical Sciences, IAJPS 2021, 08 (04), 166-181 ,ISSN 2349-7750

Sinko, P.J. Martin's Physical Pharmacy and Pharmaceutical Sciences. 6th Edition, Lippincott Williams & Wilkins, Philadelphia, 2006; pp. 563-594

Anonymous, https://www.ema.europa.eu/en/documents/scientific-guideline/ich-q-2-r1-validation_analytical-procedures-text-methodology-step-5_en.pdf, Access date: 04.03.2022

Second International Congress on Biological and Health Sciences
ONLINE 24-25-26-27 FEBRUARY 2022

Determination of Sensory and Antioxidant Properties of Black Imported Tea, Frequently Consumed in Şanlıurfa, Different Brewing Times

Kasım Takım[1], Mehmet Emin Aydemır[2]

[1]Harran University, Faculty of Veterinary, Department of Basic Sciences, Şanlıurfa, Turkey

[2]Harran University, Faculty of Veterinary, Department of Veterinary Food Hygiene and Technology, Şanlıurfa, Turkey

Corresponding author: aydemiremin23@harran.edu.tr

Abstract:
Tea is an aromatic beverage prepared by pouring hot or boiling water over the dried leaves of the plant known as *Camellia sinensis*. The chemical composition of teas can vary depending on the brewing conditions. The aim of this study is to determine the sensory and antioxidant properties of imported black tea, which is lovingly consumed by the public in Şanlıurfa, Turkey, at different brewing (infusion) times. For this purpose; analyzes of total phenolic substance, total flavonoid substance, antioxidant activity (DPPH and ABTS) and color values of the tea sample were performed after 15, 30 and 60 minutes of brewing. It was observed that there was a significant increase in the total phenolic and total flavonoid substance amounts of the tea sample during the brewing period ($p<0.01$). In the antioxidant activity of the tea sample; It was observed that DPPH and ABTS radical scavenging efficiency increased significantly in parallel with increasing the concentration amount ($p<0.01$). In addition, the highest DPPH and ABTS radical scavenging efficiency was observed in 60 min brewing time. In the color analysis of the tea sample; It was observed that L* (whiteness/darkness) and b* (yellow/blue) values increased for 30 minutes during brewing but decreased again for 60 minutes, a* (red/green) value increased during the brewing period, and its value decreased for 30 minutes and increased again for 60 minutes. It was observed that there was a positive correlation between total phenolic substance and a* and b* value, and a negative correlation between L* value. It was observed that there was a positive correlation between total flavonoid substance and L* and b* values and a negative correlation a* value. As a result, it has been concluded that imported tea, which is frequently preferred by the people in Şanlıurfa province, has high antioxidant activity and that prolonging the brewing time has a positive effect on the sensory and antioxidant properties of this tea.

Keywords: Antioxidant activity, imported black tea, brewing time, color

1. Introduction

Tea is an aromatic drink made by pouring hot or boiling water on the dried leaves obtained from the plant known as *Camellia sinensis*. After water, tea is one of the most important drinks in the world, with a history of 5000 years, and reported to be drunk by approximately two-thirds of the global population (Üstün and Demirci, 2013). In study from the UK, the USA, and Germany, it was shown that 30%-40% of the participants drank 2-3 cups of tea per day (Sedova et al., 2018).. Tea plantations are widespread and tea production is intense in India, China, Sri Lanka, Indonesia, Kenya, Turkey and Japan, with 80% of the world tea produced in these countries (Amirahmadi et al., 2013). In our country, in the Eastern Black Sea Region grown teas and imported teas are consumed. Imported teas, which are frequently consumed especially in the southeast, originate from Sri Lanka. It is loved and consumed by the people (Takım and Aydemir, 2018)

Tea is referred to as one of the best sources of polyphenolic compounds in literatüre. The polyphenols found in the tea plant have antioxidant, antimicrobial, anticancer, antiinflammatory and anti-viral effects on human health. Benefits have also been reported of lowering cholesterol, blood presssure, and the risk of cardiovascular disease, and reducing the risk of osteoporotic fractures in the elderly (Zhang et al., 2013). These benefits of tea on health are due to the phytochemicals it contains. However, the chemical composition of teas can also vary depending on the particle size of the tea used, the brewing conditions (brewing time, brewing temperature, amount of extraction, number of extractions, exposure to light) (Pastoriza ve ark., 2017).

Folk tea is brewed with a period of time that starts with a brewing time of at least 15 minutes. After brewing, it consumes up to 1 hour at the earliest. So what happens to the tea drunk in this interval? Is the phenolic content increasing or decreasing? Does the antioxidant capacity increase or decrease? Questions like this await answers. The aim of this study is to determine the sensory and antioxidant properties of imported black tea, which is lovingly consumed by the public in Şanlıurfa, Turkey, at different brewing (infusion) times.

2. Materials and Methods

The tea sample was obtained from the market in Şanlıurfa. The tea sample was brewed at the rate of 1/5 (1 g tea 5 ml tap water). Tea sample were performed after 15, 30 and 60 minutes of brewing. Analysis of the total phenolic substance, total flavonoid substance, antioxidant activity (DPPH and ABTS) and color values of the tea sample was performed.

2.1. Total phenolic substance:The Folin-Ciocalteu method was used to calculate the total amount of phenolic substances. The total amount of phenolic substance was calculated as mg Gallic acid equivalent per gram tea (Takım and Işık, 2020).

2.2. Total flavonoid substance: Determined using aluminum chloride colorimetric method. The total flavonoid content of the extract was expressed as milligrams of quercetin acid equivalents/g (Marinova et al. 2005)

2.3. Antioxidant activity: DPPH and ABTS were determined by looking at the free radical scavenging activity. Antioxidant capacity was expressed in Trolox (Takım and Işık, 2020).

2.4. Color values: Color measurements were made using the CS-10 8mm portable digital colorimeter (Tuodapu, Inc., China) The color characteristics of the tea, L* (whiteness/darkness), a* (redness/greenness) and b* (yellowness/blueness) parameters were determined.

2.5. Statistical Analysis: Analysis of variance (ANOVA) Duncan test was used using SPSS version 21.0 package program. All analyzes were performed in triplicate (SPSS, 2012).

3. Results

As a result of the analyzes made, the total phenolic and total flavonoid amounts of the tea sample are in table 1, Antioxidant activity (DPPH, ABTS) in table 2, color analysis values (L* (whiteness/darkness), a* (redness/greenness), b* (yellow/blueness)) are given in table 3, Correlation between color values of tea sample and total phenolic and total flavonoid are given in table 5.

Table 1. Total phenolic and total flavonoid amounts depending on the brewing time of the tea sample

	15 min.	30 min.	60 min.
Total phenolic (Gallic acid)	32,56±0.2	72,49±0.32	155,83±0.56
Total flavonoid (Quercetin)	20,44±0.4	22,43±0.44	104,30±0.28

Table 2. Antioxidant activity of tea sample depending on concentration and brewing time

	250 µg/ml			500 µg/ml			1000 µg/ml		
	15 min.	30 min.	60 min.	15 min.	30 min.	60 min.	15 min.	30 min.	60 min.
ABTS(Trolox)	116,98±0,24	114,76±0.25	167,99±0,17	176,86±0.29	157,79±0,41	237,19±0,16	305,95±0,98	315,27±0,4	332,12±0,91
DPPH(Trolox)	156,02±0,91	96,90± 0.21	144,80 ±0,3	191,19 ±0,5	239,60±0,46	271,20±0,17	341,54±0,76	346,12±0,56	371,60±43

Table 3. Color analysis values depending on the brewing time of the tea sample

	L*			a*			b*		
	15 min	30 min	60 min	15 min	30 min	60 min	15 min	30 dk	60 min
Tea sample	$3,97±0,37^{B}$	$6,61±0,86^{A}$	$4,41±0,56^{B}$	$-0,55±0,94^{C}$	$3,37±0,51^{B}$	$6,55±0,61^{A}$	$10,41±1,99^{B}$	$8,52±0,69^{B}$	$13,40±1,18^{A}$

A-C: The mean values with different letters in the same line are significantly different (P < 0.05).

Table 4. Correlation between color values of tea sample and total phenolic and total flavonoid

	Total phenolic			Total flavonoid		
	L*	a*	b*	L*	a*	b*
Tea sample	-0,686	0,564	1,00**	-0,947	0,11	0,886

L* (whiteness/darkness), a* (redness/greenness), b* (yellow/blueness), **(P < 0.01)

4. Discussion

It was observed that there was a significant increase in the total phenolic and total flavonoid substance amounts of the tea sample during the brewing period (p‹0.01). In the antioxidant activity of the tea sample; It was observed that DPPH and ABTS radical scavenging efficiency increased significantly in parallel with increasing the concentration amount (p‹0.01).In addition, the highest DPPH and ABTS radical scavenging efficiency was observed in 60 min brewing time. In the color analysis of the tea sample; It was observed that L* (whiteness/darkness) and b* (yellow/blue) values increased for 30 minutes during brewing but decreased again for 60 minutes, a* (red/green) value increased during the brewing period, and its value decreased for 30 minutes and increased again for 60 minutes. It was observed that there was a positive correlation between total phenolic substance and a* and b* value, and a negative correlation between L* value. It was observed that there was a positive correlation between total flavonoid substance and L* and b* values and a negative correlation a* value. It has been reported that the infusion time has an effect on the extraction of catechins, and an increase in the infusion time means the extraction of more bioactive compounds (Yu et al. 2021). Our study supported this. As the brewing times of the tea increase; the extraction rate increased, as the extraction

rates increased; The total amount of flavonoid compounds increased, and this increase affected the color of the teas and caused an increase in red color.

5. Conclusion

As a result, it was determined how the quality characteristics of Sri Lankan origin black tea, which is frequently consumed in Şanlıurfa, change at different brewing times. it has been concluded that imported tea, which is frequently preferred by the people in Şanlıurfa province, has high antioxidant activity and that prolonging the brewing time has a positive effect on the sensory and antioxidant properties of this tea. Even if the prolongation of the brewing time has positive effects on the quality criteria of the tea, we do not recommend extending the brewing time because the excess amount of antioxidants may have pro-oxidant effects and may lead to negative health consequences.

6. References

Amirahmadi M, Shoeibi S, Abdollahi M., Rastegar H, Khosrokhavar R, Hamedani MP. Monitoring of some pesticides residue in consumed tea in Tehran market. Iranian Journal of Environmental Health Science and Engineering. 2013;10(1):9.

IBM SPSS, IBM Corp. Released 2012: IBM SPSS Statistics for Windows, Version 21.0. Armonk, NY: USA

Marinova D, Ribarova F, Atanassova M. Total phenolics and total flavonoids in bulgarian fruits and vegetables. J. Univ. Chem. Technol. Met. 2005; 40:255–260

Pastoriza S, Pérez-Burillo S, Rufián-Henares JÁ. How brewing parameters affect the healthy profile of tea. Current Opinion in Food Science. 2017;14:7-12.

Sedova I, Kiseleva M, Tutelyan V. Mycotoxins in tea: occurrence, methods of determination and risk evaluation. Toxins. 2018;10(11):444.

Takım K, Işık M. Phytochemical Analysis of Paliurus spina-christi Fruit and Its Effects on Oxidative Stress and Antioxidant Enzymes in Streptozotocin-Induced Diabetic Rats. Appl. Biochem. Biotechnol. 2020;191:1353–1368.

Takım K, Aydemir ME. Şanlıurfa ilinde tüketilen kaçak çaylarda LC-MS ve GC-MS ile pestisit analizi. Tarim ve Doga Dergisi. 2018; 21(5):650.

Üstün Ç, Demirci N. Çay Bitkisinin (Camellia Sınensıs L.) tarihsel gelişimi ve tıbbi açıdan değerlendirilmesi. Lokman Hekim Journal. 2013;3(3):5- 12

Yu J, Liu Y, Zhang S, Luo L, Zeng L. Effect of brewing conditions on phytochemicals and sensory profiles of black tea infusions: A primary study on the effects of geraniol and β-ionone on taste perception of black tea infusions. Food Chemistry, 2021;354:129504.

Zhang L, Zhang ZZ, Zhou YB, Ling TJ, Wan XC. Chinese dark teas: Postfermentation, chemistry and biological activities. Food Research International, 2013;53(2):600-607.

Second International Congress on Biological and Health Sciences
ONLINE 24-25-26-27 FEBRUARY 2022

The Effect of Psychological Violence (Mobbing) Perception on Job Satisfaction in Healthcare Professionals

Bircan Türedi[1], İsmail Seçer[1], Okan Anıl Aydın[1]

[1]Beykent University, Health Science Faculty, Health Management, Istanbul, Turkey

Corresponding author: okananilaydin@gmail.com

Abstract:
In these times when the value of healthcare professionals is better understood, psychological violence experienced by healthcare workers gains a special importance. Within the scope of this study, which deals with the effect of psychological violence (mobbing) perception on health workers' job satisfaction, a research was conducted on 199 healthcare workers in Kocaeli Province. Leymann's Inventory Psychological Terror and Minnesota Satisfaction Questionnaire were used within the scope of the research. SPSS 22 package program was used for data analysis in the study. Frequency, independent t-test, one-way ANOVA, pearson correlation and linear regression analyzes were used for analysis. The total mean of the mobing scale items is 1.39 ± 0.63. The average of all the items of the job satisfaction scale is 2.71 ± 0.93. There is a positive relationship between the mobing scale and only the sub-dimension of external job satisfaction and social relations. In the regression analysis performed with external job satisfaction, a significant relationship was found with mobbing sub-dimensions and it explains 6.1% of the total variance on external job satisfaction of mobing. According to the analysis results; statistically significant differences were found between the variables of marital status and year of work at the current institution and position at work and mobbing scale. As a result of the study, mobbing was found to be low and job satisfaction was found to be moderate in health studies. In addition, it was concluded that mobbing negatively affects job satisfaction at a low level. There were also many significant differences with the socio-demographic characteristics of the participants. As a result of the study, it was concluded that the exposure of health workers to mobbing negatively affects their job satisfaction.

Keywords: psychological violence, mobbing, job satisfaction, health professional.

1. Introduction

The word ”mob“ derives from the Latin words ”möbile vulgus" "unstable crowd". In the English language; It means a group of people who are disorderly or in revolt, a gang or crowd that commits unlawful violence, a large group of people or things, and so on. Mobbing is defined as a psychological terror practiced by one or more individuals in an institution or organization, against another individual, by regularly using vindictive and immoral communication (Leymann, 1996).

It has been found that mobbing has a lot of negative effects in organizations in terms of productivity and job satisfaction of employees. The unwillingness of the employees to work due to the low job satisfaction reduces the creativity level of the employees to the lower levels. As a result of psychological violence occurring in businesses, the attention of employees distracts them from the importance of organizational goals and responsibilities. Not only the employees who are exposed to mobbing, but also those who witness the events in the process lose their faith in the business with the fear that one day mobbing may be applied to them.

1.1. Psychological Violence and Process

The theory of psychological violence found its place in the literature for the first time towards the end of the sixteenth century. Derived from the English verb “mob”, which means to form a crowd in order to attack someone, the Turkish expression “Mobbing” means “Psychological Violence”. This term was first used by the Austrian scientist Lorenz, who conducted studies on animal acts, to describe the attacks carried out by a group of small animal herds in the last quarter of the 20th century in order to frighten a single relatively larger animal (Davenport et al., 2003).

Regarding the concept, the generally accepted definition in the academic field was made by Leymann (1990). According to him, psychological violence is defined as a kind of psychological terror applied by one or a few individuals against another individual in a systematic, vindictive and immoral way.

Psychological violence, which occurs by showing itself with disturbing behaviors, starts to hurt the person exposed to psychological violence as time progresses, and events accelerate regularly; It is a formation made up of various levels. It is very important to recognize the symptoms that indicate psychological violence in this formation.

Psychological violence behavior is usually initiated by a bully individual. As time progresses, colleagues or managers cannot change the behavior of this individual, and as a result, the power of the bully rises to higher levels and even other employees in the organization participate in the behavior of psychological violence (Altuntaş, 2010).

The occurrence of psychological violence can occur only from indirect acts of violence, or only from direct acts too. It is also possible for two types of behavior to occur simultaneously. In this direction, psychological violence that starts with indirect behaviors at the first level continues with direct behaviors at the second level and may even turn into open attacks including the use of physical force over time (Zapf and Gross, 2001).

Heinz Leymann (1990) lists the steps related to this process as follows;

1.Group: Prevention of self-expression and communication

2.Group: Isolation from social relationships

3.Group: Attacks on reputation

4. Group: Attacks on the quality of life and occupational position

5.Group: Direct attacks on health

In the formation of psychological violence, there are spectators besides the victim and the perpetrator of psychological violence. These people are described as spectators from the moment they realize the phenomenon of psychological violence. Even if they are not directly involved in psychological violence, they somehow participate in, perceive and become victims of psychological violence because they are aware of this situation (Hecker, 2007).

The followers of psychological violence generally prefer to deny the negative situation in the organization and try to stay away from the victim as much as possible. The spectators may also be depressed, be afraid of negative experiences, and even consider quitting like the victims (Duffy, 2009).

1.2. Job Satisfaction

In addition to the fact that those who work in business life gain work-related knowledge, they also experience the accumulation of different emotions that occur every working day. As a result of these experiences, an individual's mental and emotional attitude towards work occurs. These attitudes are expressed as “job satisfaction”. (Eğinli, 2009).

Job satisfaction can be expressed as the financial benefits obtained from the work and the happiness of the employee to create a work with his colleagues with whom he enjoys working (Şimşek et al., 2003). If the employee can see a work that he has created, this will be a source of pride for him and he will be satisfied with this situation.

The attitudes of the employees towards their jobs and towards the organization they work for affect their performance. Since the factors affecting the attitudes of the employees are related to the opportunities provided by the management in terms of meeting their own needs and expectations and the organizational structure in terms of sustainability, ensuring job satisfaction is of particular importance for each.

Along with job satisfaction, anxiety and the discomforts that will come with anxiety decrease. Job satisfaction ensures that the person's unrevealed tensions are eliminated and his wishes come true. People have high learning potential. In addition, occupational accidents are at a very low level. The level of job satisfaction within the organization reduces the tendency of people to seek other jobs (Çetin, 2004). Likewise, it has been observed that people with high job satisfaction exhibit participatory behavior that helps others, approaches and serves customers more (Arnold and Feldman, 1986).

In world markets where there is intense competition, businesses need to use their resources effectively and efficiently in order to ensure sustainability and compete, and thus increase their overall performance. One of the most important and most volatile resources of the enterprises is their employees, and the performance of the employees is the most important factor affecting the success of the enterprises in terms of reaching the goals of the enterprise and ensuring long-term profitability. The ability of employees to show high performance and work efficiently depends on their satisfaction from their work (Erdil et al., 2004). In this respect, providing job satisfaction of employees has become one of the most basic business objectives (Bernal et al., 2005).

One of the main determinants of deteriorating working conditions in organizations is low job satisfaction. Low job satisfaction is one of the main reasons behind sudden strikes, slowing down, truancy, low productivity and similar problems. This situation constitutes a very high cost for the enterprise. In this sense, high job satisfaction both relieves managers and shows that the business is well managed (Bernal et al., 2005).

In the light of the information given above, the aim of the study is to reveal whether the psychological violence levels of health workers affect their job satisfaction, and if so, to what extent.

2. Materials and Methods

In this section, the universe and sample, research hypotheses, data collection and analysis methods of the research conducted to determine the effect of mobbing perception on job satisfaction of health workers are explained.

2.1. The Universe and Sample of the Research

The universe of the research is health workers working in health institutions in Kocaeli Province. The sample of the research is; It consists of 199 people working in District Health Directorates, Family Physicians and

Hospitals between September 9, 2020 and October 21, 2020. An online questionnaire was used as a data collection method in the research.

2.2. Data Collection Tools

In the questionnaire form, there are 9 statements that we can reach demographic data about the participants. These are the participants; their gender, age, education, profession, marital status, ways of operation, working year, year of work at the current institution and position at work. In the next two sections, scales are given.

2.2.1. Leymann Inventory of Psiychological Terror (LIPT)

The scale used to evaluate mobbing behaviors is the Leymann Inventory of Psychological Terror scale, which consists of 45 statements defined by Heinz Leymann (1996). The translation of the scale, which was originally in German, into our language was made by Osman Cem Önertoy in 2003 by publishing it in his book "Mobbing: Harassment in the Workplace".

The scale consists of five sub-dimensions; prevention of self-expression and communication, isolation from social relationships, attacks on reputation, attacks on the quality of life and occupational position and direct attacks on health. The scale is measured as a 5-point Likert type (1: Never, 2: Rarely, 3: Sometimes, 4: Often, and 5: Always).

2.2.2. Minnesota Satisfaction Questionnaire (MSQ)

Minnesota Satisfaction Questionnaire (MSQ), Weiss et al. (1967) was developed by. The scale consists of 20 statements. The Minnesota Job Satisfaction scale was introduced to the Turkish literature by Deniz and Güliz Gökçora (1985) from Hacettepe University. The scale has two sub-dimensions as internal job satisfaction and external job satisfaction. While internal job satisfaction consists of 12 expressions, external job satisfaction consists of 8 expressions (Act. Öztürk, 2004).

The internal job satisfaction score consists of items related to satisfaction related to the internal nature of the job, such as achievement, recognition or appreciation, the job itself, job responsibility, job change due to promotion and promotion. It is found by dividing the sum of the internal job satisfaction scores by 12. The external job satisfaction score consists of elements of the work environment, such as corporate policy and management, type of supervision, relations with the manager, work and subordinates, working conditions, and wages. It is found by dividing the sum of external job satisfaction scores by 8. The scale is measured as a 5-point Likert type (1: Not at all Appropriate, 2: Not Appropriate, 3: Somewhat Appropriate, 4: Appropriate, and 5: Completely Appropriate).

2.3. Analysis Methods

The data obtained from the research were transferred to the SPSS 22 program and analyzed. Before testing the hypothesis, the reliability of the data was checked. Then, the frequency distributions of the participants and the descriptive information of the scales were examined. Afterwards, correlation analyzes were performed for the relationship between the scales and regression analyzes for the effect. Finally, independent sample t-test and one-way variance (ANOVA) analyzes were applied to measure the differences in socio-demographic data on the scales.

2.4. Reliability of Scales

Table 1. Reliability Analysis Results of Scales

Scales and Sub-dimesions	Number of Item	Cronbach's Alpha
Prevention of self-expression and communication	**11**	**0,910**
Isolation from social relationships	**5**	**0,934**
Attacks on reputation	**15**	**0,971**
Attacks on the quality of life and occupational position	**9**	**0,954**
Direct attacks on health	**5**	**0,886**
Leymann Inventory of Psiychological Terror (LIPT)	**45**	**0,982**
Internal Job Satisfaction	**12**	**0,938**
External Job Satisfaction	**8**	**0,908**
Minnesota Satisfaction Questionnaire (MSQ)	**20**	**0,961**

In order to determine the reliability of the scales, the Cronbach's Alpha Coefficient was calculated with the SPSS 22 program. The data in this analysis; $0.7 \leq \alpha < 0.8$ is acceptable, $0.8 \leq \alpha < 0.9$ is good, $0.9 \leq \alpha$ is excellent. Table 1 shows the results of the reliability analysis of the scales and their sub-dimensions. According to these results, it was concluded that the data of the scales and their sub-dimensions were reliable.

2.5. Hypotheses

Depending on the purpose of the research, the following hypotheses have been developed to be tested:

H_1: There is a statistically significant relationship between mobbing and job satisfaction for the participants.

H_2: There is a statistically significant effect between mobbing and job satisfaction for the participants.

H_3: There is a statistically significant difference between mobbing and socio-demographic characteristics of the participants.

H_4: There is a statistically significant difference between the job satisfaction of the participants and their socio-demographic characteristics.

3. Results

In this section, analysis of the research results is given. First, the socio-demographic information of the participants participating in the study and the descriptive information of the scales were included, and then the hypothesis tests.

Table 2. Socio-demographic Information of Participants (n=199)

Variable		N	%
Gender	Woman	146	73,4
	Man	50	25,1
Age	20-29	32	16,1
	30-39	51	25,6
	40-49	96	48,2
	50 and above	12	6,0
Education	High School	12	6,0
	Associate Degree	37	18,6
	Bachelor	109	54,8
	Master's and Above	38	19,1
Profession	Doctor	27	13,6
	Midwife	37	18,6
	Nurse	77	38,7
	Health Officer	53	26,6
Marital status	Maried	149	74,9
	Single	46	23,1
Ways of Operation	Regular hours	136	68,3
	Shift method	25	12,6
	Watch (16-8)	14	7,0
	Other	16	8,0
Working Year	0-5	30	15,1
	6-10	40	20,1
	11-15	25	12,6
	16-20	28	14,1
	20 and above	74	37,2
Year of Work at the Current Institutio	1 and less	16	8,0
	1-5	73	36,7
	6-10	51	25,6
	11-15	26	13,1
	16-20	15	7,5
	20 and above	17	8,5
Position At Work	Worker	170	85,4
	Service Officer	19	9,5
	Manager	9	4,5

Table 2 shows the socio-demographic characteristics of the participants. When the data is examined, 74.5% of the participants are women; 50.3% are 40-49 years old; 55.6% of them are bachelor graduates; 38.7% are nurses; 76.4% are married; 71.2% of them work regular hours; 37.6% of them have been working for 20 years

or more; 36.9% of them have been working in their institution for 1-5 years and 85.9% of them are worker in the institution.

Table 3. Descriptive Findings of the Scales and their Sub-Dimensions

Scales and Sub-dimesions	Number Items	Mean ($\bar{X}$)	Standard Deviation (S.D.)
Prevention of self-expression and communication	**11**	**1,59**	**0,66**
Isolation from social relationships	**5**	**1,29**	**0,70**
Attacks on reputation	**15**	**1,31**	**0,69**
Attacks on the quality of life and occupational position	**9**	**1,41**	**0,78**
Direct attacks on health	**5**	**1,23**	**0,59**
LIPT	**45**	**1,39**	**0,63**
Internal Job Satisfaction	**12**	**2,82**	**0,98**
External Job Satisfaction	**8**	**2,56**	**0,93**
MSQ	**20**	**2,71**	**0,93**

Table 3 shows descriptive information about the LIPT and MSQ scales. The mean of LIPT expressions is 1.39 ± 0.63. Accordingly, it is seen that the participants mostly chose never and rarely expressions about mobbing expressions. When the sub-dimensions are examined; prevention of self-expression and communication 1.59 ± 0.66; isolation from social relationships 1.29 ± 0.70; attacks on reputation 1.31 ± 0.69; attacks on the quality of life and occupational position 1.41 ± 0.78 and direct attacks on health 1.23 ± 0.59 have averages. The mean of the MSQ scale is 2.71 ± 0.93. While the average of internal job satisfaction from the sub-dimensions was 2.82 ± 0.98, the average of external job satisfaction was determined as 2.56 ± 0.93.

Table 4. LIPT and MSQ Correlation Analysis Findings

		External Job Satisfaction	Internal Job Satisfaction	MSQ
Prevention of self-expression and communication	**r**	**-,095**	**-,069**	**-,082**
	p	**,189**	**,338**	**,256**
Isolation from social relationships	**r**	**,144***	**,077**	**,107**
	p	**,047**	**,291**	**,140**
Attacks on reputation	**r**	**,095**	**,056**	**,074**
	p	**,188**	**,436**	**,305**
Attacks on the quality of life and occupational position	**r**	**,047**	**,042**	**,045**
	p	**,517**	**,566**	**,534**
Direct attacks on health	**r**	**-,013**	**-,037**	**-,028**
	p	**,862**	**,614**	**,703**
LIPT	**r**	**,037**	**,016**	**,025**
	p	**,614**	**,827**	**,730**

*** The correlation is successful at the 0.05 level. (2-tailed).**

Table 4 shows the results of the pearson correlation analysis to examine the relationship between LIPT and MSQ. According to the results of the analysis, there is a statistically significant positive but weak relationship between only external job satisfaction and isolation from social relationships. Since no other relationship was found between both scales and sub-dimensions, the hypothesis about the relationship between mobbing and job satisfaction scales was rejected.

Table 5. LIPT and MSQ Regression Analysis Findings

Dependent Variables	Independent Variables	β	p	F	p (Model)	Reg. R^2
Internal Job Satisfaction	Prevention of self-expression and communication	-0,183	0,087	1,651	0,149	0,017
	Isolation from social relationships	0,127	0,372			
	Attacks on reputation	0,166	0,402			
	Attacks on the quality of life and occupational position	0,088	0,581			
	Direct attacks on health	-0,212	0,114			
External Job Satisfaction	Prevention of self-expression and communication	-0,265	0,012	3,465	0,005	0,061
	Isolation from social relationships	0,281	0,045			
	Attacks on reputation	0,209	0,283			
	Attacks on the quality of life and occupational position	-0,026	0,867			
	Direct attacks on health	-0,187	0,154			
MSQ	Prevention of self-expression and communication	-0,223	0,036	2,37	0,041	0,035
	Isolation from social relationships	0,195	0,168			
	Attacks on reputation	0,189	0,337			
	Attacks on the quality of life and occupational position	0,043	0,786			
	Direct attacks on health	-0,208	0,118			

Table 5 shows the results of multiple linear regression analysis to examine the effect of LIPT on MSQ. In the regression analysis of the internal job satisfaction sub-dimension, no significant relationship was found with the LIPT sub-dimensions. ($p>0.05$) In other words, sub-dimensions of LIPT do not affect internal job satisfaction.

In the regression analysis performed with external job satisfaction, a significant relationship was found between the sub-dimensions of LIPT and external job satisfaction ($p<0.05$), and the sub-dimensions of LIPT explain 6.1% of the total variance on external job satisfaction. With external job satisfaction, one of the sub-dimensions of LIPT, “Prevention of self-expression and communication” was negatively significant ($p=0.012$, $\beta=-0.265$), and “Isolation from social relationships” sub-dimension ($p=0.045$, $\beta=0.281$). there is a positive

significant relationship. Accordingly, while the increase in the "Prevention of self-expression and communication" sub-dimension decreases external job satisfaction, there is a positive significant relationship with the "Isolation from social relationships" sub-dimension ($p=0.045$, $\beta=0.281$). Here, an increase in "Prevention of self-expression and communication" is an expected result to increase external job satisfaction, but it is not an expected result as an increase in "Isolation from social relationships" sub-dimension increases external job satisfaction.

In the regression analysis performed with the MSQ, a significant effect was found between the sub-dimensions of LIPT ($p<0.05$) and the sub-dimensions of LIPT explain 3.5% of the total variance on the MSQ. There is a negative correlation ($p=0.036$, $\beta=-0.223$) with “Prevention of self-expression and communication”, one of the sub-dimensions of MSQ and LIPT. Accordingly, increasing the "Prevention of self-expression and communication" sub-dimension decreases the MSQ. According to these results, the hypothesis written as mobbing affects job satisfaction was accepted.

Table 6. Difference Analysis Findings of Socio-demographic Characteristics with LIPT

LIPT		N	X̄	S.D.	T	P
Gender	Woman	146	1,40	0,68	0,644	0,929
	Man	50	1,39	0,48		
Age	20-29	32	3,38	1,02	2,290	0,080
	30-39	51	3,47	0,67		
	40-49	96	3,31	0,38		
	50 and above	12	3,58	0,48		
Education	High School	12	1,12	0,16	2,021	0,112
	Associate Degree	37	1,59	0,94		
	Bachelor	109	1,37	0,57		
	Master's and Above	38	1,36	0,44		
Profession	Doctor	27	1,47	0,50	2,227	0,086
	Midwife	37	1,30	0,33		
	Nurse	77	1,29	0,42		
	Health Officer	53	1,56	0,97		
Marital status	Maried	149	1,84	1,05	3,579	0,001
	Single	46	1,26	0,34		
Ways of Operation	Regular hours	136	1,34	0,54	1,662	0,177
	Shift method	25	1,63	0,97		
	Watch (16-8)	14	1,53	0,86		
	Other	16	1,36	0,42		
Working Year	0-5	30	1,43	0,75	2,078	0,085
	6-10	40	1,61	0,99		
	11-15	25	1,27	0,30		
	16-20	28	1,22	0,27		
	20 and above	74	1,36	0,46		
Year of Work at the Current Institution	1 and less	16	1,84	1,07	2,316	0,045
	1-5	73	1,42	0,75		
	6-10	51	1,26	0,30		
	11-15	26	1,43	0,49		
	16-20	15	1,23	0,37		
	20 and above	17	1,32	0,43		
Position At Work	Worker	170	1,39	0,65	0,052	0,949
	Service Officer	19	1,35	0,39		
	Manager	9	1,36	0,66		

Table 6 shows the results of the independent sample t-test and ANOVA analysis performed to analyze whether there is a significant difference between the LIPT scale and the socio-demographic characteristics of the participants. According to the results of the analysis, while there was no statistically significant difference according to the gender, age, education, profession, ways of operation, working years and position at work, a statistically significant difference was found for marital status and year of work at the current institution. When the reasons for the difference are examined, it is seen that the LIPT scale scores of the single participants for the marital status variable are higher than the married ones. The difference was revealed by

the fact that the LIPT averages of the participants who worked at the institution for less than 1 year according to the working year were higher than the other groups. It can be stated that participants who are new to their institution feel more mobbing than other participants. As a result, the H3 hypothesis was accepted for the variables of marital status and year of work at the current institution, while it was rejected for the other variables.

Table 7. Difference Analysis Findings of Socio-demographic Characteristics with MSQ

MSQ		N	X̄	S.D.	T	P
Gender	Woman	146	2,67	0,87	0,530	0,669
	Man	50	2,73	0,95		
Age	20-29	32	2,82	1,14	2,316	0,077
	30-39	51	2,71	0,86		
	40-49	96	2,60	0,89		
	50 and above	12	3,31	0,62		
Education	High School	12	2,89	0,82	0,159	0,924
	Associate Degree	37	2,69	1,13		
	Bachelor	109	2,71	0,89		
	Master's and Above	38	2,72	0,86		
Profession	Doctor	27	2,75	0,81	0,008	0,999
	Midwife	37	2,75	0,92		
	Nurse	77	2,73	0,94		
	Health Officer	53	2,73	0,95		
Marital status	Maried	149	2,83	0,99	0,877	0,382
	Single	46	2,69	0,91		
Ways of Operation	Regular hours	136	2,76	0,91	0,455	0,714
	Shift method	25	2,68	1,13		
	Watch (16-8)	14	2,51	0,73		
	Other	16	2,56	1,09		
Working Year	0-5	30	2,79	1,00	0,979	0,420
	6-10	40	2,85	0,96		
	11-15	25	2,42	0,84		
	16-20	28	2,60	1,02		
	20 and above	74	2,74	0,89		
Year of Work at the Current Institution	1 and less	16	2,22	0,90	2,098	0,067
	1-5	73	2,84	0,88		
	6-10	51	2,54	0,88		
	11-15	26	2,82	1,09		
	16-20	15	3,07	0,99		
	20 and above	17	2,62	0,87		
Position At Work	Worker	170	2,71	0,89	2,695	0,070
	Service Officer	19	2,96	1,05		
	Manager	9	2,10	1,27		

Table 7 shows the results of the independent sample t-test and ANOVA analysis performed to analyze whether there is a significant difference between the MSQ scale and the socio-demographic characteristics of

the participants. According to the results of the analysis, no statistically significant difference was found according to the participants' gender, age, education, profession, marital status, ways of operation, working year, year of work at the current institution and position at work. Accordingly, the H4 hypothesis was rejected.

4. Discussion and Conclusion

A study was conducted on 199 health workers to determine the effect of the perception of psychological violence (mobbing) on the job satisfaction of health workers.

The total mean of the LIPT scale items is 1.39 ± 0.63. Accordingly, it is seen that the participants mostly chose never and rarely statements about mobbing items. When the sub-dimensions were examined, the average of the "prevention of self-expression and communication" sub-dimension was 1.59 ± 0.66; The average of the “isolation from social relationships” sub-dimension was 1.29 ± 0.70; The average of the “attacks on reputation” sub-dimension was 1.31 ± 0.69; The average of the sub-dimension "attacks on the quality of life and occupational position" is 1.41 ± 0.78, and the average of the sub-dimension "direct attacks on health" is 1.23 ± 0.59. Buna göre ortalaması en fazla çıkan alt boyut *kişinin kendisini göstermesi ve başkalarıyla iletişiminin engellenmesine yönelik yıldırma* davranışı alt boyutudur. Accordingly, the sub-dimension with the highest average is the sub-dimension of prevention of self-expression and communication. This result shows that the most common mobing situation of the participants is prevention of self-expression and communication. This result is similar to Gökdemir's (2016) study.

The mean of all items of the MSQ scale is 2.71 ± 0.93. While the average of internal job satisfaction from the sub-dimensions is 2.82 ± 0.98, the average of external job satisfaction is 2.56 ± 0.93. Again, in Gökdemir's (2016) study, the average of internal job satisfaction is higher than the average of external job satisfaction.

According to the results of LIPT and MSQ Pearson Correlation analysis, there is a positive relationship between external job satisfaction and isolation from social relationships sub-dimension. This result confirms the hypotheses about the relationship between job satisfaction and mobbing. In Gökdemir's (2016) study, a negative correlation was found between internal and external job satisfaction and mobbing sub-dimensions, and a different result was obtained from our findings.

According to the results of multiple linear regression analysis to examine the effect of mobbing perception on job satisfaction, no significant effect was found with LIPT sub-dimensions in the regression analysis related to the internal job satisfaction sub-dimension ($p>0.05$). In other words, LIPT sub-dimensions do not affect internal job satisfaction. In the regression analysis performed with external job satisfaction, a significant effect was found between LIPT sub-dimensions and external job satisfaction ($p<0.05$), and LIPT sub-dimensions explain 6.1% of the total variance on external job satisfaction. There is a negative significant effect with "prevention of self-expression and communication", ($p=0,012$, $\beta=-0,265$) which is one of the LIPT sub-dimensions, and a positive significant effect with the "isolation from social relationships" ($p=0,045$, $\beta=0,281$) sub-dimension on external job satisfaction. Accordingly, increasing the "prevention of self-expression and communication" sub-dimension decreases external job satisfaction, while increasing the "isolation from social relationships" sub-dimension increases external job satisfaction. Here, it is an expected result that the increase in "prevention of self-expression and communication" will increase external job satisfaction. On the

other hand, it is not an expected result that increasing the "isolation from social relationships" sub-dimension will also increase external job satisfaction. The result of negative significant effect on external job satisfaction and "prevention of self-expression and communication", one of the LIPT sub-dimensions, coincides with Gökdemir's (2016) study.

In Gökdemir (2016) study, only the "prevention of self-expression and communication" sub-dimension of LIPT has a negative effect on external job satisfaction ($p=0.041<0.05$). LIPT sub-dimensions explain 3.5% of the total variance on the MSQ. There is a negative significant ($p=0.036$, $\beta=-0.223$) effect with job satisfaction and “prevention of self-expression and communication” sub-dimensions of mobbing. Accordingly, increasing the "prevention of self-expression and communication" sub-dimension reduces job satisfaction.

According to the results of the difference analysis of mobing level and job satisfaction level by gender, the gender variable does not make a difference for mobbing perception and job satisfaction ($p>0.05$). In Gökdemir's (2016) study, gender variable internal and external job satisfaction sub-dimensions make a difference for the "prevention of self-expression and communication" sub-dimension, and a different result was obtained from our study. According to the results of the Fourth European Working Conditions Survey (2007), it is stated that women are exposed to mobbing and sexual abuse 3 times more than men. Based on the countries in the same research sample, it was stated that women in Ireland, Finland and Luxembourg were exposed to mobbing more than women in other countries. On the other hand, according to the research conducted by Bahçe (2007) on employees of five sectors operating in two public, two private and one service sectors in Ankara, it was concluded that it does not matter whether the employees in the enterprises are exposed to mobbing practices, whether they are male or female. In the study conducted by Yıldırım and Yıldırım (2010) on academics working in the field of health, it was concluded that gender has no effect on being exposed to mobbing.

According to the results of the difference analysis of LIPT and MSQ levels according to age, no significant difference was found for the age variable ($p>0.05$). Although there is no significant difference with the MSQ, it can be stated that the participants aged 50 and over have higher job satisfaction. In Gökdemir's (2016) study, the job satisfaction of participants over the age of 40 is higher.

According to the results of the difference analysis of LIPT and MSQ levels according to marital status, a difference was found between the marital status variable and LIPT ($p<0.05$). Single participants averaged higher for LIPT than married participants. Accordingly, single participants feel more mobbing perception. In Aksoy's (2008) study, it was stated that single workers were exposed to more mobbing and the reason for this was that single workers were young and inexperienced. There was no significant difference between married and single participants for MSQ ($p>0.05$). In Gökdemir's (2016) study, awareness was found only in external inner satisfaction among married and single participants.

According to the results of the difference analysis of LIPT and MSQ levels according to educational status, no significant difference was found for the education variable ($p>0.05$).

According to the results of the difference analysis of LIPT level by occupation, no significant difference was found for the occupation variable ($p>0.05$). In the study of Çöl (2008), it was stated that nurses were exposed to mobbing the most. No significant difference was found in MSQ and its sub-dimensions ($p>0.05$). In

Gökdemir's study, although there was no significant difference in mobbing sub-dimensions, it was determined in job satisfaction sub-dimensions.

According to the results of the difference analysis of the LIPT level according to ways of operation, no significant difference was found for the working type variable ($p>0.05$). There was no significant difference for MSQ either ($p>0.05$). This result coincides with Gökdemir's (2016) study. According to the results of the difference analysis of LIPT level according to working years, no significant difference was found for working years ($p>0.05$). There was no significant difference for MSQ either ($p>0.05$).

According to the results of the difference analysis of the LIPT level according to the years of work in the institution where the participants are located, no significant difference was found ($p<0.05$). In the variable of working years, the average LIPT level of the participants who worked less than 1 year in the institution they are in is higher. According to this result, it can be stated that the participants who are new to their institution feel more mobbing than the other participants. Although there is no significant difference for MSQ, it can be stated that the job satisfaction of the participants working in the institution for less than 1 year is lower than the other participants.

According to the results of the difference analysis of LIPT level according to their positions at work, no significant difference was found for the variable of their positions at work ($p>0.05$). Although there is no significant difference in job satisfaction and its sub-dimensions, it is seen that the MSQ of the service workers is higher than the other participants.

5. References

Aksoy, F. Psikolojik Şiddetin (Mobbing) Sağlık Çalışanlarına Etkisi, Marmara Üniversitesi, Sağlık Bilimleri Enstitüsü, Doktora Tezi, İstanbul, 2008.

Altuntaş, C. Mobbing kavrami ve örnekleri üzerine uygulamali bir çalişma. Journal of Yaşar University, 2010, 5.18: 2995-3015.

Arnold, J., Feldman C. Organizational Behavior, New York: McGraw- Hill International Edition Management Series, 1986.

Bahçe, Ç. Mobbing Oluşumunda Örgüt Kültürünün Rolü: Örnek Bir Uygulama, Gazi Üniversitesi Sosyal Bilimler Enstitüsü, Yüksek Lisans Tezi, Ankara, 2007.

Bernal, J. G., Gargallo, C. A., Marzo, N. M., Rıvera, T. P. Job Satisfaction: Emprical Evidence Of Gender Differences. Women İn Management Review, 2005; 20 (4), 279-288.

Çetin, M. Ö. Örgüt Kültürü ve Örgütsel Bağlılık. Ankara: Nobel Yayın Dağıtım, 2004.

Çöl Özen, S. İşyerinde psikolojik şiddet: Hastane çalışanları üzerine bir araştırma, Çalışma ve Toplum Dergisi, 2008; 4, 107-134.

Davenport, N., Swartz, R. D., ve Eliot, G. P. Mobbing: İşyerinde Duygusal Taciz, (Çev.: Osman Cem Önertoy), İstanbul: Sistem Yayıncılık, 2003.

Duffy, M. Preventing workplace mobbing and bullying with effective organizational consultation, policies, and legislation. Consulting Psychology Journal: Practice and Research, 2009; 61(3), 242–262

Eğinli, A.T. Çalışanlarda İş Doyumu: Kamu ve Özel Sektör Çalışanlarının İş Doyumuna Yönelik Bir Araştırma. Atatürk Üniversitesi, İktisadi ve İdari Bilimler Fakültesi Dergisi, 2009; 23(3): 35-32.

Erdil, O., Keskin, H., İmamoğlu, S. Z., Erat, S. Yönetim Tarzı ve Çalışma Koşulları, Arkadaşlık Ortamı ve Takdir Edilme Duygusu ile İş Tatmini Arasındaki İlişkiler: Tekstil Sektöründe Bir Uygulama, Doğuş Üniversitesi Dergisi, 2004; 17-26.

Fourth European Working Conditions Survey. Preventing Violence and Harassment in the Workplace, European Foundation for the Improvement of Living and Working Conditions, 2007; 14-16.

Gökdemir, D. Sağlık çalışanlarında mobbing algısının iş tatmini üzerindeki etkisi: Kamu hastanesinde bir araştırma. MS thesis. İstanbul Gelişim Üniversitesi Sosyal Bilimler Enstitüsü, 2016.

Hecker, T. E. Workplace Mobbing: A Discussion for Librarians. The Journal of Academic Librarianship, 2007; 33 (4), 439-445.

Leymann, H. Mobbing and Psychological Terror at Workplaces. Violence and Victims, 1990; 5 (2), 119-126.

Leymann, H. The content and development of mobbing at work. European journal of work and organizational psychology, 1996, 5.2: 165-184.

Özyurt, A. İstanbul Hekimlerinin İş Doyum ve Tükenmişlik Düzeyleri, (Yayımlanmamış Yüksek Lisans Tezi), İstanbul: Marmara Üniversitesi, Saglık Bilimler Enstitüsü, 2004.

Şimşek, M. Ş., Akgemci, T., Çelik, A. Davranış Bilimlerine Giriş ve Örgütsel Davranış (8.Baskı). Ankara: Nobel Yayıncılık, 2013.

Weiss, D. J., Dawis, R. V., England, G. W., Lofquist, L. H. Minnesota Satisfaction Questionnaire. Minneapolis, MN: University of Minnesota, Vocational Psychology Research, 1967.

Yıldırım, D., Yıldırım, A. Sağlık alanında çalışan akademisyenlerin karşılaştıkları psikolojik şiddet davranışları ve bu davranışların etkileri, Türkiye Klinikleri Tıp Bilimleri Dergisi, 2010; 2, 559-570.

Zapf, D., C. Gross, Conflict Escalation and Coping With Workplace Bullying: A Replication and Extension. European Journal of Work and Organizational Psychology, 2001; 10 (4), 497- 522.

Second International Congress on Biological and Health Sciences
ONLINE 24-25-26-27 FEBRUARY 2022

The Histological Effect of CoQ10 on Spermatogenesis in Rats

Sinem İnal[1], Yonca Betil Kabak[1]

[1]Ondokuz Mayis University, Faculty of Veterinary Medicine, Department of Pathology, Samsun, Turkey

Corresponding author: sinem.inal@omu.edu.tr

Abstract:

The histological effects of CoQ10 supplementation were investigated by examining seminiferous tubule morphometry in rat testicles in this study. For this purpose, a total of 30 Sprague Dawley rats obtained from DEHAM (Ondokuz Mayis University Experimental Animal Application and Research Center, Samsun Turkey) were used and divided into three groups; control (n=10), vehicle (n=10), and CoQ10 (n=10). The control group was given only pellet feed and water during the study. While the vehicle group was given only olive oil by oral gavage for 23 days, the CoQ10 group was given 20 mg/kg CoQ10 by oral gavage after being dissolved in olive oil for 23 days. At the end of the experiment, rats were euthanized under ketamine xylazine anesthesia. Testicular tissues were removed and fixed in Bouin's solution. Epithelial thickness and diameters of 10 seminiferous tubules were measured for each rat. In addition, histology of the epididymis was evaluated. While the diameter values did not differ significantly between the groups, a statistically significant difference was observed between the control and CoQ10 groups in epithelial thickness ($P<0.05$). Sperm density in the epididymis did not differ significantly between groups. The increase in the thickness of the seminiferous tubular epithelium containing germ cells can be considered as a factor indicating increased spermatogenesis. As a result, this increase in thickness suggested that CoQ10 may have a positive effect on spermatogenesis.

Keywords: CoQ10, rat, seminiferous tubule

#This study was supported by Ondokuz Mayıs University Scientific Research Projects Commission (PYO.VET.1904.19.013).

1. Introduction

Infertility is caused by a host of intrinsic and extrinsic factors. Male fertility may be adversely affected by many causes such as drugs, infections, pollutants or radiation exposure (Olayemi 2010; Wong et al. 2000). Healthy male germ cells require a certain amount of reactive oxygen radicals (reactive oxygen species - ROS) for the

regulation of spermatogenesis. However, if too much oxidative stress is present, fertility is negatively affected (Tafuri et al. 2015). The main adverse effects of oxidative stress include reduced sperm motility, count and pathological changes in sperm morphology (Aitken and Fisher 1994).

The use of antioxidizing agents may reverse or prevent this unwanted process. The use of supplements such as Vitamin E and Vitamin C is known to reduce sperm DNA damage (Ahmadi et al. 2016). Also, previous studies suggest that the administration of antioxidants increases sperm motility and count (Hadwan et al. 2012, 2014). CoQ10 has been successfully used for antioxidative properties. It has been widely used for oxidative stress studies in experimental testicular damage models (Güleş et al. 2019; Mazen and Elnegris 2013).

The aim of this study is to determine the effects of CoQ10 on the seminiferous tubules of healthy adult male Sprague-Dawley rats by histological morphometric evaluation.

2. Materials and Methods

A total of 30 Sprague Dawley rats was obtained from DEHAM (Ondokuz Mayis University Experimental Animal Application and Research Center, Samsun, Turkey). For this experimental study, approval was provided from Ondokuz Mayıs University Animal Experiments Local Ethics Committee (No: 2018/50). They were kept under standard conditions of temperature, humidity and light and dark cycles. Rats divided into three groups; control (n=10), vehicle (n=10), and CoQ10 (n=10). The control group was given only pellet feed and water during the study. While the vehicle group was given only olive oil by oral gavage for 23 days, the CoQ10 group was given 20 mg/kg CoQ10 (Roth, Germany) by oral gavage after being dissolved in olive oil for 23 days. At the end of the experiment, rats were euthanized under ketamine xylazine anesthesia. Testicular tissues were removed and fixed in Bouin's solution. After tissue samples were embedded paraffin, sections were cut 4-5 µm and stained with hematoxylin-eosin. For histopathological evaluations, epithelial thickness and diameters of 10 seminiferous tubules were measured for each rat. In addition, histology of the epididymis was evaluated. Statistical analyses were performed using the GraphPad Prism version 5.00 (GraphPad Software, San Diego California USA). Significant differences among means were analyzed with one-way analysis of variance ANOVA followed by Dunnett’s posthoc test. p-value of <0.05 was considered significant.

3. Results

The normal histological structure that the germ cells at different stages in the seminiferous tubules were arranged in a certain order, and Sertoli cells were found in the basal lamina of the seminiferous tubules in all groups. (Figure 1) The mean diameters of the seminiferous tubules were measured as 278.4 µm in the control group, 272.9 µm in the vehicle group, and 277.9 µm in the CoQ10 group. Epithelial thicknesses of tubules

were measured as 65.51 µm, 66.83 µm and 71.02 µm, respectively. (Figure 2) While the diameter values did not differ significantly between the groups, a statistically significant difference was observed between the control and CoQ10 groups in epithelial thicknesses ($P<0.05$). Sperm density in the epididymis did not differ significantly between CoQ10 and control groups. (Figure 3)

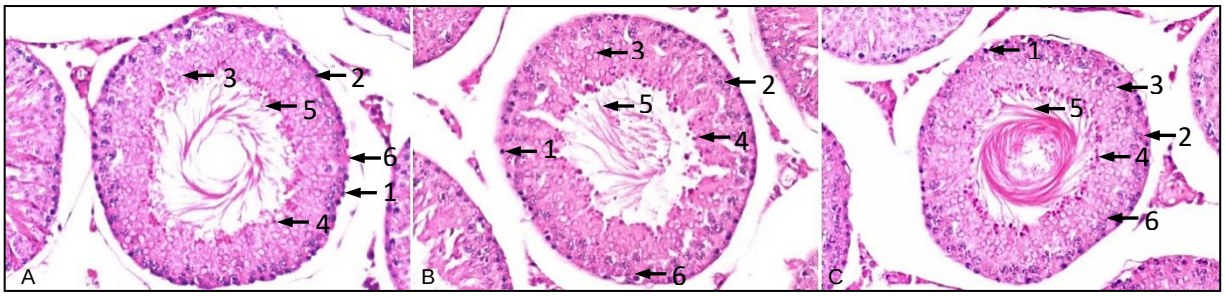

Figure 1. Seminiferous tubule (1) Tip A Spermatogonium, (2) pachytene spermatocyte, (3) step 7 round spermatid, (4) residual body, (5) mature spermatid, (6) sertoli cell. A) control group x20, B) vehicle group x20, C) CoQ10 group x20

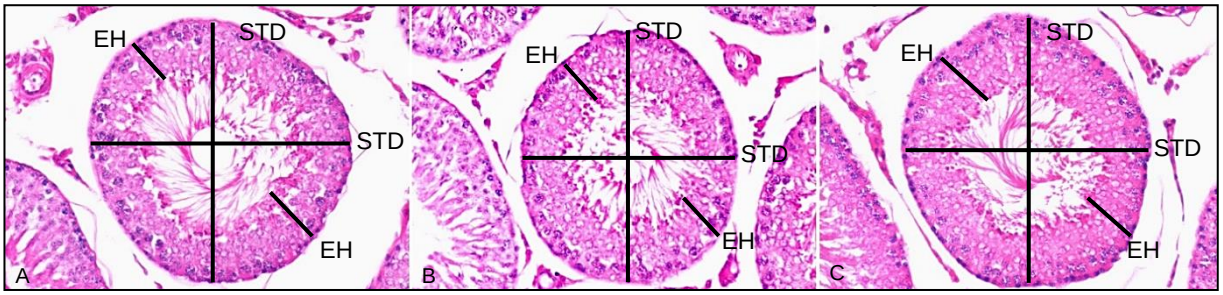

Figure 2. Diameters of the seminiferous tubules (STD) and epithelial heights (EH). A) control group x20, B) vehicle group x20, C) CoQ10 group x20

Figure 3. Epididymis A) control group x4, B) vehicle group x4, C) CoQ10 group x4

4. Discussion

In this study, the effect of supplemental CoQ10 administration on spermatogenesis was investigated histologically in Sprague Dawley rats kept under physiological conditions. The use of antioxidant supplements in male fertility has been the focus of many studies. Antioxidants such as zinc (Ebisch et al. 2006), vitamin C (Colagar and Marzony 2009) and vitamin E (Ross et al. 2010), carnitine (Lenzi et al. 2004), selenium and N-acetyl-cysteine (Safarinejad and Safarinejad 2009) are used to improve semen parameters. CoQ10, also known

as ubiquinone, is one of the important antioxidants (Ernster and Forsmark-Andree 1993). A positive correlation between CoQ10 concentration and sperm motility has been reported (Gvozdjáková et al. 2015). Histological evaluation of testicular tissue is performed with semi-quantitative and quantitative methods. Morphometry of the seminiferous tubules is one of the methods used to evaluate testicular tissue (Yalçın et al. 2020). During spermatogenesis, spermatogonial cells transform into spermatozoa within the seminiferous tubule (Hess and Franca 2009). Thickening of the seminiferous tubules is previously reported to positively affect fertility (Tripathi et al. 2015). Previous reports show a correlation between reduced spermatogenesis and thinning of the epithelial layer (Kianifard et al. 2012). The results of our study show that there was an increase in epithelial height in the seminiferous tubules in the CoQ10 group compared to the control group.

5. Conclusion

The increase in thickness of the seminiferous tubule epithelium containing germ cells can be considered as a factor indicating increased spermatogenesis. As a result, this increase in thickness suggested that CoQ10 may have a positive effect on spermatogenesis.

6. References

Ahmadi S, Bashiri R, Ghadiri-Anari A, Nadjarzadeh A. Antioxidant supplements and semen parameters: An evidence based review. International Journal of Reproductive Biomedicine. 2016; 14 (12): 729.

Aitken J, Fisher H. Reactive oxygen species generation and human spermatozoa: the balance of benefit and risk. Bioessays. 1994; 16 (4): 259-267.

Colagar AH, Marzony ET. Ascorbic Acid in human seminal plasma: determination and its relationship to sperm quality. Journal of Clinical Biochemistry and Nutrition. 2009; 45 (2): 144-149.

Ebisch I, Pierik F, De Jong F, Thomas C, Steegers-Theunissen R. Does folic acid and zinc sulphate intervention affect endocrine parameters and sperm characteristics in men? International Journal of Andrology. 2006; 29 (2): 339-345.

Ernster L, Forsmark-Andree P. Ubiquinol: an endogenous antioxidant in aerobic organisms. The Clinical Investigator. 1993; 71 (8): S60-S65.

Güleş Ö, Kum Ş, Yıldız M, Boyacıoğlu M, Ahmad E, Naseer Z, Eren Ü. Protective effect of coenzyme Q10 against bisphenol-A-induced toxicity in the rat testes. Toxicology and Industrial Health. 2019; 35 (7): 466-481.

Gvozdjáková A, Kucharská J, Dubravicky J, Mojto V, Singh RB. Coenzyme Q10, α-tocopherol, and oxidative stress could be important metabolic biomarkers of male infertility. Disease Markers. 2015; 2015: 1-6.

Hadwan MH, Almashhedy LA, Alsalman ARS. Oral zinc supplementation restore high molecular weight seminal zinc binding protein to normal value in Iraqi infertile men. BMC Urology. 2012; 12 (1): 1-6.

Hadwan MH, Almashhedy LA, Alsalman ARS. Study of the effects of oral zinc supplementation on peroxynitrite levels, arginase activity and NO synthase activity in seminal plasma of Iraqi asthenospermic patients. Reproductive Biology and Endocrinology. 2014; 12 (1): 1-8.

Hess RA, Franca LRD. Spermatogenesis and cycle of the seminiferous epithelium; in Molecular Mechanisms in Spermatogenesis: Volume 636: Cheng C. Y (Ed.). Springer Science. 2008; pp. 1-15.

Kianifard D, Sadrkhanlou RA, Hasanzadeh S. The ultrastructural changes of the sertoli and leydig cells following streptozotocin induced diabetes. Iranian Journal of Basic Medical Sciences. 2012; 15 (1): 623-635.

Lenzi A, Sgro P, Salacone P, Paoli D, Gilio B, Lombardo F, Santulli M, Agarwal A, Gandini L. A placebo-controlled double-blind randomized trial of the use of combined l-carnitine and l-acetyl-carnitine treatment in men with asthenozoospermia. Fertility and Sterility. 2004; 81 (6): 1578-1584.

Mazen NF, Elnegris HM. Role of coenzyme Q10 in testicular damage induced by acrylamide in weaned albino rats: a histological and immunohistochemical study. Egyptian Journal of Histology. 2013; 36 (1): 164-174.

Olayemi F. Review on some causes of male infertility. African Journal of Biotechnology. 2010; 9 (20): 2834-2842.

Ross C, Morriss A, Khairy M, Khalaf Y, Braude P, Coomarasamy A, El-Toukhy T. A systematic review of the effect of oral antioxidants on male infertility. Reproductive Biomedicine Online. 2010; 20 (6): 711-723.

Safarinejad MR, Safarinejad S. Efficacy of selenium and/or N-acetyl-cysteine for improving semen parameters in infertile men: a double-blind, placebo controlled, randomized study. The Journal of Urology. 2009; 181 (2): 741-751.

Tafuri S, Ciani F, Iorio EL, Esposito L, Cocchia N. Reactive oxygen species (ROS) and male fertility; in New Discoveries in Embryology: IntechOpen. Wu B. (Ed.). 2015; pp 19-33.

Tripathi UK, Chhillar S, Kumaresan A, Aslam MM, Rajak S, Nayak S, Manimaran A, Mohanty T, Yadav S. Morphometric evaluation of seminiferous tubule and proportionate numerical analysis of Sertoli and spermatogenic cells indicate differences between crossbred and purebred bulls. Veterinary World. 2015; 8 (5): 645-650.

Wong WY, Thomas CM, Merkus JM, Zielhuis GA, Steegers-Theunissen RP. Male factor subfertility: possible causes and the impact of nutritional factors. Fertility and Sterility. 2000; 73 (3): 435-442.

Yalçın T, Sercan K, Tektemur NK, Ozan İE. The methods used in histopathological evaluation of testis tissues. Batman Üniversitesi Yaşam Bilimleri Dergisi. 2020; 10 (1): 148-157.

Second International Congress on Biological and Health Sciences
ONLINE 24-25-26-27 FEBRUARY 2022

Comparison of Glucose Oxidase Method and Electro Biochemical Glucose Sensor Method in Determination of Glucose

Umut Kökbaş[1],

[1]Nevşehir Hacı Bektaş Veli University, Dental Faculty, Medical Biochemistry Department. Nevşehir /Turkey

Corresponding author: umutkokbas@gmail.com

Abstract:
Glucose level is used as a marker in diabetes mellitus. Since complications such as retinopathy due to diabetes mellitus may occur, it is very important to make a quick and easy determination. In this study, it is aimed to compare the electrobiochemical glucose method and glucose oxidase method, which can be an alternative to glucose determination, which is important in terms of diagnosis and follow-up of treatment. For method comparison studies, a total of 200 results were obtained from 5 different solutions containing different amounts of glucose. All samples were analyzed with both the electrobiochemical glucose sensor and the spectrophotometric glucose oxidase method. Analysis results were compared statistically. In the ANOVA test performed according to the results of the samples used in the comparison of the obtained values, it was determined that the results of the two methods were in correlation with each other. In addition, ROC (Receiver Operation Characteristics, Receiver Operating Characteristic) curve has been drawn and its acceptability as an alternative method has been shown. In our study we obtain ROC curve value as 66,5 %. This shown that both of two methods can use a new laboratory method for glucose determination. Electro biochemical glucose sensor method can be evaluated as an alternative method to glucose oxidase method.

Keywords: glucose oxidase, electro biochemistry, glucose.

1. Introduction

Diabetes mellitus (DM) is a chronic disease with an increase in blood glucose level. Diabetes occurs as a result of the absence or lack of insulin secretion, decreased effect of insulin or decreased insulin receptor sensitivity Ingrosso et al. (2022). Genetic causes, immunological factors, environmental factors play a role in the etiology Hussein Al-Ansary et al. (2021). Today, DM; It is classified under four main headings as Type I DM, Type II DM, Gestational DM and other specific types (Beta cell functional disorder, insulin dysfunction, exocrine pancreatic disease, drugs, infections, genetic syndromes, etc.) Alizadeh et al. (2022).

Hyperglycemia and lack of insulin cause various organ dysfunctions in patients with DM. Diabetes has negative effects on the eyes and lungs as well as on other organs. Lung complications; infections, pulmonary function abnormalities, pleural effusion, obstructive sleep apnea Mehta et al. (2022).

Glucose level is used as a marker in diabetes mellitus Achmad et al. (2022). Since complications such as retinopathy due to diabetes mellitus may occur, it is very important to make a quick and easy determination. In this study, it is aimed to compare the electrobiochemical glucose method and glucose oxidase method, which can be an alternative to glucose determination, which is important in terms of diagnosis and follow-up of treatment.

2. Materials and Methods

Glucose oxidase method: The glucose oxidase enzyme reacts with glucose to form gluconic acid and hydrogen peroxide. Hydrogen peroxide reacts with oxygen acceptor substances in the presence of peroxidase enzyme to form a pink colored complex. It is based on the spectrophotometric detection of the color formed at a wavelength of 546 nm Xu et al. (2021).

Electrobiochemical sensor method: In this method, glucose oxidase enzyme and hydrogen peroxidase enzyme were immobilized to the graphite electrode by bovine serum albumin (BSA) and gelatin. The principle of this method is bienzymatic and it is based on the principle of electrobiochemical measurement of the potential change resulting from the oxidation of hydrogen peroxide, which is formed as a result of the reaction of the glucose oxidase enzyme immobilized on the graphite electrode surface, with glucose around +0,70 V with the help of a biosensor.

In both methods, the amount of glucose is measured indirectly. When blood sample was used in the working environment, glucose was studied in a way that corresponds to 80, 100, 150, 200 and 300 mg/dL glucose concentrations. Solutions corresponding to five different concentrations used in method comparison were measured 20 times each. 200 measurements were taken with each method, a total of 200 results were obtained.

2.1. Statistical analysis

ANOVA test was performed using the data obtained from both methods using the SPPS 22.0 statistical program. In addition, since the electrobiochemical sensor is a new method, ROC (Receiver operating characteristic) analysis was performed and its curve was drawn in order to compare it with the Glucose oxidase method.

3. Results

In the results obtained for the five concentrations studied, a separate ANOVA test was performed for each concentration. No statistically significant difference was found in either method. ($P>0.005$) The averages of the results of the study conducted with a total of 200 samples from each concentration according to five different concentrations are given in Table 1.

Table 1. International congress on biological and health sciences

	Electrobiochemical sensor method (n=100)	Glucose oxidase method (n=100)
80 mg/dL Glucose	82,75	84,16
100 mg/dL Glucose	101,97	98,13
150 mg/dL Glucose	149,06	154,32
200 mg/dL Glucose	201,29	204,58
300 mg/dL Glucose	297,86	306,41

The ROC curve is used to compare the two analytical methods. A comparison of specificity and sensitivity is made on the ROC curve. When the comparative analysis of the test results is made, as seen in Figure 1, the area under the blue line constitutes 66.5% of the total area. If the area under the curve in the ROC analysis is over 50%, that method indicates that acceptable results are obtained.

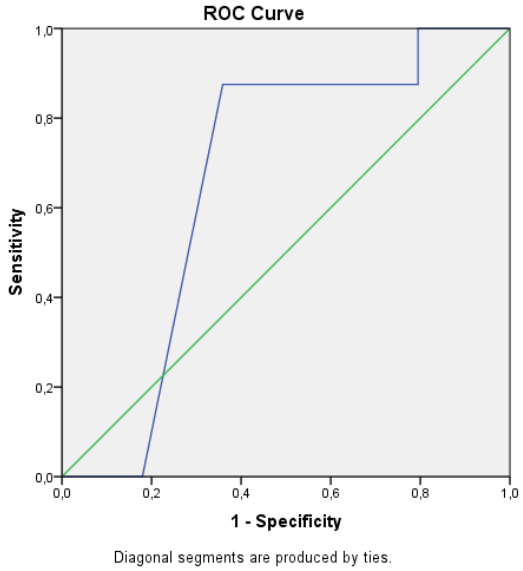

Figure 1. ROC curve of the results obtained from the electrobiochemical glucose sensor study according to the glucose results obtained from the Glucose oxidase method.

4. Discussion

Hyperglycemia and lack of insulin cause various organ dysfunctions in patients with DM. Diabetes has negative effects on the eyes and lungs as well as on other organs. Lung complications; infections, pulmonary function

abnormalities, pleural effusion, obstructive sleep apnea. According to the literature, the prevalence of hyperglucosemia in our country has reached approximately 12% in our country's population. Due to this feature, glucose is one of the important parameters among the continuous examination requests.

In our study, the results obtained from the electrobiochemical sensor and the glucose oxidase method were compared according to the glucose levels in equivalent amounts. Statistically, there was a correlation between the two methods. It is seen in the drawn ROC curve that the electrobiochemical sensor can be used as an alternative to the Glucose oxidase method. (Figure 1) The methods that remain above the green 50% area line added by the program in the ROC curve are considered as alternative methods to the compared method.

5. Conclusion

As a result, it is seen that electrobiochemical studies are faster, cheaper and more practical than traditional methods in the literature. From this point of view, it is expected that the use of electrobiochemical sensors will become widespread for a valuable parameter such as glucose, which is also used as an emergency test.

6. References

1. Achmad, C., et al. Relation between Glycemic Control and Cardiac Autonomic Neuropathy in Patients with Diabetes Mellitus type 2. Curr Probl Cardiol. 2022; 101135.

2. Alizadeh, Y., M. M. Jalali and A. Sehati. Association of different severity of diabetic retinopathy and hearing loss in type 2 diabetes mellitus. Am J Otolaryngol. 2022; 43: 103383.

3. Hussein Al-Ansary, K. A., M. S. Khudhair and A. W. Ashor. The correlation of pro- and anti-inflammatory markers with glycaemic indices in healthy participants and in patients with type 2 diabetes mellitus. J Pak Med Assoc. 2021; 71(Suppl 8): S72-S76.

4. Ingrosso, D. M. F., M. Primavera, S. Samvelyan, V. M. Tagi and F. Chiarelli. Stress and Diabetes Mellitus: Pathogenetic Mechanisms and clinical outcome. Horm Res Paediatr. 2022;

5. Mehta, C., D. Cohen, P. Jaisinghani and P. Parikh. Internal Medicine Resident Adherence to Evidence-Based Practices in Management of Diabetes Mellitus. J Med Educ Curric Dev. 2022; 9: 23821205221076659.

6. Xu, X., Y. Ma, S. Ding and Y. Li. Glucose oxidase@zinc-doped zeolitic imidazolate framework-67 as an effective cascade catalyst for one-step chemiluminescence sensing of glucose. Mikrochim Acta. 2021; 188: 427.

Second International Congress on Biological and Health Sciences
ONLINE 24-25-26-27 FEBRUARY 2022

Antimicrobial, Anti-quorum Sensing, Anti-biofilm and Anti-swarming Activities of Ethanolic Chestnut Propolis Extracts

Ülkü Zeynep Üreyen Esertaş[1], Ali Osman Kılıç[1], Sevgi Kolaylı[2]

[1]Karadeniz Technique University, Faculty of Medicine, Department of Microbiology, Trabzon, Türkiye

[2]Karadeniz Technique University, Faculty of Science, Department of Chemistry, Trabzon, Türkiye

Corresponding author: biyolog_ulku@hotmail.com

Abstract:

Antibiotic resistance, which has increased rapidly in recent years as a result of uncontrolled and unconscious antibiotic consumption, poses a great threat to public health. The inadequacy of existing antibiotics has increased the need for new effective and less toxic antibiotic raw materials or antibiotic derivatives. Propolis is a resinous mixture that honey bees collect from nature for the hygiene and safety of their hives. This natural bee mixture contains many different polyphenols, and volatile oils has wide biological active properties is frequently used in complementary medicine. Raw propolis is usually extracted in 70% ethanol, and used as antimicrobial and antiviral agent. In this study, the antimicrobial activity of ethanolic chestnut propolis was investigated. Antibacterial activity was investigated against *Staphylococcus aureus*, *Mycobacterium smegmatis, Chromobacterium violaceum* and *Candida albicans* was by agar well diffusion assay. Anti-quorum sensing, anti-biofilm and anti-swarming activities were investigated against *Chromo bacterium violaceum*ATCC31532, *Chromo bacterium violaceum* ATCC 12472 and *Pseudomonas aeruginosa* PAO1 respectively. The results were showed that the chestnut Turkish propolis extract were showed high antimicrobial and anti-quorum sensing activity. The high antimicrobial capacity of ethanolic propolis extracts against bacteria with strong resistance to antibiotics needs to be clarified by further research.

Keywords: Chestnut, anti-swarming, propolis, anti-quorum sensing, anti-biofilm

1. Introduction

Propolis is a bee product and is collected as raw propolis by scraping from honeybees' hives. Honeybee propolis is a paste-like mixture created by processing the resinous products collected from the bark and leaves of trees with their own secretions (Salatino et al. 2005). It can be used as a plug in the cracks, cavities and holes of the hives, and its main function is to protect the hygiene and health of the colony. It has a wide range of biological activities such as antioxidant, antibacterial, antiviral, antitumoral and anti-inflammatory. Propolis is an important natural product for human health as well as the health of bee colonies, and it has recently been widely used as a complementary medicine agent. The composition of the balsamic part of propolis is a mixture of secondary metabolites consisting mostly of polyphenols and completely herbal agents. Polyphenols

family, on the other hand, are secondary metabolites of plants and consist of natural organic molecules with nearly 10 thousand members. They are aromatic cyclic structures with very large members, including phenolic acids, flavonoids, coumarins, stilbenes, lignins, procyanins, anthocyanins and their subclasses (Hano, & Tungmunnithum, 2020).

The effectiveness of existing antibiotics on microorganisms has been decreasing rapidly in recent years. With the increase in antibiotic resistance, this problem poses a great threat to public health (Ekşi et al., 2020).

Propolis is a natural mixture whose composition varies according to the flora of the region where it is collected, and consists of high amounts of phenolic acid, flavonoids, stilbenes and lignin. However, the most common sources of propolis are poplar propolis (poplar spp.), and chestnut, pine, oak, juniper, spruce, fir, linden, fruit trees and citrus fruits are important sources. Black Sea Region is rich in chestnut forests and has a high propolis yield, dark red colored of chestnut propolis is an unknown species in the world, and antimicrobial activity of the chestnut propolis was investigated in this study.

2. Materials and Methods

2.1. Sample

The chestnut propolis was supplied from Zonguldak region of Turkey, and the raw material was extracted ethanol (70%). For this extraction, 10 g powdered propolis was mixed 50 ml 70% ethanol, and shaked at 24 h. After filtrations, the solutions was used for tests.

2.1. Antimicrobial activity

Staphylococcus aureus (ATCC 25923),*Mycobacterium smegmatis* (ATCC 607), *Chromo bacterium violaceum* (ATCC 12472), *Candida albicans* (ATCC 10231) were used in the screening of the extract.

The antimicrobial activity was measured by agar diffusion assay with 50 µL of the extracts. Petri dishes were incubated for 18 h for bacteria and 36 h for *Candida*. Minimal Inhibitory Concentration (MIC) was determined using BHIB for *M. smegmatis* and Mueller Hinton broth-II for other bacteria (Woods et al. 2003). RPMI 1640 with 0.2% glucose was used to determine the MIC of *Candida* species (CLSI, 2008). To determine the Minimum Bactericidal Concentration (MBC), 50 µL samples were taken from the MIC well and the previous three wells, inoculated into plates with the relevant medium, and incubated at 37°C for their species times for each microorganism (Woods et al. 2003). The MIC value before the first well where growth started was determined as MBC before it.

2.2. Anti-quorum sensing activity

Sub-Mic concentrations were determined for the violacein pigment suppression activity of the extracts in *C. violaceum* strains. Before the experiment, *Chromobacterium* strains were incubated in 5 mL of LB medium at 37°C overnight at 175 rpm. For the study 50 µL of *C. violaceum* strains was added to 5 mL of soft LB agar, poured onto LB agar petri dishes and left to dry. 50 µL of the determined Sub-Mic concentrations of the extracts were added to the wells opened on LB agar and allowed to incubate overnight. Extracts in which

growth occurred, but no pigment formation was observed in *C. violaceum* strains and that formed a transparent zone were accepted as positive (Franklin et al. 2015).

2.3. Anti-biofilm activity

P. aeruginosa PAO1 strain was adjusted to a McFarland concentration of 0.5 and diluted to 1%. Each well of the micro-plates was adjusted to 125 µL of LB medium, 40 µL of extract and 35 µL of *P. aeruginosa* PAO1. Prepared micro-plates were incubated for 24 hours at 37°C. Micro-plates were washed three times with distilled water and kept in 0.3% crystal violet for 15 minutes. Then, the micro-plates were washed three more times with distilled water, kept in 95% ethanol for 15 min and absorbance was measured at 570 nm (McLean et al. 2004; Truchado et al. 2009). The graph was created by taking the mean value of three repeated experiments.

2.4. Anti-swarming activity

The sub-MIC values of the extracts were determined againts *P. aeruginosa* PAO1 strain and a lower value was used with this value. Relevant concentrations of the extracts were added into 5 mL LB soft agar medium, poured into LB agar petri dishes and left to solidify. A colony from the LB agar culture of *P. aeruginosa* strain was added to the middle of the petri dishes containing "swarming" medium with a sterile tooth pick and incubated for 16-18 hours at 37°C (Rashid and Kornberg 2000; Rice et al. 2005). Swarming action was tested by measuring the diameter of the scatter from the point of inoculation to the periphery. The results were evaluated by comparing with the PAO1 strain without plant extract added.

3. Results

3.1. Antimicrobial activity

Table 1. Antimicrobial activity results

Microorganisms	**Zon diameter (mm)**	**MIC (µg/mL)**	**MBC (µg/mL)**	**Controls**
S. aureus	**22.66±0.57**	**125**	**250**	**30.00±3.0**
C. violaceum	**14.66 ±1.15**	**125**	**250**	**26.00±0.0**
C. albicans	**26.00±1.00**	**62.50**	**125**	**30.66±0.5**
M. smegmatis	**25.00±1.0**	**62.50**	**125**	**30.00±1.0**

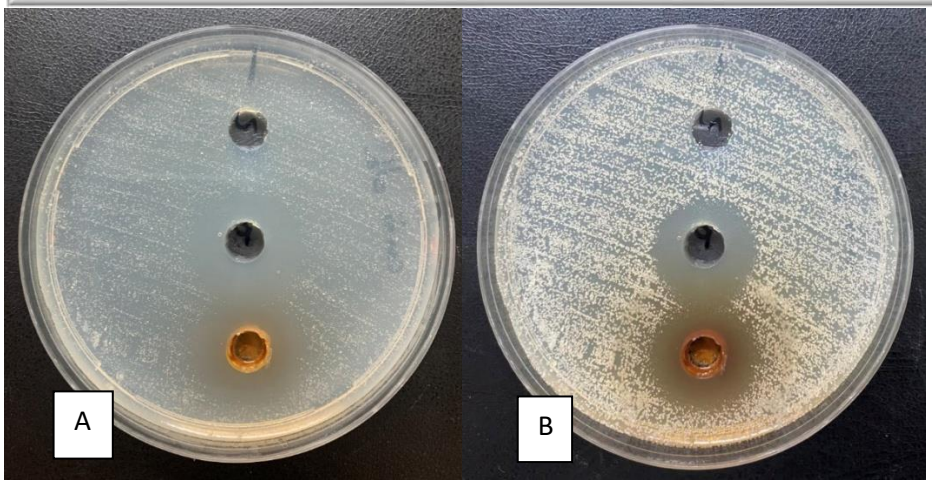

Figure 1. *C. albicans* antimicrobial activity results; A; first day, B; Second day.

3.2. Anti-quorum sensing

Table 1. Anti-quorum sensing activity results

Propolis extract	***C. violaceum* ATCC 12472**	***C. violaceum* ATCC 31532**
	+	+

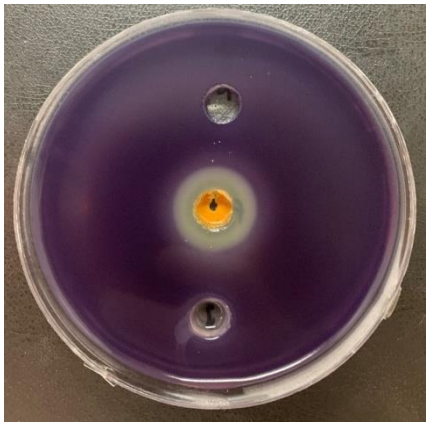

Figure 2. Anti-quorum sensing activity results

3.3. Anti-biofilm and anti-swarming activity

It was determined that ethanolic chestnut propolis extract did not show anti swarming activity. The extract was found to have anti-biofilm activity, but the results of the repeated experiments were not statistically significant.

4. Discussion

The antimicrobial activity of propolis against many pathogens has been investigated and widely known for many years (Temiz et al., 2011). Numerous studies have demonstrated that propolis possesses a marked antibacterial and moderate antifungal activities. But, chestnut propolis is not studied in detailed. Similar to our study, Sorucu and Ceylan (2021) determined that propolis extracts showed antimicrobial and anti-quorum

sensing activity, but different kind of propolis samples were showed similar effects. They mention that there is no activity against gram negatives in their studies and literature. However, antimicrobial activity against gram-negative bacteria *C. violaceum* was determined in this study. This study results shows a stronger result than the literature by showing high antifungal activity against *C. albicans* fungus. Lamberte et al. (2011) determined the ethanol extract propolis has anti-QS activity against *C. violaceum* ATCC 12472. While Lamberte et al. (2011) reveal that low doses prevented biofilm formation than the high doses, the present study was increasing the dose-dependent. Similarly, this study shows that anti-biofilm activity is dose dependent.

5. Conclusion

The results of the study showed that chestnut ethanolic propolis extract has high antimicrobial and anti-quorum sensing potential.

6. References

Clinical and Laboratory Standards Institute. Reference method for broth dilution antifungal susceptibility testing of yeasts; approved standard, 3rd ed., CLSI document M27-A3. Clinical and Laboratory Standards Institute, Wayne, PA.2008.

Ekşi S, Esertaş ÜZÜ, Kilic AO, Ejder N, Uzunok B. (2020) Determination of the antimicrobial and antibiofilm effects and 'Quorum Sensing' inhibition potentials of *Castanea sativa* Mill. extracts. Notulae Botanicae Horti Agrobotanici Cluj-Napoca, 48(1), 66-78. https://doi.org/10.15835/nbha48111736.

Franklin MJ, Chang C, Akiyama T, Bothner B. New technologies for studying biofilms. Microbial Biofilms. 2015; 1-32.https://doi.org/10.1128/9781555817466.ch1.

Hano, C., & Tungmunnithum, D. (2020). Plant polyphenols, more than just simple natural antioxidants: Oxidative stress, aging and age-related diseases. Medicines, 7(5), 26.

Lamberte LE, Cabrera EC, Rivera WL. Pseudomonas aeruginosa'da Chromobacterium violaceum ve Virülans Faktörü Üretiminde Çekirdek Algılama Aracılı Pigment Üretiminin Potansiyel İnhibitörü Olarak Propolis Etanolik Ekstraktının (EEP) Aktivitesi. Philipp Tarım Bilimi. 2011; 94, 14-22.

McLean RJC, Pierson LS, Fuquac C. A simple screening protocol for the identification of quorum signal antagonist. J Microbiol Methods. 2004;58(3):351-60.

Rashid MH, Kornberg A. In organic polyphosphate is needed for swimming, swarming, and twitching motilities of Pseudomonas aeruginosa. Proceedings of the National Academy Sciences of the United States of America. 2000; 97(9):4885-4890. https://doi. org/ 10.1073ypnas.060030097

Rice SA, Koh KS, Queck SY, Labbate M. Lam KW, Kjelleberg S. Biofilm formation and sloughing in *Serratia marcescens* are controlled by quorum sensing and nutrient cues. J Bacteriol. 2005; 187(10), 3477-3485.https://doi.org/10.1128/JB.187.10.3477-3485.2005.

Salatino, A., Teixeira, É. W., & Negri, G. (2005). Origin and chemical variation of Brazilian propolis. Evidence-based complementary and alternative medicine, 2(1), 33-38.

Sorucu A, Ceylan Ö. Propolisin su ve etanol ekstraktlarının antimikrobiyal ve anti-quorum algılama aktivitelerinin belirlenmesi. Ankara Üniv Vet Fak Derg. 2021;68, 373-381.

Temiz A, Sener A, Tuylu AO, Sorkun K, Salih B. Antibacterial activity of bee propolis samples from different geographical regions of Turkey against two foodborne pathogens, Salmonella enteritidis and Listeria monocytogenes. Turkish Journal of Biology 2011; 35(4): 503-511. doi: 10.3906/biy-0908-22.

Truchado P, Gil-Izqierdo A, Tomas-Barberan F, Allenda A. Inhibition by chestnut honey of N-Acyl-L-homo serine lactones and biofilm formation in *Erwinia carotovora*, *Yersinia enterocolitica* and *Aeromonas hydrophila*. J Agric Food Chem. 2009; 57(23):11186-11193. https://doi.org/10.1021/jf9029139.

Woods GL, Brown-Elliott BA, Desmond EP, Hall GS, Heifets L, et al. Susceptibility testing of mycobacteria, nocardiae, and other aerobic actinomycetes; Approved Standard. NCCLS document M24-A,2003; 23 (18).

Second International Congress on Biological and Health Sciences
ONLINE 24-25-26-27 FEBRUARY 2022

Biologically Active Properties of Sunflower Honey

Merve Keskin[1], Yakup Kara[2], Sevgi Kolaylı[2]

[1]Vocational School of Health Services, Bilecik Seyh Edebali University, Bilecik, Turkey

[2]Department of Chemistry, Faculty of Science, Karadeniz Technical University, Trabzon, Turkey

Corresponding author: skolayli61@yahoo.com

Abstract:
Honey is a natural bee product that is produced by collecting the nectar (flower honey) in the flowers of plants or the sweet secretions (secretory honey) produced by some insects by making use of the living parts of the plants, collected by honey bees, modified and stored in the honeycomb cells. Sunflower honey is a flower honey produced mostly in Marmara and Thrace regions in Turkey. Since this honey crystallizes very easily, it is not preferred among the people. In this study, the bioactive components and antioxidant properties of sunflower honey were investigated. Moisture, pH, conductivity, color, optical rotation values and proline were determined as physicochemical properties. Total polyphenol, total flavonoid and total antioxidant values were calculated. Total phenolic content of the honey was found 21.35 ±1,30 mg GAE/100 g, and total antioxidant capacity was 2030 µmol $Fe_2SO_4.7H_2O$/g. The phenolic profile was performed with 19 phenolic standard HPLC-UV and determined sunflower honey was rich in myricetin and chrysin. It was determined that sunflower honey also contains p-OH benzoic acid, catechin, syringic acid, caffeic acid, protocatecquic acid, catechin, p-coumaric acid, ferulic acid, resveratrol, luteolin, t-cinnamic acid, pinosembrin and daidzein phenolic acid and different flavonoids in varying amounts. It was determined that sunflower honey, which is a light-colored flower honey, has rich content in terms of bioactive components.

Keywords: Sunflower honey, phenolics, antioxidant capacity, flavonoids, flower honey

1. Introduction

Honey is a natural bee product that is produced by collecting the nectar (blossom honey) in the flowers of plants or the sweet secretions (dew honey) produced by some insects by making use of the living parts of the plants, collected by honey bees, modified and stored in the honeycomb cells. Today honey is accepted as a functional food, with a wide range of biological active properties, and functions. The biological value of this natural product, which consists of 95% sugar by dry weight, depends on 5% differences. The features that make honey different from each other are due to the bioactive compounds of honey, such as polyphenols, pigments, vitamins, minerals and volatile aroma compounds (Küçük et al. 2007; Can et al. 2015; Kanbur et al. 2021).

Turkey is at the intersection of three continents and has rich flora according to the climate characteristics of Asia, Europe and Africa. It is also home to a rich variety of honeys depending on the variety of rich honey plants. The most produced honeys as flower honeys in Turkey are heterofloral highland honeys, as well as thyme, astragalus, blackthorn, acacia, linden, chestnut, heather, citrus, cotton, lavender and sunflower honeys. Sunflower honey is an industrial plant honey produced in the regions where sunflowers are produced intensively, especially in the Marmara and Thrace regions (Sert et al. 2011). This honey, which is very high in terms of monofloral value, is a bright yellow colored, unique aroma and very easily crystallized honey. The biological value of this honey, which is not preferred by the Turkish people because it crystallizes easily, is not known exactly. The aim of this study is to reveal the chemical properties and bioactive components of sunflower honey.

2. Materials and Methods

Sunflower honey was supplied from Silivri region of Istanbul, Turkiye, by Silivri Municipality. The authentic structure of honey was determined by melisopalynological analysis and honeys containing more than 45% sunflower pollen are considered monofloral honey(Louveaux et al. (1978).

2.1 Physicochemical analysis

The physico-chemical parameters of pH, Brix (%), moisture (%), electrical conductivity (mS/cm^2), and optical rotations were determined by the in agreement with the Honey Codex (Can et al. 2015). Sugar analysis of the honey were carried out according a high-performance liquid chromatography (HPLC-RID) with a refractive index detector(Can et al. 2015).Prolin content was measured by spectrophotometric method (Meda, et al. 2005). The results were expressed in mg/kg.

2.1.1 Total phenolic contents (TPC)

Ethanolic extracts of the samples were prepared. 3 g of honey was dissolved in 30 ml of ethanol (99%) and stirred for 24 hours, then filtered first with a coarse and then with a fine filter paper. The total phenolic content(TPC) of the honey samples were measured using Folin-Ciocalteu's assay (Slinkard and Singleton, 1977). Total phenolic content of the samples was calculated as mg gallic acid equivalents (GAE)/g sample using a standard curve. For preparation of the standard curve, gallic acid standards (from 0.031 to 1.0 mg GAE/mL) were used.

2.1.2 Total flavanoid contents (TFC)

Total flavonoid content (TFC) of the samples were measured according to Fukumoto and Mazza (2000). TFC was expressed as mg quercetin equivalent (QUE)/g sample using a standard curve. For preparation of the standard curve, quercetin standards (from 0.031 to 0.5 mg QUE/mL) were used.

2.1.3 Ferric reducing antioxidant power (FRAP)

Total antioxidant capacity of the samples was measured using the ferric reducing antioxidant power assay (FRAP) method (Benzie and Strain, 1999). For preparation of the standard curve, different concentrations of $FeSO_4.7H_2O$ (from 1000 to 31.25 µmol/ml) were used to prepare the standard curve. The results were expressed as µmol $FeSO_4.7H_2O$ equivalents/g sample using the curve.

2.1.4. Determination of phenolic profiles

Nineteen phenolic standards of were analyzed using HPLC (Elite LaChrom Hitachi, Japan) in a UV–VIS detector, and C18 column (150mm x 4.6 mm, 5 mm; Fortis). The mobile phase consisted of (A) 2% acetic acid in water and (B) acetonitrile: water (70:30). The samples and standard injection volume were 25 mL, with a column temperature of 30 °C and flow rate of 1.5 mL/min. The programmed solvent used began with a linear gradient held at 95% A for 3 min, decreasing to 80% A at 10 min, 60% A at 20 min, 20% A at 30 min, and finally 95% A at 50 min (Can et al., 2015). For quantitative determination, all phenolic component calibration curves were between 0.998 and 1.000.

3. Results

The results of the palynological and physicochemical analysis of the sunflower honey are summarized in Table 1. It was determined that honeydew major pollen was 80% sunflower pollen and it was one of the honeys with high unifloral honey quality.

Table 1. Palynological and physicochemical analysis

Parameter	Values
Sunflower pollen %	**72±1.2**
Moisture %	**17±0.9**
pH	**4.40±0.1**
Optical Rotations	**-2.20±0.01**
Electrical Conductivimetry (mS/cm)	**0.40±0.02**
Prolin (mg/kg)	**476±2.11**
Fructose (%)	**37.80±0.9**
Glucose (%)	**35.87±0.9**
Sucrose (%)	**0.56±0.01**
Maltose (%)	**2.05±0.01**

Table 2 shows the phenolic content and antioxidant value of sunflower honey. One of the most important bioactive components of honey is polyphenols, and it was determined as 21.35 mg / 100 g in sunflower honey.

Table 2. Total phenolic and antioxidant capacity of the honey

Total phenolic contents (mg Gallic acid/ 100 g)	**21.35 ±1.30**
Total Flavanoid contents (mg Quercetin/100 g)	**0.50±0.10**
Total antioxidant Capacity µmol $Fe_2SO_4.7H_2O$/g	**2030±56.30**

Table 3. Phenolic composition of the sunflower honey by HPLC-UV (µg /100g)

Gallic acid	**102**
Protocatequic acid	**34**
***p*-OH benzoic acid**	**243**
Catechin	**-**
Caffeic Acid	**144**
Syringic Acid	**35**
Epicatechin	**164**
p-coumaric acid	**56**
Ferulic acid	**88**
Rutin	**-**
Myrecetin	**264**
Resveratrol	**-**
Daidzein	**18**
Luteolin	**-**
t-cinnamic acid	**-**
Hesperetin	**30**
Cyrisin	**-**
Pinocembrin	**323**
CAPE	**159**

The phenolic composition is summarized in Table 3. In the study in which 19 standards were used, Pinocembrin and myricetin were the highest phenolic compounds, followed by hydroxy benzoic acid, caffeic acid, CAPE, epicatechin.

4. Discussion

The high negative content of the optical rotation value supports that the honey is flower honey. While this value is always positive in dew honeys, it is negative in flower honeys. While the conductivity value of honey was determined as 0.4 mS/cm, it was found to be suitable for Flower honeys. It is reported in the honey codex that this value should be greater than 0.8 mS/cm in dew honeys (Kolaylı et al. 2018). While the proline value is determined as 476 mg/kg, the minimum value is 300 mg/kg according to the Turkish honey codex (Can et al. 2015). While the F/G ratio of honey was found to be 1.05, low amounts of sucrose and maltose were determined. It is stated in the literature that there is a correlation between the F/G ratio and the

crystallization value of honey. This value is higher than 1.4 in chestnut, pine and oak honeys that do not crystallize easily, and the low F/G ratio (1.05) is an important reason for sunflower honey to crystallize easily (Suriwong et al. 2020). Easy crystallization does not mean that honey is bad. It was determined that the physicochemical values of sunflower honey were compatible with the literature (Pauliuc, & Oroian, 2020). It was reported that TPC value was to be approximately 100 mg GAE/100 g in chestnut honey, and 16 mg GAE/100 g was detected in acacia honey (Can et al. 2015). It contains total polyphenols, similar to light-colored flower honeys. It was not possible to compare the TPC values of sunflower honey because there was not much study in the literature. Depending on the total phenolic substance content, the total flavonoid amount was also found to be lower than the dark-colored flower honeys (Kaygusuz et al. 2016). While total antioxidant capacity was determined according to FRAP type, it was found that honey had higher antioxidant value than light colored honey (Can et al. 2015). In a study conducted in 1992, it was reported that this honey is rich in pinocembrin, similar to our study, followed by chrysin and galangin (Sabatier et al. 1992). In a study conducted on Romanian honeys, it was reported that sunflower honey is rich in pinocembrin (Oroian & Ropciuc, 2017).

5. Conclusion

Sunflower honey is one of the light colored monofloral honeys. Its production is quite high in Turkey, especially in the Thrace region. In this study, the physicochemical and biochemical properties of sunflower honey were determined. It was determined that sunflower honey, which is a light-colored flower honey, has rich content in terms of bioactive components. It is clear that sunflower honey has potential for apitherapy applications.

6. References

Benzie IFF, Strain JJ. Ferric Reducing/Antioxidant Power Assay: Direct measure of total antioxidant activity of biological fluids and modified version for simultaneous measurement of total antioxidant power and ascorbic acid concentration. Methods in Enzym. 1999; 299: 15–27.

Can Z, Yildiz O, Sahin H, Turumtay EA, Silici S, Kolayli S. An investigation of Turkish honeys: their physico-chemical properties, antioxidant capacities and phenolic profiles. Food Chemistry. 2015; 180: 133-141.

Fukumoto LR, Mazza G. Assessing antioxidant and prooxidant activities of phenolic compounds. Journal Agriculture Food Chemistry. 200; 48: 3597-3604.

Kaygusuz H, Tezcan F, Erim FB, Yildiz O, Sahin H, Can Z, Kolayli S. Characterization of Anatolian honeys based on minerals, bioactive components and principal component analysis. LWT-Food Science and Technology. 2016; 68: 273-279.

Kanbur ED, Yuksek T, Atamov V, Ozcelik AE. A comparison of the physicochemical properties of chestnut and highland honey: The case of Senoz Valley in the Rize province of Turkey. Food Chemistry, 2021; 345: 128864.

Küçük M, Kolaylı S, Karaoğlu Ş, Ulusoy E, Baltacı C, Candan, F. Biological activities and chemical composition of three honeys of different types from Anatolia. Food Chemistry. 2007; 100(2): 526-534.

Oroian M, Ropciuc S. Honey authentication based on physicochemical parameters and phenolic compounds. Computers and Electronics in Agriculture. 2017; 138: 148-156.

Pauliuc D, Oroian M. Organic acids and physico-chemical parameters of romanian sunflower honey. Food and Environment Safety Journal, 2020; 19(2).

Sabatier S, Amiot MJ, Tacchini M, Aubert S. (1992). Identification of flavonoids in sunflower honey. Journal of Food Science. 1992; 57(3): 773-774.

Sert D, Akin N, Dertli E. Effects of sunflower honey on the physicochemical, microbiological and sensory characteristics in set type yoghurt during refrigerated storage. International Journal of Dairy Technology, 2011; 64(1): 99-107.

Slinkard K, Singleton VL. Total phenol analysis: automation and comparison with manual methods. Am J Enol Viticult. 1977; 28: 49-55.

Suriwong V, Jaturonglumlert S, Varith J, Narkprasom K, Nitatwichit C. Crystallisation behaviour of sunflower and longan honey with glucose addition by absorbance measurement. International Food Research Journal. 2020; 27(4).

Second International Congress on Biological and Health Sciences
ONLINE 24-25-26-27 FEBRUARY 2022

Multi-class, Multi-residue LC-MS/MS Method For Veterinary Drug Residues, Mycotoxins And Pesticide In Urine

Zehra Hajrulai-Musliu[1], Risto Uzunov[1], Maksud Krluku[2], Aleksandra Angeleska[1], Elizabeta Dimitrieska-Stojkovikj[1], James Jacob Sasanya[3]

[1]Faculty of Veterinary Medicine-Skopje, "Ss. Cyril and Methodius" University in Skopje, Lazar Pop-Trajkov 5/7, 1000 Skopje, Republic of North Macedonia
[2]Veterinary ambulance Maksi, str. Amdi Leshi, Debar, Republic of North Macedonia
[3]International Atomic Energy Agency, Vienna International Centre, P. O. Box 100, A-1400, Vienna, Austria

Corresponding author: zhajrulai@fvm.ukim.edu.mk

Abstract:
In this work, an liquid chromatography- tandem mass spectrometry (LC-MS/MS) methodology is proposed for the multi-class multi-residue screening of veterinary drugs, pesticides and mycotoxins in bovine urine, using an LS-MS/MS both in positive and negative mode.The method currently covers 72 analytes belonging to different families such as antibiotics, steroid hormones, β-agonists, lactones, thyreostatics and contaminants such as pesticides and mycotoxins. After comparing different sample preparation procedures, extraction with sodium acetate and phosphate buffer followed by enzymatic hydrolyze with β-glucuronidase and solid phase extraction with OASIS cartridges was selected as the most appropriate methodology. In the validation study were included linearity, limit of detection, limit of quantification, decision limit, detection capability, accuracy and precision of the method. The method was linear with R^2>0.99. The limit of quantification were established between 0.19 µg/l and 16.7 µg/l, demonstrating the usefulnes of LC-MS/MS as an ideal tool for compliance monitoring in regulatory laboratories. The results for accuracy, expressed as recovery, were with values from 65 – 115%. Intra-day precision (repeatability) and inter-day precision (reproducibility) were expressed thought coefficient of variation. The CV was from 1.26 to 23.31 % for intra-day precision and from 2.29 to 29.42 % for inter-day precision. The results for accuracy and precision fulfill the criteria prescribed in the Commission Decision 2002/657/EC. The method was successfully applied for routine analysis of bovine urine samples. The routine analysis showed that the target components were not detected in the bovine urine samples.

Key words: veterinary drug residues, pesticide residues, mycotoxins, bovine urine,validation study, LC-MS/MS

This work was supported by the IAEA project Integrated radiometric and complementary techniques for mixed contaminants and residues in food (D52041).

1. Introduction

Veterinary drugs such as different class of antibiotics are widely administered in food-producing animals to prevent or treat of diseases. Also, some veterinary drugs like anabolic hormones, β-agonists, thyreostats show growth-promoting effects and are commonly used for these purposes. The residues of veterinary drugs in food from animal origin cause side effects on human health. Due to the side effects, the monitoring of veterinary drug residues in live animals and animal tissues is very important to protect public health (Biselli et al. 2013; Uzunov et al. 2019). The measures to monitor the residue of veterinary drugs in live animals and

food from animal origin are prescribes in Council Directive 96/23/EC (96/23/EC). Also, animals are often simultaneously exposed to mycotoxins mixtures along with other contaminants such as pesticides or heavy metals, making multi-residual and multi-toxin exposure study relevant from a public health perspective. (Agriopoulou et al. 2020; Chinaza et al. 2021).

The development of analytical methods for the determination of residues and contaminants in food of animal origin plays a key role in the protection of public health. Therefore, a large number of analytical method for determination of residues and contaminants separately, but only several multi-residue and multi-class analytical methods have been established for the determination of veterinary drug residues and contaminants such us pesticides and mycotoxins in food matrices (Zhan et al. 2013; Hajrulai-Musliu et al. 2021; Danezis et al, 2016; Gómez-Pérez et al. 2015). On the other hand, methods for the simultaneous determination of residues and contaminants in urine (multi-class and multi-residue methods) are very rare or non-existent. There are a lot of published sensitive and reliable analytical methods, both for screening and confirmation purposes, for determination of residues and contaminants in urine. Most of these methods have been developed for the analysis of each group of residues and contaminants separately. (Ahn et al. 2010; Akre and Mizuno 2016; Escrivá et al. 2017; Uzunov et al. 2019).

The aim of this study is to develop and validate a reliable quantitative method for determination and quantification of a total of 72 residues and contaminants as follow: veterinary drug residues, pesticides and mycotoxins in bovine urine utilizing liquid chromatography-tandem mass spectrometry (LC-MS/MS).

2. Materials and Methods

2.1. Chemicals and reagents

Methanol, acetonitrile and water with LC-MS/MS grade, ethylacetate, dichloromethane, ammonium hydroxide, acetic acid, ammonium acetate (HPLC grade) were purchased from Carlo Erba Reagent S.A.S (Val de Reuil, France); formic acid (LC-MS/MS grade), sodium acetate (p.a.), sodium dihydrogen phosphate hydrate (p.a.), disodium hydrogen phosphate dihydrate (p.a.), sodium chloride (p.a.), β-glucuronidase aryl sulfatase and trichloroacetic acid (≥99.5 %) and Oasis HLB cartridges (500mg/6ml) were from Waters (Milford, MA, USA).

2.2. Analytical standards

Amoxicillin (99.6 %), ampicillin (99.8 %), benzylpenicillin (99.3 %), cloxacillin (98.7 %), oxacillin (98.4 %), lincomycin (100.3 %), tylosin (87.9 %), trimethoprim (99.5 %), tetracyclin (96.8%), cephapirin (98.5%), clenbuterol HCl (99.1 %), isoxsuprine HCl (100 %), salbutamol (99.4 %), zilpaterol HCl (96.0 %), ractopamine HCl (95.5 %), terbutaline hemisulfate salt (100.0 %), taleranol (99.5 %), 19 nortestosterone (99.8 %), clostebol (99.1 %), boldenone (99.1 %), methyltestosterone (99.5 %), testosterone (100.0 %), carbofuran (99.9 %), carbaryl (99.9 %), parathion (99.7 %), malathion (99.2 %), diazinon (98.3 %), dimethoate (99.8 %), atrazine (99.5 %), cypermethrin (98.4 %), permethrin (98.1 %), deltamethrin (99.9 %), coumaphos (99.7 %), dichlorvos (99.8 %), chlorpyrifos (99.8 %), boscalid (99.5 %), fentoate (98.8 %), fenthion (98.5 %), fenvalerate (99.4 %), monocrotophos (99.8 %), malaoxon (99.0 %), methamidophos (98.1 %), metacrifos (96.1 %), amitraz (99.8 %), omethoate (98.4 %), vamidothion (≥98.0 %), phosmet (99.8 %), thiouracil (100 %), propylthiouracil (99.6 %),

methylthiouracil (≥ 98.0 %), tapazol (99.7 %), heptenophos (98.7 %), bifenthrin (99.0 %), methomyl (99.0 %), were purchased from Sigma-Aldrich (St. Louis, MO, USA). Brombuterol (98.0 %), mabuterol HCl (98.0 %), cimbuterol (98.0 %), clenpenterol HCl (98.0 %) were obtained from Witega (Berlin, Germany). Zeranol (99.9 %), stanozolol (99.8 %), ceftiofur (98.01 %), cephalexin (96.6 %), oxytetracycline (96.5 %), enrofloxacin (99.74 %), ciprofloxacin (98.0 %), sulfadimidine (99.6 %), sulfamethoxazole (99.7 %), sulfadiazine (99.8 %), sulfachloropyridazine (99.1 %) and sulfadimethoxine (99.7 %) were obtained from Dr. Ehrenstorfer GmbH (Augsburg, Germany); ochratoxin A (≥ 98.0%) and zearalenone (99.0%) were obtained from Trylogy Analytical Laboratory, Inc. (Washington, USA).

2.3. Preparation of stock standard solutions, intermediate and working standard solutions

The individual stock standard solutions were prepared in methanol. The concentration of individual stock solutions was in range from 0.5 to 1.0 mg/ml. In the next step, mixed working solutions from standards for construction of calibration curve and fortification of the samples were prepared in methanol. The concentration of these standard solutions was 10 µg/ml.

2.4. Sample preparation

In the first step, 30 ml urine was centrifuged 5 minutes, on 2000 rpm, at room temperature. After centrifugation, 5 ml of urine sample was fortified with the standards. Prior to extraction the samples were left to stand for 10 min at room temperature. In the next step, 5 ml of 0.2 M sodium acetate buffer (pH=5) and 5 ml 0.02 M Phosphate buffer (PBS) (pH=7.2) (1:1, v/v) were added, then the samples were shaken for 1 min on a vortex and 20 µL of β-glucuronidase aryl sulfatase was added. The samples were incubated 17 h at 37°C. After cooling at room temperature, samples were centrifuged 5 minutes, on 2000 rpm, at room temperature.
The Oasis HLB cartridges were used for clean-up procedure. The cartridges were activated and conditioned with 5 ml of methanol and 5 ml of water. The whole extract was passed through the cartridges at one drop per second and the cartridge dried, washed with 5 ml of water and dried again. The residues were eluted with two eluent mixtures, first 4 ml of eluent mixture I (48.5:48.5:3, v/v/v, methanol:acetonitrile:ammonium hydroxide) and then with 4 ml of eluent mixtute II (1.5:8.5, v/v, methanol:dichlormethane).
In the next step the solution was evaporated under nitrogen to near dryness at 35°C. The residue was reconstituted with 1 mL of the mobile phase (95:5, v/v, Mobile phase A: Mobile phase B). Prior to LC–MS/MS analysis the extracts were filtered through a 0.45µm membrane filter into 2 mL autosampler vials.

2.5. LC-MS/MS analysis

LC-MS/MS (Waters, Milford, MA, USA) were used for identification and quantification of the target compounds. LC-MS/MS is equipped with a binary pump, vacuum degasser, thermostatted autosampler, thermostatted column manager and triple quadrupole detector. For chromatographic separation was used LC column Kinetex C18 (50 x 2.1 mm, 2.6 µm, Phenomenex, Torrance, CA, USA). For instrument control, data acquisition and processing of results was used software (MassLynx version 4.1, Waters, Milford, MA, USA).
The LC conditions were as follow: flow rate of mobile phase: 0.2 ml/min; column temperature: 40°C, elution program: 0–1 min, 95-80 % A; 1–4 min, 80-60 % A; 4–8 min, 60-95 % A; 8-12 min, 95 % A; mobile phase A contains: water with 5 mMol ammonium acetate, 0.01 % formic acid and 0.01 % trichloroacetic acid; mobile phase B contains: methanol with 0.1% formic acid, temperature in sample chamber: 4°C; injection volume: 5 µL. The MS/MS conditions were optimized as follows: capillary voltage of 3.0 kV; source temperature of 150°C; desolvation temperature of 400°C; cone gas at 100 L/h; desolvation gas at 300 L/h.

3. Results

3.1. MS/MS optimization

For optimization of MS/MS conditions and selection of appropriate diagnostic ions the standard working solution with concentration of 1.0 µg/mL were infused to the MS/MS detector. ESI in both positive and negative ion modes was evaluated for detection of 72 compounds included in the study. The optimal parameters for each compound, such as: polarity, precursor ion, product ions, collision energy, cone voltage and retention time are shown in Table 1. The optimal dwell time which provides suitable signal to noise and good peak shape was 0.025 s.

Table 1. MRM parameters

Standard	Polarity	Precursor ion (m/z)	Product ion (m/z)	Collision energy	Cone voltage	Retention time
Thiouracil TU	+	128.80	112.0 69.86 59.77	20 18 18	30	1.43
Methylthiouracil MTU	+	142.83	125.90 83.85 41.86	18 22 18	30	1.55
Propyltiouracil PTU	+	170.88	154.30 111.91 69.86	20 24 22	32	1.90
Tapazole TAP	+	114.82	110.15 87.83 56.84	16 16	36	0.82
Testosteron TEST	+	289.16	108.99 96.95 178.18	24 28 28	36	6.78
Methyltestosteron MES	+	303.22	96.96 109.0 178.18	28 24 24	36	7.05
Boldenon BOLD	+	287.16	121.03 135.02 171.20	24 16 20	34	6.55
19 Nortestosteron 19 N	+	275.14	80.56 109.0 93.18	34 26 32	38	6.68
Stanozolol STZL	+	329.22	80.95 95.00	46 46	64	7.52

			121.00	42		
Clostebol CLBL	+	323.16	130.98 142.96 157.13	26 26 22	40	7.14
Zeranol ZENL	-	321.03	90.87 40.90 259.2	40 40 36	74	6.34
Taleranol TANL	-	321.03	90.87 40.90 259.2	34 40 42	74	6.70
Clenbuterol CLEN	+	276.97	202.95 131.87 166.77	16 30 30	22	3.84
Brombuterol BROM	+	366.90	292.84 211.42 57.00	20 34 38	26	4.34
Mabuterol MABT	+	310.95	236.99 216.96 57.00	18 26 30	24	4.51
Clenpenterol CLEP	+	291.00	202.92 131.89 167.79	16 30 28	28	4.60
Isoxuprin ISOX	+	302.04	106.96 164.01 120.95	30 16 28	26	3.31
Cimbuterol IMB	+	234.03	159.98 142.94 57.0	16 28 26	22	2.26
Ractopamine RACT	+	302.04	164.01 106.96 120.95	16 28 24	24	3.86
Salbutamol SALB	+	240.03	147.96 165.98 56.94	20 14 24	22	1.99
Zilpaterol HCl ZILP	+	262.03	202.05 185.01 156.98	22 24 32	22	1.95
Terbutalin hemisulfate TERB	+	226.00	152.00 106.97 170.00	14 30 16	26	1.87
Amoxicillin AMOX	+	367.07	159.96	16	28	5.55

			90.89	40		
Ampicillin AMP	+	349.97	105.95 159.94	20 14	34	3.93
Benzylpenicillin BNPC	+	334.99	90.96 80.94	42 52	44	5.52
Lincomycin LINK	+	407.06	126.02 41.75	34 72	22	2.80
Tylosin TYLS	+	916.3	173.99 100.88	46 52	74	6.31
Trimethoprim TRIP	+	290.97	122.94 229.94	28 24	26	2.90
Cephapirin CEPR	+	423.93	291.93 151.89	14 28	42	2.04
Tetracycline TETC	+	445.03	410.01 153.90	20 34	40	5.33
Cloxacillin CLCN	+	435.94	159.97 276.96	18 14	26	6.15
Oxacillin OXIN	+	402.05	159.96 243.03	10 12	24	5.95
Cefalexin CEFA	+	347.97	157.86 173.93	8 14	30	2.75
Ceftiofur CEFT	+	523.96	241.00 125.17	16 58	34	4.90
Enrofloxacin ENRO	+	360.05	245.09 72.02	30 36	36	3.68
Ciprofloxacin CIPR	+	332.01	245.05 230.94	40 28	38	3.56
Oxytetracyclin OXTT	+	462.01	426.02 200.93	38 30	36	3.17
Sulfachloropyridazin SUPZ	+	284.90	155.93 91.93	16 34	28	2.93
Sulfadiazin SUDI	+	250.97	91.93 155.93	30 14	28	1.92
Sulfadimetoxin SUDM	+	310.97	155.93 91.93	20 32	36	4.36
Sulfadimidin SULD	+	278.95	185.93 91.93	18 36	34	2.71
Sulfamethoxazol SULM	+	253.91	92.00 155.94	30 16	28	3.01
Carbofuran CRL	+	222.1	165.0 123.0	12 22	32	5.38

Carbaryl CRB	+	202.0	145.05 127.0	10 32	26	5.74
Parathion PTN	+	292.0	210.0 180.0	12 26	30	6.02
Malathion MTN	+	331.1	98.93 127.0	14 26	30	6.76
Diazinon DNN	+	304.97	168.94 153.00	24 24	44	7.38
Dimethoate DIM	+	229.90	198.83 124.84	10 20	30	3.36
Atrazine ATRZ	+	216.0	174.22 104.14	15 30	32	7.00
Permethrin PEMT	+	390.97	355.02 182.92	6 12	34	8.68
Cypermethrin CIRM	+	433.0	192.80 90.93	20 12	28	8.27
Deltamethrin DELM	+	229.84	198.83 124.85	30 14	30	3.37
Coumaphos COU	+	362.90	226.86 306.86	26 18	52	7.39
Dichlorophos DIRP	+	220.78	108.89 78.83	20 30	44	5.25
Chlorpyrifos CHRS	+	351.78	96.79 199.77	32 16	38	8.11
Fenvalerat FERT	+	419.97	166.89 124.88	14 42	38	8.33
Boskalid BOS	+	342.94	306.94 139.85	20 20	56	6.68
Fentoate FETE	+	320.86	162.87 246.84	12 12	28	7.25
Fenthion FEON	+	278.82	168.87 104.86	18 28	38	7.33
Monocrotophos MOCR	+	223.16	192.87 97.83	8 12	30	2.70
Malaoxon MAON	+	314.94	126.84 98.80	14 26	38	5.60
Methamidophos MEDF	+	141.78	93.80 46.82	14 24	38	1.96
Metacrifos MECF	+	240.93	208.83 124.83	8 20	32	6.40
Amitraz AMRZ	+	294.05	162.96	14	30	7.87

			121.91	32		
Omethoat OMAT	+	213.84	182.82 154.84	12 18	32	1.78
Vamidothion VAON	+	287.78	145.92 117.87	14 24	30	3.59
Phosmet FOST	+	320.86	246.84 162.87	14 58	32	6.90
Heptenophos HEPH	+	250.78	126.83 89.04	16 34	42	6.26
Bifenitrin BFNT	+	440.03	180.96 165.87	22 42	24	8.65
Methomyl MEML	+	162.84	87.88 105.90	8 10	30	2.35
Zearalenone ZEAN	-	316.97	130.87 174.91	30 26	62	6.85
Ochratoxin A OTAA	+	404.03	238.92 101.8	30 10	46	6.92

3.2. Optimization of mobile phase

During the development of the method due to the differences in the chemical structure between components included in this study six different mobile phases were investigated. The composition of the mobile phases is shown in Table 2.

Table 2. Composition of mobile phases

No.	Mobile phase A	Mobile phase B
1	Water with 5 mM ammonium acetate ar 0.1 % formic acid	Acetonitrile with 0.1% formic acid
2	Water with 5 mM ammonium acetate ar 0.1 % formic acid	Acetonitrile:methanol (50/50; v/v) wi 0.1% formic acid
3	Water with 5 mM ammonium acetate ar 0.1 % formic acid	Methanol with 0.1% formic acid
4	Water with 5 mM ammonium acetate ar 0.01 % formic acid	Methanol with 0.1% formic acid
5	Water with 5 mM ammonium acetate, 0 % formic acid and 0.01 % trichloroacet acid (TCA)	Methanol with 0.1% formic acid
6	Water with 5 mM ammonium acetat 0.01 % formic acid and 0.01 % TCA	Methanol with 0.1% formic acid

The results of the investigation of mobile phases from 1 to 5 (Table 2) showed that some compounds were not detected, moreover, poor separation, bad peak shape, low signal intensity or detection only one daughter ion. The chromatograms for poor separation and bad peak shape are shown in Figure 1 and Figure 2, respectively.

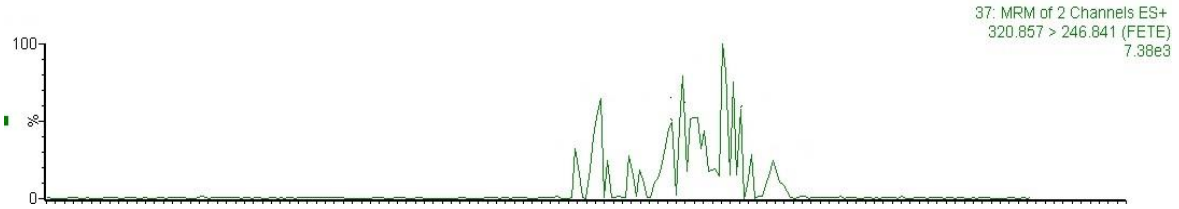

Figure 1. Chromatogram of fentoate – poor separation

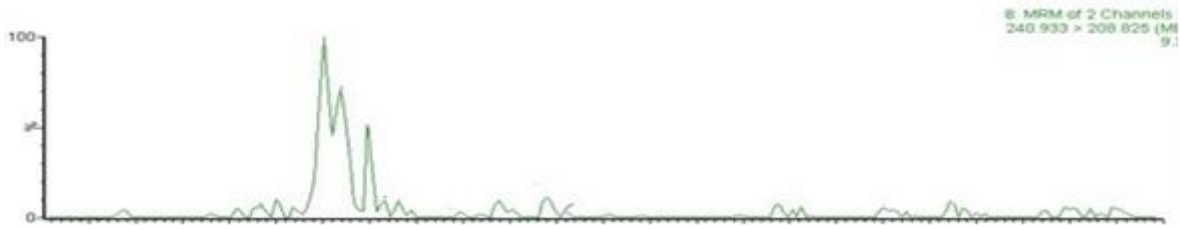

Figure 2. Chromatogram of metacrifos – bead peak shape

The optimal mobile phase which provides improved separation, good peak shape, high signal intensity, the best peak symmetry and resolution as well as detection of all target components was water with 5 mM ammonium acetate, 0.01 % formic acid and 0.01 % TCA as mobile phase A and methanol with 0.1% formic acid as mobile phase B. The chromatograms are given in Figure 3 and Figure 4.

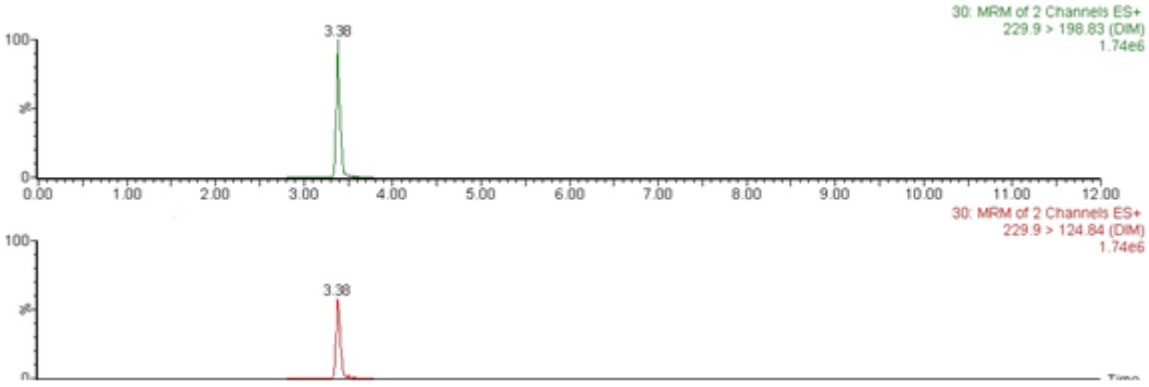

Figure 3. Chromatogram of dimethoate

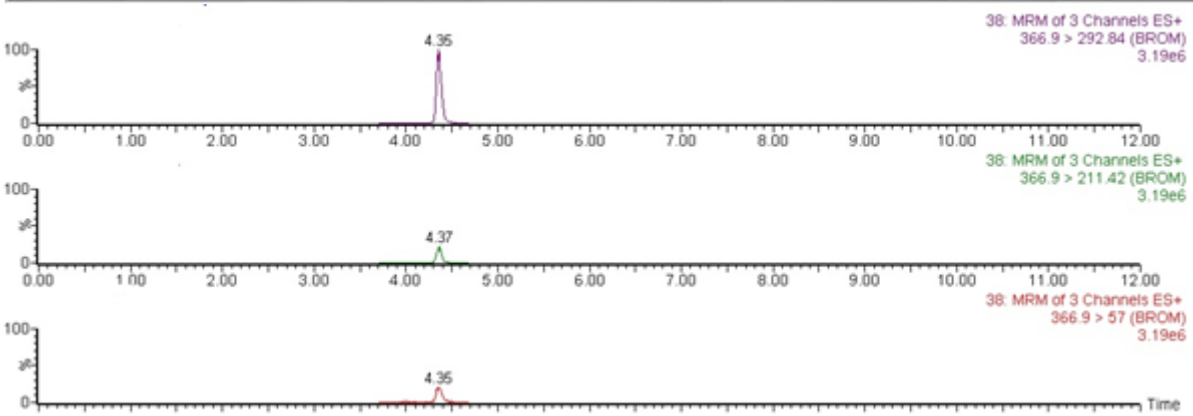

Figure 4. Chromatogram of brombuterol

3.3. Optimisation of the sample preparation

Four extraction protocols were investigated for the extraction of 72 compounds from urine. In the first protocol was used liquid-liquid (LLE) extraction without enzymatic hydrolyze, in the second protocol was used LLE with enzymatic hydrolyze, in third extraction protocols were used solid phase extraction (SPE) without enzymatic hydrolyze, while in fourth protocol was used SPE with enzymatic hydrolyze. The enzymatic hydrolyze was performed with β-glucuronidase aryl sulfatase from Helix pomatia. In the first step, for all protocols, 30 ml urine samples were centrifuged 5 minutes, on 2000 rpm, at room temperature. This step was used to remove the proteins.

In the first and second protocols with LLE, after centrifugation, 5 ml of urine samples was fortified with the standards. Prior to extraction the samples were left to stand for 10 min at room temperature. In the next step, 5 ml of 0.2 M sodium acetate buffer (pH=5) and 5 ml 0.02 M Phosphate buffer (PBS) (pH=7.2) (1:1, v/v) were added, the samples were shaken for 1 min on a vortex. After this step, in the first protocol, samples were centrifuged 5 minutes, on 2000 rpm, at room temperature and the next step was LLE, while in the second protocol for the enzymatic hydrolyze 20 µL of β-glucuronidase aryl sulfatase was added. The samples were incubated 17 h at 37°C. After cooling at room temperature, samples were centrifuged 5 minutes, on 2000 rpm, at room temperature. LLE was the same for both extraction protocols, as follows. In the first step from LLE was used 10 ml methanol:acetonitrile:acetic acid (49:49:2, v/v/v). The samples were shaken for 1 min on a vortex and centrifuged 5 minutes, on 2000 rpm, at room temperature. After that, the supernatant was transferred in test tubes. In the second LLE step 10 ml of ethylacetate:hexane (40:60, v/v) was used. The samples were shaken for 1 min on a vortex and centrifuged 5 minutes, on 2000 rpm, at room temperature. The supernatant was fused to the first supernatant. The samples were evaporated under nitrogen to near dryness at 35°C. The residue was reconstituted with 1 mL of the mobile phase (95:5, v/v, Mobile phase A: Mobile phase B). Prior to LC–MS/MS analysis the extracts were filtered through a 0.45µm membrane filter into 2 mL autosampler vials.

In the third and fourth protocols after centrifugation, 5 ml of urine sample was fortified with the standards. Prior to extraction the samples were left to stand for 10 min, at room temperature. In the next step, 5 ml of 0.2 M sodium acetate buffer (pH=5) and 5 ml 0.02 M Phosphate buffer (PBS) (pH=7.2) (1:1, v/v) were added, the samples were shaken for 1 min on a vortex. After cooling at room temperature, samples were centrifuged

5 minutes, on 2000 rpm, at room temperature. The next step in the third protocol is SPE extraction, while in the fourth protocol the next step is enzymatic hydrolysis. For this purpose, 20 µL of β-glucuronidase aryl sulfatase was added. The samples were incubated 17 h at 37°C. After cooling at room temperature, samples were centrifuged 5 minutes, on 2000 rpm, at room temperature. The SPE step is the same in the both protocols. SPE: Oasis HLB cartridges were activated and conditioned with 5 ml of methanol and 5 ml of water. The reconstituted extract (10 ml) was passed through the cartridges at one drop per second and the cartridge dried, washed with 5 ml of water and dried again. The residues were eluted with two eluent mixtures, first 4 ml of eluent mixture I (48.5:48.5:3, v/v/v, methanol:acetonitrile:ammonium hydroxide) and then with 4 ml of eluent mixture II (1.5:8.5, v/v, methanol:dichlormethane).

After solid phase extraction the eluent was evaporated under nitrogen to near dryness at 35°C. The residue was reconstituted with 1 mL of the mobile phase (95:5, v/v, Mobile phase A: Mobile phase B). Prior to LC–MS/MS analysis the extracts were filtered through a 0.45µm membrane filter into 2 mL autosampler vials.

For optimization of extraction procedure, for all extraction protocols, blank urine samples were spiked with standards at 3 concentration levels.

The thyreostats were not detected with LLE protocols. In the protocols with SPE extraction without enzymatic hydrolysis the results shown low recovery < 55 % for anabolic steroids and zeranol. Stanozolol and taleranol with this protocol were not detected. The optimal recoveries were obtained by SPE extraction with enzymatic hydrolysis and the recoveries were from 65.0 % for mabuterol (spiked at concentration at 0.2 µg/L) to 115.0 % for brombuterol (spiked at concentration at 0.2 and 0.4 µg/L).

3.4. Method validation

3.4.1. Linearity

The linearity of the method was evaluated using matrix-matched calibration curve. The blank urine samples were fortified at six concentration levels. For each concentration levels three replications were performed. The linearity along the research range presented values for coefficient of correlation (R2) from 0.9904 for cypermethrin to 0.9997 for lincomycin and ochratoxin A. The range of calibration curve and R^2 for all compounds are given in Table 3.

Table 3. Linearity of the method

Analytes	Calibration range (µg/L)	R^2
Thiouracil TU	0-100.0	0.9920
Methylthiouracil MTU	0-100.0	0.9942
Propyltiouracil PTU	0-100.0	0.9931
Tapazole TAP	0-100.0	0.9954
Testosteron TEST	0-100.0	0.9968
Methyltestosteron MEST	0-100.0	0.9940
Boldenon BOLD	0-100.0	0.9952
19 Nortestosteron 19 NO	0-100.0	0.9917
Stanozolol STZL	0-100.0	0.9948
Clostebol CLBL	0-100.0	0.9987
Zeranol ZENL	0-100.0	0.9935
Taleranol TANL	0-100.0	0.9972
Clenbuterol CLEN	0-50.0	0.9914
Brombuterol BROM	0-50.0	0.9931
Mabuterol MABT	0-50.0	0.9973
Clenpenterol CLEP	0-50.0	0.9935
Isoxuprin ISOX	0-50.0	0.9995
Cimbuterol CIMB	0-50.0	0.9931
Ractopamine RACT	0-100.0	0.9931
Salbutamol SALB	0-100.0	0.9964
ZilpaterolHCl ZILP	0-100.0	0.9959
TerbutalinTERB	0-100.0	0.9919
Amoxicillin AMOX	0-100.0	0.9965
Ampicillin AMP	0-100.0	0.9913
Benzylpenicillin BNPC	0-100.0	0.9936
Linkomycin LINK	0-100.0	0.9997
Tylosin TYLS	0-100.0	0.9993
Trimetoprim TRIP	0-100.0	0.9963
Cephapirin CEPR	0-100.0	0.9981
Tetracyclin TETC	0-100.0	0.9962
Cloxacillin CLCN	0-100.0	0.9986
Oxacillin OXIN	0-100.0	0.9954
Cefalexin CEFA	0-100.0	0.9996
Ceftiofur CEFT	0-100.0	0.9940
Enrofloxacin ENRO	0-100.0	0.9964
Ciprofloxacin CIPR	0-100.0	0.9932
Oxytetracyclin OXTT	0-100.0	0.9936

Sulfachloropyridazin SUPZ	**0-100.0**	**0.9980**
Sulfadiazin SUDI	**0-100.0**	**0.9931**
Sulfadimetoxin SUDM	**0-100.0**	**0.9944**
Sulfadimidin SULD	**0-100.0**	**0.9910**
Sulfamethoxazol SULM	**0-100.0**	**0.9968**
Carbofuran CRL	**0-100.0**	**0.9921**
Carbaryl CRB	**0-100.0**	**0.9915**
Paration PTN	**0-100.0**	**0.9964**
Malation MTN	**0-100.0**	**0.9910**
Diazinon DNN	**0-100.0**	**0.9914**
Dimethoat DIM	**0-100.0**	**0.9975**
Atrazine ATRZ	**0-100.0**	**0.9985**
Permetrin PEMT	**0-100.0**	**0.9959**
Cypermetrin CIRM	**0-100.0**	**0.9904**
Deltametrin DELM	**0-100.0**	**0.9946**
Coumaphos COU	**0-100.0**	**0.9934**
Dichlorophos DIRP	**0-100.0**	**0.9943**
Chloropyrifos CHRS	**0-100.0**	**0.9940**
Fenvalerat FERT	**0-100.0**	**0.9943**
Boskalid BOS	**0-100.0**	**0.9925**
Fentoate FETE	**0-100.0**	**0.9913**
Fention FEON	**0-100.0**	**0.9963**
Monocrotophos MOCR	**0-100.0**	**0.9991**
Malaoxon MAON	**0-100.0**	**0.9945**
Methamidophos MEDF	**0-100.0**	**0.9941**
Metacrifos MECF	**0-100.0**	**0.9956**
Amitraz AMRZ	**0-100.0**	**0.9973**
Omethoat OMAT	**0-100.0**	**0.9921**
Vamidothion VAON	**0-100.0**	**0.9951**
Phosmet FOST	**0-100.0**	**0.9925**
Heptenophos HEPH	**0-100.0**	**0.9920**
Bifenitrin BFNT	**0-100.0**	**0.9959**
Methomyl MEML	**0-100.0**	**0.9974**
Zearalenone ZEAN	**0-100.0**	**0.9935**
Ochratoxin A OTAA	**0-100.0**	**0.9997**

3.4.2. LOD, LOQ, CCα and CCβ

The LODs and LOQs were determined as the lowest concentration of the standards which were used for construction of calibration curve (n=20). The LOD was calculated as the mean value plus 3.3 times the

calculated standard deviation (SD), while the LOQ was calculated as the mean value plus 10 times the calculated SD. The LODs were from 0.06 µg/L for clenbuterol to 5.51 µg/L for metacrifos, while the LOQs were from 0.17 µg/L for clenbuterol to 16.70 µg/L to metacrifos. The CCα and CCβ were determined according to the criteria prescribes in the Commission Decision 2002/657/EC. CCα were ranged from 0.11 µg/L for clenbuterol to 10.88 µg/L for cephapirin, while CCβ were ranged from 0.15 µg/L for clenbuterol to 15.23 µg/L for tylosin. The results are shown in Table 4.

Table 4. CCα, CCβ, LOD, LOQ and MRPL

Analytes	CCα (µg/L)	CCβ (µg/L)	LOD (µg/L)	LOQ (µg/L)	MRPL (µg/L
Thiouracil TU	7.17	9.46	2.03	5.08	10
Methylthiouracil MTU	2.26	4.88	1.64	3.56	10
Propylthiouracil PTU	2.23	5.22	2.48	4.75	10
Tapazole TAP	5.03	8.42	4.22	7.15	10
Testosterone TEST	9.86	12.35	2.46	7.45	/
Methyltestosterone MEST	1.36	1.78	0.47	1.45	2
Boldenone BOLD	0.69	0.95	0.31	0.95	1
19 Nortestosterone 19 NO	0.55	0.88	0.21	0.63	1
Stanozolol STZL	1.15	1.64	0.62	1.88	2
Clostebol CLBL	4.36	8.02	2.22	6.80	/
Zeranol ZENL	1.77	1.93	0.65	1.84	2
Taleranol TANL	1.27	1.83	0.42	1.29	2
Clenbuterol CLEN	0.11	0.15	0.06	0.17	0.2
Brombuterol BROM	0.13	0.16	0.07	0.19	0.2
Mabuterol MABT	0.13	0.18	0.07	0.19	0.2
Clenpenterol CLEP	0.32	0.47	0.12	0.36	0.5
Isoxuprin ISOX	0.28	0.38	0.17	0.32	0.5
Cimbuterol CIMB	0.25	0.41	0.13	0.41	0.5
Ractopamine RACT	0.48	0.67	0.18	0.56	1.0
Salbutamol SALB	0.71	0.92	0.22	0.66	1.0
Zilpaterol ZILP	0.56	0.78	0.14	0.40	1.0
Terbutaline	1.77	2.62	0.76	2.30	3.0
Amoxicillin AMOX	7.86	11.54	3.08	9.28	/
Ampicillin AMP	9.22	10.56	2.04	6.15	/
Benzylpenicillin BNPC	9.88	13.54	4.07	12.33	/
Lincomycin LINK	6.64	9.51	4.48	13.28	/
Tylosin TYLS	10.15	15.23	3.28	9.90	/
Trimethoprim TRIP	3.79	6.14	5.08	15.40	/
Cephapirine CEPR	10.88	13.56	2.12	6.51	/
Tetracyclin TETC	4.46	8.78	5.00	8.86	/
Cloxacillin CLCN	8.76	10.15	3.32	10.06	/
Oxacilln OXIN	7.86	9.22	3.12	9.35	/
Cefalexin CEFA	9.13	7.11	4.51	13.70	/
Ceftiofur CEFT	6.54	9.25	3.88	11.65	/
Enrofloxacin ENRO	4.12	8.01	4.52	13.25	/
Ciprofloxacin CIPR	6.57	8.22	2.12	6.35	/
Oxytetracycline OXTT	5.00	7.54	3.36	9.98	/
Sulfachloropyridazin SUPZ	5.36	7.48	2.11	6.48	/
Sulfadiazine SUDI	4.28	8.20	2.88	7.01	/

Sulfadimetoxine SUDM	**8.32**	**11.56**	**3.51**	**10.23**	**/**
Sulfadimidine SULD	**7.15**	**10.02**	**3.13**	**9.56**	**/**
Sulfamethoxazole SULM	**7.28**	**10.78**	**4.01**	**12.15**	**/**
Carbofuran CRL	**5.23**	**8.11**	**3.35**	**10.15**	**/**
Carbaryl CRB	**5.78**	**9.01**	**2.02**	**6.10**	**/**
Parathion PTN	**7.81**	**9.94**	**4.38**	**13.15**	**/**
Malathion MTN	**9.14**	**13.25**	**1.11**	**3.40**	**/**
Diazinon DNN	**8.64**	**12.08**	**3.88**	**11.65**	**/**
Dimethoate DIM	**7.35**	**10.11**	**2.31**	**7.00**	**/**
Atrazine ATRZ	**7.22**	**9.21**	**2.78**	**8.45**	**/**
Permethrin PEMT	**4.36**	**6.58**	**3.56**	**10.51**	**/**
Cypermethrin CIRM	**8.54**	**10.12**	**3.11**	**9.42**	**/**
Deltamethrin DELM	**7.12**	**9.54**	**4.02**	**12.18**	**/**
Coumaphos COU	**5.48**	**8.82**	**2.57**	**7.65**	**/**
Dichlorvos DIRP	**6.54**	**9.11**	**3.11**	**9.39**	**/**
Chlorpyrifos CHRS	**6.78**	**9.82**	**1.56**	**4.80**	**/**
Fenvalerate FERT	**8.25**	**11.34**	**3.11**	**9.50**	**/**
Boskalid BOS	**6.34**	**8.14**	**2.78**	**7.90**	**/**
Fentoate FETE	**7.85**	**10.26**	**2.33**	**7.41**	**/**
Fenthion FEON	**7.00**	**9.11**	**3.56**	**10.70**	**/**
Monocrotophos MOCR	**6.29**	**9.54**	**4.01**	**12.20**	**/**
Malaoxon MAON	**8.48**	**12.08**	**4.09**	**12.40**	**/**
Methamidophos MEDF	**4.35**	**7.95**	**3.37**	**10.15**	**/**
Metacrifos MECF	**6.88**	**9.02**	**5.51**	**16.70**	**/**
Amitraz AMRZ	**4.64**	**7.12**	**2.92**	**8.80**	**/**
Omethoat OMAT	**6.58**	**9.04**	**2.11**	**6.55**	**/**
Vamidothion VAON	**6.12**	**9.15**	**2.64**	**8.02**	**/**
Phosmet FOST	**7.32**	**10.48**	**3.22**	**9.70**	**/**
Heptenophos HEPH	**10.12**	**14.11**	**4.11**	**12.20**	**/**
Bifenthrin BFNT	**8.22**	**12.56**	**3.51**	**10.50**	**/**
Methomyl MEML	**6.48**	**10.14**	**2.31**	**7.48**	**/**
Zearalenone ZEAN	**5.29**	**7.78**	**4.68**	**14.20**	**/**
Ochratoxin A OTAA	**7.79**	**10.64**	**4.00**	**12.10**	**/**

3.4.3. Accuracy and precision

Recovery of the method was used for evaluation of the accuracy. Recovery was studied at three concentration levels obtained by fortification of urine samples by mixed standard solution. The recovery range was from 65 % for mabuterol to 115 % for brombuterol. The intra-day precision (repeatability) and inter-day precision (reproducibility) were studied, as well as recovery, but for inter-day precision the fortified samples at three concentration levels were prepared and tested at three consecutive days. Intra-day and inter-ay precision were expressed thought coefficient of variation (CV, %). The CV for intra-day precision was from 1.26 % for lincomycin to 23.31 % for malathion, while the CV for reproducibility (inter-day precision) was from 2.29 % for lincomycin to 29.42 % for carbaryl. The results are summarized in Table 5.

Table 5. Accuracy and precision of the method

Analytes	Added concentration (µg/L)	Average concentration in the samples (µg/L) (n=6)	Standard deviation (µg/L)	Recovery (%)	Repeatability (CVr, %)	Reproducibi-lity (CV_R, %)
Thiouracil TU	10	9.44	1.06	94.40	11.23	16.54
	15	13.27	1.78	88.47	13.41	18.28
	20	18.25	2.55	91.25	13.97	17.36
Methylthiouracil MTU	10	8.55	0.74	85.50	8.65	13.53
	15	14.02	2.56	93.47	18.27	21.00
	20	18.54	3.04	92.70	16.40	19.88
Propyltiouracil PTU	10	8.11	0.98	81.10	12.08	16.46
	15	16.42	1.15	109.47	7.00	13.08
	20	21.54	1.95	107.70	8.87	12.95
Tapazole TAP	10	8.45	1.12	84.52	13.25	17.00
	15	13.80	2.04	92.00	14.78	18.54
	20	19.14	2.46	95.70	12.85	16.48
Testosteron TEST	10	10.79	2.26	107.3	20.95	22.94
	15	15.90	1.80	106.0	11.32	15.38
	20	20.20	3.74	101.0	18.51	24.35
Methyltestosteron MES	2.0	1.46	0.22	73.0	15.07	20.80
	3.0	2.74	0.41	91.3	14.96	17.46
	4.0	3.56	0.61	89.0	21.07	22.38
Boldenon BOLD	1.0	1.01	0.14	101.0	13.86	17.45
	1.5	1.62	0.17	108.0	10.49	13.12
	2.0	2.16	0.45	108.0	17.13	21.35
19 Nortestosteron 19 N	1.0	0.84	0.11	84.0	13.10	17.10
	1.5	1.23	0.22	82.0	17.89	19.46
	2.0	1.76	0.17	88.0	9.66	12.08
Stanozolol STZL	2.0	1.79	0.13	89.5	7.26	9.92
	3.0	3.30	0.51	110.0	15.45	19.46
	4.0	4.31	0.28	107.8	6.50	9.12
Clostebol CLBL	10	10.25	1.36	102.5	13.27	16.35
	15	14.60	2.17	97.3	14.86	16.87
	20	19.88	3.51	99.4	17.65	22.14
Zeranol ZENL	2.0	1.55	0.08	77.5	5.16	7.17
	3.0	2.48	0.21	82.7	8.47	10.02
	4.0	3.41	0.19	85.3	5.57	6.46
Taleranol TANL	2.0	1.64	0.12	82.0	7.32	9.01

	3.0	2.78	0.35	92.7	12.59	15.38
	4.0	4.01	0.40	100.3	9.98	14.46
	0.2	0.14	0.02	70.0	14.29	16.01
Clenbuterol CLEN	0.3	0.22	0.04	73.3	18.18	21.35
	0.4	0.34	0.06	85.0	17.65	19.12
	0.2	0.23	0.04	115.0	17.39	20.48
Brombuterol BROM	0.3	0.33	0.03	110.0	9.09	13.04
	0.4	0.46	0.09	115.0	19.56	22.56
	0.2	0.13	0.01	65.0	7.69	8.12
Mabuterol MABT	0.3	0.21	0.04	70.0	19.05	21.03
	0.4	0.30	0.06	75.0	20.0	22.74
	0.5	0.56	0.04	112.0	7.14	10.46
Clenpenterol CLEP	0.75	0.69	0.07	92.0	10.14	12.88
	1.0	0.87	0.05	87.0	5.75	7.46
	0.5	0.40	0.02	80.0	5.00	9.25
Isoxuprin ISOX	0.75	0.72	0.07	96.0	9.72	12.23
	1.0	0.94	0.17	94.0	18.09	21.08
	0.5	0.48	0.05	96.0	10.42	16.35
Cimbuterol CIMB	0.75	0.63	0.03	84.0	4.76	7.04
	1.0	0.84	0.11	84.0	13.10	16.12
	1.0	0.85	0.04	85.0	4.71	6.12
Ractopamine RACT	1.5	1.55	0.12	103.3	7.74	8.45
	2.0	2.10	0.14	105.0	6.67	9.12
	1.0	0.90	0.07	90.0	7.78	10.15
Salbutamol SALB	1.5	1.50	0.21	100.0	14.0	19.23
	2.0	2.14	0.27	107.0	12.62	16.08
	1.0	0.77	0.04	77.0	5.20	7.78
ZilpaterolHCl ZILP	1.5	1.22	0.13	81.3	10.70	18.14
	2.0	1.78	0.27	89.0	15.20	18.37
	3.0	2.90	0.22	96.7	7.58	8.24
TerbutalinTERB	4.5	4.73	0.57	105.1	12.05	15.31
	6.0	5.44	0.89	90.7	16.36	17.08
	10.0	9.77	0.52	97.7	5.32	8.46
Amoxicillin AMOX	15.0	15.46	1.31	103.1	8.47	9.12
	20.0	20.07	1.12	100.4	5.58	7.68
	10.0	10.46	1.43	104.6	13.67	15.21
Ampicillin AMP	15.0	16.45	2.15	109.7	13.07	16.35
	20.0	19.56	3.78	97.8	19.33	22.18
	10.0	8.22	0.76	82.2	9.25	13.35
Benzylpenicillin BNPC	15.0	12.78	1.74	85.2	13.62	16.08
	20.0	17.56	1.22	87.8	6.95	8.57

Linkomycin LINK	10.0	11.13	0.14	111.3	1.26	2.29
	15.0	16.51	1.40	110.1	8.48	13.58
	20.0	20.85	1.78	104.3	8.54	9.88
Tylosin TYLS	10.0	11.00	0.56	110.0	5.09	8.19
	15.0	16.38	1.12	109.2	6.84	9.38
	20.0	20.17	1.35	100.9	6.69	9.56
Trimetoprim TRIP	10.0	11.00	2.01	110.0	18.27	22.89
	15.0	16.25	2.64	108.3	16.24	17.23
	20.0	21.41	3.51	107.1	16.39	21.64
Cephapirin CEPR	10.0	10.85	0.45	108.5	4.15	7.08
	15.0	16.04	1.13	106.9	7.04	10.12
	20.0	21.52	1.46	107.6	6.78	8.68
Tetracyclin TETC	10.0	10.14	0.28	101.4	2.76	6.02
	15.0	16.39	0.36	109.3	2.20	3.88
	20.0	19.86	0.75	99.3	3.78	7.45
Cloxacillin CLCN	10.0	10.01	1.46	100.1	14.59	22.14
	15.0	16.20	2.05	108.0	12.65	14.65
	20.0	21.08	2.26	105.4	10.72	14.78
Oxacillin OXIN	10.0	8.43	0.86	84.4	10.20	14.56
	15.0	14.48	1.33	96.5	9.19	15.02
	20.0	18.35	1.78	91.9	9.70	13.06
Cefalexin CEFA	10.0	8.13	1.22	81.3	15.01	19.25
	15.0	12.78	2.01	85.2	15.73	18.48
	20.0	16.90	2.26	84.5	13.37	16.30
Ceftiofur CEFT	10.0	8.22	1.45	82.2	17.64	22.11
	15.0	12.05	2.18	80.3	18.09	22.08
	20.0	16.11	2.48	80.6	15.39	17.66
Enrofloxacin ENRO	10.0	9.72	0.88	97.2	9.05	14.46
	15.0	14.05	1.12	93.7	7.97	10.12
	20.0	18.65	2.41	93.3	12.92	15.11
Ciprofloxacin CIPR	10.0	10.77	0.67	107.7	6.22	8.99
	15.0	15.52	0.69	103.5	4.45	9.05
	20.0	20.90	1.25	104.5	5.98	10.12
Oxytetracyclin OXTT	10.0	9.46	1.45	94.6	15.33	18.14
	15.0	15.05	1.33	100.3	8.84	11.68
	20.0	17.96	2.08	89.8	11.58	15.12
Sulfachloropyridazin SUPZ	10.0	10.67	1.41	106.7	13.21	16.18
	15.0	16.07	2.28	107.1	14.19	20.08
	20.0	19.07	3.04	95.35	15.94	18.81
Sulfadiazin SUDI	10.0	9.20	0.45	92.0	4.89	7.00
	15.0	14.23	1.48	94.87	10.40	13.56

	20.0	20.18	2.03	100.9	10.06	11.12
Sulfadimetoxin SUDM	10.0	10.73	0.44	107.3	4.10	6.48
	15.0	15.21	0.92	101.4	6.05	12.21
	20.0	21.12	2.08	105.6	9.85	14.03
Sulfadimidin SULD	10.0	11.00	1.35	110.0	12.27	14.64
	15.0	15.56	1.78	103.7	11.43	14.92
	20.0	21.64	3.45	108.2	15.94	21.08
Sulfamethoxazol SULM	10.0	10.96	2.04	109.6	18.16	22.46
	15.0	15.79	2.95	105.3	18.68	20.51
	20.0	19.66	3.66	98.3	18.61	21.03
Carbofuran CRL	10.0	9.90	0.48	99.0	4.85	7.01
	15.0	16.02	0.75	106.8	4.68	8.12
	20.0	21.08	2.31	105.4	10.96	15.36
Carbaryl CRB	10.0	8.04	1.74	80.40	21.64	29.42
	15.0	13.80	2.04	92.00	14.78	19.58
	20.0	17.36	1.46	86.80	8.41	12.35
Paration PTN	10.0	8.20	1.35	82.00	16.46	21.02
	15.0	13.46	1.74	87.73	12.93	17.46
	20.0	18.20	2.07	91.00	11.37	16.58
Malation MTN	10.0	8.75	2.04	87.50	23.31	29.11
	15.0	12.64	2.51	82.27	19.86	23.46
	20.0	16.58	4.02	82.90	19.93	21.35
Diazinon DNN	10.0	9.94	1.36	99.4	13.68	17.46
	15.0	15.80	2.08	105.3	13.16	15.21
	20.0	19.10	2.41	95.5	12.62	17.88
Dimethoat DIM	10.0	10.64	1.46	106.4	13.72	16.99
	15.0	14.82	1.02	98.8	6.88	12.08
	20.0	19.43	3.12	97.18	16.06	19.35
Atrazine ATRZ	10.0	9.35	0.66	93.5	7.06	9.78
	15.0	14.47	0.88	94.47	6.08	9.65
	20.0	21.68	2.51	108.4	11.58	15.48
Permetrin PEMT	10.0	8.95	1.11	89.50	12.40	15.35
	15.0	14.88	1.45	99.20	9.74	10.18
	20.0	21.34	2.96	106.70	13.87	17.48
Cypermetrin CIRM	10.0	9.28	0.48	92.80	5.17	8.87
	15.0	13.00	1.92	86.67	14.77	21.23
	20.0	17.48	3.01	87.40	17.22	19.48
Deltametrin DELM	10.0	8.39	0.25	83.9	2.98	5.96
	15.0	14.00	0.61	93.3	4.36	8.11
	20.0	20.43	1.48	102.2	7.24	9.08
Coumaphos COU	10.0	9.23	0.14	92.30	1.52	3.99

	15.0	16.04	0.75	106.93	4.68	5.80
	20.0	20.14	1.95	100.70	9.68	14.03
	10.0	8.01	1.15	80.10	14.36	16.08
Dichlorophos DIRP	15.0	13.50	1.75	90.00	12.96	16.69
	20.0	18.35	3.14	91.75	17.11	21.36
	10.0	10.08	1.12	100.8	11.11	16.22
Chloropyrifos CHRS	15.0	14.86	2.35	99.1	15.81	22.08
	20.0	21.80	2.78	109.0	12.75	14.35
	10.0	9.23	0.21	92.30	2.28	6.02
Fenvalerat FERT	15.0	13.51	2.04	90.07	15.09	16.33
	20.0	18.64	3.22	93.20	17.27	22.18
	10.0	10.45	0.92	104.5	8.80	16.35
Boskalid BOS	15.0	14.83	1.95	98.87	13.15	17.18
	20.0	18.94	2.08	94.7	10.98	14.46
	10.0	8.88	0.65	88.80	7.32	10.56
Fentoate FETE	15.0	14.41	2.13	96.07	14.78	18.68
	20.0	17.56	3.07	87.80	17.48	22.95
	10.0	9.80	0.88	98.0	8.98	13.01
Fention FEON	15.0	14.65	1.02	97.67	6.96	11.35
	20.0	21.32	1.95	106.60	9.15	17.12
	10.0	8.95	1.45	89.5	16.20	21.08
Monocrotophos MOCR	15.0	15.12	1.52	100.8	10.05	12.06
	20.0	18.46	2.03	92.3	11.00	13.88
	10.0	10.42	1.88	104.20	18.04	22.01
Malaoxon MAON	15.0	15.78	3.15	105.20	19.96	22.96
	20.0	19.35	3.02	96.75	15.61	17.36
	10.0	8.12	1.25	81.20	15.39	18.48
Methamidophos MEDF	15.0	12.99	2.08	86.60	16.01	20.02
	20.0	17.84	2.14	89.20	12.00	16.11
	10.0	9.35	0.88	93.50	9.41	12.36
Metacrifos MECF	15.0	14.48	1.36	96.53	9.39	14.08
	20.0	21.04	1.22	105.20	5.80	8.01
	10.0	9.98	0.65	99.80	6.51	9.66
Amitraz AMRZ	15.0	15.35	0.99	102.33	6.45	7.35
	20.0	21.85	2.04	109.25	9.34	11.08
	10.0	8.46	1.04	84.60	12.29	13.06
Omethoat OMAT	15.0	16.35	1.22	109.00	7.46	9.54
	20.0	21.53	1.95	107.65	9.06	12.03
	10.0	8.98	0.48	89.8	5.35	7.08
Vamidothion VAON	15.0	13.10	0.61	87.3	4.66	6.36
	20.0	19.44	0.77	97.2	3.96	5.12

Phosmet FOST	**10.0** **15.0** **20.0**	**9.24** **14.61** **17.46**	**1.23** **1.35** **3.04**	**92.40** **97.40** **87.30**	**13.31** **9.24** **17.41**	**15.64** **10.66** **21.88**
Heptenophos HEPH	**10.0** **15.0** **20.0**	**8.05** **14.46** **18.48**	**0.27** **1.54** **1.95**	**80.50** **97.40** **92.40**	**3.35** **10.65** **10.55**	**5.12** **14.45** **12.95**
Bifenitrin BFNT	**10.0** **15.0** **20.0**	**9.00** **16.43** **21.24**	**0.62** **1.13** **3.35**	**90.0** **109.5** **106.2**	**6.89** **6.88** **15.77**	**9.35** **8.18** **16.35**
Methomyl MEML	**10.0** **15.0** **20.0**	**9.54** **14.23** **22.35**	**1.25** **1.17** **3.06**	**95.4** **94.9** **111.8**	**13.10** **8.22** **13.69**	**15.64** **17.82** **16.38**
Zearalenone ZEAN	**10.0** **15.0** **20.0**	**10.34** **15.58** **21.38**	**0.22** **0.95** **1.36**	**103.4** **103.9** **97.2**	**2.13** **6.10** **6.36**	**3.56** **8.81** **11.25**
Ochratoxin A OTAA	**10.0** **15.0** **20.0**	**10.63** **15.37** **18.05**	**0.45** **1.92** **2.04**	**106.3** **102.5** **90.25**	**4.23** **12.49** **11.30**	**6.64** **13.58** **14.61**

4. Discussion

According to Commission Decision 2002/657/EC for banned substances, thyreostats, anabolic hormones, lactones and β-agonists were selected one precursor ion and three product ions, while for other substances, antibiotics, pesticides and mycotoxins were selected one product and two precursor ions. The most abundant product ion was used for quantification, while the second product ion was used for confirmation.

Sample preparation is the critical step during the application of methods for simultaneous detection of different class of compounds from samples and the crucial steps in achieving the purifying effect and satisfactory recovery simultaneously are extraction procedure and clean up (Hajrulai-Musliu et al., 2021). The preparation of urine samples can be relatively convenient and easy in conditions when aqueous characteristic of urine is combined with LC-MS/MS as one of the advanced separation techniques. Urine is widely used to monitor the illegal use of growth-promoting agents and veterinary drugs, besides that these substances in the urine generally show high clearance rates (Stolker and Th Brinkman 2005; Stolker et al. 2007). The simplest methods for detection of pesticides in urine are direct injection of urine samples or dilute-and-shoot procedures but urinary salts or macromolecules cause major problems such as decrease of the instrument sensitivity, clogging on the injection syringe or clogging on the ESI probe. To avoid adverse effects and to achieve more efficiency are used solid phase extraction (SPE) and liquid-liquid extraction (LLE) for residues from veterinary drugs and contaminants extraction ([a]Kaufmann et al. 2008; [b]Kaufmann et al. 2011; Hu et al. 2005).

In this study four extraction protocols were tested. The optimal recoveries were obtained by SPE extraction with enzymatic hydrolysis. The results are comparable with Kellman et. all (2009) and Makarov et al., (2006) who conclude that the LLE is simpler and easier than SPE, but interferences from urine may remain in the extract and cause a serious matrix effect or lead to low extraction efficiency.

From the validation study can conclude that the results for R^2 showed good linearity for all compounds included in the study. The gained results for LOD, LOQ, CCα and CCβ showed that the method was sensitive, while from the results for recovery and precision can conclude that the analytical method demonstrated good accuracy and precision. The results are in agreement with the criteria described in 2002/657/EC and would be useful for multi-class and multi-residue screening of veterinary drugs, pesticides and mycotoxins in bovine urine.

4.1. Real sample analysis

In order to test the applicability of the developed method, the method was applied to the analysis of real bovine urine samples. A total of 65 local samples from bovine urine were collected and tested. According to gained results can conclude that residues of the target compounds weren't detected in bovine urine samples.

5. Conclusion

The method describes extraction, clean up, identification and quantification of 72 residues of veterinary drugs and other contaminants in bovine urine. In the method development were optimized MS/MS methods and extraction procedure, while in the validation study were evaluated linearity, LOD, LOQ, CCα, CCβ, accuracy and precision of the method. The gained results fulfill the performances prescribed in the Commission Decision 2002/657/EC. Consequently, the method could be used in routine analysis of bovine urine samples for simultaneous detection of veterinary drug residues and contaminants.

6. References

Agriopoulou S, Stamatelopoulou E, Varzakas T. Advances in occurrence, importance, and mycotoxin control strategies: prevention and detoxification in foods. Foods. 2020; 9 (2): 137.

Ahn J, Kim D, Kim H, Jahng KY. Quantitative determination of mycotoxins in urine by LC-MS/MS. Food Additives & Contaminants: Part A. 2010; 27 (12): 1674–1682.

Akre C, Mizuno M. A screening and determinative method for the analysis of natural and synthetic steroids, stilbenes and resorcyclic acid lactones in bovine urine. Drug Testing and Analysis. 2016; 8 (5-6): 448-57.

Biselli S, Schwalb S, Meyer A, Hartig L. A multi-class, multi-analyte method for routine analysis of 84 veterinary drugs in chicken muscle using simple extraction and LC-MS/MS. Food Additives & Contaminants: Part A. 2013; 30 (6): 921-939.

Chinaza GA, Erick NO, Chukwuka UO, Anjani KU, Katarzyna B, Charles OR, Okpala MK, Raquel PFG. Mycotoxins affecting animals, foods, humans, and plants: types, occurrence, toxicities, action mechanisms, prevention, and detoxification strategies—a revisit. Foods. 2021; 10 (6): 1279.

Commission of the European Communities: Council Directive96/23/EC of 29 April 1996 on measures to monitor certain substancesand residues thereof in live animals and animal products and repealingDirectives 85/358/EEC and 86/469/EEC and Decisions 89/187EEC and91/664/EEC. OJEC, L125, 10-32, 1996.

Commission of the European Communities: Commission Decision 2002/657/EC of 12th August 2002 implementing Council Directive 96/23/EC concerning the performance of analytical methods and the interpretation of results. OJEC, L221, 2002

Danezis GP, Anagnostopoulos CJ, Liapis K, Koupparis MA. Multi-residue analysis of pesticides, plant hormones, veterinary drugs and mycotoxins using HILIC chromatography—MS/MS in various food matrices. Analytica Chimica Acta. 2016; 942: 121-138.

Escrivá L, Oueslati S, Font G, Manyes L. Alternaria Mycotoxins in Food and Feed: An Overview. Journal of Food Quality. 2017; 5: 1-20.

Gómez-Pérez ML, Romero-González R, Vidal JLM, Frenich AG. Analysis of pesticide and veterinary drug residues in baby food by liquid chromatography coupled to Orbitrap high resolution mass spectrometry. Talanta. 2015; 131: 1-7.

Hajrulai-Musliu Z, Uzunov R, Jovanov S, Jankuloski D, Stojkovski V, Pendovski L, Sanya, JJ. A new LC–MS/MS method for multiple residues/contaminants in bovine meat. BMC Chemistry. 2021; 15 (1): 62.

Hu Q, Noll RJ, Li H, Makarov A, Hardman M, Graham Cooks R. The Orbitrap: a new mass spectrometer. 2005; 40 (4): 430-43.

[a]Kaufmann A, Butcher P, Maden K, Widmer M. Quantitative multiresidue method for about 100 veterinary drugs in different meat matrices by sub-2-microm particulate high-performance liquid chromatography coupled to time-of-flight mass spectrometry. Journal of Chromatography A. 2008; 1194 (1): 66-79

[b]Kaufmann A, Butcher P, Maden K, Walker S, Widmer M. Semi-targeted residue screening in complex matrices with liquid chromatography coupled to high resolution mass spectrometry: current possibilities and limitations. Analyst. 2011; 136: 1898-1909.

Kellman M, Muenster H, Zomer P, Mol H. Full scan MS in comprehensive qualitative and quantitative residue analysis in food and feed matrices: How much resolving power is needed? Journal of the American Society for Mass Spectrometry. 2009; 20 (8): 1464–1476.

Makarov A, Denisov E, Lange O, Horning S. Dynamic range of mass accuracy in LTQ Orbitrap hybrid mass spectrometer. Journal of the American Society for Mass Spectrometry. 2006; 17 (7): 977-982.

Stolker AAM, Th Brinkman UA. Analytical strategies for residue analysis of veterinary drugs and growth-promoting agents in food-producing animals--a review. Journal of Chromatography A. 2005; 1067 (1-2): 15-53.

Stolker AAM, Zuidema T, Nielen MWF. Residue analysis of veterinary drugs and growth-promoting agents.Trends in Analytical Chemistry. 2007; 26 (10): 967-979.

Uzunov R, Hajrulai-Musliu Z, Stojkovski V, Dimitrieska-Stojkovic E, Stojanovska-Dimzoska B, Sekulovski P, Jankuloski D. Development and validation of LC-MS/MS method for determination of ten beta agonists in bovine urine. Kafkas Universitesi Veteriner Fakultesi Dergisi. 2019; 25 (1): 55-60.

Zhan J, Xu DM, Wang SJ, Sun J, Xu YJ, Ni ML, Yin JY, Chen J, Yu XJ, Huang ZQ. Comprehensive screening for multi-class veterinary drug residues andother contaminants in muscle using column-switching UPLC–MS/MS. Food Additives & Contaminants: Part A. 2013; 30 (11); 1888-1899.

Second International Congress on Biological and Health Sciences
ONLINE 24-25-26-27 FEBRUARY 2022

Investigation of triterpene saponins from the berries of common ivy (*Hedera helix* L.) growing in Azerbaijan

Saida Akberova[1], Gaibverdi Iskenderov[2]

[1, 2]Azerbaijan Medical University

Saida Akberova: musayeva_saida@mail.ru

Abstract:
In order to search for new sources of plant raw materials for the creation of medicines containing triterpene glycosides, we studied the triterpene saponins of common ivy (*Hedera helix* L.) from the flora of Azerbaijan. The aim of the study is to develop a method for the efficient isolation of saponins from common ivy berries based on certain optimal conditions. The paper presents the results of chemical investigation of triterpene saponins (substances A, B, C and D), isolated from the berries of common ivy. Applying classical chemical methods, such as acid, alkaline, and analytical partial hydrolysis, methylation with diazomethane, complete methylation followed by methanolysis, periodate oxidation as well as IR spectroscopy and thin layer chromatography (TLC) were established that two saponins are biosids of corresponding sapogenins. The carbohydrate chain of these compounds consist of one molecule L-arabinose and L-rhamnose. It has been found that is saponin A $C_{41}H_{66}O_{11}$ oleanolic acid 3-O-[α-L-rhamnopyranosyl-(1 → 2)-α-L-arabopiranosyd] (β-hederin) and saponin B $C_{41}H_{66}O_{12}$ has the same carbohydrate chain associated with hederagenin (α-hederin). Saponin C is pentaosid of oleanolic acid. The carbohydrate chain includes one molecule of L-rhamnose, D-glucose, D-galactose and two molecules of L-arabinose. On the basis of results of the experiments and their analysis found complete chemical structure of individual glycoside as oleanolic acid 3-O-α-L-arabinopiranozyl-(1→2)-β-D-galaktopyranosyl-(1→2)-[β-D-glucopyranosyl-(1→4)]-α-L-rhamnopyranosyl-(1→2)-α-L-arabinopiranozyl. This glycoside is isolated from the berries of common ivy for the first time. For the first time, triterpene saponins from raw materials were isolated separately by a special approach - sequential fractional extraction and their physicochemical properties were studied.

Key words: triterpene saponins, oleanolic acid, hederagenin, α-hederin, β-hederin.

1. Introduction

The search for new sources of plant materials for the creation of medicines is of great importance for pharmaceutical science. Based on this, it is of great interest to study the plant flora of Azerbaijan in this direction. The object of the study was common ivy *Hedera helix* L., widespread in Azerbaijan, containing triterpene saponins. Older European medical literature suggests that children develop significant toxicity including vomiting, diarrhea, respiratory depression, and coma after ingestion of berries or leaves from *Hedera helix* [1].
The aim of the study is to develop a method for the efficient isolation of saponins from common ivy berries based on certain optimal conditions.

2. Materials and methods

Dried and crushed ivy berries, which grow in Azerbaijan, were used as raw materials. To determine the number of triterpene saponins and aglycones, thin-layer chromatography (TLC) was used. As a stationary

phase, standard Silufol and Sorbfil plates were taken, and systems of various solvents were taken as a mobile phase: solvent system I - n-butanol - ethanol - 25% ammonia (10 : 2 : 5), solvents system II - chloroform - ethanol - water (15 : 15 : 5), solvent system III - ethyl acetate - isopropyl alcohol - water (65 : 23 : 12); solvent system IV - benzene - methanol - acetic acid (1: 3: 1). The last two systems were used for the determination of monosaccharides. For the detection of substances in the chromatogram, a 25% alcohol solution of phosphotungstic acid was used, followed by heating for 5–10 minutes at a temperature of 100^0 C [2]. Monosaccharides and methyl derivatives were detected on the chromatogram with aniline phthalate. The melting point of the substances was determined using a Kofler bench, and the specific rotation was measured using a P-161 polarimeter. IR spectra of triterpene saponins were recorded on an Agilent Cary 630 FTIR spectrometer from Agilent Technologies in the range of 600-4000 cm^{-1}.

1.2 kg of raw material was degreased first with petroleum ether, then with benzene. From the rest of the raw material, polar glycosides were extracted first with 50% ethanol, then low-polarity glycosides, with 80%. After appropriate purification processes, low polar and polar glycosidic fractions were obtained, each of which consists of two glycosides. These fractions were then separated into individual glycosides by silica gel adsorption column chromatography (2.5 x 40 cm). Glycosides A and B were isolated from the less polar fraction, glycosides C and D were isolated from the polar fraction. Individual glycosides A, B and C were subjected to a deeper chemical study [3,4].

3. Results

R_f values of isolated individual triterpene glycosides in solvent systems I and II: for glycoside A were 0.84 and 0.75; for glycoside B were 0.81 and 0.71; for glycoside C were 0.46 and 0.40. Glycoside A has the composition $C_{41}H_{66}O_{11}$, molecular weight 734, melting point 228-230^0 C, $[\alpha]_D^{20}$ =+17.8^0 (c 0.5; 80% ethanol). Glycoside B has the composition $C_{41}H_{66}O_{12}$, molecular weight 750, melting point 236-238^0 C, $[\alpha]_D^{20}$=+16.2^0 (c 0.7; 80% ethanol). Glycoside C has the composition $C_{58}H_{94}O_{25}$, molecular weight 1190, melting point 188-190^0 C, $[\alpha]_D^{20}$=+9^0 (c 0.1; 50% ethanol).

4. Discussion

The results of experimental studies on the above triterpene glycosides showed that glycoside A is a biosid of oleanolic acid, the carbohydrate chain of which includes one molecule of L-rhamnose and L-arabinose each. This glycoside has the following chemical structure: oleanolic acid 3-O-α-L-rhamnopyranosyl-(1→2)-O-α-L-arabinopyranoside and is a well-known glycoside β-hederin. Glycoside B is also a biosid, but contains hederagenin as an aglycone. The carbohydrate chain of this glycoside has a similar set and sequence of monosaccharides, as in glycoside A. The chemical structure of glycoside B is identical to α-hederin. As shown by the results of a chemical study of glycoside C, it is a pentaosid of oleanolic acid, the composition of the carbohydrate chain of the molecule of which includes one molecule of L-rhamnose, D-glucose, D-galactose and two molecules of L-arabinose. Moreover, all monosaccharides are interconnected, forming one carbohydrate chain at the hydroxyl in position 3 of the oleanolic acid molecule.

5. Conclusion

For the first time, triterpene saponins from raw materials were isolated separately (glycosides A, B, C and D) by a special approach - sequential fractional extraction and their physicochemical properties were studied. The chemical structures of individual saponins were determined: glycoside A is biosid of oleanolic acid, glycoside B is biosid of hederagenin, glycoside C is pentaosid of oleanolic acid. Glycoside C was first obtained from this raw material, and its chemical structure was fully determined.

6. References

1. Donald G.B. Medical toxicology of natural substances: foods, fungi, medicinal herbs, plants, and venomous animals: John Wiley & Sons Inc. 2008; pp. 865-866.

2. Yakovishin L.A. Molecular complexes of triterpene glycosides with biologically active substances: preparation, chemical-pharmaceutical properties and biological activity: dissertation of the doctor of chemical sciences. Sevastopol, 2018; p. 218.

3. Iskenderov G.B., Musayeva S.Sh. Chemical investigation of the less polar saponins from the fruts of Common Ivy (*Hedera helix* L.). Journal of Qafqaz University. 2013; 1 (1): pp. 83-88.

4. Iskenderov G.B., Musayeva S.Sh. Chemical investigation of polar triterpene glycosides from the berries of Common Ivy. Journal of Qafqaz University. 2014; 2 (1): pp. 40-47.

Second International Congress on Biological and Health Sciences
ONLINE 24-25-26-27 FEBRUARY 2022

Doxorubicin and Zinc Oxide Encapsulated Albumin Nanoparticles Exhibits Ph-Sensitive Drug Release Profile

Habibe YILMAZ[1,2,3]

[1] Department of Pharmaceutical Biotechnology, Faculty of Pharmacy, Trakya University, Edirne, TURKEY.
[2] Department of Biochemistry, Faculty of Science, Ege University, Izmir, TURKEY.
[3] Research and Application Center of Drug Development and Pharmacokinetics, Ege University, Izmir, TURKEY.

Corresponding author: habibeyilmaz@trakya.edu.tr

Abstract:

Many drug delivery systems are being studied for biomedical purposes. Among these, nanoparticular systems are of great interest. Zinc oxide nanoparticles (ZnO NP) are among the few nanoparticles classified as safe by the FDA. It has been shown to have anti-tumoral and antimicrobial effects. In addition, it can also be used in bioimaging due to its unique optical properties. Its use as a drug delivery system continues to be investigated. Albumin (Alb) is a protein synthesized in the liver and abundant in plasma. The use of albumin as a nano drug delivery system has advantages such as being non-toxic, non-antigenic and biodegradable. Doxorubicin (Dox) is a highly effective and widely used anti-cancer drug. However, it has serious side effects such as vomiting, myelosuppression and cardiotoxicity. Therefore, studies are still being carried out on many smart drug delivery systems to reduce the side effects of doxorubicin and increase its therapeutic index.
The aim of this work is to synthesize zinc oxide and doxorubicin-carrying nanoparticulate formulation that can have controlled release of the drug especially at acidic region resulting in improved therapeutic index for cancer therapy.
In this study, aqueous synthesis of zinc oxide nanoparticle was carried out. Then, the obtained zinc oxide nanoparticles were encapsulated with albumin using desolvation method. Doxorubicin loading was carried out simultaneously with the encapsulation of zinc oxide nanoparticles, and albumin nanoparticles loaded with doxorubicin and zinc oxide nanoparticles (Dox-Alb-ZnO NP) were obtained. Nanoparticles were characterized with SEM, TEM and FTIR. It was found that nanoparticles are in spherical shape. Also, FTIR analysis revealed that encapsulation was successful. Drug loading and desolvation yield was calculated and found as 51.8% and 98.2%, respectively. Cumulative drug release was monitored for 48 hours against buffers at pH 5.5 and pH 7.4. Slower drug release rate was observed at pH 5.5 compared to pH 7.4. When the release study data were evaluated in terms of kinetic modeling, it was found to be suitable for the Kors-Meyer Peppas model. Therefore, it was concluded that the nano drug delivery system is pH sensitive and can be used for chemotherapeutic purposes.

Keywords: Zinc oxide nanoparticles, doxorubicin, albumin, drug release, drug loading.

1. Introduction

Zinc has been used biomedically for many years. However, although many metal ions have a role in controlling biological processes, their use in high amounts can cause toxicities. Therefore, researchers are trying to modulate these undesirable effects by developing metallic nanoparticles. Zinc oxide nanoparticles are also highly preferred in the biomedical sense due to their essential role in biochemical

reactions, being used for a long time, biocompatibility, biodegradability, easy functionalization, drug loading, ease of synthesis and low cost. Its use against many diseases such as wound healing, cardiovascular and ischemic diseases, use as a microbial agent and cancer is being investigated (Bariu et al., 2018). Zinc oxide nanoparticles also exhibit beneficial optical properties. For example, it can be used as a cell imaging agent because of its excitonic blue and near-UV emission. In addition, it can generate reactive oxygen species (ROS) due to UV illumination, indicating that it can be used for photodynamic therapy purposes. In addition to these, many properties such as high catalytic activity, high absorption capacity, high isoelectric point that can provide protein adsorption, and semiconducting property allow them to be used in biosensors (Zhang et al., 2013).

Albumin is the globular protein synthesized in the liver and the most abundant protein in plasma. The use of albumin in nanomedicine is preferred due to its easy availability, water solubility, low immunogenicity, non-toxicity, biocompatibility and biodegradability. Abraxane™ and Albunex™ which are based on human serum albumin, have been on the market since 2005 following FDA approval and used in the treatment of breast cancer. In addition to being used alone in the preparation of nanoparticle form, it is a good coating agent that can be used for purposes such as solving the aggregation problem and increasing biocompatibility, especially in metallic nanoparticles (Nosrati et al., 2018; Ak et al., 2014).

Cancer is now the largest cause of death following cardiovascular disease. In addition to applications such as surgery and radiotherapy for cancer treatment, chemotherapeutics is being widely used. Doxorubicin is one of the frequently used chemotherapeutics. Doxorubicin, like many chemotherapeutics, causes systemic toxicities with low selectivity, such as vomiting, cardiotoxicity, myelosuppression, and hair loss. Therefore, nanomedical solutions are being developed to reduce side effects and increase the therapeutic index. FDA-approved Doxil™ is one of the results from these efforts. However, research on the development of more effective and biocompatible drug delivery systems with lower doses of chemotherapeutics is still ongoing.

The aim of this work is to synthesize zinc oxide and doxorubicin-carrying nanoparticulate formulation that can have controlled release of the drug especially at acidic region resulting in improved therapeutic index for cancer therapy.

2. Materials and Methods

2.1 Materials

BSA was purchased from Sigma-Aldrich, 1-ethyl-3-carbodiimide hydrochloride (EDC) was obtained from Merck and Dox was supplied commercially. All the other reagents were of analytical grade. Fouirer Transform Infrared (FT-IR) spectroscopy analysis was performed at Ege University Research and Application Center of Drug Development and Pharmocokinetics, scanning electron microscopy (SEM) analysis was performed at Ege University Central Research Test and Analysis Laboratory Application and Research Center (MATAL) and transmission electron microscopy (TEM) analysis was performed at Çanakkale Onsekiz Mart University Science and Technology Application and Research Center (ÇOMÜ-ÇOBİLTUM).

2.2 Synthesis of Zinc Oxide Nanoparticles (ZnO NP)

0.2 M zinc sulphate dissolved in distilled water and mixed with mechanical stirrer at 3000 rpm and 60°C. 0.5 M NaOH heated to 60°C was rapidly added to it. The reaction is continued for 1 hour at 60°C and with mechanical stirring at 3000 rpm. At the end of the time, the mixture containing the nanoparticles formed is cooled to room temperature. Nanoparticles were precipitated by centrifugation at 9000 rpm, washed 3 times in distilled water, and then dispersed in pure water. The dispersed nanoparticles were subjected to ultrasonication 4 times for 15 minutes. The obtained product was dried at 80°C, then ground in a mortar and dried at 60°C overnight (Pourrahimi et al., 2014).

Morphological evaluation was performed by SEM analysis and structural evaluation was performed by FT-IR analysis.

2.3 Synthesis of Albumin Coated Zinc Oxide Nanoparticles (Alb-ZnO NP)

A combination of methods from Kumar et al. 2013, Nosrati et al. 2018 and our previous study were used in the synthesis of albumin-coated zinc oxide nanoparticles (Kumar et al., 2013; Ak G. et al., 2014; Nosrati et al., 2018). Briefly, 15 mg ZnO NPs dispersed in 1.5 mL distilled water with ultrasonication for 10 minutes. 0.25 mL distilled water and 0.5 mL of albumin solution with a concentration ranging from 5 to 50 mg/mL is added to 0.25 mL of ZnO NP suspension and mixed thoroughly at 300 rpm for 15 minutes in orbital shaker. Then, 4 mL of acetone is dropped at a flow rate of 1 mL/min. Immediately after the addition of acetone, 100 µL of 10 mg/mL EDC is added and allowed to react for 2 hours at room temperature. At the end of the time period, the formed nanoparticles were precipitated by centrifugation at 13.000 rpm for 30 min and washed with distilled water 3 times under same conditions. The desolvation efficiency was determined by measuring the amount of albumin remaining in the supernatant using the Bradford method and was calculated using the equation below (Bradford M.M., 1976; Ak G. et al, 2014).

$$\textit{Desolvation Efficiency (\%)} = \left(\textit{Initial protein amount (mg)} - \textit{Protein amount in supernatant (mg)} \right) / \textit{Initial protein amount (mg)} \quad \textbf{Eq.1}$$

Morphological evaluation was performed by TEM analysis and structural evaluation was performed by FT-IR analysis.

2.4 Doxorubicin Loading to Alb-ZnO NP (Dox-Alb-ZnO NP)

0.5 mL of 20 mg/mL concentration of albumin solution and 0.25 mL of Dox solution in concentrations ranging from 1 to 10 mg/mL were added onto the dispersed ZnO NP suspension at a concentration of 10 mg/mL and a volume of 0.25 mL. Then, 4 mL of acetone is dropped at a flow rate of 1 mL/min. Immediately after the addition of acetone, 100 µL of 10 mg/mL EDC is added and allowed to react for 2 hours at room temperature. At the end of the period, the formed nanoparticles were precipitated by centrifugation at 13.000 rpm for 30 min and washed with distilled water 3 times under same conditions.

The drug loading yield was calculated by measuring the Dox at the supernatant spectrophotometrically at 480 nm. Dox loading yield was calculated by using the equation below (Ak G. et al, 2014).

DLY (%) = Initial Dox amount (mg) – (Dox amount in supernatant (mg) / Initial Dox amount (mg) **Eq. 2**

Morphological evaluation was performed by TEM analysis and structural evaluation was performed by FT-IR analysis.

2.5. *In vitro* Drug Release Studies and Kinetics

The nanoparticles were dispersed 10 mM acetate buffer at pH 5.5 and, 10 mM phosphate buffer at pH 7.4 and sealed in dialysis tubing (12000 MWCO). In addition, free Dox solution was prepared in the relevant buffers and placed in dialysis tubing (12000 MWCO). The dialysis tubings were placed in 10 mM acetate buffer at pH 5.5 and, 10 mM phosphate buffer at pH 7.4 containing vessels and then set in a water bath at 37°C under constant shaking. Samples were taken at predetermined time intervals and replaced with pre-warmed fresh buffer. The amount of Dox released in collected sample was measured spectrophotometrically at 480 nm. The cumulative fraction of released Dox versus time was expressed by the following equation (Ak G. et al, 2014).

Cumulative Drug Release (%) = Released Dox (mg) / Initial Dox amount (mg) **Eq. 3**

Various kinetic models (zero-order release, first-order release, Higuchi's model, Korsmeyer–Peppas model, and Hixon–Crowell model) were studied to evaluate the data to determine drug release kinetics behavior. Correlation coefficient (R^2) value was used in the evaluation of the model. The highest R^2 value indicates the best-fit model (Ak G. et al., 2021).

3. Results

3.1. Synthesis of Zinc Oxide Nanoparticles (ZnO NP)

SEM analysis was performed to determine the morphological structure and size of the synthesized zinc oxide nanoparticles. SEM images showed that it was morphologically almost spherical in shape and ranged in size from 30 to 60 nm. FTIR of ZnO NPs showed broad peak in the region of 3385 cm^{-1} which corresponds to the O–H bond while peak at 891 cm^{-1} might be due to the bending of inorganic carbonate group. Also, the sharp peak in the region of 560–400 cm^{-1} is the characteristic peak at of Zn–O bond present in the ZnO nanoparticles.

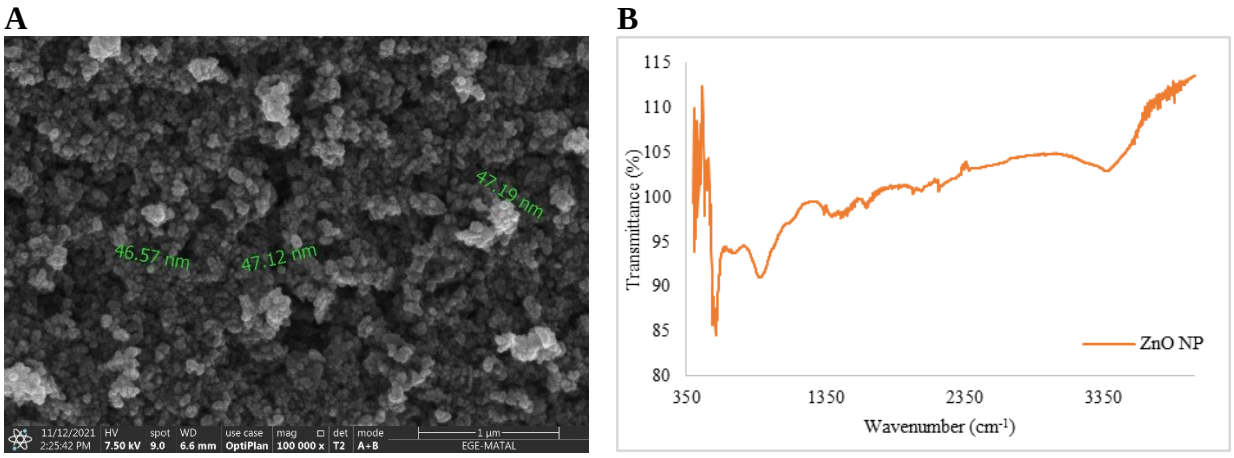

Figure 1. A) SEM image of ZnO NPs, B) FTIR analysis data of ZnO NP.

3.2 Synthesis of Albumin Coated Zinc Oxide Nanoparticles (Alb-ZnO NP)

Desolvation efficiency was found to be over 90% at all albumin concentrations. It was observed that the yield was 98.2% at 20 mg/mL concentration and there was no significant difference at higher concentrations. Therefore, it was decided that the optimal albumin concentration was 20 mg/mL. In TEM images, it is understood that the morphological structures of nanoparticles are close to spherical. It is noteworthy that as a result of albumin coating, the dimensions reach a size close to 100 nm.

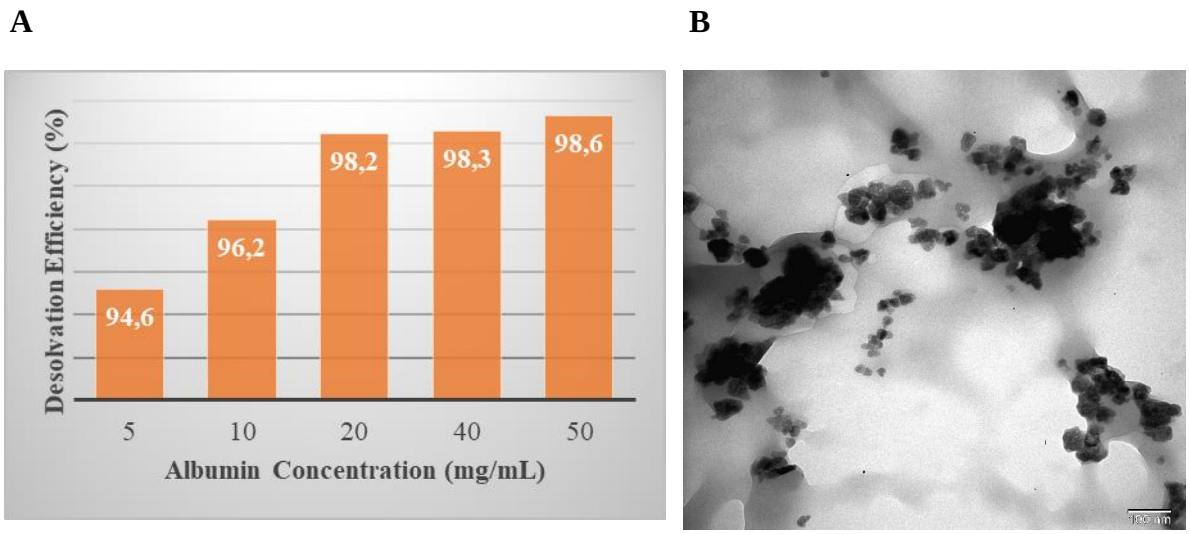

Figure 2. A) Desolvation efficiency and B) TEM image of Alb-ZnO-NPs.

In the comparative FTIR analysis, a decrease is observed in the carboxylic acid signals of albumin at 3072 cm^{-1} and 2953 cm^{-1} after coating with ZnO NP. Similarly, there is a decrease in the signals from ketone and carboxylic acid groups in the range of 1400 cm^{-1} to 1082 cm^{-1}.

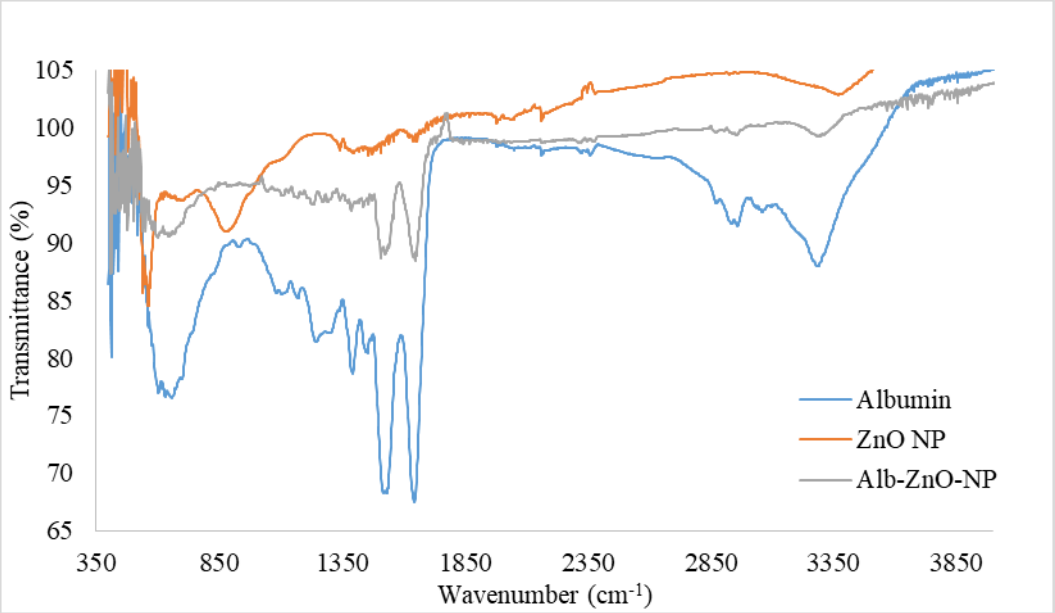

Figure 3. Comparative FT-IR analysis data of albumin, ZnO NP and Alb-ZnO-NP.

3.3 Doxorubicin Loading to Alb-ZnO NP (Dox-Alb-ZnO NP)

When the drug loading efficiency at 5 to 10 mg/mL concentrations was examined, it was seen that it ranged from 48% to 52%. However, it was determined that the optimum concentration was 7.5 mg/mL with 51.8% yield among the varying concentrations in doxorubicin loading. In the TEM images obtained after drug loading, it was observed that the size of drug-loaded nanoparticles increased to around 200 nm.

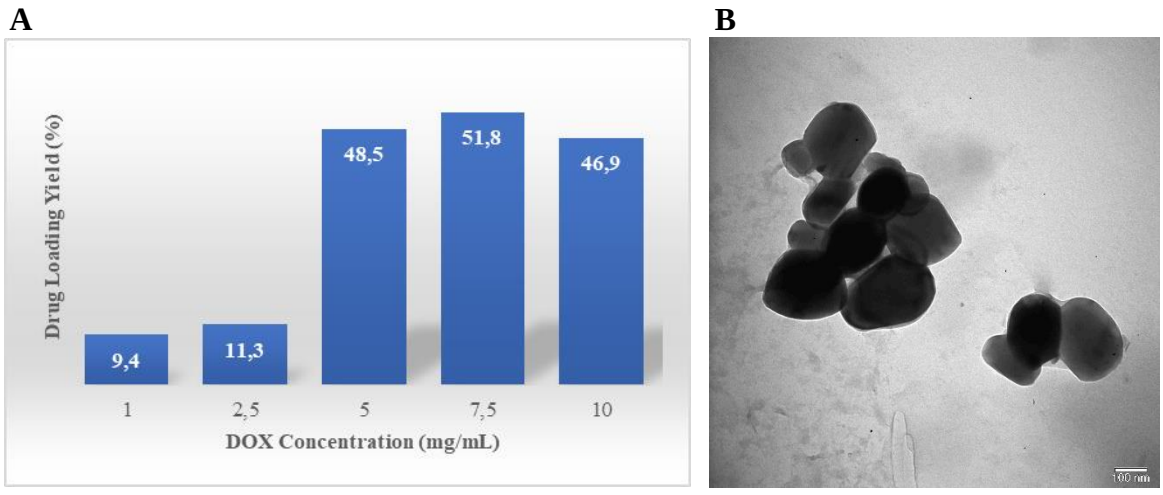

Figure 4. A) Doxorubicin loading yield and B) TEM image of Dox-Alb-ZnO-NPs.

When the FT-IR data of Alb-ZnO NP and Dox-Alb-ZnO NP are overlapped, signals from Dox are seen in the region of 2850 cm^{-1} and 3350 cm^{-1}. Although the signals between 1400 cm^{-1} to 1600 cm^{-1} appear to be masked, the signals in the Dox-Alb-ZnO NP in the range of 1200 cm^{-1} to 1400 cm^{-1} depend on the Dox.

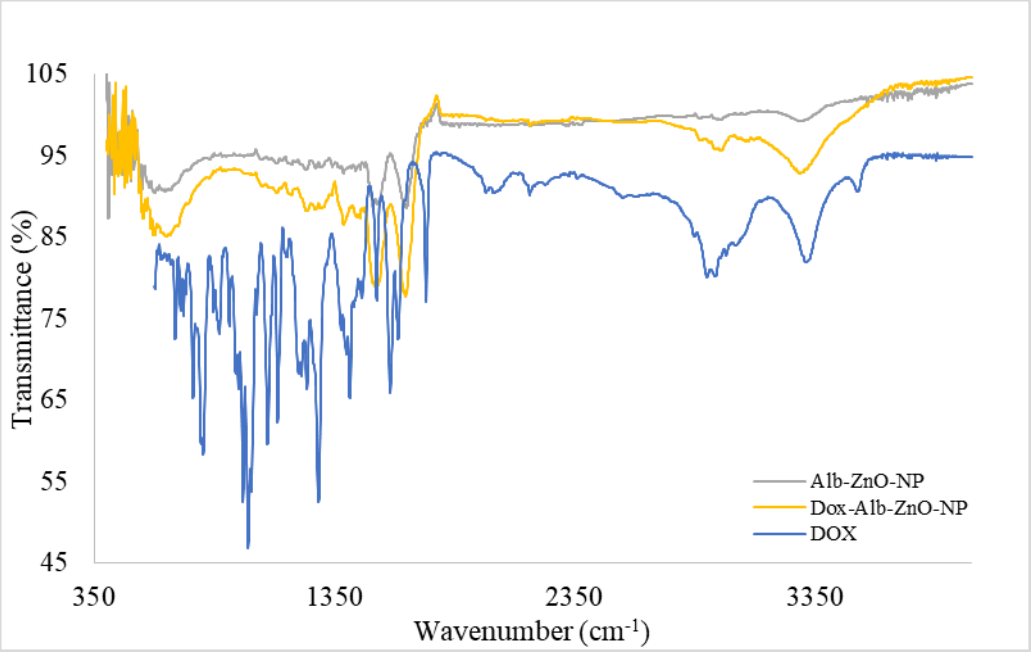

Figure 5. Comparative FT-IR analysis data of Alb-ZnO NP and Dox-Alb-ZnO NP.

3.4 *In vitro* Drug Release Studies and Kinetics

The drug release study was performed in buffer at pH 5.5 to mimic intracellular lysosomal space and, pH 7.4 to mimic physiological conditions. Drug release was monitored for 48 hours. According to the 48 hours drug release results, Dox release from nanoparticles is higher at pH 5.5 compared to pH 7.4. On the other hand, it is seen that free doxorubicin reaches a similar release amount in 6 hours.

A

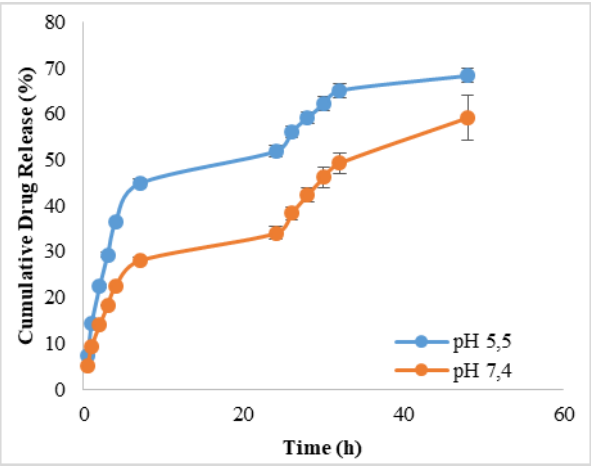

B

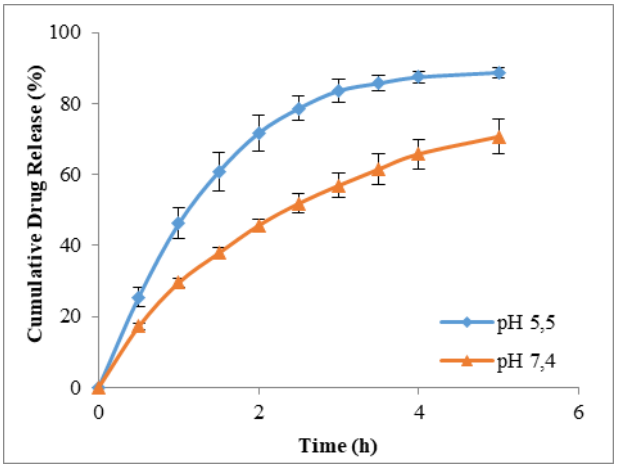

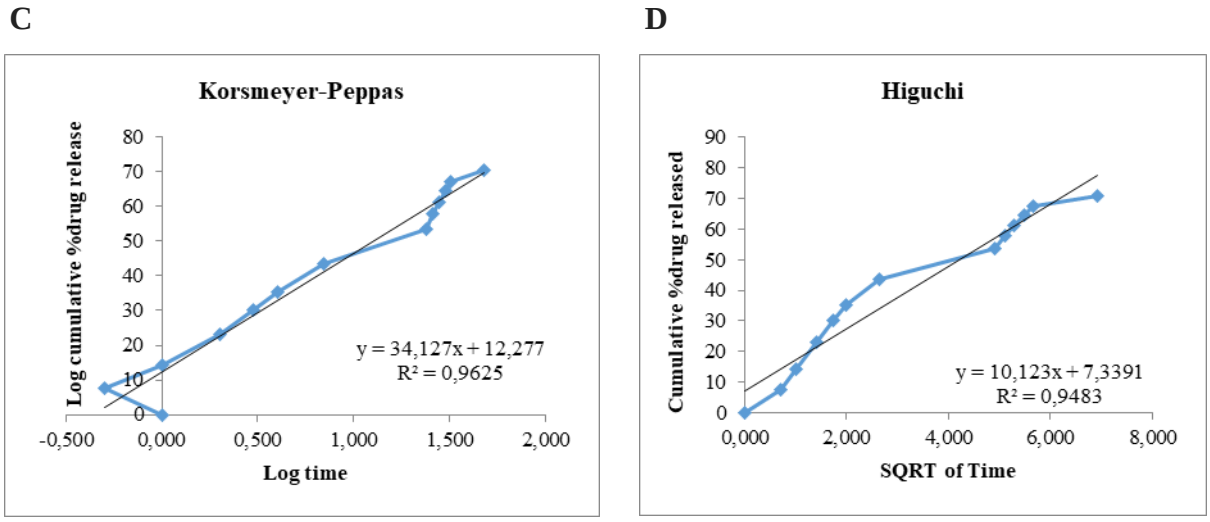

Figure 6. A) Doxorubicin release profile from Dox-Alb-ZnO NPs at pH 5.5 and 7.4, B) Free doxorubicin release profile at pH 5.5 and 7.4, C) Korsmeyer-Peppas drug release kinetics and, D) Higuchi drug release kinetics model.

First-order, zero-order, Higuchi, Korsmeyer-Peppas and Hixson Crowell models were studied to determine drug release kinetics model. The two models with the highest R^2 value among the studied models are shown in Figure 6. It was determined from the R^2 value that the best model describing the drug release kinetics was Korsmeyer-Peppas model, and the n value was calculated as 0.17.

4. Discussion

The dimensions of the zinc oxide nanoparticles obtained in a study carried out in 2017 were found to be approximately 44 nm in size and spherical by TEM imaging (Kim et al., 2017). Similar results were obtained with publication in which the synthesis method was used (Pourrahimi et al., 2014). The shape and size of the synthesized zinc oxide nanoparticles were correlated with the literature. The FT-IR analysis is similar to the study carried out in 2021. In the related study, -OH group signals on the surface of zinc oxide nanoparticles were detected at 3215 cm^{-1} and Zn-O signals between 457-545 cm^{-1} which is similar to the performed study (Batool et al., 2021).

When the desolvation efficiency of albumin nanoparticles was evaluated, it was observed that nanoparticles that were coacerved with ethanol and cross-linked with glutaraldehyde has 80% desolvation efficiency (Ak G., 2014). However, in my work, unlike the other study, coacervation was performed with acetone and crosslinking was performed with EDC. The desolvation efficiency was found to be approximately 98% for 20 mg/mL albumin concentration. The obtained data shows that cross-linking is more effective with EDC for synthesis of albumin nanoparticles and only 2% of the synthesized albumin remains unreacted. The method shows superiority in terms of reaction efficiency. According to the FT-IR results, signals from albumin at 3288 cm^{-1} are seen at 3298 cm^{-1} in albumin-coated zinc oxide nanoparticles, and signals from 1643 cm^{-1} to 1529 cm^{-1} are seen at 1687 cm^{-1} and 1527 cm^{-1}. The signal of Zn-O overlaps with the signal from albumin. This finding indicates that zinc oxide nanoparticles are successfully coated with albumin. It has been suggested that the size not increasing significantly after

coating with albumin is because of the tight packing of the structure due to the intense electrostatic interactions.

In the Dox loading study of zinc oxide nanoparticles carried out in 2017, it was reported that 1.32% of the 4 mg drug (52.8 µg Dox), incorporated in the nanoparticle structure (Kim et al., 2017). In another study, doxorubicin was loaded onto PEG-coated and uncoated zinc oxide nanoparticles via adsorption. The loading efficiency for the uncoated zinc oxide nanoparticles was 35% and the loading efficiency for the coated ones was 65%. In the study, it was observed that the drug loading of zinc oxide nanoparticles was increased by coating. They suggested that the loading efficiency of doxorubicin was due to electrostatic interactions for zinc oxide nanoparticles, whereas in coated ones this was due to the large molecular core of PEG (Batool et al., 2021). Ak et al. found the drug loading efficiency of albumin nanoparticles as 65.5% (Ak et al., 2014). When the literature information and the available data are evaluated, in this study, the drug loading efficiency is high and the albumin coating has an increasing effect on this efficiency. Based on FT-IR analysis performed after drug loading, signals from Dox was found at 3273 cm^{-1}, 2953 cm^{-1}, 1388 cm^{-1} and 1238 cm^{-1} which suggests the drug was successfully loaded to the nanoparticles. In addition, the enlargement of the structure in the TEM analysis also indicates that drug loading has occurred.

In a study conducted in 2017, DOX release was monitored for 144 hours at a pH value of 5.5, which mimics intracellular conditions. It was stated that the drug release was 29% in 6 hours and 92.8% in 144 hours with sustained release (Kim et al., 2017). In our study, it is seen that 29% drug release is reached in 3 hours and 80% drug release is observed in 48 hours.

In drug systems, drug release is dependent on diffusion and dissolution. The Higuchi model is one of the most widely used models to explain the controlled drug release pattern. Drug delivery system developed in the study is following Higuchi drug release model as the drug release profile is very close to trend line or regression line and there is a high value of coefficient of correlation (R^2=0,9483). The diffusion type of the release profile following the Higuchi model was explained by the Korsmeyer-Peppas model. According to the data obtained, the n value is less than 0.45 which indicates the nanoparticle exhibits a Fickian release because the relaxation time (tr) is greater than the characteristic solvent diffusion time (td) (Dash et al., 2010; Gouda et al., 2017).

5. Conclusion

In the study, anti-cancer drug delivery system was successfully synthesized. When evaluated together with the information in the literature, it is expected that zinc oxide nanoparticles will contribute to cytotoxicity together with doxorubicin. Again, the optical properties of zinc oxide nanoparticles are suitable for photodynamic therapy, suggesting that the synthesized drug delivery system may have such property. Therefore, future studies will be performed to assess if this feature exists. The drug release profile showed that the developed drug delivery system is pH-sensitive and, exhibits controlled and prolonged release. In the light of these data, the developed drug delivery system has the potential to be used for anti-cancer treatment and its further studies may be beneficial.

6. References

Ak G., Yeilmaz H., Sanleier S.H. Preparation of magnetically responsive albumin nanospheres and in vitro drug release studies. Artificial Cells, Nanomedicine and Biotechnology. 2014; 42(1): 18-26.

Ak G., Bozkaya Ü.F., Yılmaz H., Sarı Turgut Ö., Bilgin İ., Tomruk C., Uyanıkgil Y., Hamarat Şanlıer Ş. An intravenous application of magnetic nanoparticles for osteomyelitis treatment: An efficient alternative. International Journal of Pharmaceutics. 2021; 592: 119999.

Bariu A.K., Kotcherlakota R., Patra C.R. Inorganic Frameworks as Smart Nanomedicines: Volume 6: Biomedical applications of zinc oxide nanoparticles. Grumezescu A.M (Ed). William Andrew. Elsevier. 2018; pp 239-278.

Batool M., Khursid S., Daoush W.M., Siddique S.A., Nadeem T. Green Synthesis and Biomedical Applications of ZnO Nanoparticles: Role of PEGylated-ZnO Nanoparticles as Doxorubicin Drug Carrier against MDA-MB-231(TNBC) Cells Line. Crystals. 2021; 11: 344 – 363.

Bradford MM. A rapid and sensitive method for the quantitation of microgram quantities of protein utilizing the principle of protein dye binding. Analytical Biochemistry. 1976; 72: 248-254.

Dash S., Murthy P.N., Nath L., Chowdhury P. Kinetic Modeling on Drug Release from Controlled Drug Delivery Systems. Acta Poloniae Pharmaceutica - Drug Research. 2010; 67(3): 217-223.

Gouda R., Baishya H., Qing Z. Application of Mathematical Models in Drug Release Kinetics of Carbidopa and Levodopa ER Tablets. Journal of Developing Drugs. 2017; 6(2): 1000171.

Kim S., Lee S.Y., Cho H.J. Doxorubicin-Wrapped Zinc Oxide Nanoclusters for the Therapy of Colorectal Adenocarcinoma. Nanomaterials (Basel). 2014; 7(11): 354 – 367.

Kumar P., Kumar P., Deep A., Bharadwaj L.M. Synthesis and conjugation of ZnO nanoparticles with bovine serum albumin for biological applications. Applied Nanoscience. 2013; 3: 141-144.

Nosrati H., Salehiabar M., Manjili H.K., Danafar H., Davaran S. Preparation of magnetic albumin nanoparticles via a simple and one-pot desolvation and co-precipitation method for medical and pharmaceutical applications. International Journal of Biological Macromolecules. 2018; 108: 909-915.

Pourrahimi A.M., Liu D., Pallon L.K.H., Andersson R.L., Martínez Abad A., Lagarón J.M., Hedengvist M.S., Ström V., Gedde U.W., Olsson R.T. Water-based synthesis and cleaning methods for high purity ZnO nanoparticles – comparing acetate, chloride, sulphate and nitrate zinc salt precursors. RCS Advances. 2014; 4: 35568.

Zhang Y., Nayak T.R., Hong H., Cai W. Biomedical Applications of Zinc Oxide Nanomaterials. Current Molecular Medicine. 2013; 13(10): 1633-1645.

Second International Congress on Biological and Health Sciences
ONLINE 24-25-26-27 FEBRUARY 2022

Investigation of The Synergistic Effect of Phenolic Compounds on Acetylcholinesterase

Melike Karaman[1], Emine Toraman[1]

[1]Atatürk University, Science Faculty, Department of Molecular Biology and Genetics, Erzurum, Turkey

Corresponding author: melike.yildiz@atauni.edu.tr

Abstract:

Acetylcholinesterase (AChE) hydrolyzes acetylcholine, a neurotransmitter, into acetic acid and choline. AChE activity enhances in the age-related neurological disorders. Thus, the inhibition of AChE is a crucial therapeutic approach to treat the cognitive disorder such as Alzheimer's disease. Natural compounds derived from plants are widely investigated as sources of AChE inhibitors. It has been reported that phenolic compounds naturally found in plants and fruits have the potential to inhibit AChE activity. Gallic acid (GA) and vanillic acid (VA) are phenolic acid derivatives found in plants. These compounds are bioactive molecules with anti-inflammatory, antioxidant, antibacterial and antimicrobial effects. In this study, the effect of different doses of GA and VA mixture on AChE activity was investigated. A mixture of GA and VA was prepared at 50 and 100 µM concentrations of both compounds. This mixture was applied to third instar fly larvae. After the application, the heads of adult flies were dissected and homogenized. AChE activity was measured by Ellman's method for each group. When the results were examined, it was found that 50 µM of GA-VA mixture did not show a significant difference in enzyme activity, but 100 µM of GA-VA mixture caused a significant decrease in enzyme activity. It could be beneficial to use the synergistic effect of phenolic compounds in the investigation of AChE inhibitors.

Keywords: ache activity, gallic acid, phenolic acid, vanillic acid.

1. Introduction

Acetylcholinesterase (AChE, EC 3.1.1.7) is an enzyme belonging to the family of cholinesterases, a special class of carboxylic ester hydrolases. AChE is existed at cholinergic synapses and neuromuscular junctions in the nervous system. After activation of acetylcholine receptors on the postsynaptic membrane, it hydrolyzes acetylcholine to choline and acetate. As it helps to terminate synaptic transmission at nerve endings, AChE activity is necessary for the nervous system to function normally (Lionetto et al. 2013). Alteration of AChE activity causes some congenital and acquired diseases (Martyn and Fagerlund 2020).

Alzheimer's disease (AD) is the most common type of dementia. This neurodegenerative disease is characterized by neurofibrillary tangles and neuritic plaques as a result of accumulation of amyloid-beta peptides in the brain. In addition, atrophy due to neural, neuropil and synaptic losses is observed in AD (Breijyeh and Karaman 2020). Disruption of cholinergic neurons and loss of neurotransmission in the brain are the main causes of decreased cognitive function in the patients with AD (Ferreira-Vieira et al. 2016). It is reported that there is a decrease in the level of acetylcholine in the brain of these patients due to cholinergic impairment. One of the treatment strategies of AD is the use of acetylcholinesterase inhibitors to increase the acetylcholine level (Fullwood 2007).

Phenolic acids are one of the most common bioactive compounds and occur naturally in plants. Various phenolic acid derivatives possess antioxidants, cardioprotective, anticancer, hepatoprotective, antimicrobial, anti-diabetic and antiulcer (Saibabu et al. 2015). In addition, these compounds have the inhibitory potential on AChE activity (Jabir et al. 2018). Gallic Acid (GA) is the main phenolic acid in tea. Vanillic Acid (VA) is a phenolic acid derivative found in several fruits, cereal grains, olives and wine (Kiokias et al. 2020). It has been reported that GA inhibits AChE activity in a dose-dependent manner (Balkrishna et al. 2019).

In this study, the inhibition properties of GA and VA mixture on AChE activity was investigated. The AChE activity was measured in the samples treated with the different concentrations of the mixture.

2. Materials and Methods

Acetylthiocholine iodate (Sigma), sodium citrate (Sigma), sodiumphosphate dibasic (Sigma), 5,5'-dithiobis 2-nitrobenzoic acid (Sigma), Ethylenediamine tetraacetic acid (Sigma), Vanillic acid (Merk), Gallic acid (Merk) and instant medium (Carolina) were used in this study.

Third instar larvae of *Drosophila melanogaster* were grown in the instant medium treated with 50 and 100 µM concentrations of gallic acid and vanillic acid mixtures. AChE activity was measured in adult flies obtained from the larvae. After the heads of the flies were dissected, they were homogenized using 0.1 M phosphate buffer (containing 0.5% Triton X-100, pH: 7.4). The supernatant was used as the enzyme source (Hsiao et al. 2004). AChE activity was determined according to Ellman's spectrophotometric method (Ellman et al. 1961). AChE activity was determined according to Ellman's method. For this purpose, a mixture containing Tris-HCl solution (1 M, pH 8.0), 5,5'-dithiobis 2-nitrobenzoic acid (0.5 mM), acetylthiocholine iodide (10 mM) and sample was prepared. The absorbance was measured at 412

nm with kinetic read. One unit of AChE activity was defined as the amount of enzyme needed to hydrolyze 1 µmol of the substrate per min.

Statistical analysis of the data obtained from the studies was performed using the Graphpad prism program. One-way ANOVA test was used for statistical evaluation. Statistical significance level was considered as $p<0.05$.

3. Results

To determine the inhibitory effect of gallic and vanillic acid mixture on AChE activity, stock solutions of these compounds were prepared. Then, 50 and 100 µM concentrations of these solutions were applied to the larvae. AChE activity in the heads of adult flies developing from these larvae was determined. As a result, it was found that 50 µM of GA-VA mixture did not affect the AChE activity statistically compared to the control ($p>0.05$). However, 100 µM of GA-VA mixture caused a statistically significant decrease in AChE activity compared to control ($p<0.05$). The graph of AChE activity results is given in Figure 1.

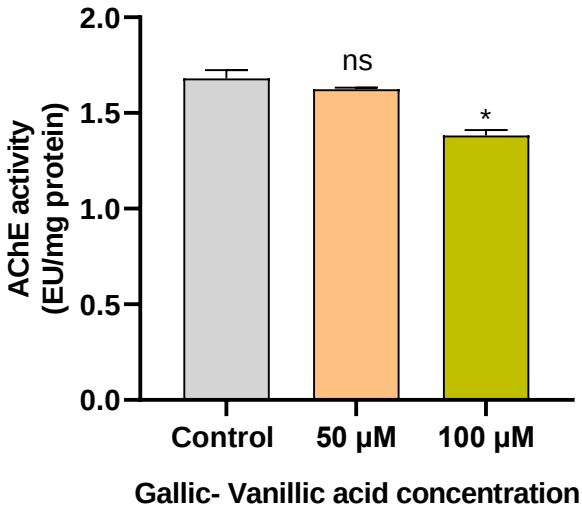

Figure 1. AChE activity in the heads of flies treated with GA-VA mixtures (GA: gallic acid, VA: vanillic acid, ns: not significant, *: p-value <0.05)

4. Discussion

A decrease in the level of a neurotransmitter acetylcholine causes significant changes in the brain and cognitive disorders such as Alzheimer's disease (AD). Therefore, AChE inhibitors are used to restore acetylcholine levels. Various plant species have shown pharmacological activities related to the treatment of cognitive disorders (Howes and Houghton 2003). Therefore, the therapeutic potential of compounds isolated from plants in the treatment of cognitive disorders and neurodegenerative diseases

is being investigated. Polyphenols and phenolic acids from the plants has been the subject of increasing interest due to their health benefits and investigated for their acetylcholinesterase inhibitory activity (Roseiro et al. 2012). In a study, the possible in vitro inhibitory potentials of a number of phenolic compounds and flavonoid derivatives against AChE and BChE at 1 mg/ml concentration were investigated. It has been reported that some phenolic acids and flavonoids in the prepared solutions exhibit beneficial inhibitory activity against AChE and BChE (Orhan et al. 2007). In another study, the anticholinesterase activities of nine phenolic acids and six flavonoids, alone or in combination, were measured. As a result, p-Hydroxyphenylpyruvic, caffeic, chlorogenic, gentisic, homogentisic, nordihydroguaiaretic and rosmarinic acids in pairs exhibited a lower inhibitory activity than the sum of the activities of the single compounds. However, inhibitory activity was not observed in some combinations (Szwajgier 2015). In this study, it was found that the mixtures prepared from phenolic acid derivative gallic acid and vanillic acid showed an inhibitory effect depending on the dose. Studies have shown that the anticholinesterase activity of phenolic acids varies according to the compound studied. This may depend on the structure of the compound used, the number and/or position of functional groupsin the compound.

5. Conclusion

In this study, AChE inhibitory activities of different concentrations of gallic acid and vanillic acid mixture were investigated. The results showed that the mixture could have inhibitory capacity depending on the dose. It may be useful to use a combination of phenolic compounds in the investigation of AChE inhibitors. However, further in vivo studies should be performed to evaluate and confirm the potential of phenolic compounds as therapeutic AChE inhibitors.

6. References

Balkrishna A, Pokhrel S, Tomer M, Verma S, Kumar A, Nain P, Gupta A, Varshney A. Anti-Acetylcholinesterase Activities of Mono-Herbal Extracts and Exhibited Synergistic Effects of the Phytoconstituents: A Biochemical and Computational Study. Molecules. 2019; 24 (22):

Breijyeh Z, Karaman R. Comprehensive Review on Alzheimer's Disease: Causes and Treatment. Molecules. 2020; 25 (24):

Ellman GL, Courtney KD, Andres V, Jr., Feather-Stone RM. A new and rapid colorimetric determination of acetylcholinesterase activity. Biochem Pharmacol. 1961; 7 88-95.

Ferreira-Vieira TH, Guimaraes IM, Silva FR, Ribeiro FM. Alzheimer's Disease: Targeting the Cholinergic System. Current Neuropharmacology. 2016; 14 (1): 101-115.

Fullwood NJ. Neural stem cells, acetylcholine and Alzheimer's disease. Nature Chemical Biology. 2007; 3 (8): 435-435.

Howes MJR, Houghton PJ. Plants used in Chinese and Indian traditional medicine for improvement of memory and cognitive function. Pharmacology Biochemistry and Behavior. 2003; 75 (3): 513-527.

Hsiao YM, Lai JY, Liao HY, Feng HT. Purification and characterization of acetylcholinesterase from oriental fruit fly [Bactrocera dorsalis (Hendel)] (Diptera : Tephritidae). Journal of Agricultural and Food Chemistry. 2004; 52 (17): 5340-5346.

Jabir NR, Khan FR, Tabrez S. Cholinesterase targeting by polyphenols: A therapeutic approach for the treatment of Alzheimer's disease. Cns Neuroscience & Therapeutics. 2018; 24 (9): 753-762.

Kiokias S, Proestos C, Oreopoulou V. Phenolic Acids of Plant Origin-A Review on Their Antioxidant Activity In Vitro (O/W Emulsion Systems) Along with Their in Vivo Health Biochemical Properties. Foods. 2020; 9 (4):

Lionetto MG, Caricato R, Calisi A, Giordano ME, Schettino T. Acetylcholinesterase as a Biomarker in Environmental and Occupational Medicine: New Insights and Future Perspectives. Biomed Research International. 2013; 2013 1-8.

Martyn JAJ, Fagerlund MJ. 12 Neuromuscular Physiology and Pharmacology: Volume 2: In Miller's Anesthesia. Gropper, M. A., MD, PhD (Eds.). Elsevier. 2020; pp. 333-353.

Orhan I, Kartal M, Tosun F, Sener B. Screening of various phenolic acids and flavonoid derivatives for their anticholinesterase potential. Zeitschrift Fur Naturforschung Section C-a Journal of Biosciences. 2007; 62 (11-12): 829-832.

Roseiro LB, Rauter AP, Serralheiro MLM. Polyphenols as acetylcholinesterase inhibitors: structural specificity and impact on human disease. Nutrition and Aging. 2012; 1 (2): 99-111.

Saibabu V, Fatima Z, Khan LA, Hameed S. Therapeutic Potential of Dietary Phenolic Acids. Advances in Pharmacological Sciences. 2015; 2015

Szwajgier D. Anticholinesterase activity of selected phenolic acids and flavonoids - interaction testing in model solutions. Annals of Agricultural and Environmental Medicine. 2015; 22 (4): 690-694.

Second International Congress on Biological and Health Sciences
ONLINE 24-25-26-27 FEBRUARY 2022

Is It A Part of Tectorial Membrane?

Burak Karip[1], Özlem Öztürk Köse[2] Gülseli Berivan Sezen [3]

[1] Department of Anatomy, Faculty of Medicine, University of Health Sciences, Istanbul, Turkey

[2] Department of Anatomy, Faculty of Medicine, Biruni University, Istanbul, Turkey

[3] Department of Neurosurgery, Gaziosmanpaşa Training and Research Hospital, Istanbul, Turkey

Corresponding author: krpbrk@gmail.com

Abstract:
The craniocervical junction is the main structure that is related to the stability of the cervical region. The most important and principal formations of the junction are atlanto-occipital and atlanto-axial joints. In terms of atlanto-axial joint, there are many different ligaments that serve as a protector for the joint. Whereas some of them (transverse ligament of atlas, alar ligaments, apical ligament of dens, superior longitudinal band, and inferior longitudinal band of cruciform ligament) seem more important, a few of them (Arnold's ligament, Gerber's ligament) may be overlooked. Arnold's ligament is known as accessory atlantoaxial ligaments which can seem deep parts of the tectorial membrane. In this case, during the routine dissection on a caucasian male cadaver, after removing the bodies of the vertebrae, spinal cord, and tectorial membrane, we found an abnormal ligament. According to its position, it seems like Arnold's ligament but in terms of its coursing, it didn't like a part of the ligaments. Although many anatomists overlooked or ignored the ligaments, for surgeons, they are really important for some functions and the prognosis of the surgeries. This ligament which we found in that area may be a deep part of the tectorial membrane. So there are still unclear pieces of knowledge about the craniocervical junction.

Keywords: Craniocervical junction, tectorial membrane, accessory atlantoaxial ligaments, atlantaxial joints

1. Introduction

Even though atlanto-axial joint seems a basic structure, there are many different ligaments in this area. The main reason is the articulation between the atlas and the axis. These structures are known as the first cervical vertebra and the second cervical vertebra respectively. Especially the articulation process of the joint performs among the dens (also called the odontoid process) and the anterior arch of the atlas (Koller & Robinson, 2019).

The ligamentous structure which covers the articulation is consist of the transverse ligament of atlas, alar ligaments, apical ligament of dens, superior longitudinal band, and inferior longitudinal band of cruciform ligament. Except those ligaments, there are a few other ligaments that are not well defined (Standring, 2015). The first one is Gerber's ligament which is defined as an accessory band below the superıor longitudinal band of cruciform ligament (Ishak et al., 2019). The second important one is

accessory atlantoaxial ligaments (also called Arnold's ligament) which course obliquely from the medial part of the axis to lateral mass of the atlas. At the same time, all of these structures are parts of the craniocervical junction (Debernardi et al., 2015). Beyond these structures, there is an important protector which is called as the tectorial membrane. The tectorial membrane is the superıor continuation of the posterior longitudinal ligament and has superficial and deep parts. Some of the ligaments we mentioned are thought to be related to these parts.

2. Case Report

During the routine dissection for education on a caucasian male cadaver, after removing the bodies of vertebrae to remove the spinal cord, we noticed an abnormal structure around the craniocervical junction (Figure 1). First of all, we removed the spinal cord and tectorial membrane gently from that area. We could identify the superior and inferior longitudinal band of the cruciform ligament clearly. But there was still an abnormal structure that seem like a deep part of the tectorial membrane.

Figure 1. Posterior aspect of atlantoaxial region. *Our finding

3. Discussion

Though accessory atlantoaxial ligaments and tectorial membrane are rarely encountered in the literature and textbooks, it has been mentioned in various books for over 100 years. Actually, these ligaments have some connections with the transverse ligament of atlas, alar ligaments, the atlas, the axis, and occiput (Bodon et al., 2019). The coursing pattern of the ligaments is towards the lateral side to the medial side (Niknejad, van Calenbergh, Demaerel, & van Loon, 2016). In terms of their functions, the ligaments have some important features such as assisting alar ligaments to limit the rotation of the craniocervical junction (Ishak et al., 2019; Yuksel, Heiserman, & Sonntag, 2006). On the other hand, the ligaments can assist to the transverse ligament of atlas to limit the rotation of the atlanto-occipital joints as well (Tubbs, Salter, & Oakes, 2004). Although our finding resembles the ligaments in that it appears just below the membrane, it can be a variation of the ligaments or a deep part of the membrane. Due to the high variability and vital importance of the region, this study may give the surgeon a different perspective.

4. References

Bodon, G., Kiraly, K., Tunyogi-Csapo, M., Hirt, B., Wilke, H. J., Harms, J., & Patonay, L. (2019). Introducing the craniocervical Y-ligament. *Surg Radiol Anat, 41*(2), 197-202. doi:10.1007/s00276-018-2116-z

Debernardi, A., D'Aliberti, G., Talamonti, G., Villa, F., Piparo, M., & Collice, M. (2015). The Craniovertebral Junction Area and the Role of the Ligaments and Membranes. *Neurosurgery, 76*(suppl_1), S22-S32. doi:10.1227/01.neu.0000462075.73701.d2 %J Neurosurgery

Ishak, B., Gnanadev, R., Dupont, G., Kikuta, S., Altafulla, J., Iwanaga, J., & Tubbs, R. S. (2019). Gerber's Ligament—A Forgotten Structure of the Craniocervical Junction. *World Neurosurgery, 124*, e707-e709. doi:https://doi.org/10.1016/j.wneu.2018.12.198

Koller, H., & Robinson, Y. (2019). *Cervical Spine Surgery: Standard and Advanced Techniques*. In.

Niknejad, H. R., van Calenbergh, F., Demaerel, P., & van Loon, J. (2016). Accessory atlantoaxial ligament avulsion fracture of the axis: Are there any clinical implications? *J Craniovertebr Junction Spine, 7*(4), 273-275. doi:10.4103/0974-8237.193259

Standring, S. (2015). *Gray's Anatomy- The Anatomical Basis of Clinical Practice* (S. Standring Ed. 41th ed.): Elsevier.

Tubbs, R. S., Salter, E. G., & Oakes, W. J. (2004). The accessory atlantoaxial ligament. *Neurosurgery, 55*(2), 400-402; discussion 402-404. doi:10.1227/01.neu.0000129699.37854.77

Yuksel, M., Heiserman, J. E., & Sonntag, V. K. (2006). Magnetic resonance imaging of the craniocervical junction at 3-T: observation of the accessory atlantoaxial ligaments. *Neurosurgery, 59*(4), 888-892; discussion 892-883. doi:10.1227/01.Neu.0000232661.24547.06

Second International Congress on Biological and Health Sciences
ONLINE 24-25-26-27 FEBRUARY 2022

Bioinformatics Analysis to Identify and Evaluate the Critical Driver Genes and Pathways Involved in COVID-19

Hamid Ceylan[1]

[1]Atatürk University, Faculty of Science, Department of Molecular Biology and Genetics, Erzurum, Turkey

Corresponding author: hamid.ceylan@atauni.edu.tr

Abstract:
The novel coronavirus (COVID-19) outbreak was declared as a global pandemic by The World Health Organization (WHO) on March 11, 2020. Since then, a large number of omics data has been generated from different experimental and clinical studies. Due to the complex nature of the disease, the clinical use of existing data against COVID-19 remains insufficient. The present study aims to identify critical genes and associated main pathways using a bioinformatics approach to elucidate the gene-disease relationship. For this purpose, disease-related genes were identified using the Comparative Toxicogenomics Database (CTD). The first 100 genes ranked by inference score were used for further analyses. The protein-protein interaction (PPI) network of the identified genes was mapped by the STRING database. Thereafter, the MCODE plug-in of Cytoscape software was used to identify significant clusters in the PPI network. Finally, the most critical hub gene candidates were determined based on the Maximal Clique Centrality (MCC) algorithm scores of Cytohubba plug-in of Cytoscape. The ToppGene (ToppFun) tool was used to identify functional categories and biochemical pathways. In total, ten genes (*TNF, IL4, CXCL8, IL6, CCL2, STAT3, JUN, IL1B, IL10,* and *ICAM1*) were identified as highly critical hub genes for the disease. The findings of the current study support the hypothesis that core genes involved in important mechanisms such as the TNF signaling pathway, Jak-STAT signaling pathway, and FoxO signaling pathway may be crucial targets for understanding and managing COVID-19-related complications.

Keywords: bioinformatics, covid-19, hub genes, network

1. Introduction

The 2019 coronavirus disease (COVID-19) has complex clinical manifestations and is therefore different from many respiratory-associated viral infections. Although it is known that the most important feature of COVID-19 is respiratory involvement, many studies from the beginning of the pandemic to the present have revealed the effects of COVID-19 on diverse organ systems (Deer et al. 2021).

As we know, the most common clinical symptoms of the disease include cough, shortness of breath, fever, headache, and fatigue (Gorna et al. 2021). However, it also leads to the emergence of many complications as it targets multiple organs and tissues such as the kidneys, large intestine, and heart, especially. Different manifestations including encephalitis, loss of smell and taste, and disorientation have been reported in COVID-19 positive patients even in the absence of other respiratory symptoms

(Asadi-Pooya and Simani 2020). Cheng et al. reported that advanced kidney disease is associated with a poor prognosis in patients with COVID-19 (Cheng et al. 2020). Previous studies show that the disease is also associated with irregular liver functions (Fan et al. 2020; Jothimani et al. 2020). Additionally, our latest study also showed that this disease can contribute to new late-onset cardiovascular anomalies in the near future (Ceylan 2021).

It is well known that non-communicable diseases (NCDs) including cardiovascular diseases, diabetes, and cancer are the dominant causes of death worldwide. Moreover, people with underlying such health conditions have a higher risk of severe COVID-19 disease (Nikoloski et al. 2021). Given the complexity observed in these diseases, the identification of key genes and pathways using bioinformatics-based analyses can help us to reveal specific events and molecular mechanisms for therapeutic interventions.
As we gain more insight into the drivers of COVID-19, it will be easier to predict the post-COVID conditions and long-term effects of the disease and to identify effective treatment strategies. In this work, the potential molecular mechanisms that drive long-term ramifications of COVID-19 infection were evaluated by bioinformatics analysis.

2. Materials and Methods

2.1. COVID-19 related gene screening

Target genes associated with COVID-19 were mined from the publicly available Comparative Toxicogenomics Database (CTD) (Davis et al. 2019). The first 100 genes ranked by inference score were used for further analyses.

2.2. Protein-protein interaction (PPI) network and sub-module identification analyses

Using the STRING (Search Tool for the Retrieval of Interacting Genes) online tool (Jensen et al. 2009), a protein-protein interaction network was constructed to evaluate the relationships among selected genes. PPI network was visualized and analyzed by using Cytoscape software (Shannon et al. 2003). Then, MCODE (Molecular Complex Detection) plug-in was applied to explore important nodes in the PPI network. Finally, hub genes were determined according to the Maximal Clique Centrality (MCC) algorithm of the cytoHubba plug-in of Cytoscape.

2.3. Functional enrichment analysis

To identify genes at the biologically functional level, hub genes determined by MCC analysis were submitted to the DAVID (Database for Annotation, Visualization, and Integrated Discovery) online analysis resource (Huang et al. 2009). p-value <0.05 was set as cut-off criteria

3. Results

3.1. Screening of disease-related genes

According to CTD, a total of 9861 genes are associated with COVID-19 or its descendants. However, mentioned previously, the first 100 genes ranked by inference score were selected for further analyses. Top genes are summarized in Table 1.

Table 1. Top 100 disease (COVID-19, MESH:D000086382) related genes obtained from CTD.

Rank	Gene Symbol	Inference Score	Rank	Gene Symbol	Inference Score	Rank	Gene Symbol	Inference Score
1	*TP53*	32,1	34	*MAP1LC3B*	20,07	68	*CASP7*	17,16
2	*CCL2*	31,9	35	*MCL1*	20,01	69	*MAP2*	17,14
3	*NFKBIA*	28,84	36	*NR1H4*	20,01	70	*INS1*	17,12
4	*RELA*	28,56	37	*CDH1*	19,93	71	*EDN1*	16,84
5	*TNF*	27,64	38	*BCL2L1*	19,84	72	*PPARG*	16,65
6	*NFKB1*	26,92	39	*VEGFA*	19,8	73	*DDIT3*	16,62
7	*CASP3*	26,48	40	*IL2*	19,71	74	*ABCC2*	16,6
8	*CASP8*	25,73	41	*SQSTM1*	19,66	75	*CTNNB1*	16,46
9	*ABCB1*	25,43	42	*MYC*	19,6	76	*APP*	16,45
10	*IL6*	25,4	43	*STAT1*	19,45	77	*ACTA2*	16,44
11	*CXCL8*	25,21	44	*GLB1*	19,38	78	*CASP12*	16,16
12	*AKT1*	24,44	45	*FOS*	19,25	79	*CD36*	16,08
13	*NOS2*	24,24	46	*IFNG*	19,24	80	*FAS*	16,03
14	*IL10*	24,2	47	*NOS3*	19,08	81	*CYP2D6*	15,97
15	*IL1B*	23,89	48	*ESR1*	19,02	82	*ABCB11*	15,92
16	*CDKN1A*	23,22	49	*SERPINE1*	18,97	83	*NFE2L2*	15,84
17	*ICAM1*	22,32	50	*GPT*	18,8	84	*MAPK3*	15,78
18	*SOD2*	22,31	51	*AGT*	18,71	85	*MAPK1*	15,76
19	*TGFB1*	22,02	52	*BBC3*	18,6	86	*IL4*	15,61
20	*IL1A*	21,96	53	*ALB*	18,58	87	*MKI67*	15,6
21	*CCND1*	21,83	54	*CS*	18,52	88	*CYP2C9*	15,51
22	*PCNA*	21,73	55	*RUNX2*	17,99	89	*CAT*	15,48
23	*CYP3A4*	21,69	56	*MAP2K1*	17,9	90	*HSF1*	15,42
24	*BAX*	21,63	57	*MMP9*	17,85	91	*CYP3A23*	15,26
25	*HSPA5*	21,59	58	*TLR4*	17,85	92	*ABCB1A*	15,25
26	*COL1A1*	21,54	59	*MT2A*	17,81	93	*JUN*	15,24
27	*STAT3*	20,74	60	*LEP*	17,77	94	*BAK1*	15,15
28	*BECN1*	20,7	61	*CTSK*	17,73	95	*EGFR*	15,1
29	*BCL2*	20,67	62	*RB1*	17,52	96	*RAF1*	15,09
30	*HMOX1*	20,6	63	*CREB1*	17,45	97	*CTSB*	15,05
31	*CTSL*	20,35	64	*MAPK8*	17,37	98	*PTGS2*	15,03
32	*PARP1*	20,14	65	*CYP27A1*	17,36	99	*TIMP2*	15,03
33	*SRC*	20,12	66	*CASP9*	17,33	100	*CCND2*	15,01
			67	*MYH7*	17,27			

3.2. PPI network analysis and identification of hub genes

A PPI network was constructed based on the STRING to analyze the biological functions of the genes (Figure 1). Then PPI network was imported into Cytoscape. Subnetwork analysis by using MCODE showed two clusters (Figure 2a and 2b). Finally, the top 10 genes, computed using the topological scoring method of MCC, from the PPI network were selected as hub genes (Figure 3). Further analysis was done using the these ten (*TNF, IL4, CXCL8, IL6, CCL2, STAT3, JUN, IL1B, IL10,* and *ICAM1*) genes.

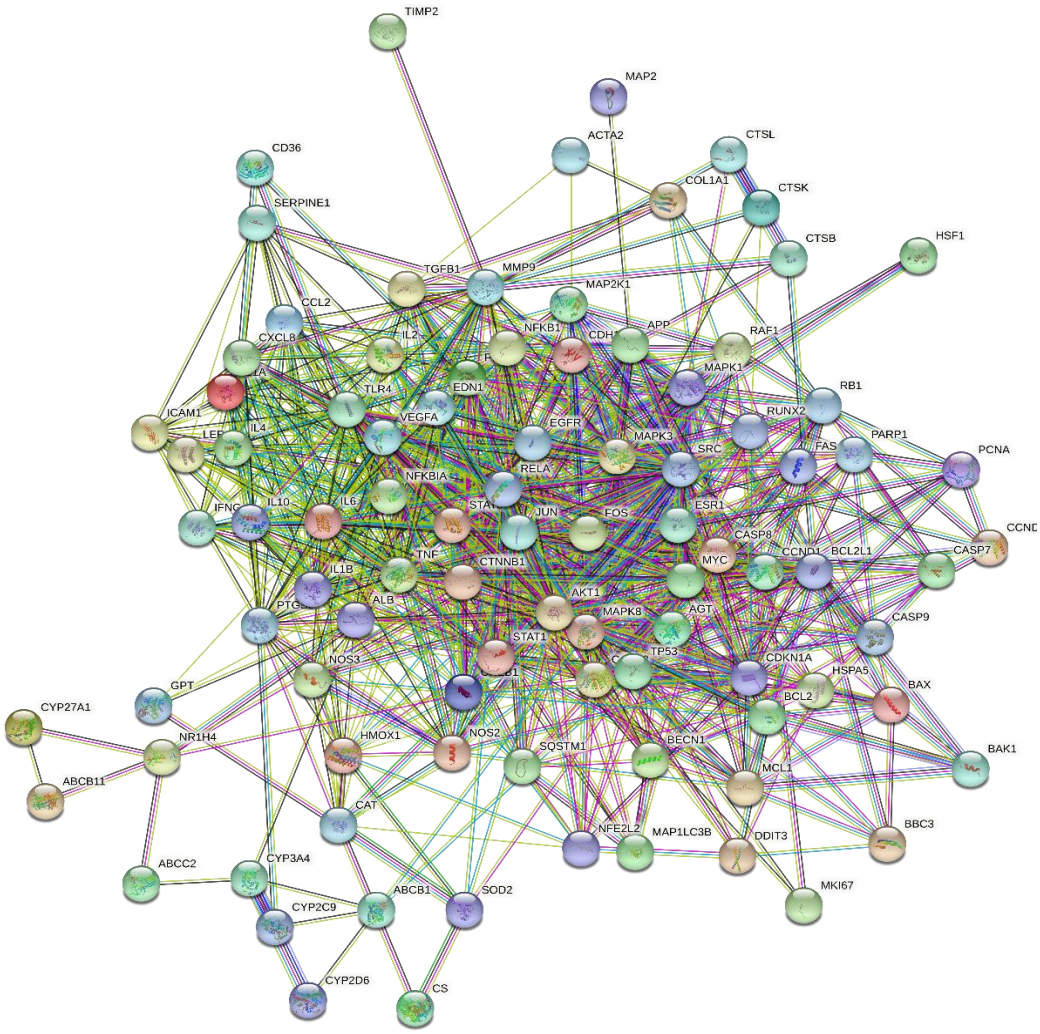

Figure 1. Protein-Protein interaction (PPI) network obtained from STRING database for all genes.

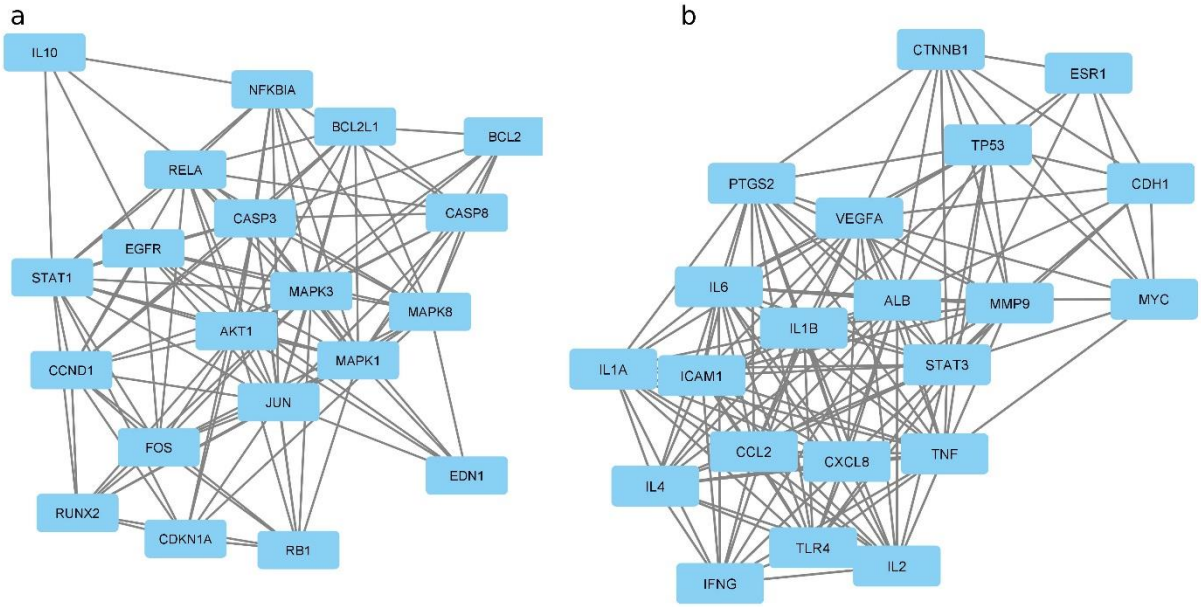

Figure 2. The functional sub-network analysis of PPI network. a) Module 1, b) Module 2

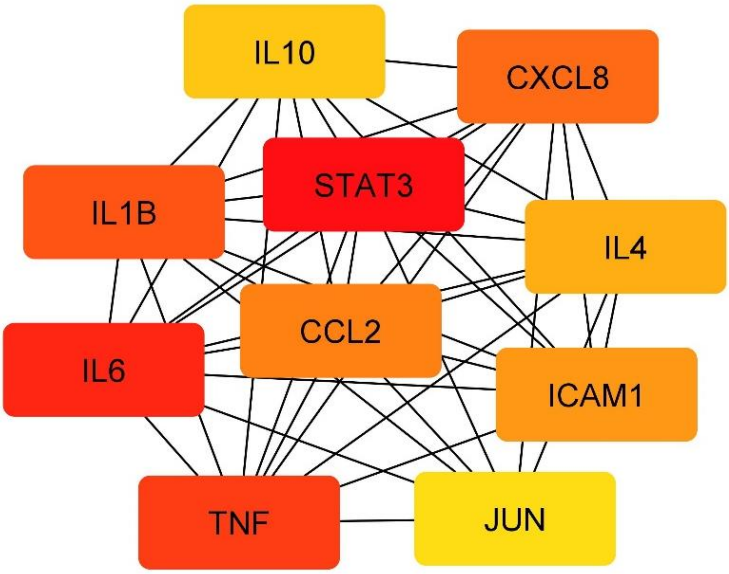

Figure 3. Visualization of the hub genes using cytoHubba plugin. The red to yellow color grade represents decreasing MCC scores.

3.3. Enrichment analysis of GO term and KEGG pathways

GO analysis further classified the hub genes into three categories; biological process (BP), cellular component (CC), and molecular function (MF), as summarized in Table 2. The results of the KEGG pathway enrichment analysis revealed that these genes are involved in many processes that are very critical for the cell, including TNF signaling pathway, NF-kappa B signaling pathway, Pathways in cancer, and FoxO signaling pathway. The detailed results are shown in Table 3.

Table 2. Gene ontology enrichment analysis of the genes. GO, Gene Ontology; MF, molecular function; BP, biological process; CC, cellular component.

Category	GO Term	p-value	Genes
BP	immune response	1,89E-08	*IL10, IL4, IL6, CXCL8, IL1B, CCL2, TNF*
	positive regulation of transcription, DNA-templated	6,28E-08	*IL10, IL4, IL6, JUN, IL1B, STAT3, TNF*
	positive regulation of sequence-specific DNA binding transcription factor activity	1,78E-07	*IL10, IL4, IL6, IL1B, TNF*
	response to drug	2,23E-07	*IL10, IL4, IL6, JUN, STAT3, ICAM1*
	inflammatory response	6,67E-07	*IL10, IL6, CXCL8, IL1B, CCL2, TNF*
	negative regulation of cell proliferation	8,29E-07	*IL10, IL6, JUN, CXCL8, IL1B, STAT3*
	aging	1,09E-06	*IL10, IL6, JUN, STAT3, CCL2*
	positive regulation of nitric oxide biosynthetic process	1,30E-06	*IL6, IL1B, TNF, ICAM1*
	positive regulation of ERK1 and ERK2 cascade	1,38E-06	*IL6, JUN, CCL2, TNF, ICAM1*
	positive regulation of transcription from RNA polymerase II promoter	2,82E-06	*IL10, IL4, IL6, JUN, IL1B, STAT3, TNF*
	cellular response to interleukin-1	5,97E-06	*IL6, CXCL8, CCL2, ICAM1*
	positive regulation of chemokine biosynthetic process	1,15E-05	*IL4, IL1B, TNF*
	positive regulation of heterotypic cell-cell adhesion	1,40E-05	*IL10, IL1B, TNF*
	response to ethanol	1,94E-05	*IL4, STAT3, CCL2, ICAM1*
	cellular response to tumor necrosis factor	2,23E-05	*IL6, CXCL8, CCL2, ICAM1*
	cytokine-mediated signaling pathway	3,77E-05	*IL6, IL1B, STAT3, CCL2*
CC	extracellular space	3,74E-07	*IL10, IL4, IL6, CXCL8, IL1B, CCL2, TNF, ICAM1*
	extracellular region	3,13E-05	*IL10, IL4, IL6, CXCL8, IL1B, CCL2, TNF*
	external side of plasma membrane	1,26E-04	*IL4, IL6, TNF, ICAM1*
MF	cytokine activity	1,38E-06	*IL10, IL4, IL6, IL1B, TNF*
	growth factor activity	0,003	*IL10, IL4, IL6*
	transcription regulatory region DNA binding	0,005	*JUN, STAT3, TNF*
	chemokine activity	0,026	*CXCL8, CCL2*

Table 3. KEGG pathway enrichment analysis of the genes. KEGG, Kyoto Encyclopedia of Genes and Genomes

Category	Term	p-value	Genes
KEGG	TNF signaling pathway	9,90E-08	*IL6, JUN, IL1B, CCL2, TNF, ICAM1*
	Cytokine-cytokine receptor interaction	1,40E-07	*IL10, IL4, IL6, CXCL8, IL1B, CCL2, TNF*
	Toll-like receptor signaling pathway	6,30E-06	*IL6, JUN, CXCL8, IL1B, TNF*
	NF-kappa B signaling pathway	1,60E-04	*CXCL8, IL1B, TNF, ICAM1*
	T cell receptor signaling pathway	2,40E-04	*IL10, IL4, JUN, TNF*
	Asthma	6,50E-04	*IL10, IL4, TNF*
	Jak-STAT signaling pathway	7,00E-04	*IL10, IL4, IL6, STAT3*
	Insulin resistance	8,20E-03	*IL6, STAT3, TNF*
	Pathways in cancer	1,20E-02	*IL6, JUN, CXCL8, STAT3*
	FoxO signaling pathway	1,20E-02	*IL10, IL6, STAT3*
	Chemokine signaling pathway	2,30E-02	*CXCL8, STAT3, CCL2*
	MAPK signaling pathway	4,10E-02	*JUN, IL1B, TNF*

4. Discussion

According to the latest WHO report, more than 400 million people worldwide have been infected, and almost 6 million people have died from the coronavirus disease 2019 (COVID-19). Scientific and medical studies have led to significant developments in the diagnosis, treatment, and prevention of COVID-19. However, there are many blurry points that are not yet fully understood about the effects after the acute phase of the disease.

Today, there are different effective therapeutic approaches for COVID-19. These approaches are aimed at restoring and protecting individual health only in the acute stages of the disease. However, it remains unclear what kind of health problems someone who has an illness will face in the process called “long COVID-19 or post COVID-19 syndrome", which covers the long-term effects of the disease. Therefore, in order to predict the long-term effects of the disease, it is considered very important to identify the genes whose expression changes depending on the disease and the molecular mechanisms in which these genes are involved. The present study was carried out to identify the critical driver genes and pathways involved in COVID-19 by using bioinformatics analysis.

Analysis of COVID-19 related genes obtained from the Comparative Toxicogenomics Database (CTD) revealed that these genes are associated with many critical molecular pathways (see Table 3). According to the latest findings, brain damage caused by COVID-19 is associated with TNF signaling. Recent studies

have shown that respiratory symptoms can be accompanied by short- and long-term neuropsychiatric symptoms (NPs) and long-term brain sequelae (Roman and Irwin 2020).

Toll-like receptor (TLR) signaling pathway, which plays a role in the triggering and progression of many diseases including I/R (ischemia-reperfusion) injury, cancer, and hypertension, is also associated with COVID-19. It has been reported that abnormal TLR signaling in COVID-19 patients may be the cause of SARS-CoV-2-induced myocarditis (Aboudounya and Heads 2021).

The FoxO signaling pathway is another essential mechanism for many cellular physiological events. Transcription factors (The forkhead box O; FoxO family) in this pathway regulate the expression of genes in important cellular physiological events such as cell cycle control, oxidative stress resistance, longevity, and apoptosis (Cheema et al. 2021). The evidence considers FoxO regulation as the arsenal for clinical management of COVID-19. Since changes in this pathway are associated with the abnormal regulation of molecular drivers underlying many diseases, it has the potential to cause various long-term COVID19-related complications (Barh et al. 2021).

5. Conclusion

Although knowledge about COVID-19 has been provided, there are still vital information gaps in terms of systems biology. Due to its complex nature, determining a holistic approach strategy with multi-omics analysis can provide useful information regarding COVID-19 management. New or adapted therapeutics for the pathways identified in this study may provide useful information for controlling potential COVID-19 associated long-term complications.

6. References

Aboudounya MM and Heads RJ. COVID-19 and Toll-Like Receptor 4 (TLR4): SARS-CoV-2 May Bind and Activate TLR4 to Increase ACE2 Expression, Facilitating Entry and Causing Hyperinflammation. Mediators Inflamm. 2021; 2021:8874339. https://doi.org/10.1155/2021/8874339

Asadi-Pooya AA and Simani L. Central nervous system manifestations of COVID-19: A systematic review. J Neurol Sci. 2020; 413:116832. https://doi.org/10.1016/j.jns.2020.116832

Barh D, Aljabali AA, Tambuwala MM, Tiwari S, Serrano-Aroca A, Alzahrani KJ, Silva Andrade B, Azevedo V et al. Predicting COVID-19-Comorbidity Pathway Crosstalk-Based Targets and Drugs: Towards Personalized COVID-19 Management. Biomedicines. 2021; 9. https://doi.org/10.3390/biomedicines9050556

Ceylan H. A bioinformatics approach for identifying potential molecular mechanisms and key genes involved in COVID-19 associated cardiac remodeling. Gene Rep. 2021; 24:101246. https://doi.org/10.1016/j.genrep.2021.101246

Cheema PS, Nandi D and Nag A. Exploring the therapeutic potential of forkhead box O for outfoxing COVID-19. Open Biol. 2021; 11:210069. https://doi.org/10.1098/rsob.210069

Cheng Y, Luo R, Wang K, Zhang M, Wang Z, Dong L, Li J, Yao Y et al. Kidney disease is associated with in-hospital death of patients with COVID-19. Kidney Int. 2020; 97:829-838. https://doi.org/10.1016/j.kint.2020.03.005

Davis AP, Grondin CJ, Johnson RJ, Sciaky D, McMorran R, Wiegers J, Wiegers TC and Mattingly CJ. The Comparative Toxicogenomics Database: update 2019. Nucleic Acids Res. 2019; 47:D948-D954. https://doi.org/10.1093/nar/gky868

Deer RR, Rock MA, Vasilevsky N, Carmody L, Rando H, Anzalone AJ, Basson MD, Bennett TD et al. Characterizing Long COVID: Deep Phenotype of a Complex Condition. EBioMedicine. 2021; 74:103722. https://doi.org/10.1016/j.ebiom.2021.103722

Fan Z, Chen L, Li J, Cheng X, Yang J, Tian C, Zhang Y, Huang S et al. Clinical Features of COVID-19-Related Liver Functional Abnormality. Clin Gastroenterol Hepatol. 2020; 18:1561-1566. https://doi.org/10.1016/j.cgh.2020.04.002

Gorna R, MacDermott N, Rayner C, O'Hara M, Evans S, Agyen L, Nutland W, Rogers N and Hastie C. Long COVID guidelines need to reflect lived experience. Lancet. 2021; 397:455-457. https://doi.org/10.1016/S0140-6736(20)32705-7

Huang DW, Sherman BT and Lempicki RA. Bioinformatics enrichment tools: paths toward the comprehensive functional analysis of large gene lists. Nucleic acids research. 2009; 37:1-13.

Jensen LJ, Kuhn M, Stark M, Chaffron S, Creevey C, Muller J, Doerks T, Julien P et al. STRING 8--a global view on proteins and their functional interactions in 630 organisms. Nucleic Acids Res. 2009; 37:D412-6. https://doi.org/10.1093/nar/gkn760

Jothimani D, Venugopal R, Abedin MF, Kaliamoorthy I and Rela M. COVID-19 and the liver. J Hepatol. 2020; 73:1231-1240. https://doi.org/10.1016/j.jhep.2020.06.006

Nikoloski Z, Alqunaibet AM, Alfawaz RA, Almudarra SS, Herbst CH, El-Saharty S, Alsukait R and Algwizani A. Covid-19 and non-communicable diseases: evidence from a systematic literature review. BMC Public Health. 2021; 21:1068. https://doi.org/10.1186/s12889-021-11116-w

Roman M and Irwin MR. Novel neuroimmunologic therapeutics in depression: A clinical perspective on what we know so far. Brain Behav Immun. 2020; 83:7-21. https://doi.org/10.1016/j.bbi.2019.09.016

Shannon P, Markiel A, Ozier O, Baliga NS, Wang JT, Ramage D, Amin N, Schwikowski B and Ideker T. Cytoscape: a software environment for integrated models of biomolecular interaction networks. Genome research. 2003; 13:2498-2504.

Production of Amylase from *Aeribacillus pallidus* AO7 using Potato Peel Powder

Mehmet Akif OMEROGLU[1], Seyda ALBAYRAK[1], Mustafa Ozkan BALTACI[1], Ahmet ADIGUZEL[1]

[1]Deparment of Molecular Biology and Genetics, Faculty of Science, Atatürk University, Erzurum, Turkey

Corresponding author: akif.omeroglu@atauni.edu.tr

Abstract:
Amylases are a group of hydrolase enzymes having ability to degrade starch and similar molecules, reducing starch to simple sugars. Amylases are considered as one of the most crucial industrial enzymes. There is a large number of applications of amylases in various industries such as food, paper, textile and detergents. Moreover, amylase enzymes for industrial applications are supposed to have high temperature activity and stability. Thermostable amylases which would be isolated mainly from thermophilic microorganisms have found a wide number of commercial applications owing to their decent overall stability. The current study focuses on investigation of amylolytic activity of thermophilic bacterium AO7 which was isolated from the hot spring situated in Turkey. Genetic analysis performed by 16S rRNA sequences demonstrated that the isolated strain AO7 belonged to *Aeribacillus pallidus*. In order to make the production process more cost-effective, Potato Peel Powder (PPP), which is regarded as waste and has high starch content, was used as substrate for amylase production. As a result of optimisation studies for production of amylase enzyme with *Aeribacillus pallidus* AO7, the optimal parameters were determined as PPP concentration of 50 g/L, temperature of 55 °C, initial pH of 7.0 and incubation time of 48 h. As a consequence of experiments carried out under optimised culture conditions, the amylase activity was detected as 65 U/mL.

Keywords: Amylase, Potato Peel Powder, *Aeribacillus pallidus* AO7

1. Introductıon

Enzymes are biological molecules with a protein structure. They are synthesized under genetic control and known as organic catalysts. Enzymes, which have very important metabolic functions in cells, have entered daily life to be used for various purposes. Enzymes used in almost all areas of industry are generally obtained from microorganisms. This is because enzymes from microorganisms have higher catalytic activity, are more stable and cheaper than plant and animal enzymes and can be obtained in large quantities (1).

Amylases are a group of hydrolase enzymes reducing starch to simple sugars. They have the ability to degrade starch and similar molecules. Another important feature of amylases is their ability to break down glycosidic bonds between glucose units making up amylopectin, amylose, and glycogen (2).

Amylases of microbial origin are valuable as they have the potential to be used as an alternative to the chemical breakdown of starch. For this reason, studies on the isolation of enzymes from different

sources are crucial and there is an intense desire to discover microorganisms with high enzyme production capacity (3).

Microorganisms are among the first sources to meet industrial amylase enzyme requirements due to their various technological advantages, including high-throughput production in short amount of time and thermal stability. Microbial amylolytic enzymes which break down starch are of great industrial importance. Industrially, the production of amylase highly performed using by bacteria and fungi. It is reported that microorganisms such as *Aspergillus niger*, *Aspergillus oryzae*, *Bacillus subtilis*, *Bacillus licheniformis*, *Micrococcus halobius* have amylase enzyme activity (4).

The purpose of the current study is to perform isolation of bacteria, which has ability to produce amylase enzyme, from the hot spring and is to optimise culture conditions for the best enzyme activity.

2. Materıal and Method

2.1. Preparation of Substrate

In order to make the production more cost-effective, Potato Peel Powder (PPP) containing high starch content was used as subtrate. For this purpose, potato peels were first washed and were dried at 80 °C. Then, the dried peels were ground into fine particles.

2.2. Isolation of Bacteria Producing Amylase

Water samples were collected from the hot spring situated in Erzurum, Turkey and they were brought to laboratory under aseptic conditions. A serial of dilutions with sterile-saline water (0.9%) was prepared (from 10^{-1} to 10^{-6}) and they were spread on the agar plates containing 1% starch as carbon source. Colonies grown on starch agar plates were selected and purified. It was detected that 5 different bacteria have ability to produce amylase enzyme. Among isolates with amylase activity, the isolate coded with AO7 was determined to demonstrate the best activity.

2.3. Identification of the isolate coded with AO7

First of all, DNA isolation of the bacteria was performed. 16S rRNA gene region was amplified using universal primers [27F (5’-AGA GTT TGA TCC TGG CTC AG- 3’) and 1492R (5’-GGT TAC CTT GTT ACG ACT T-3’)] by PCR. The amplified PCR products were cloned into pGEM-T Easy Vector. Then, the clones obtained were sequenced at Macrogen. The obtained sequence was compared with the complementary sequences within GenBank and Eztaxon (5).

2.4. Production Medium

The production processes were performed in 250 mL flasks containing 100 mL of the sterilized medium composed of 10 g/L PPP and some mineral salts (1.5 g/L KH_2PO_4, 0.5 g/L $MgSO_4$ and 0.01 g/L $CaCl_2$) (pH 7.0).

2.5 Optimisation of Production Medium

To optimise the culture conditions for the best production of amylase with the isolate coded with AO7, different parameters such PPP concentration (10-60 g/L), temperature (35-60 °C), pH (4-9) and incubation time (12-72 h) were tested.

2.6. Amylase Activity Assay

For determining amylase activity, soluble starch solution was prepared in 0.1 M phosphate buffer (pH 7.5) and the solution was used as substrate. It was centrifuged at 5000 rpm and then 0.1 mL of supernatant was mixed with 1 mL of soluble starch solution and the mixture left to incubation at 55 °C for 10 min. Following this, 1 mL of 3,5-dinitrosalicylic acid (DNS) solution was added to the mixture and the final mixture was incubated in a water bath at 95 °C for 10 min. After cooling to room temperature, the absorbance was measured at 540 nm [6].

3. Results

3.1. Identification of the isolate coded with AO7

Identification of the thermophilic isolate from hot water samples was performed at species level by molecular method. Amplification of 16S rRNA gene region, which would be evolutionarily conserved, was carried out after extracting the total DNA from the test isolate. The sequence of the isolate was compared with 16S rRNA sequences of other bacteria in the GenBank and the nucleotides were analysed using BLAST and EzTaxon. As a consequence of sequence analysis, it was determined that the isolate coded with AO7 showed similarity to *Aeribacillus pallidus* with the rate of 99%.

3.2. Effect of PPP Concentration on the Enzyme Activity

While determining PPP concentrations on the amylase activity, the optimal PPP concentration was determined to be 50 g/L and enzyme activity was noted as 40.8 U/L.

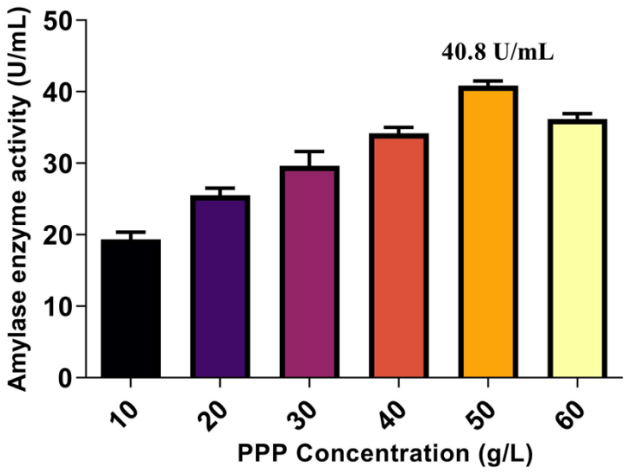

Figure 1. Effect of PPP Concentration on the Enzyme Activity

3.3. Effect of Temperature on the Enzyme Activity

The enzyme activity was investigated at different temperature values (35-60 °C). It was noted that optimum activity was obtained at 55 °C as 47.5 U/L.

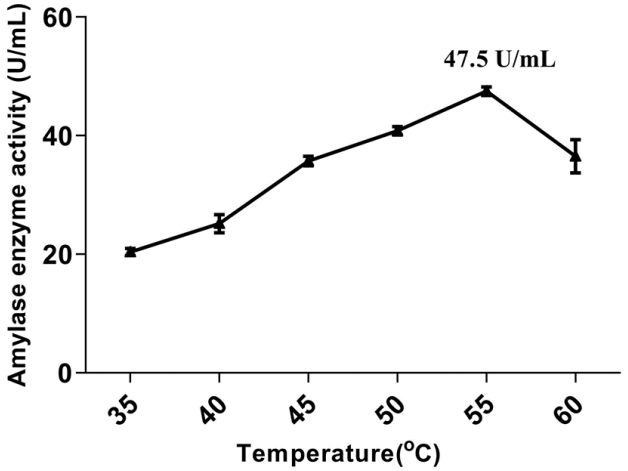

Figure 2. Effect of Temperature on the Enzyme Activity

3.4. Effect of pH on the Enzyme Activity

To designate optimum pH value for the enzyme activity, different pH values were tested (4-9) and the best activity was observed at pH 7 as 54.6 U/L.

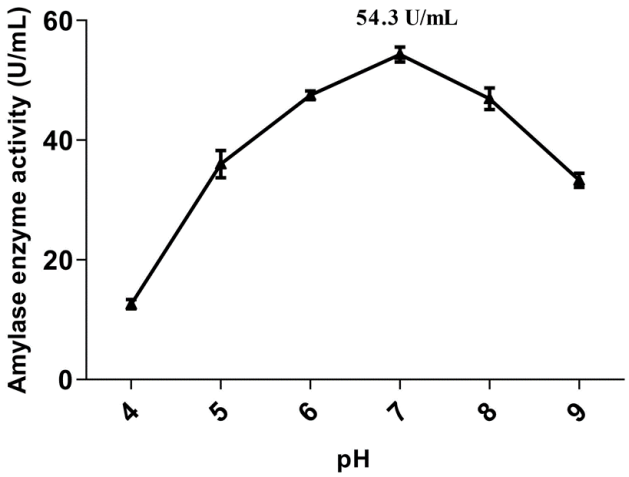

Figure 3. Effect of pH on the Enzyme Activity

3.5. Effect of Incubation Time on the Enzyme Activity

To understand the effect of incubation time on the enzyme activity, 6 different incubation times were examined and the optimum incubation time was determined to be 48 h with 65 U/L enzyme activity.

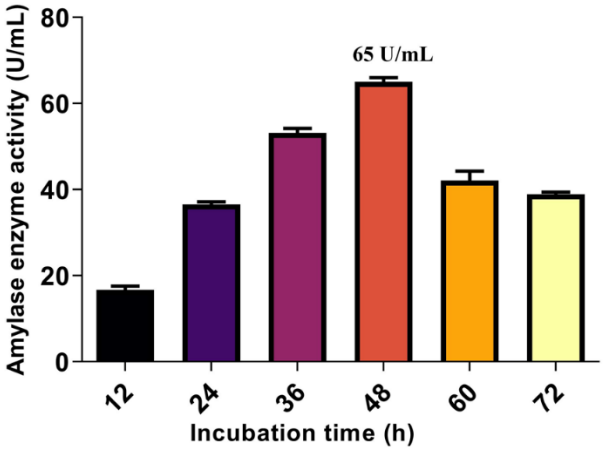

Figure 4. Effect of incubation time on the Enzyme Activity

4. Discussion

In the current study, some culture parameters (substrate concentration, temperature, pH and incubation time) were optimised. Initially, different concentrations of PPP from 10 to 60 g/L were tested and it was designated that the maximal production of amylase (40.8 U/mL) was achieved in the growth medium supplemented with 50 g/L PPP.

The optimal enzyme activity was obtained at 55 °C as 47.5 U/L in spite of the fact that the isolate was able to produce amylase enzyme in a wide temperature range from 35-60 °C.

While the optimum pH for amylase production was determined, a pH range from 4 to 9 at 55 °C was investigated. Maximum amylase production was obtained at pH 7.0 as as 54.6 U/L.

After determining the optimal parameters for PPP concentration, temperature and pH, optimum incubation time for the enzyme activity was also examined in the study. Various incubation times from 12 to 72 hours were investigated. It was observed that the optimum incubation time was noted as 48 hours and the maximal enzyme production was 65 U/L as a consequence of the experiments performed under optimised conditions.

5. Conclusion

The current study revealed that *Aeribacillus pallidus* AO7 isolated from the hot spring would be able to produce amylase enzyme on waste potato peels. It was observed that production of the enzyme can be considerably increased by means of the optimisation of the culture conditions.

6. References

1- Nigam P. S. Microbial enzymes with special characteristics for biotechnological applications. Biomolecules. 2013; 3(3): 597-611.

2- Guzmán-Maldonado H. Paredes-López O. Biliaderis C. G. Amylolytic enzymes and products derived from starch: a review. Critical Reviews in Food Science & Nutrition. 1995; 35(5): 373-403.

3- Souza PMD. Application of microbial α-amylase in industry-A review. Brazilian journal of microbiology. 2010; 41(4): 850-861.

4- Gopinath SC. Anbu P. Arshad MM. Lakshmipriya T. Voon CH. Hashim U. Chinni SV. Biotechnological processes in microbial amylase production. BioMed research international. 2017; 2017.

5- Adiguzel A. Ozkan H. Baris O. Inan K. Gulluce M. Sahin F. Identification and characterization of thermophilic bacteria isolated from hot springs in Turkey. Journal of Microbiological Methods. 2009; 79: 321–328.

6- Miller GL. Use of dinitrosalicylic acid reagent for determination of reducing sugar. Analytical Chemistry. 1959; 31: 426–428.